Фазовые превращения и дефекты в кристаллах

Б.Б.Страумал

ИФТТ РАН, НЦЧ РАН

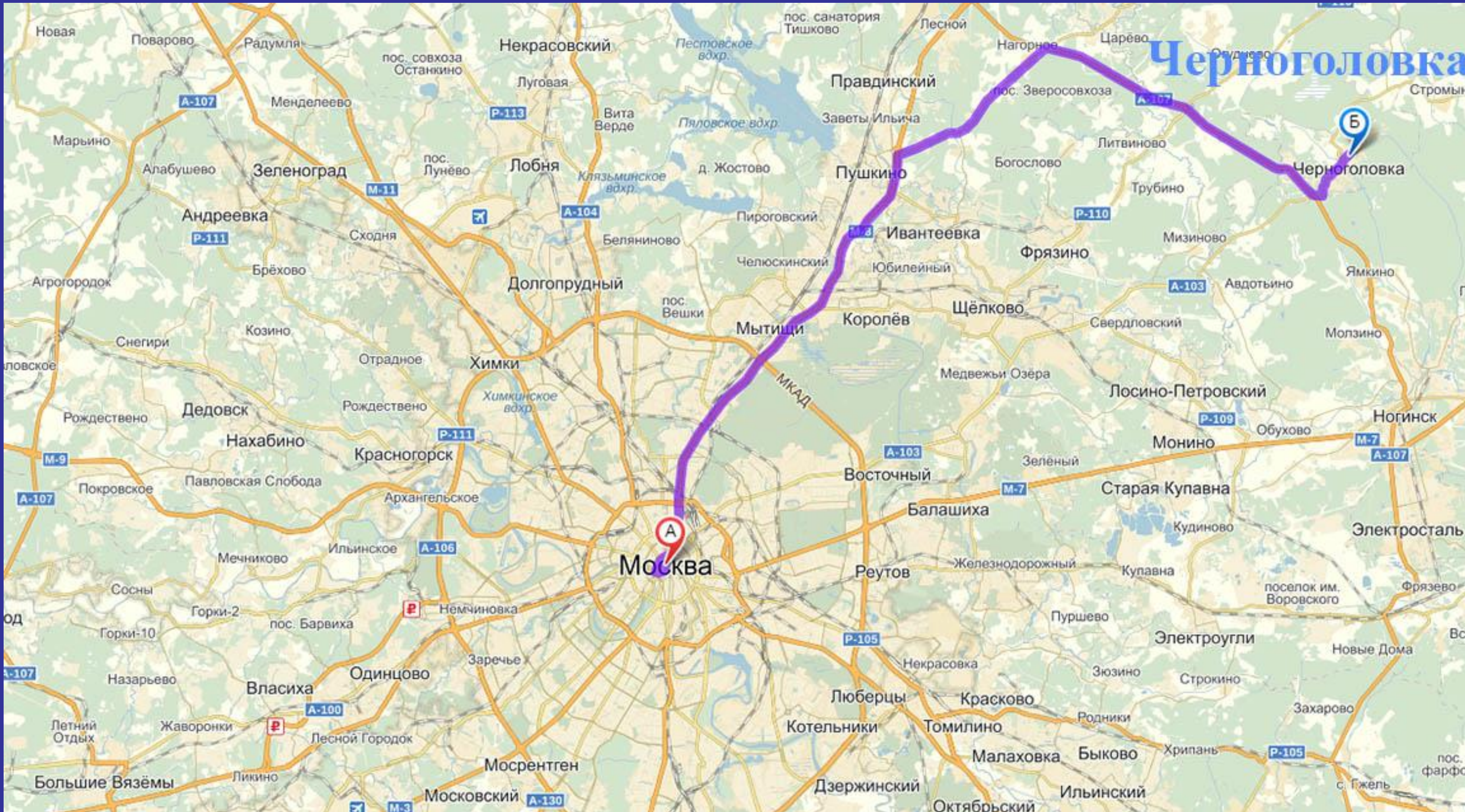

Черноголовка, где это?

Черноголовка, вид сверху

Черноголовка, вид сверху

Черноголовка, основатели

Фазовые превращения:
-- в объеме
-- на внешних и внутренних границах раздела

Фазовые превращения:

-- на внешних поверхностях (огранение-потеря огранки)

Why the facets of surfaces and interfaces appear?

Two amorhous phases: smooth interface

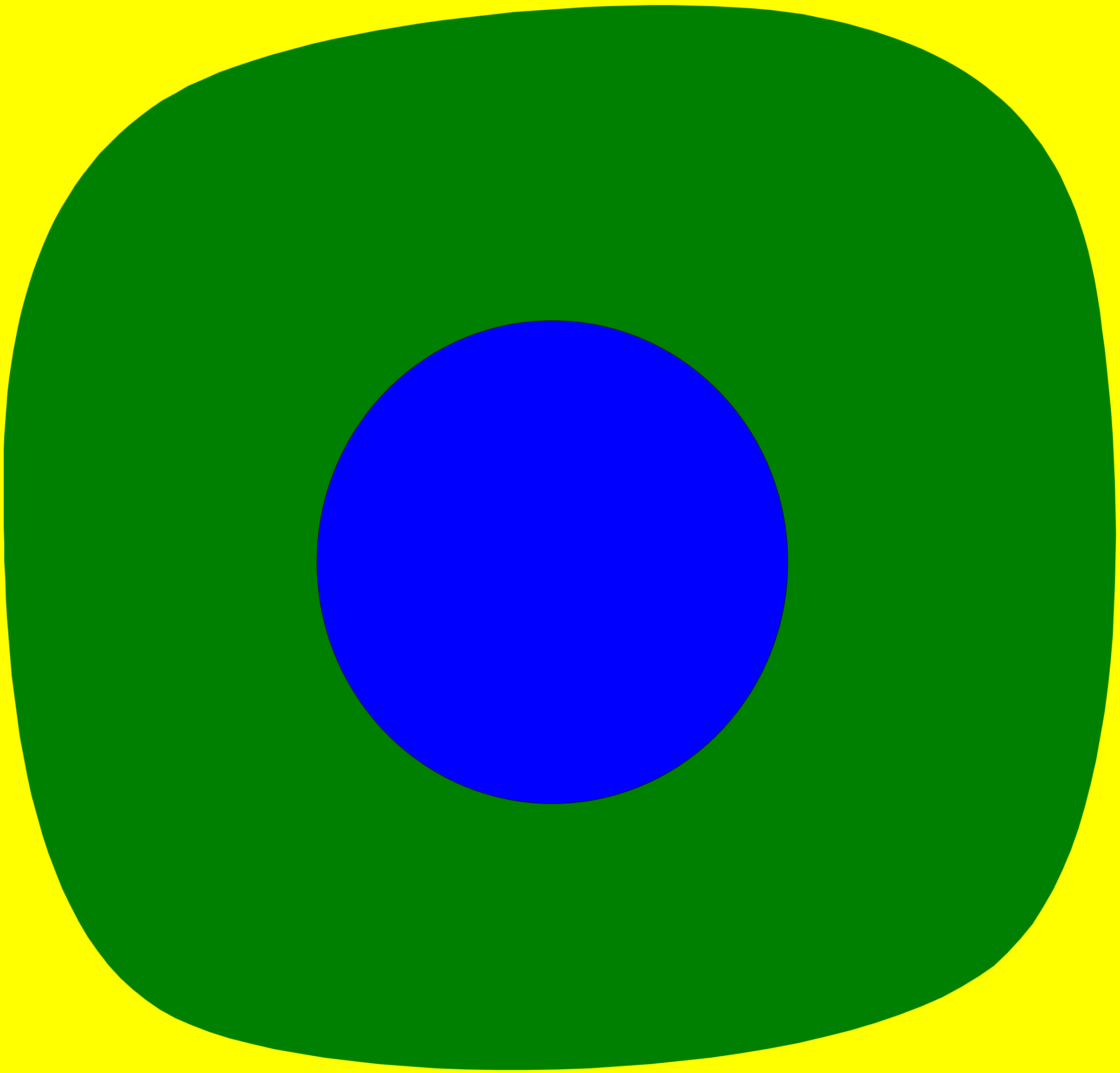

Crystal inside of an amorphous phase

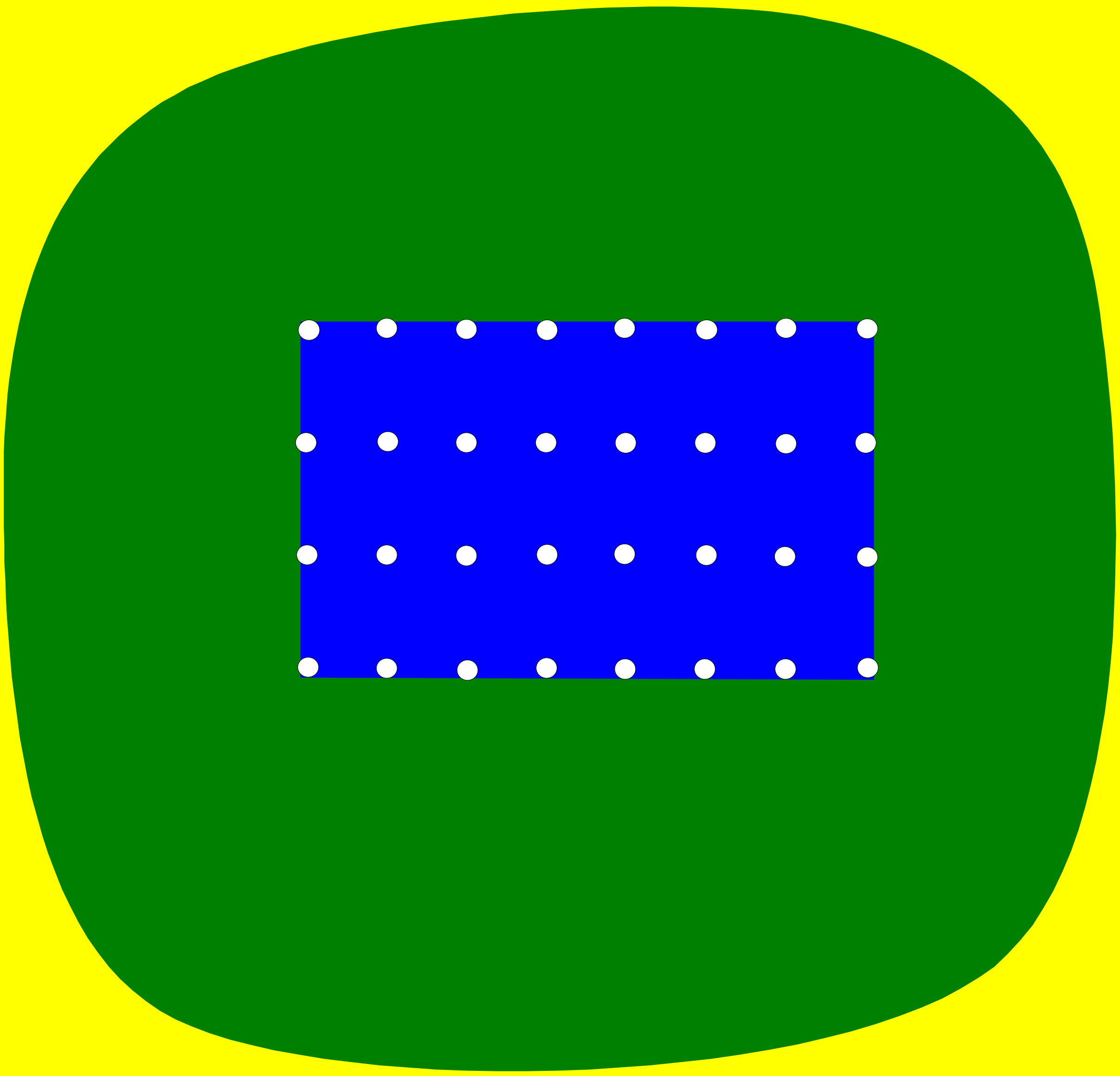

Equilibrium shape of the crystal surface

Вульфъ Г.В. О скорости роста и растворенія кристалловъ
Тр. Варшавск. общ. естествоисп. 1894–1895. Т. 6. вып. 9. С. 7–11.

Вульфъ Г.В. Къ вопросу о скоростяхъ роста и растворенія кристаллическихъ граней
Изв. Варшавск. ун-та, 1895 (кн. 7–9). 1896 (кн. 1,2). С. 1–120.

Wulff G. Zur Frage der Geschwindigkeit des Wachstums und der Auflösung der Krystallflächen
Zeitschrift für Krystallographie 1901. Vol. 34. P. 449–530.

Temperature influence on the equilibrium shape of the surface

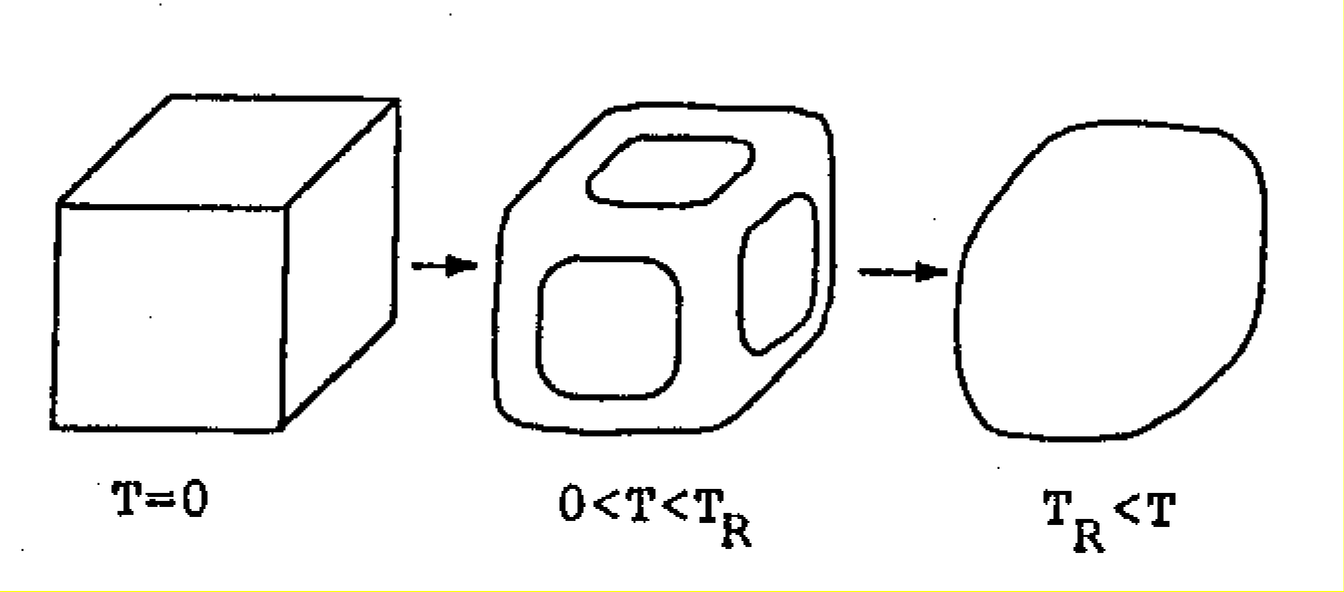

Temperature influence….

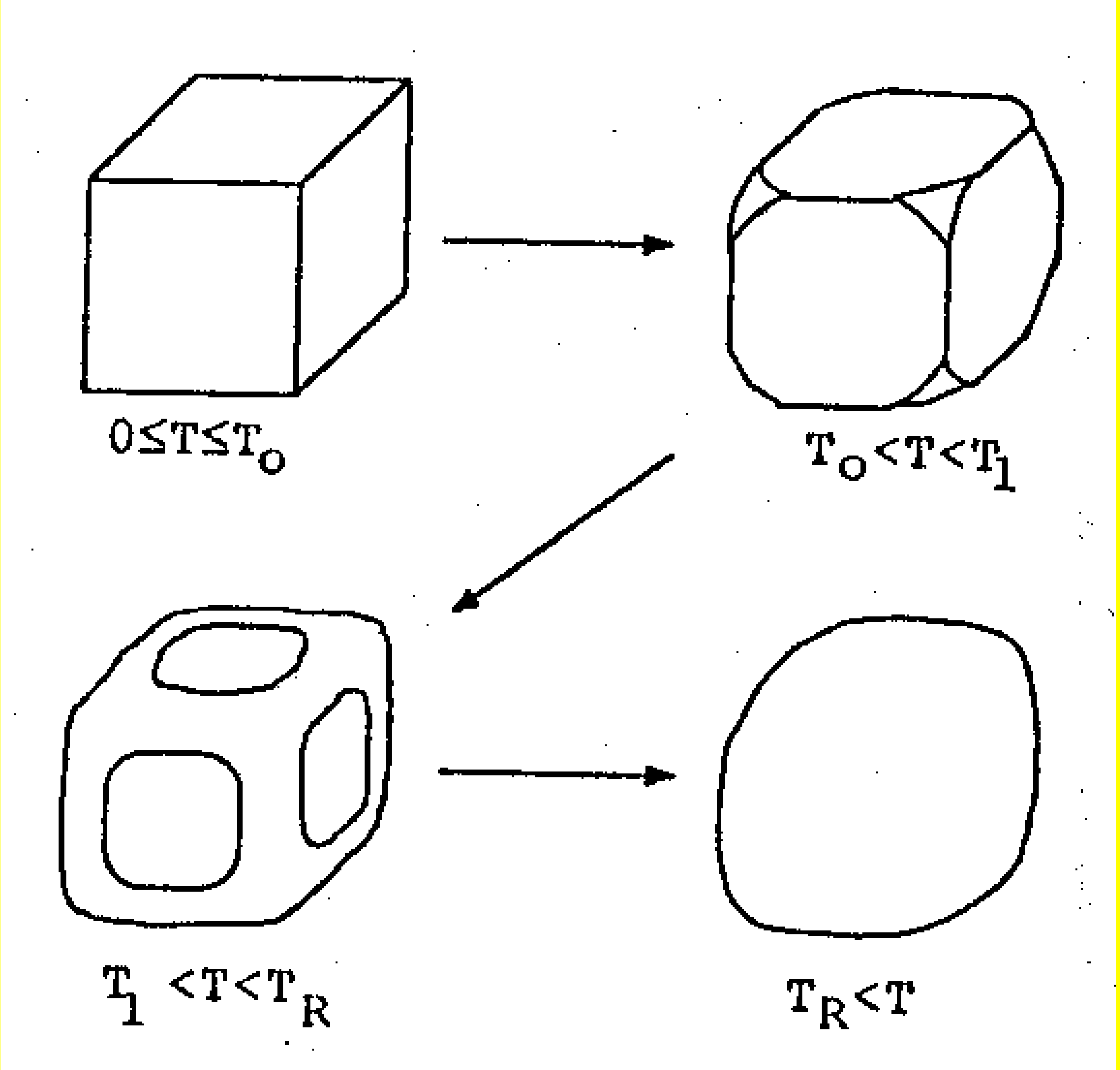

Temperature influence….

NaCl: (100) facets

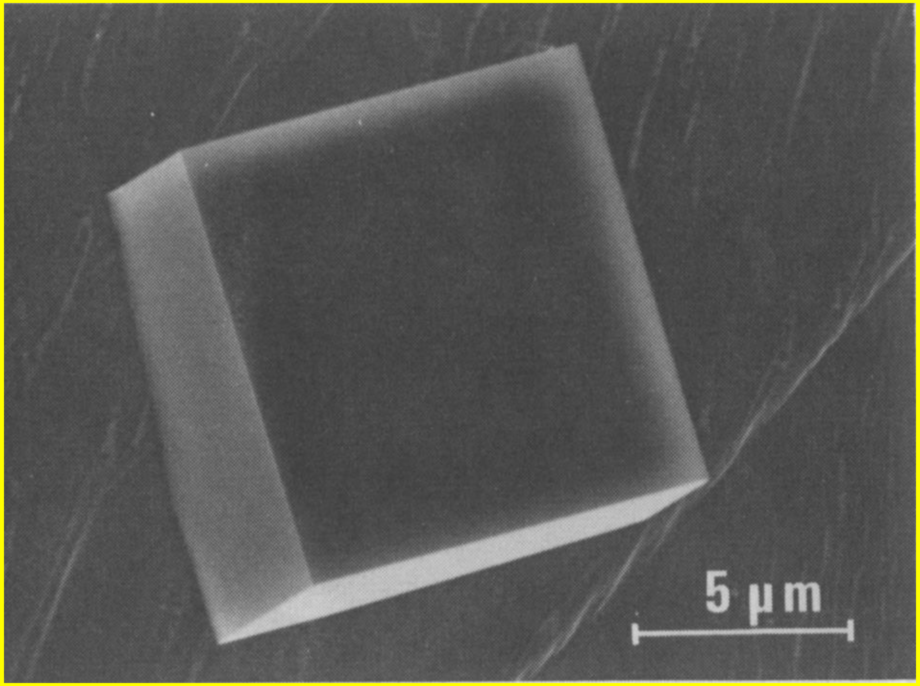

T = 620°C

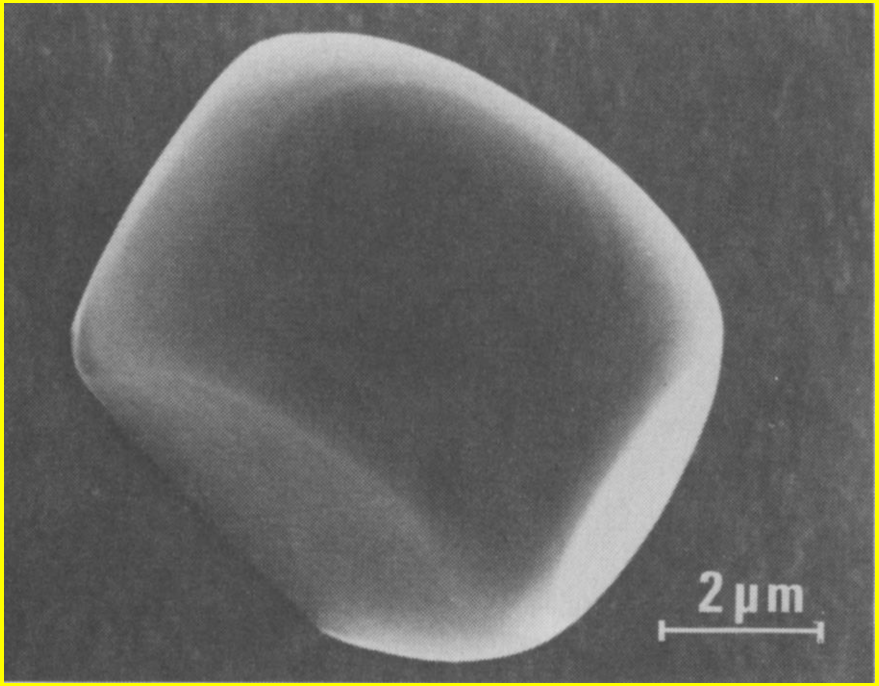

T = 710 °C

J.C. Heyraud, J.J. Mėtois, *J. Crystal Growth* 84 (1987) 503

Temperature influence on the equilibrium shape of the surface

NaCl: (100) facets

***T* = 710 °C**

J.C. Heyraud, J.J. Mėtois,
J. Crystal Growth 84 (1987) 503

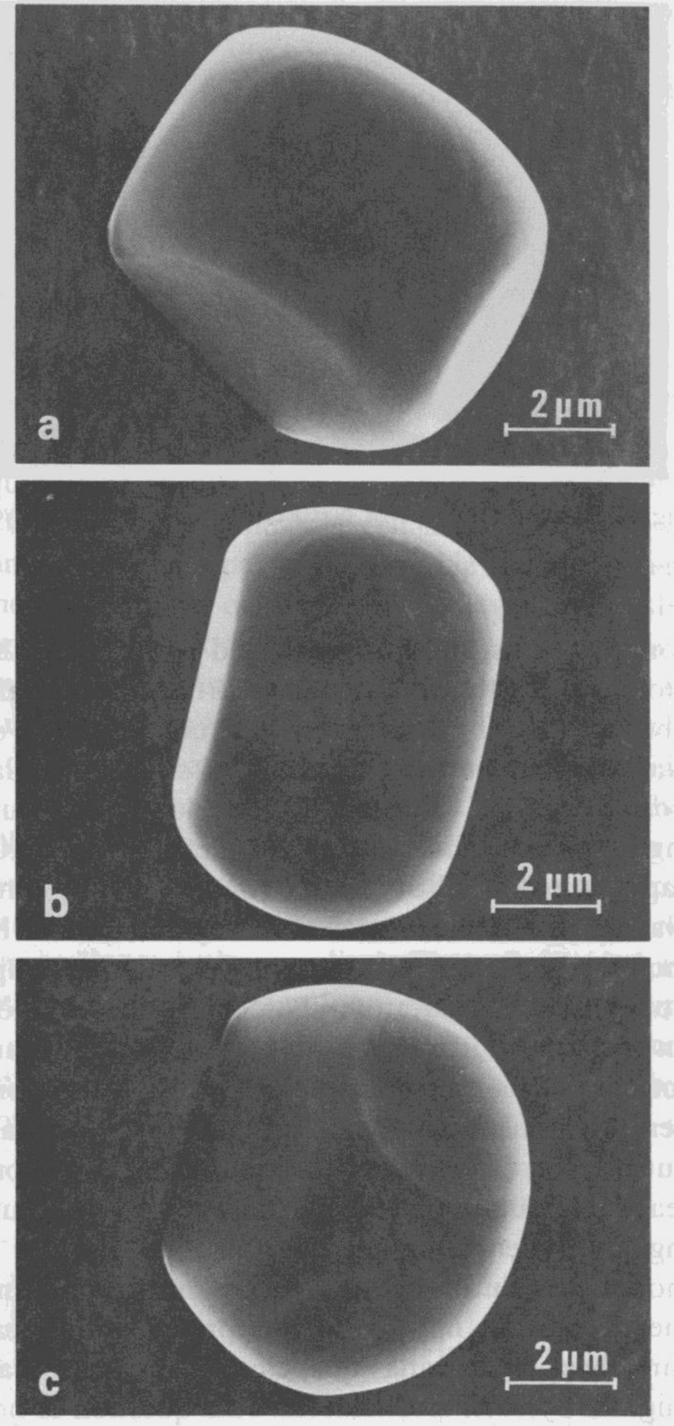

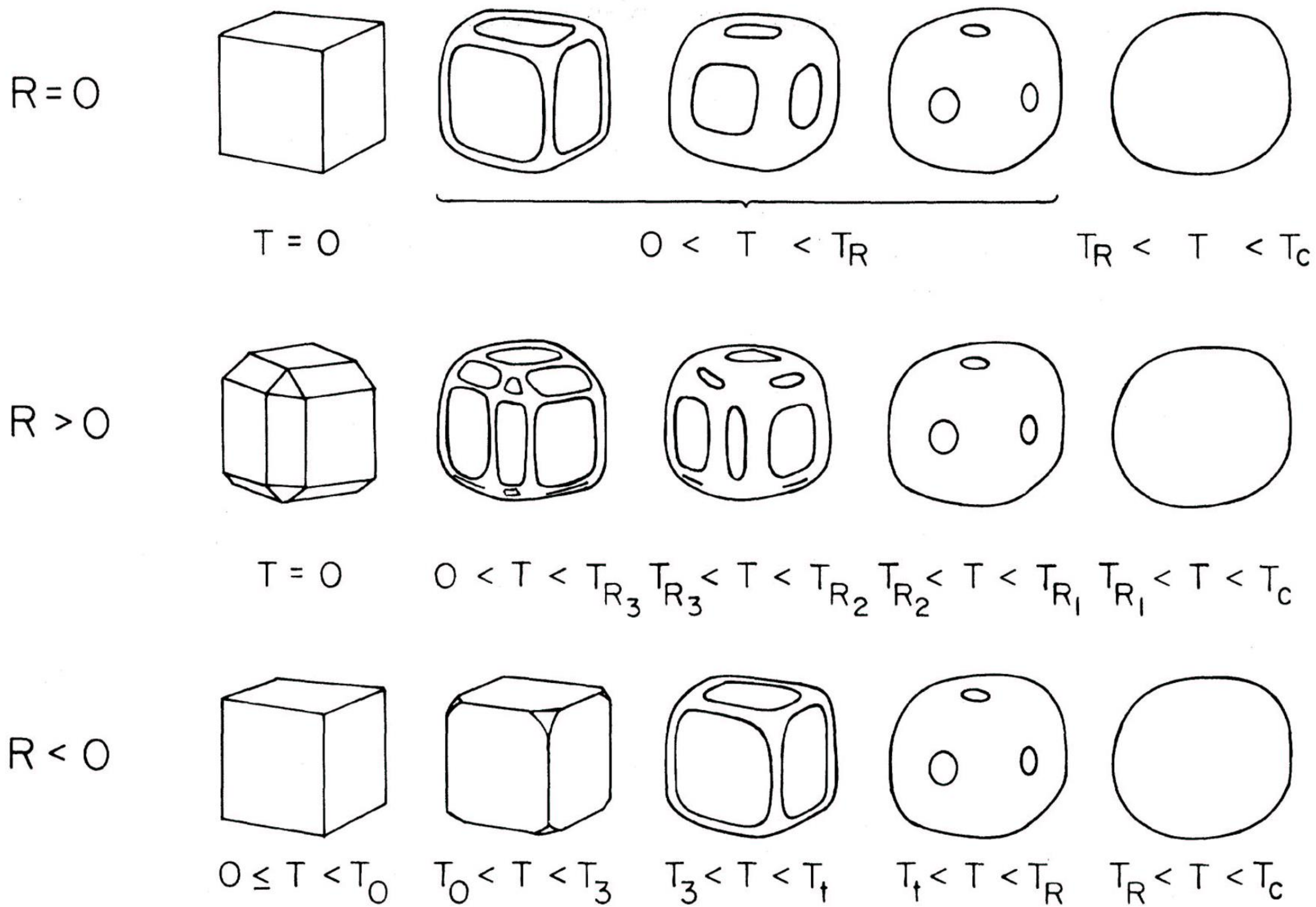

Lattice gas model with NN and NNN interactions

C. Rottman, R. Wortis, *Phys. Rev. B* 29 (1984) 328

Temperature influence….

He^4: third roughening transition

T = 0.4 K

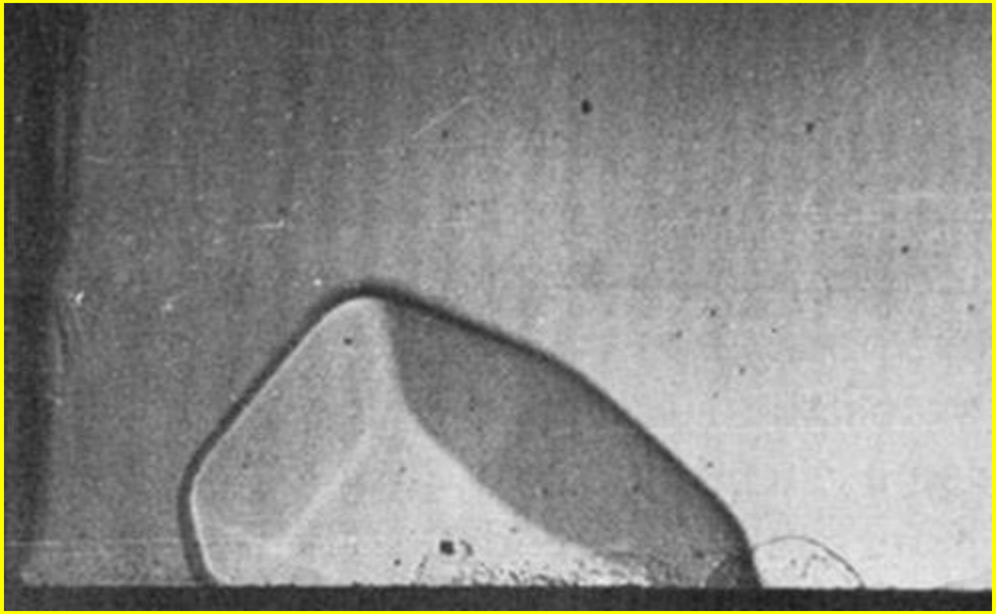

T = 0.35 K

R.E.Wolf, S. Balibar, *Phys. Rev. Lett.* 51 (1983) 1366

Temperature influence….

He^3: (100), (110) and (112) facets

***T* = 0.022 K**

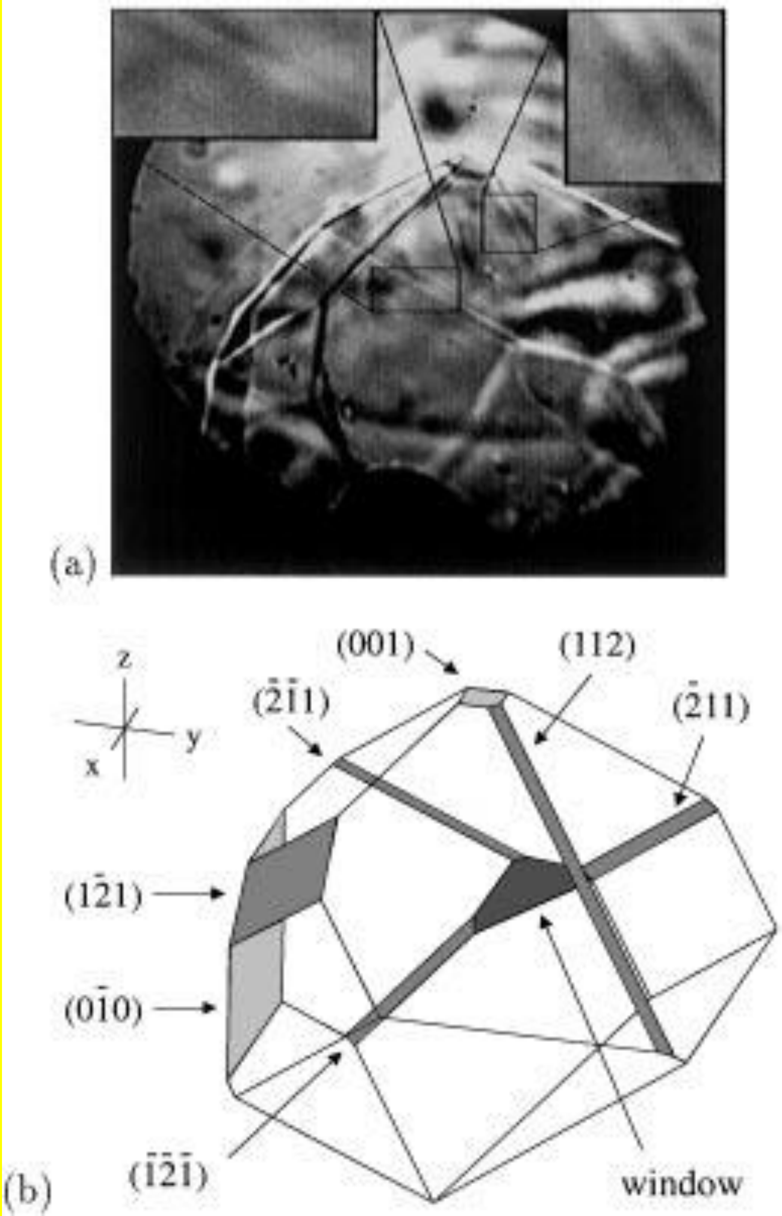

R. Wagner, S.C. Steel, O.A. Andreeva, R. Jochemsen, G. Frossati. *Phys. Rev. Lett.* 76 (1996) 263

Au single crystals at 0.95 T_m

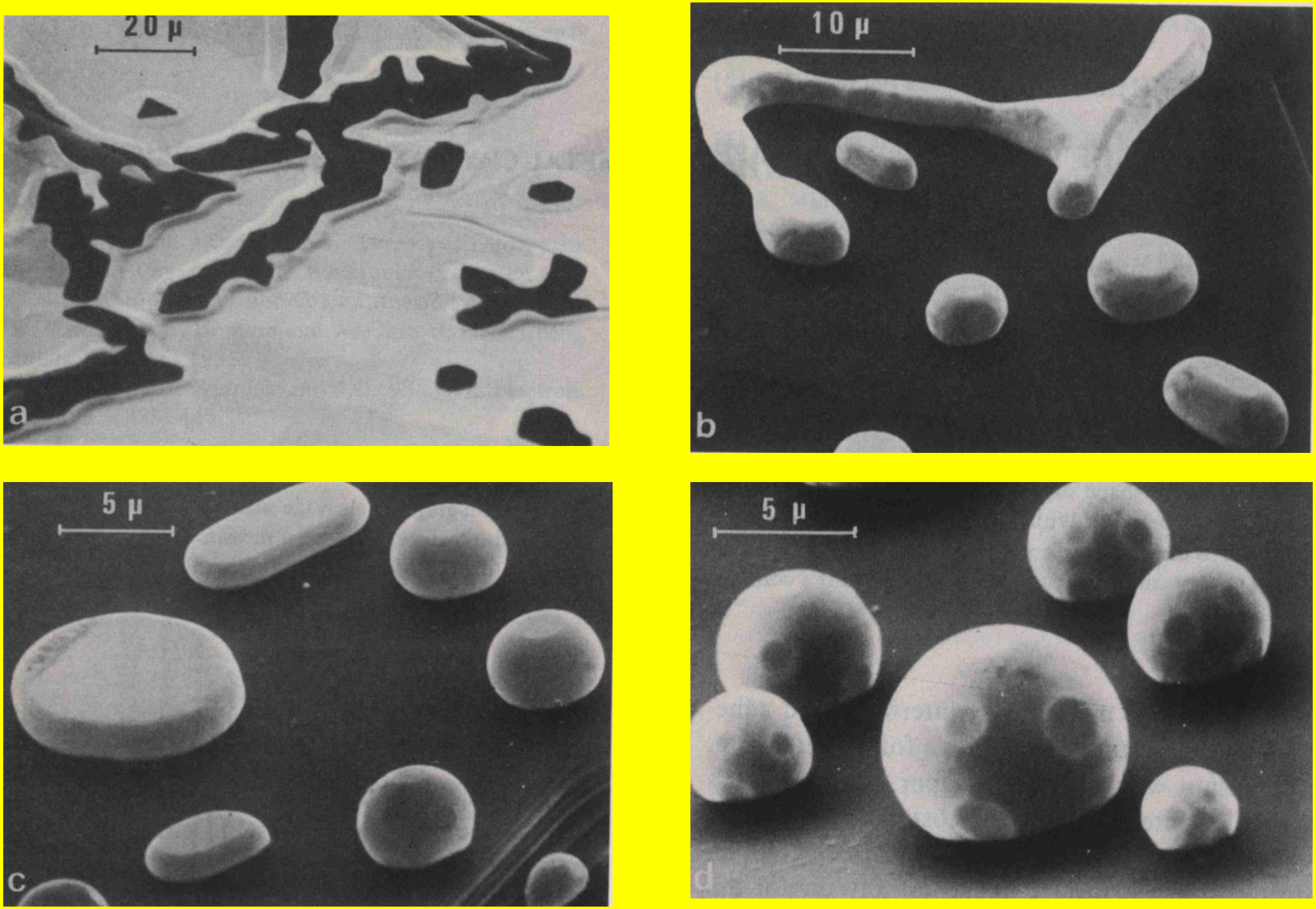

J.C. Heyraud, J.J. Metois: J. Cryst. Growth 50, 571 (1980)

Au single crystal at 0.95 T_m. (111) and (100) facets

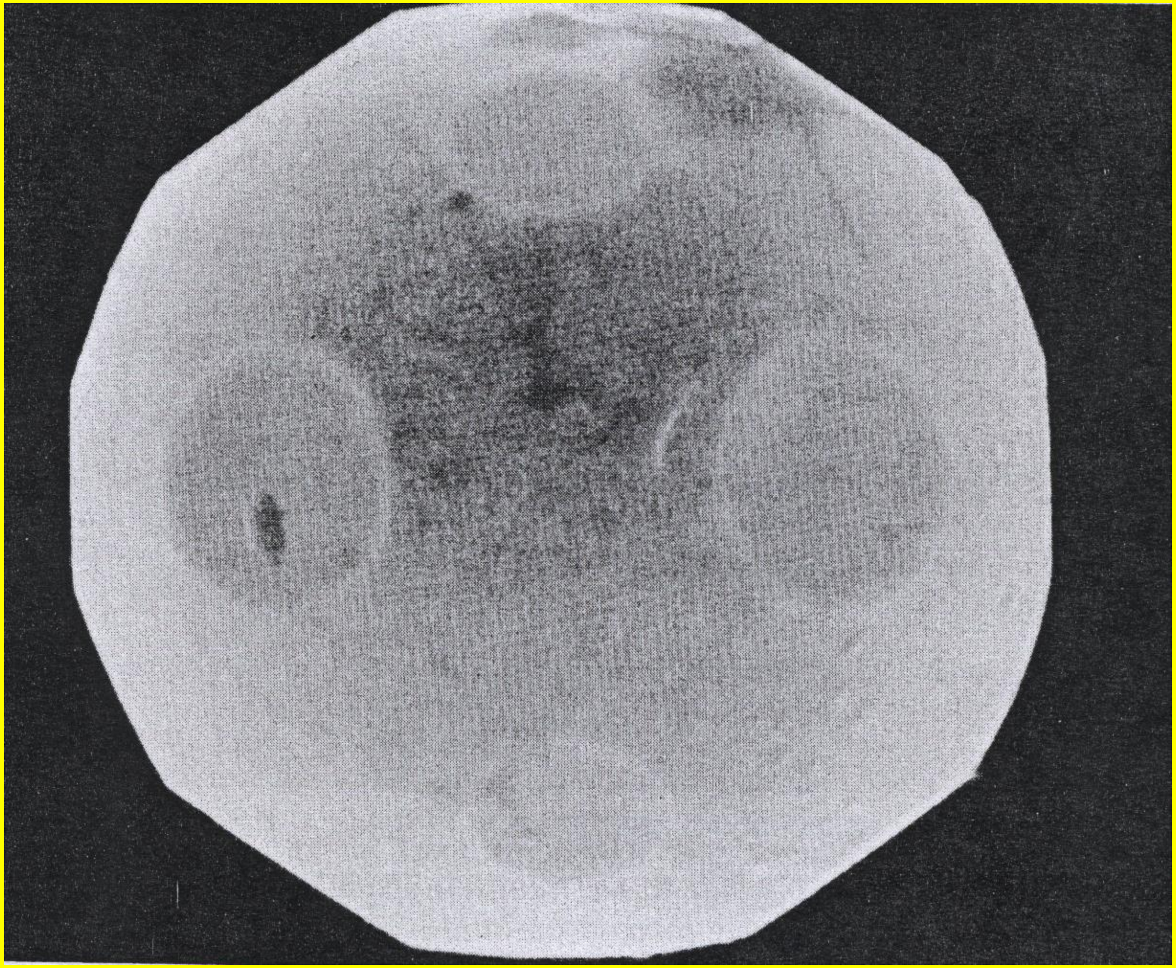

J.C. Heyraud, J.J. Metois: J. Cryst. Growth 50, 571 (1980)

Au single crystal at 0.95 T_m. (111) and (100) facets

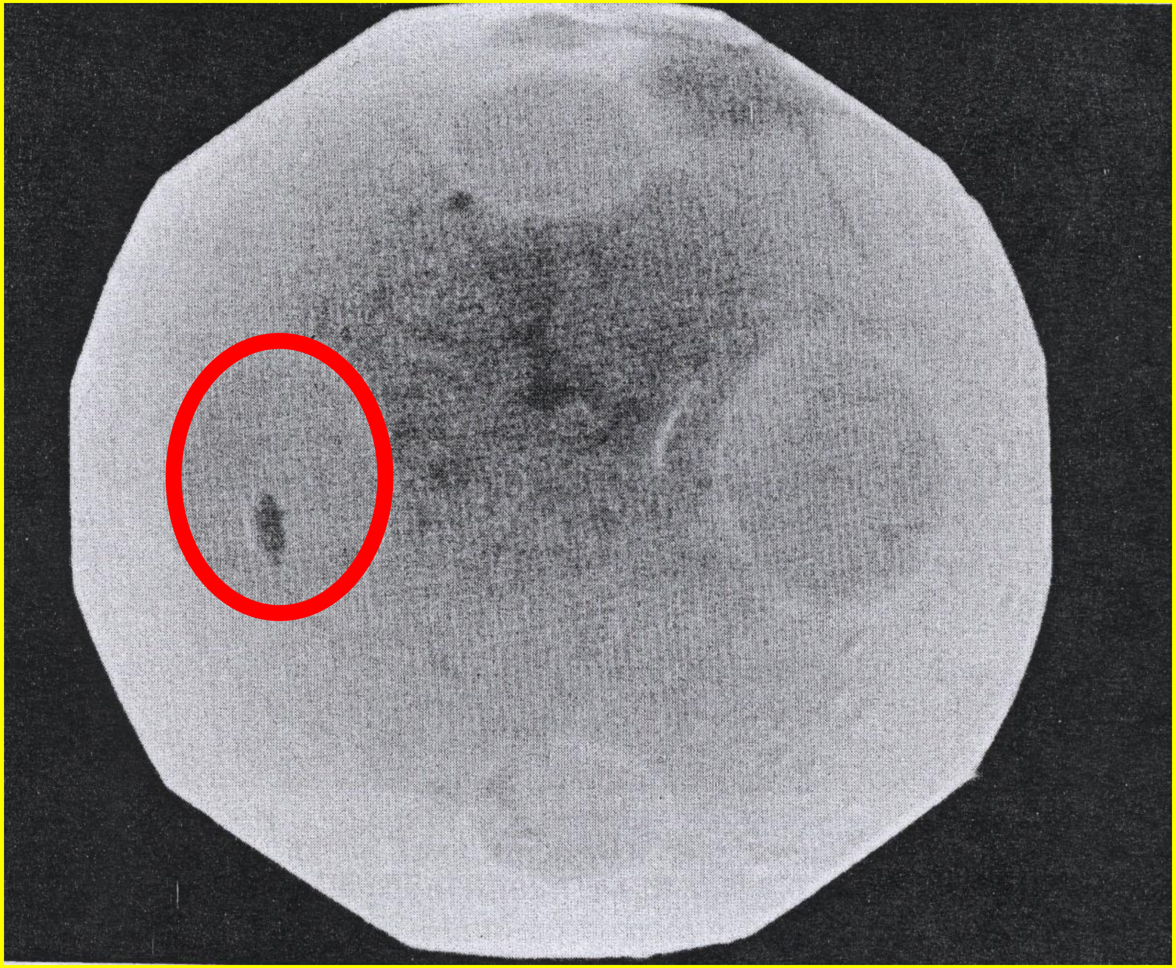

J.C. Heyraud, J.J. Metois: J. Cryst. Growth 50, 571 (1980)

Au single crystal at 0.95 T_m: (111) and (100) facets

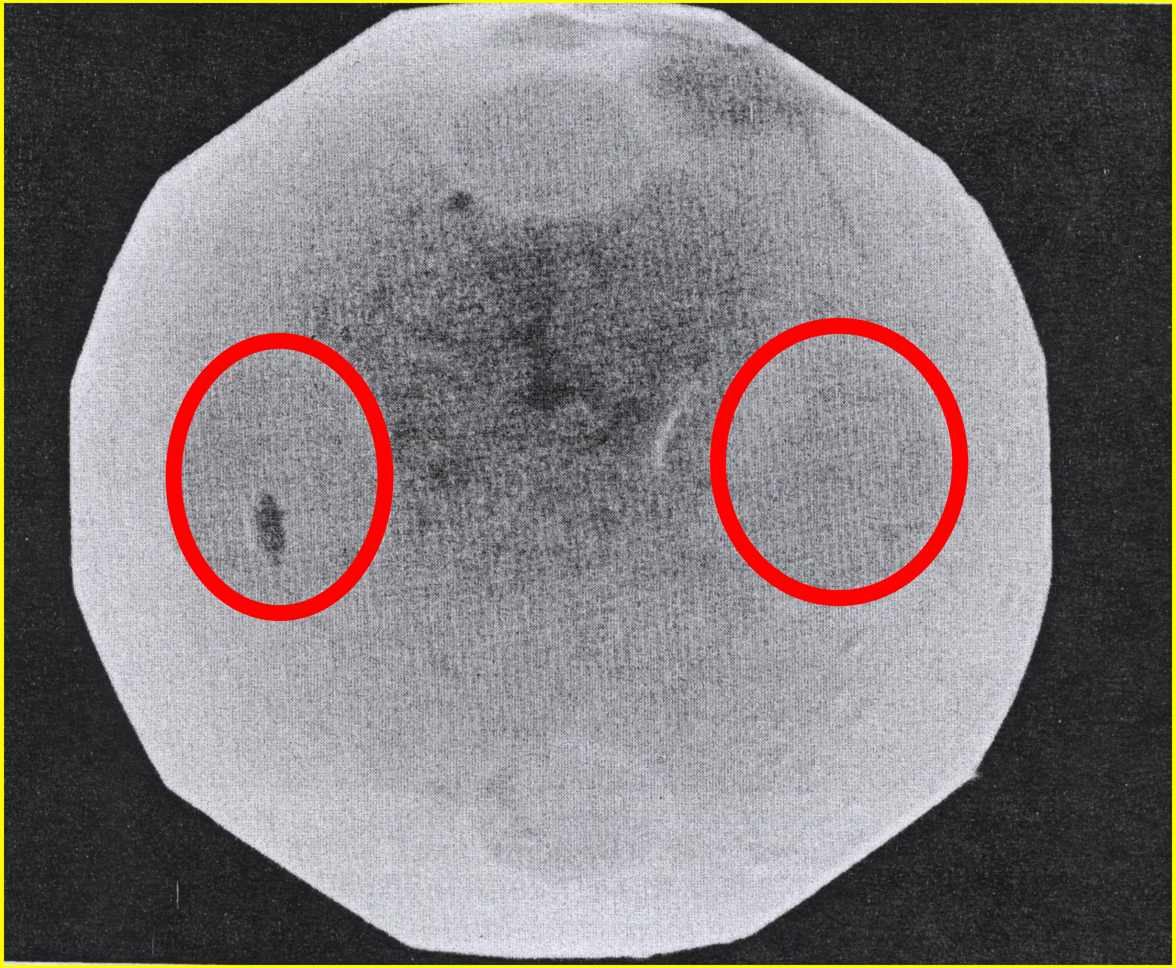

J.C. Heyraud, J.J. Metois: J. Cryst. Growth 50, 571 (1980)

Au single crystal at 0.95 T_m. (111) and (100) facets

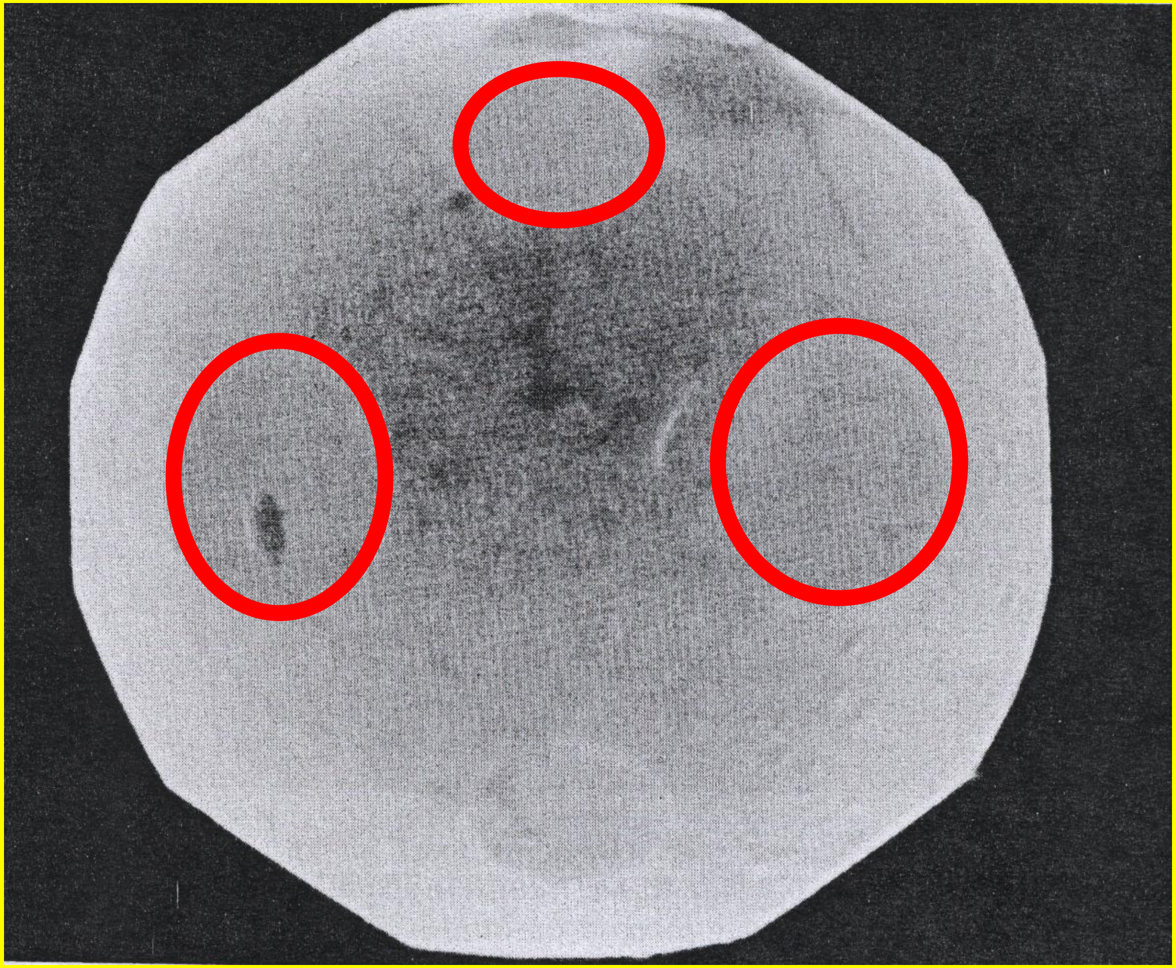

J.C. Heyraud, J.J. Metois: J. Cryst. Growth 50, 571 (1980)

Au single crystal at 0.95 T_m. (111) and (100) facets

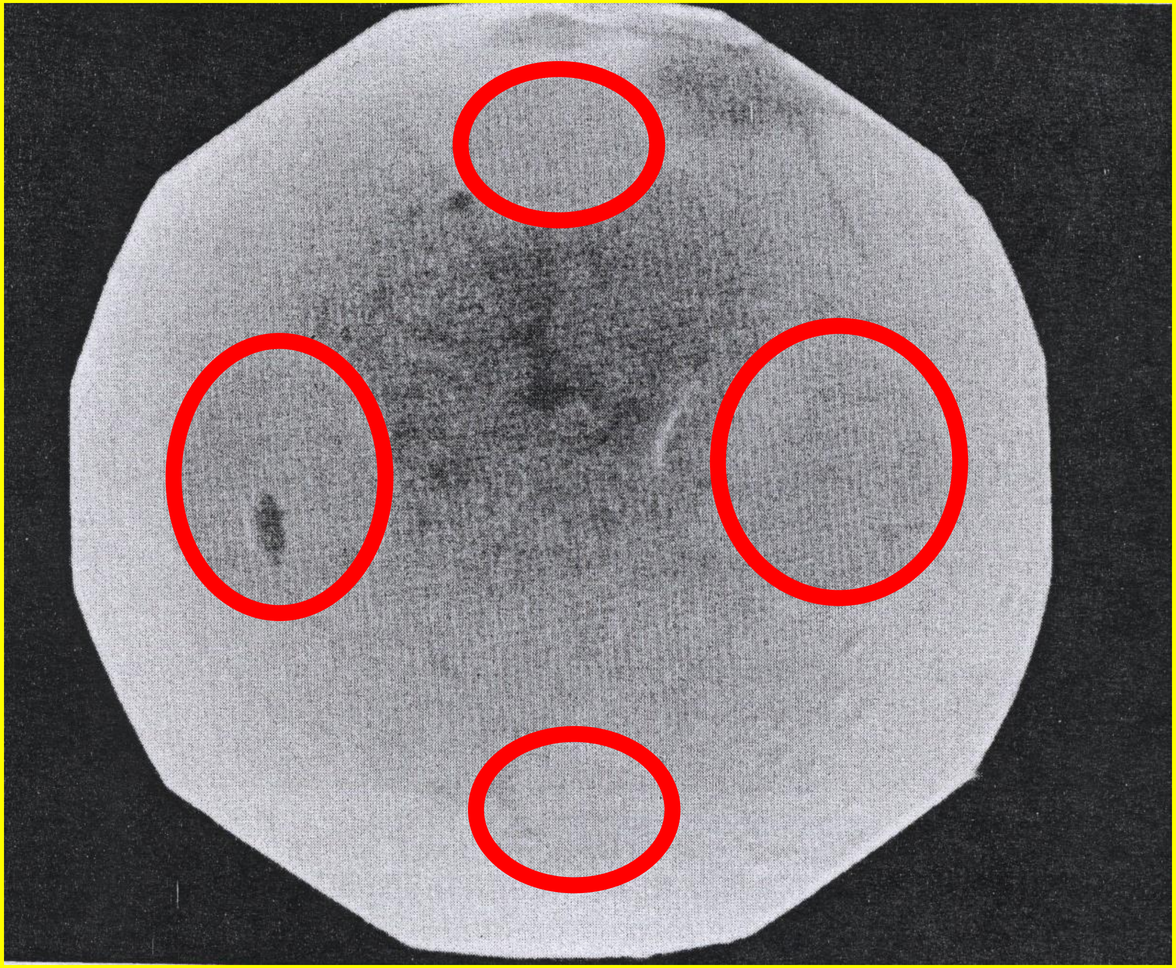

J.C. Heyraud, J.J. Metois: J. Cryst. Growth 50, 571 (1980)

Au single crystal at 0.95 T_m. Shape discontinuities

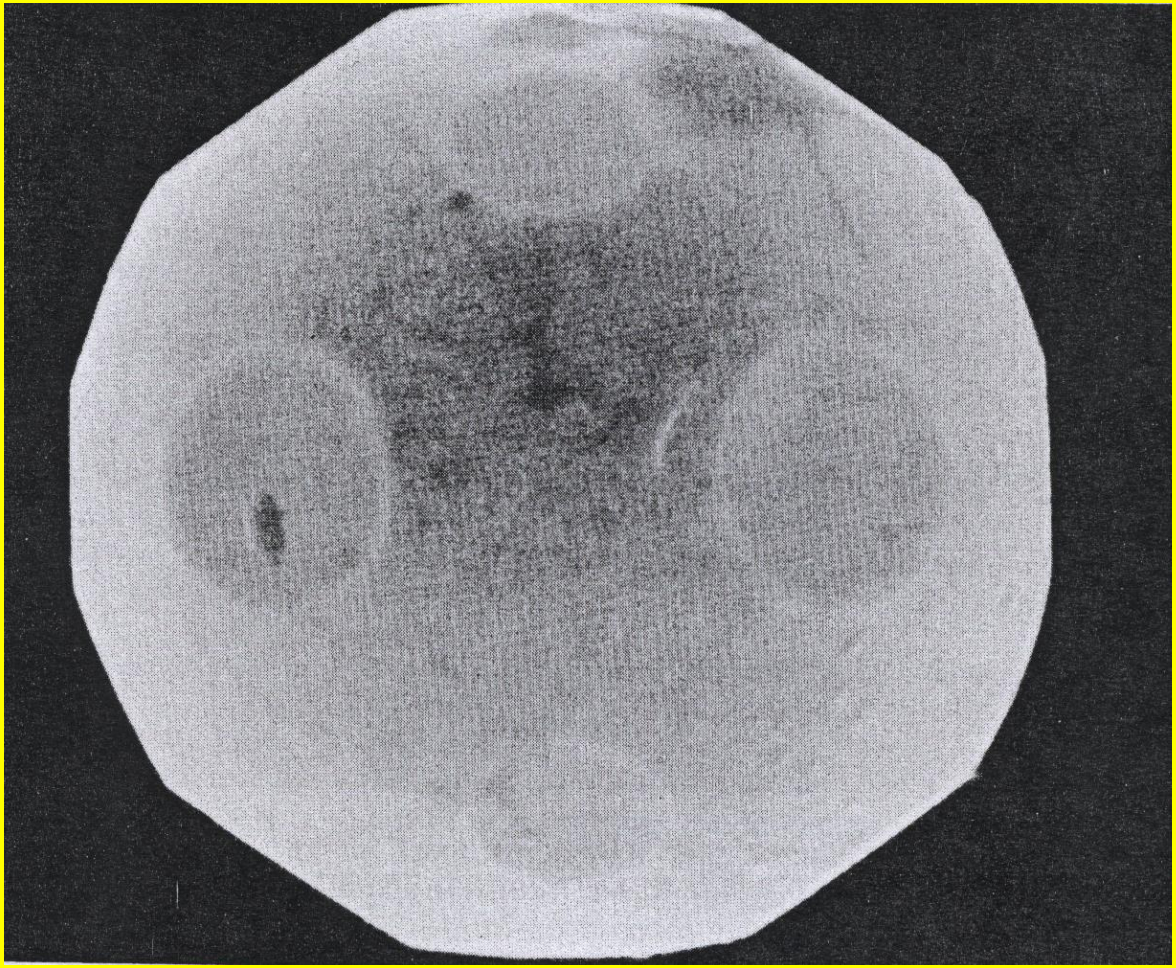

J.C. Heyraud, J.J. Metois: J. Cryst. Growth 50, 571 (1980)

Au single crystal at 0.95 T_m. Shape discontinuities

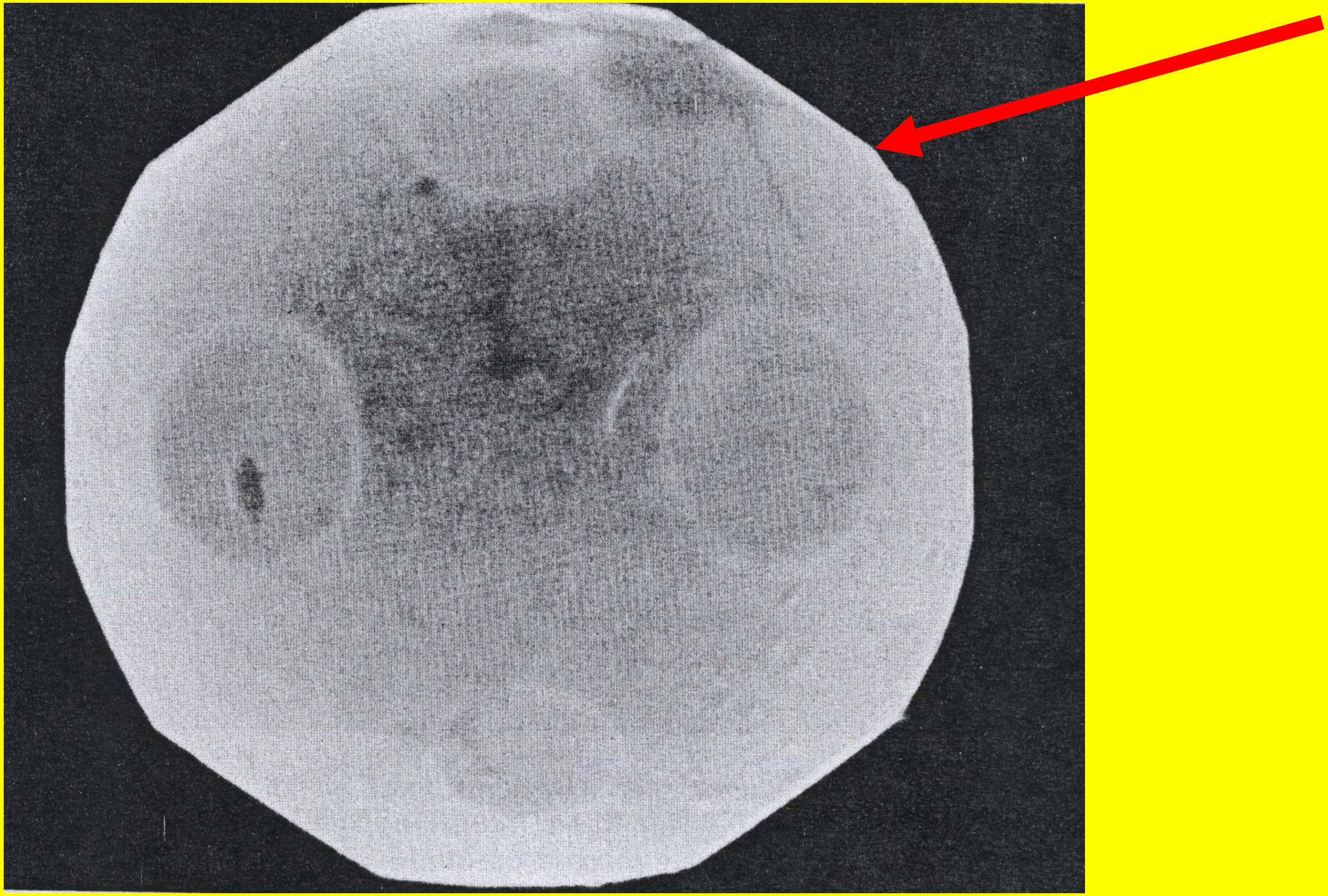

J.C. Heyraud, J.J. Metois: J. Cryst. Growth 50, 571 (1980)

Au single crystal at 0.95 T_m. Shape discontinuities

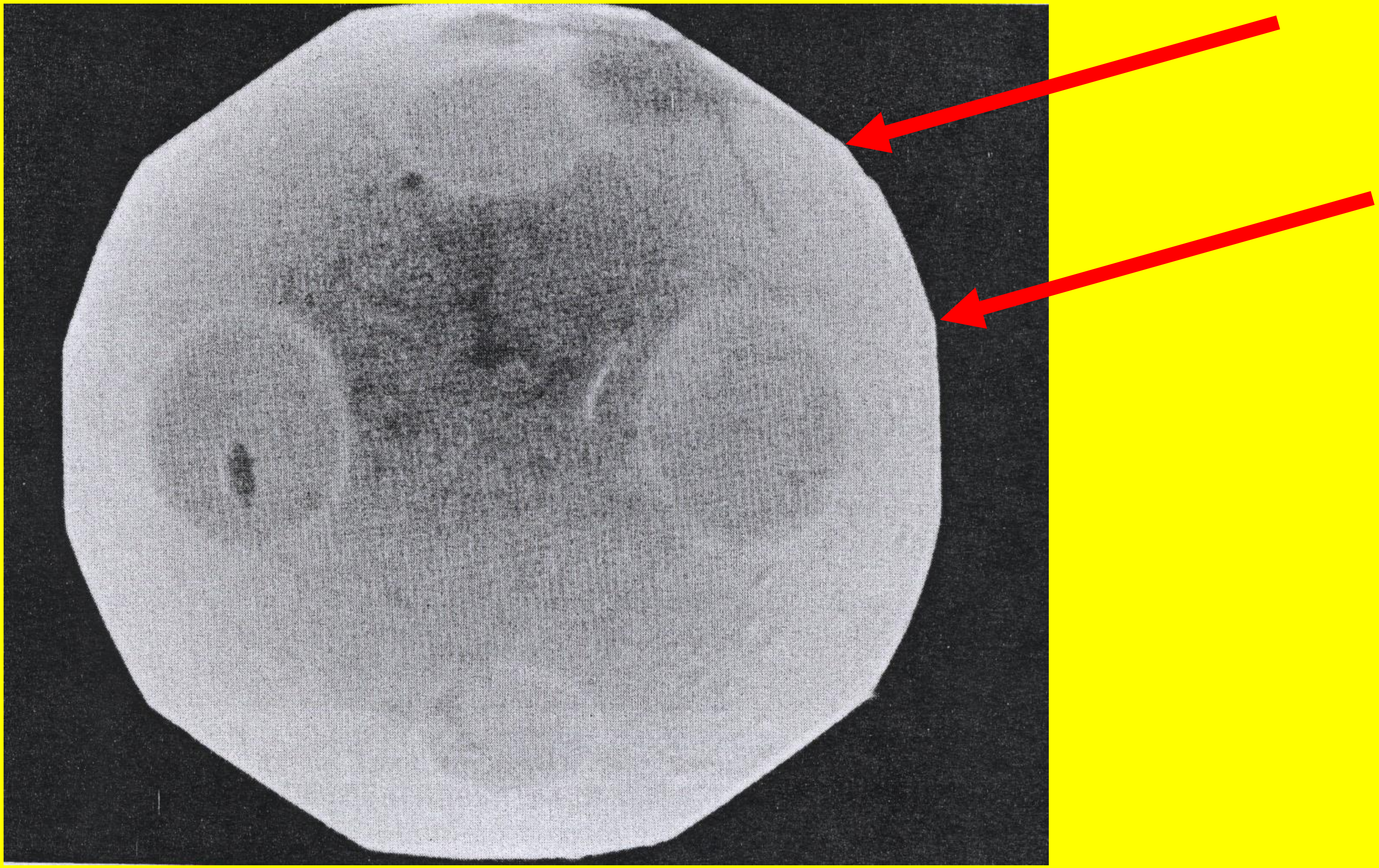

J.C. Heyraud, J.J. Metois: J. Cryst. Growth 50, 571 (1980)

Pb single crystals at 0.97 T_m. No shape discontinuities

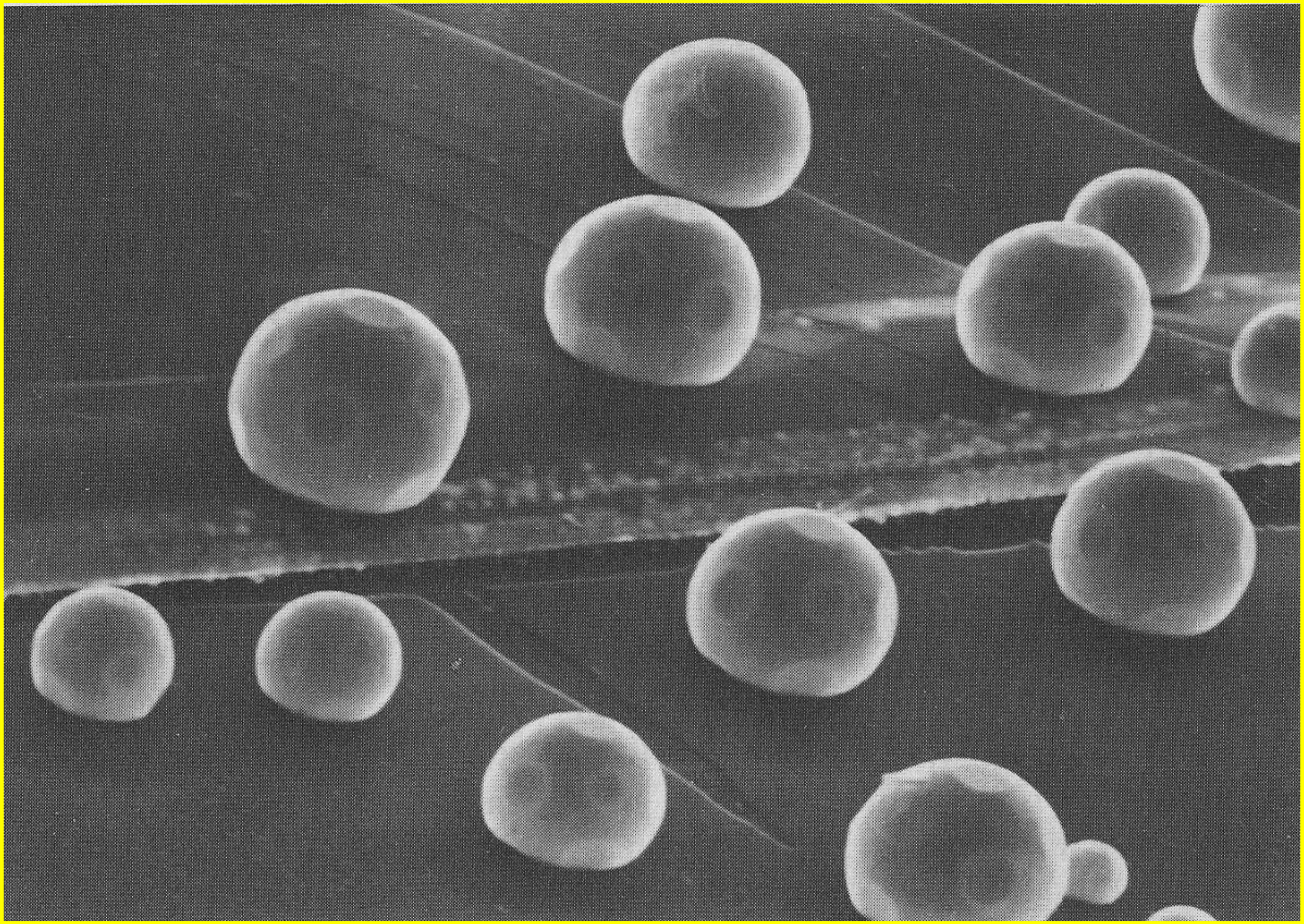

J.C. Heyraud, J.J. Metois: Surf. Sci, 128, 334 (1983)

How the Pb facets grow...

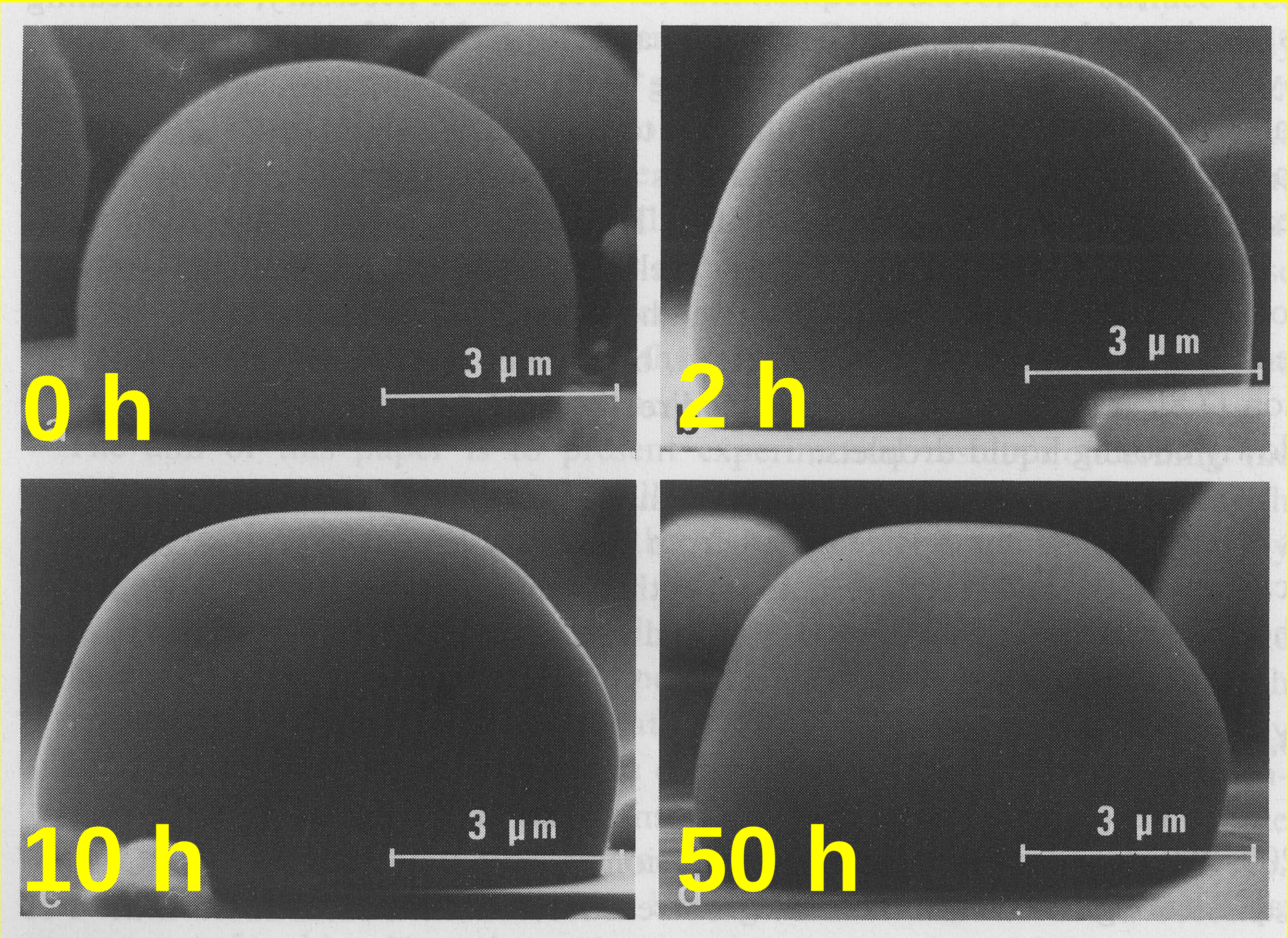

J.C. Heyraud, J.J. Metois: Surf. Sci, 128, 334 (1983)

Pb single crystal at 0.97 T_m.
No shape discontinuities

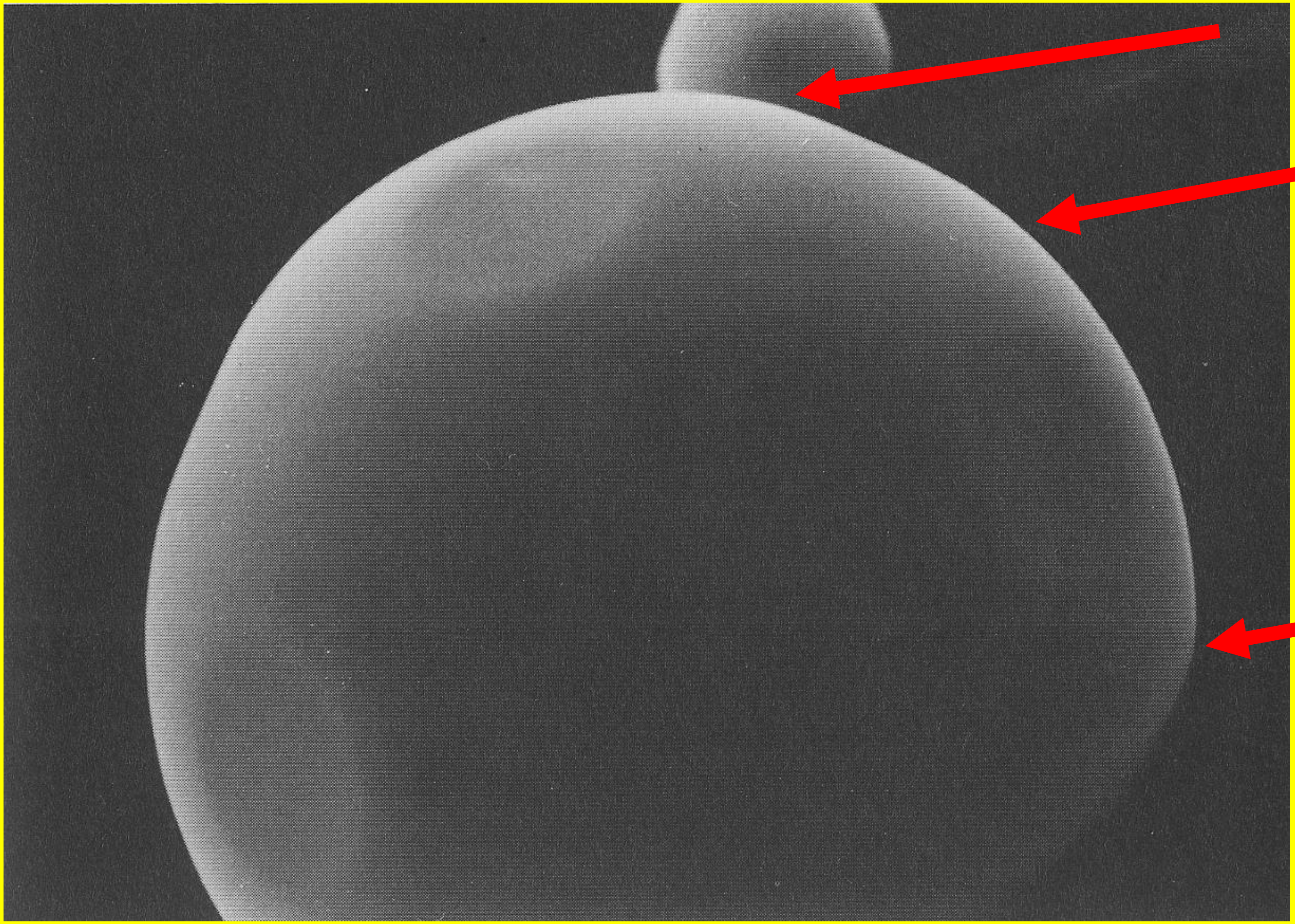

J.C. Heyraud, J.J. Metois: Surf. Sci, 128, 334 (1983)

Surfaces of pure metals.
Experiment:

- no more than two crystallographically different facets

- facets are isolated and separated by portions of rough surfaces

Roughening of Pb surfaces: P-T behaviour

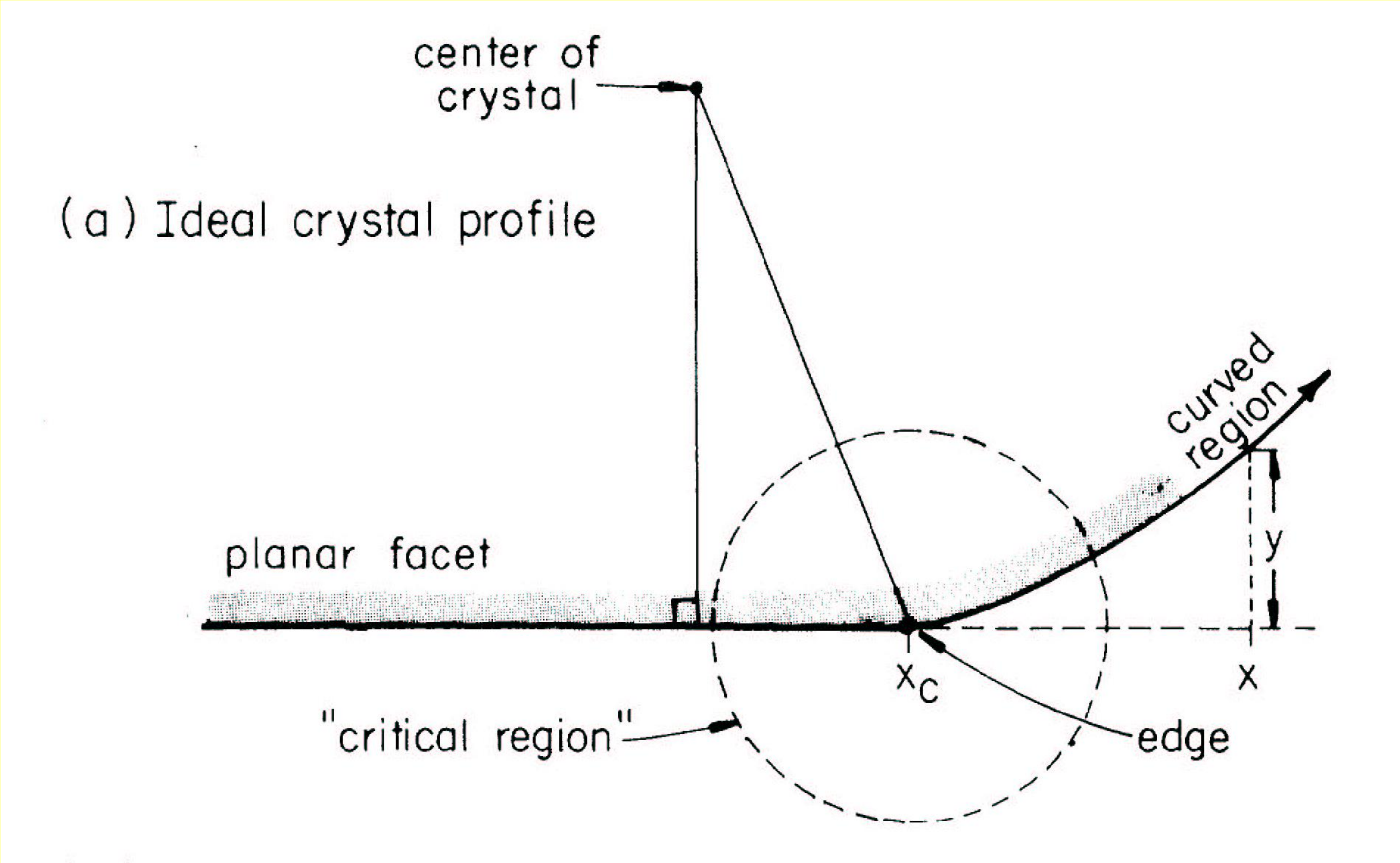

C. Rottman, R. Wortis, J.C. Heyraud, J.J. Mėtois. *PRL* 52 (1984) 1009

Rounding near cristal facet

$$y = A(x - x_c)^{\theta} \text{ + higher order terms}$$

Andreev theory (mean-field approximation):

$\theta = 2$

Pokrovsky-Talapov theory (including fluctuations):

$\theta = 3/2$

A.F. Andreev. *Zh.Eksp.Teor.Fiz.* 79 (1981) 2042

V.L. Pokrovsky, A.L. Talapov. *PRL* 42 (1979) 65 and *Zh.Eksp.Teor.Fiz.* 78 (1980) 269

Roughening of Pb surfaces: P-T behaviour

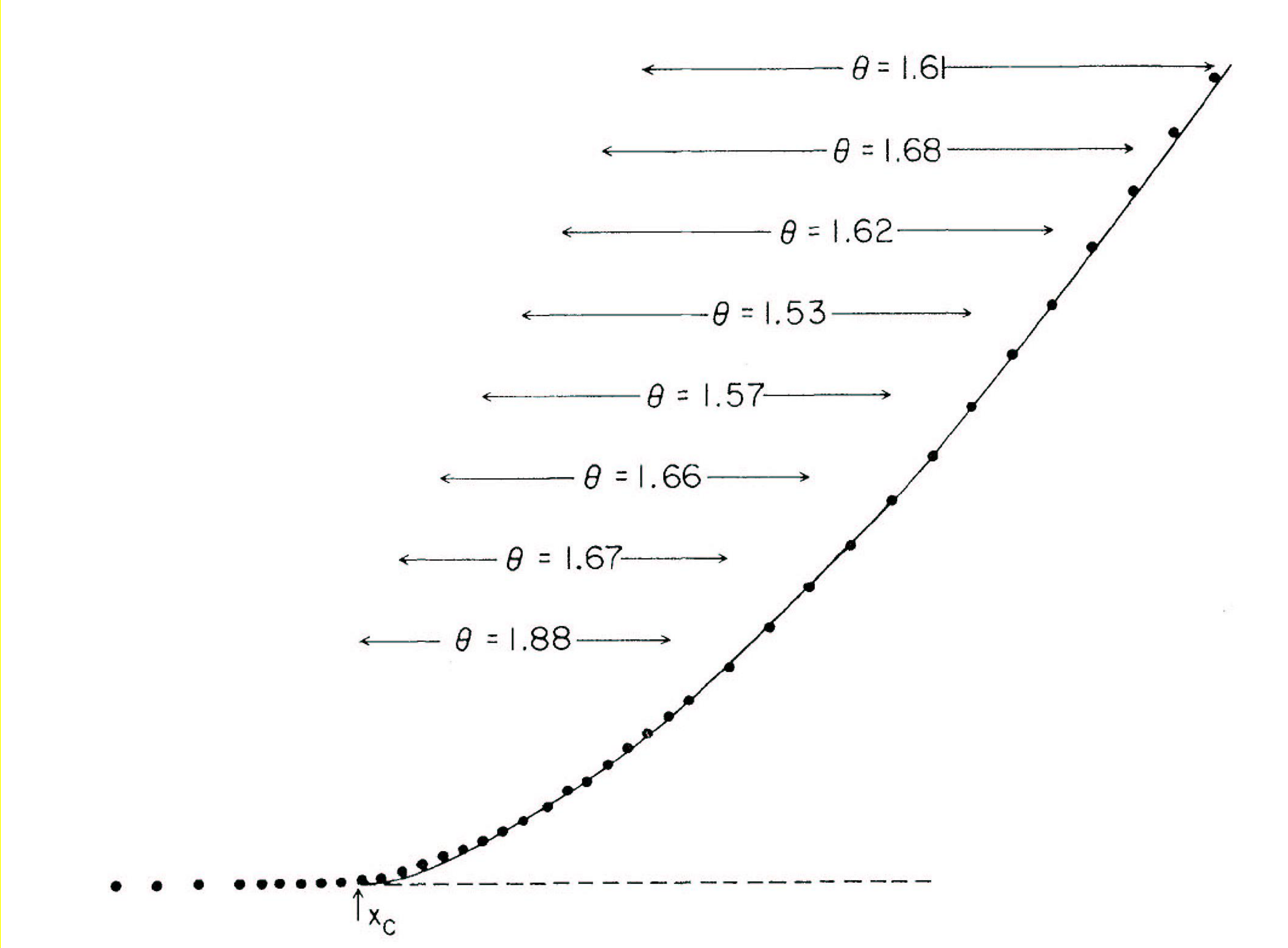

C. Rottman, R. Wortis, J.C. Heyraud, J.J. Mėtois. *PRL* 52 (1984) 1009

Equilibrium crystal shapes in the BCSOS model with enhanced interaction range

(a) ECS in the exactly soluble square lattice BCSOS model with stochastic FRE point.

(b) ECS with a first-order line extending into the rough area.

(c) ECS with first-order facet-to-round boundaries and PTE points.

(d) ECS with a spontaneous tilted rough phase, i.e., with a **<u>first order ridge inside the rough phase</u>**.

D. Davidson, M. den Nijs. *PRL* 84 (2000) 326

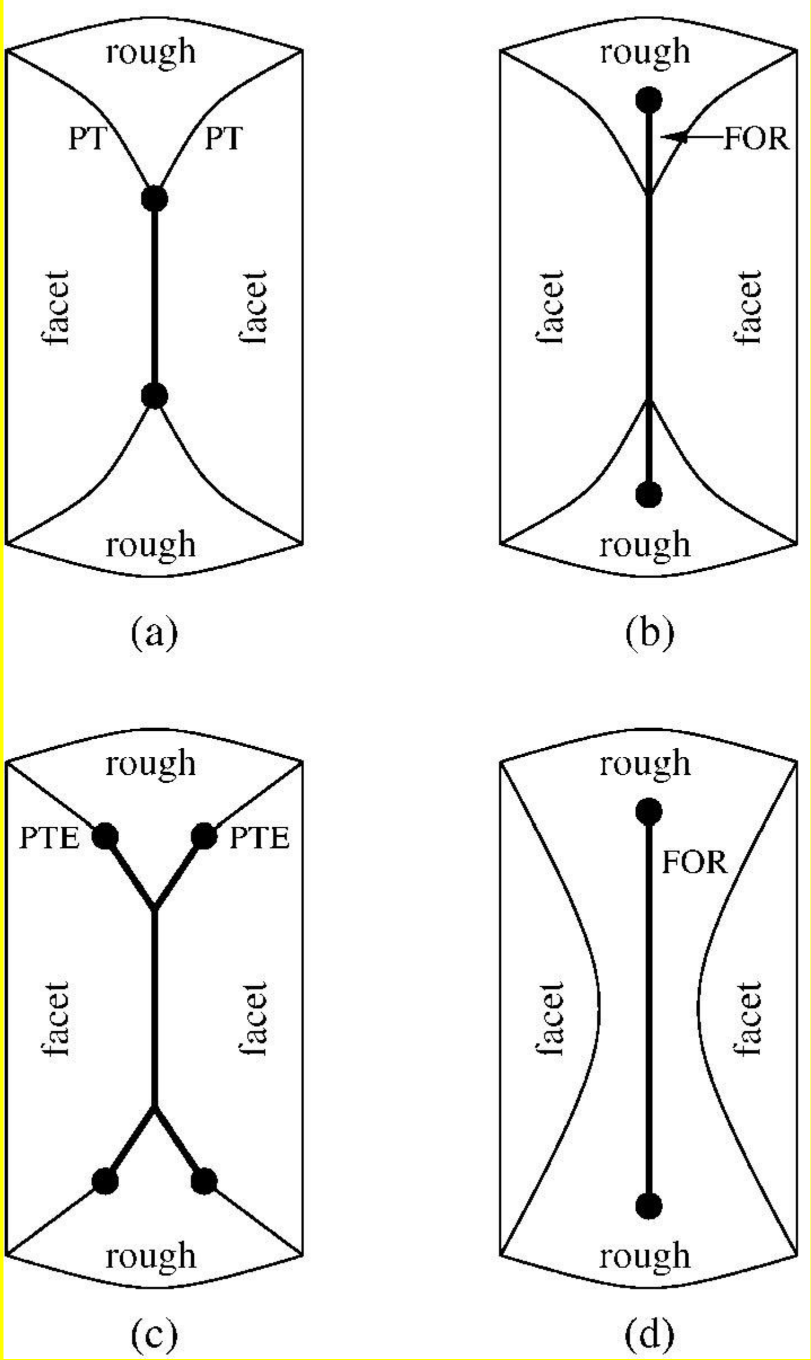

Фазовые превращения:

-- на внутренних границах раздела (огранение-потеря огранки)

Low angle grain boundary:

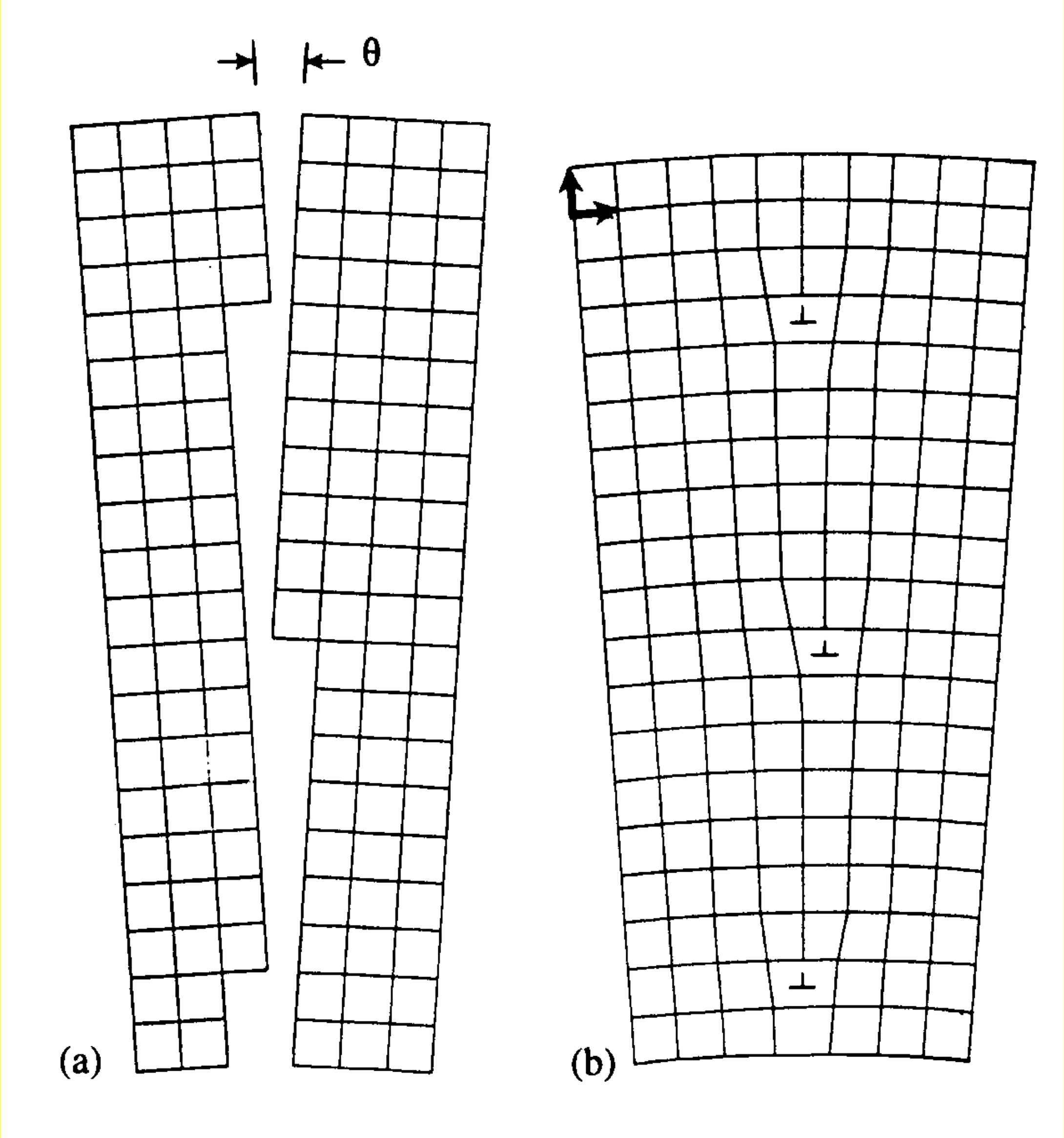

Symmetric tilt boundary, individual lattice dislocations

Reed (1953)

Краевая дислокация (edge dislocation)

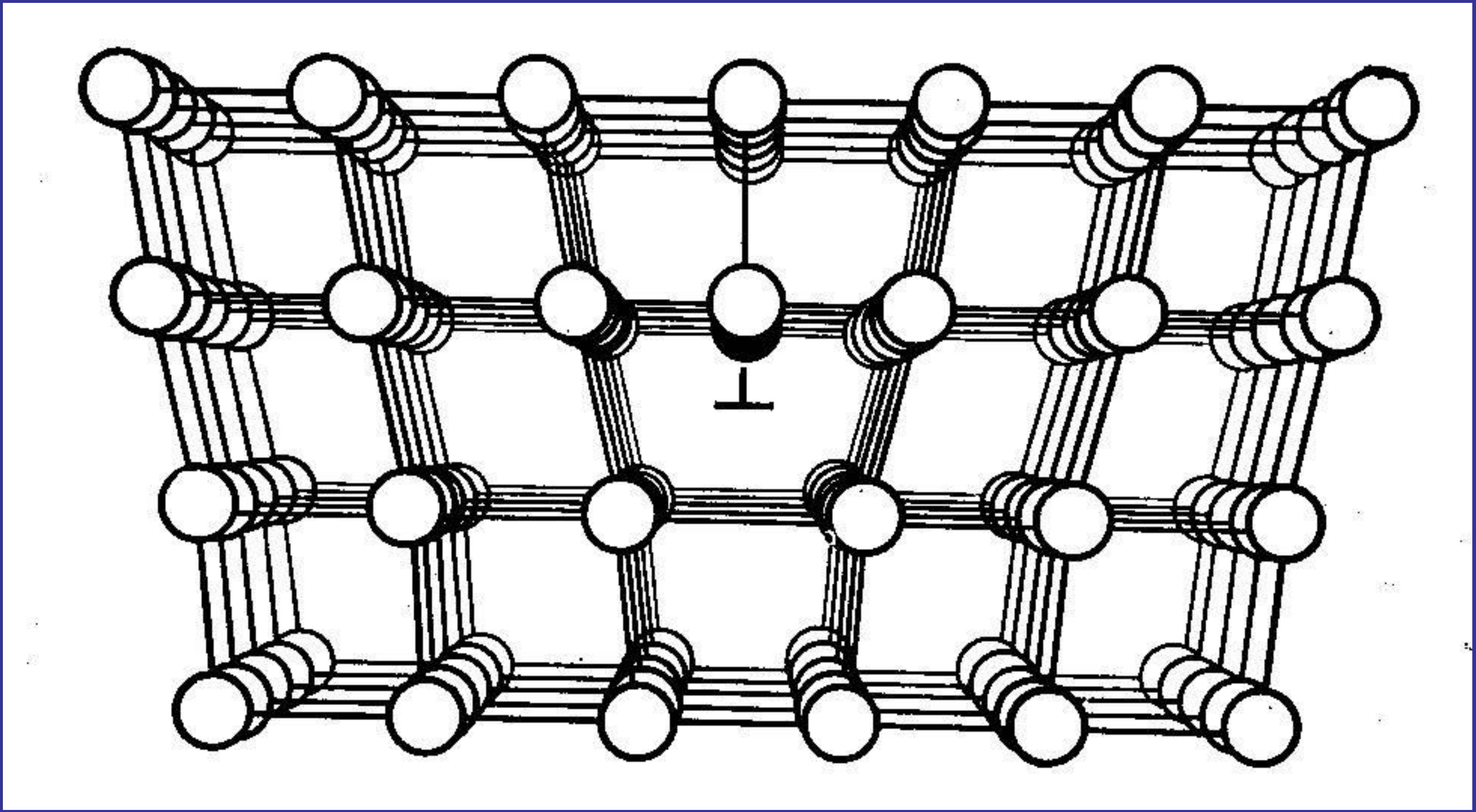

Energy, σ of a low angle grain boundary in dependence on misorientation θ

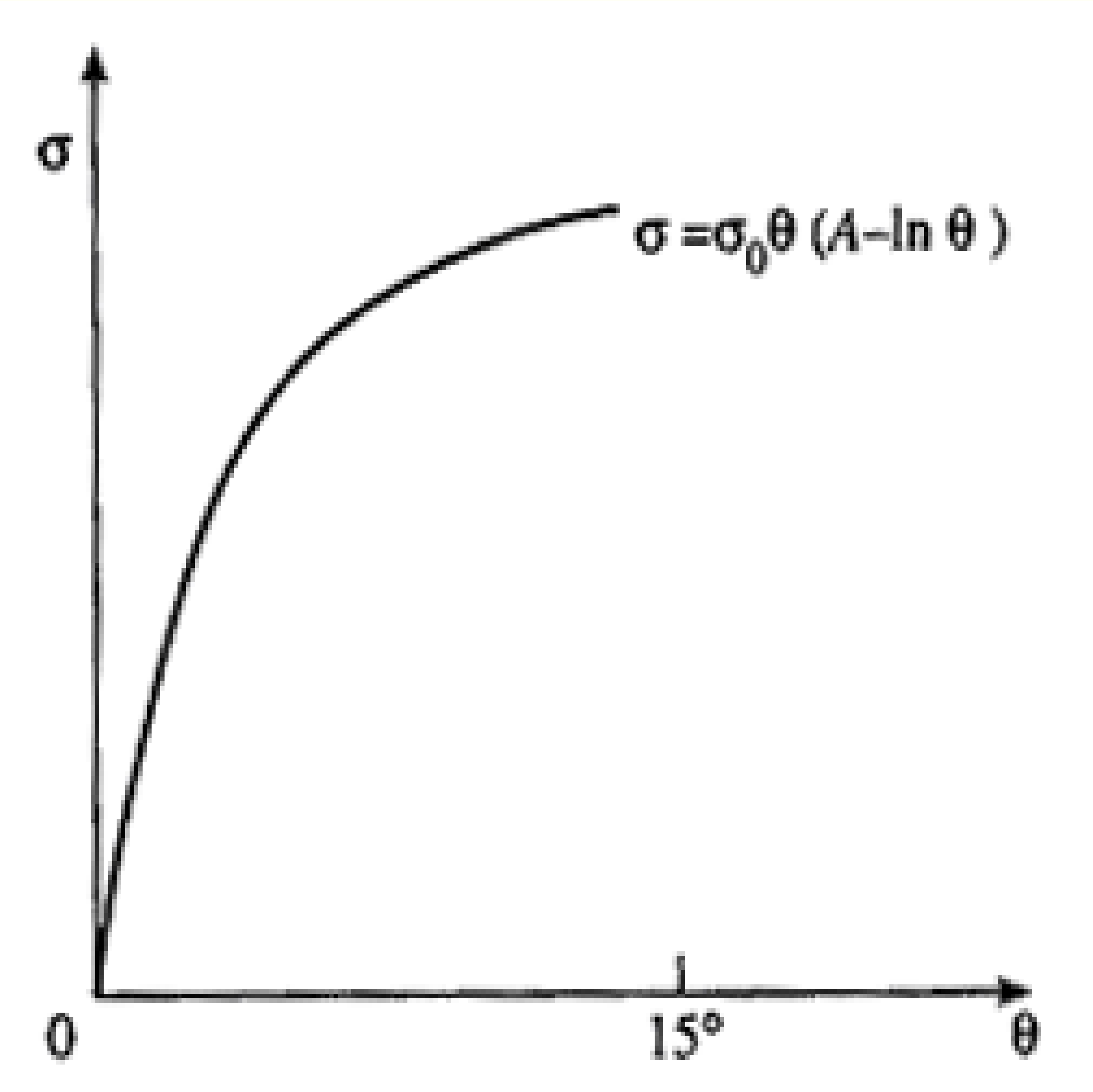

Reed (1953)

High angle grain boundary

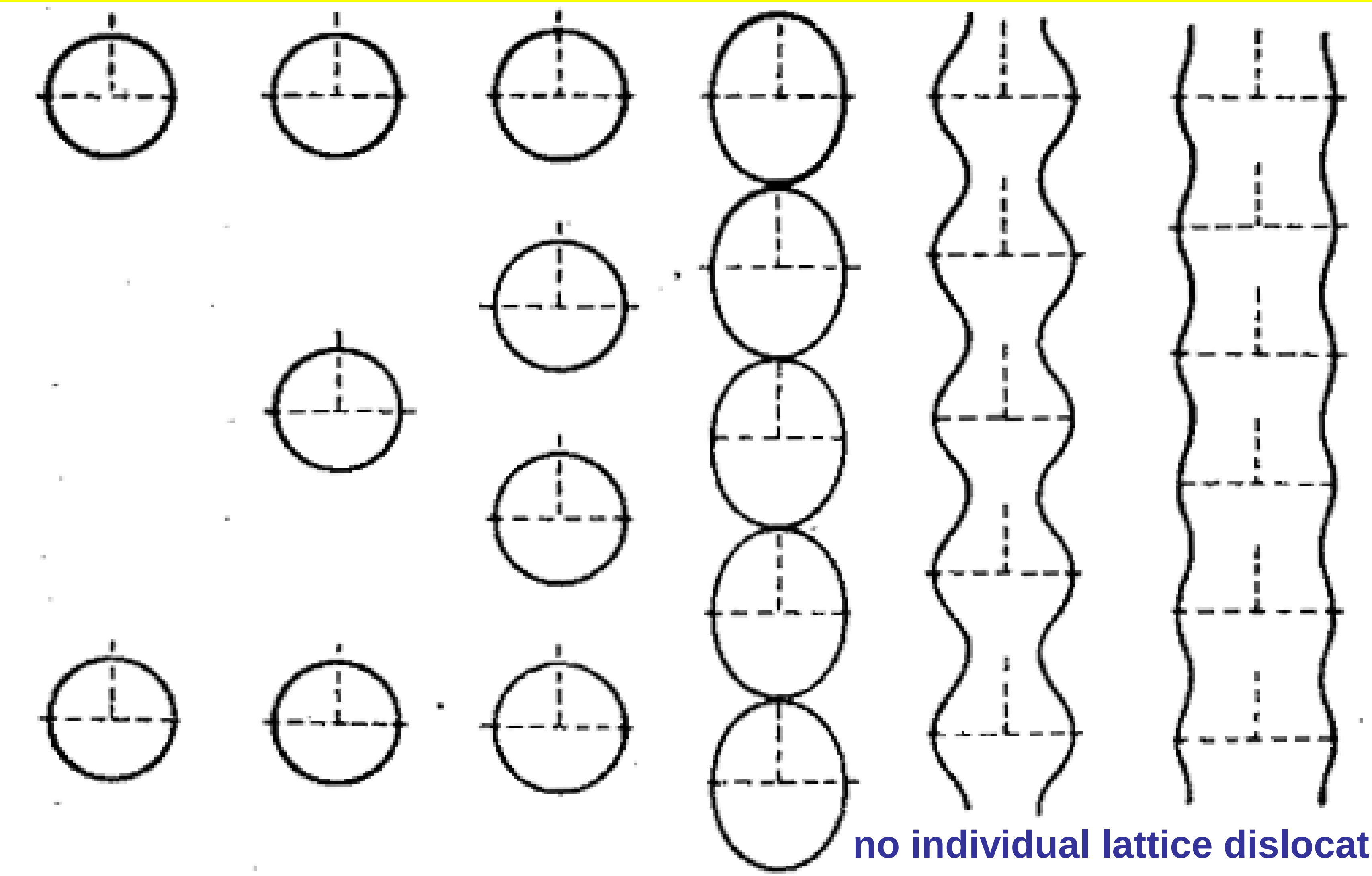

Misorientation, $\theta \rightarrow$

Two lattices: coincidence site lattice

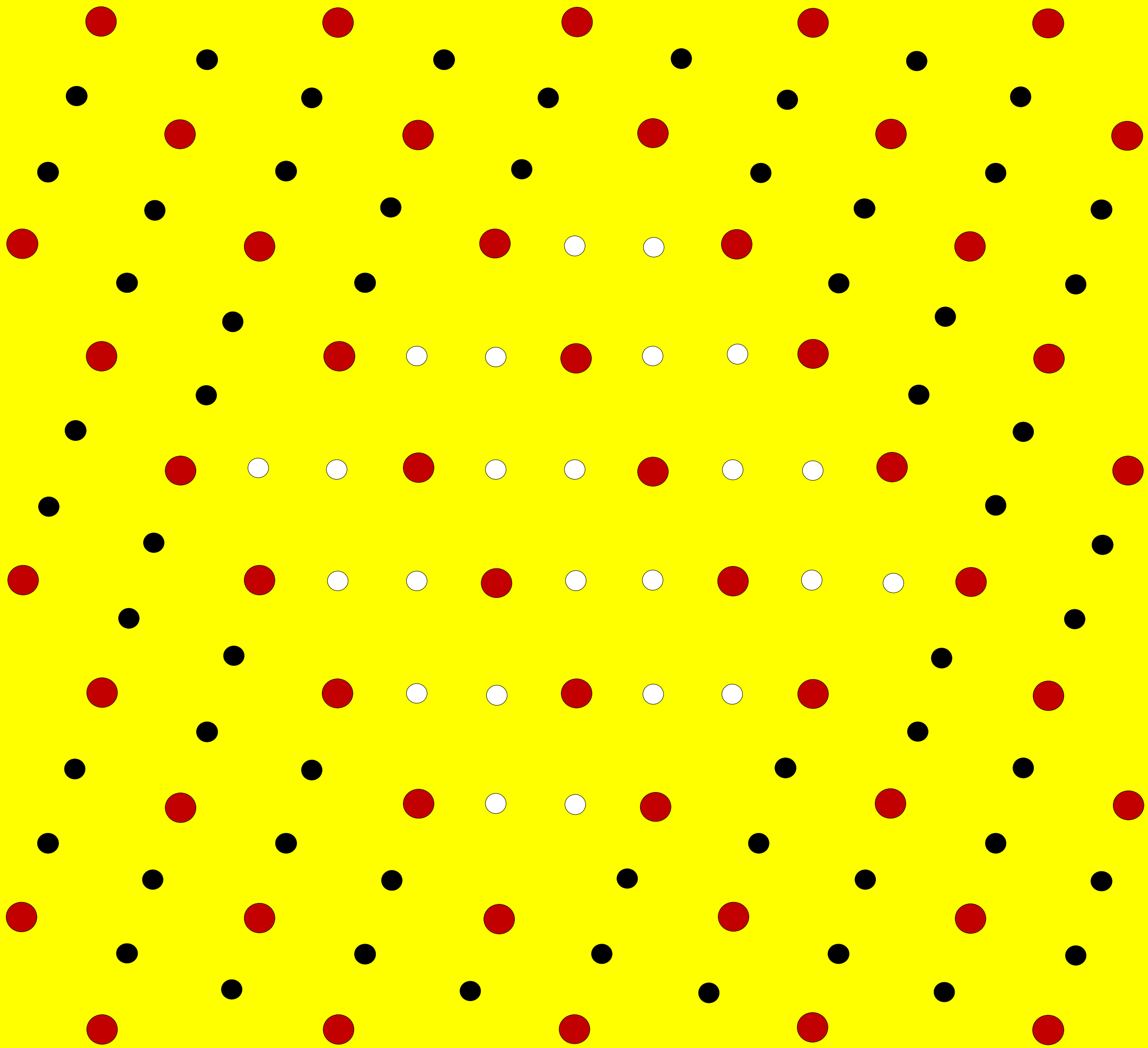

Two grains with coincidence site lattice

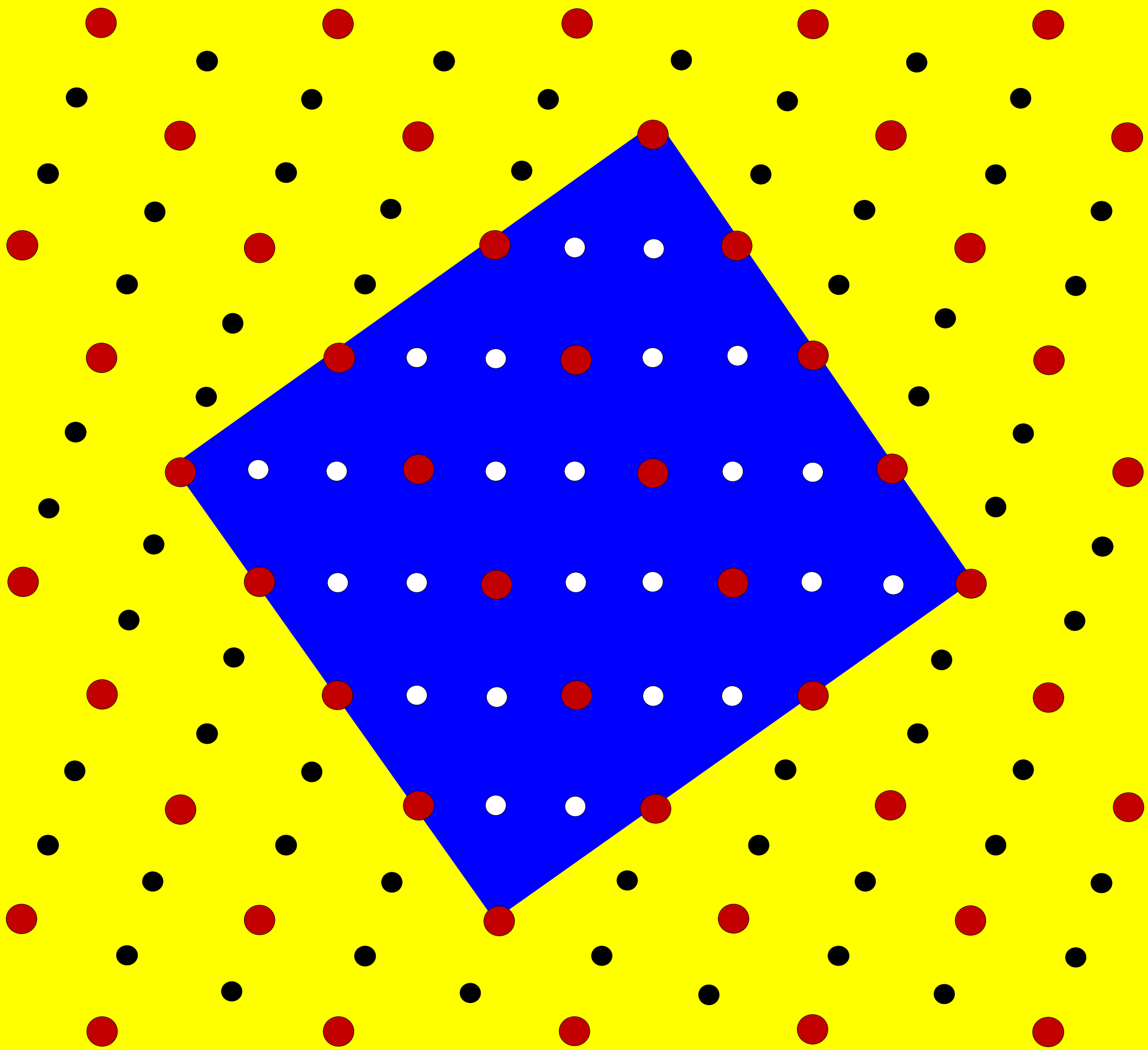

Two grains with coincidence site lattice

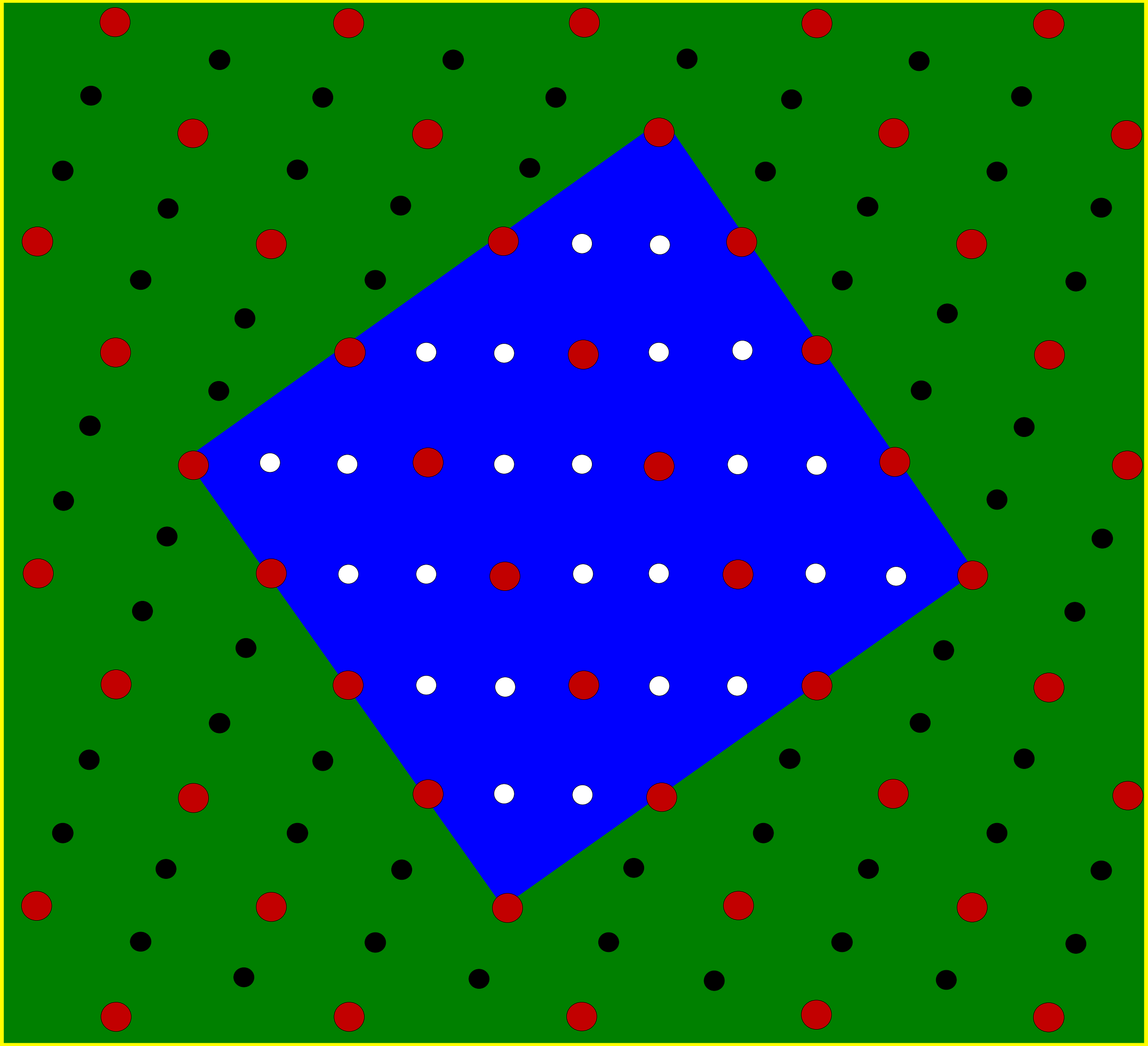

Two amorhous phases: smooth interface

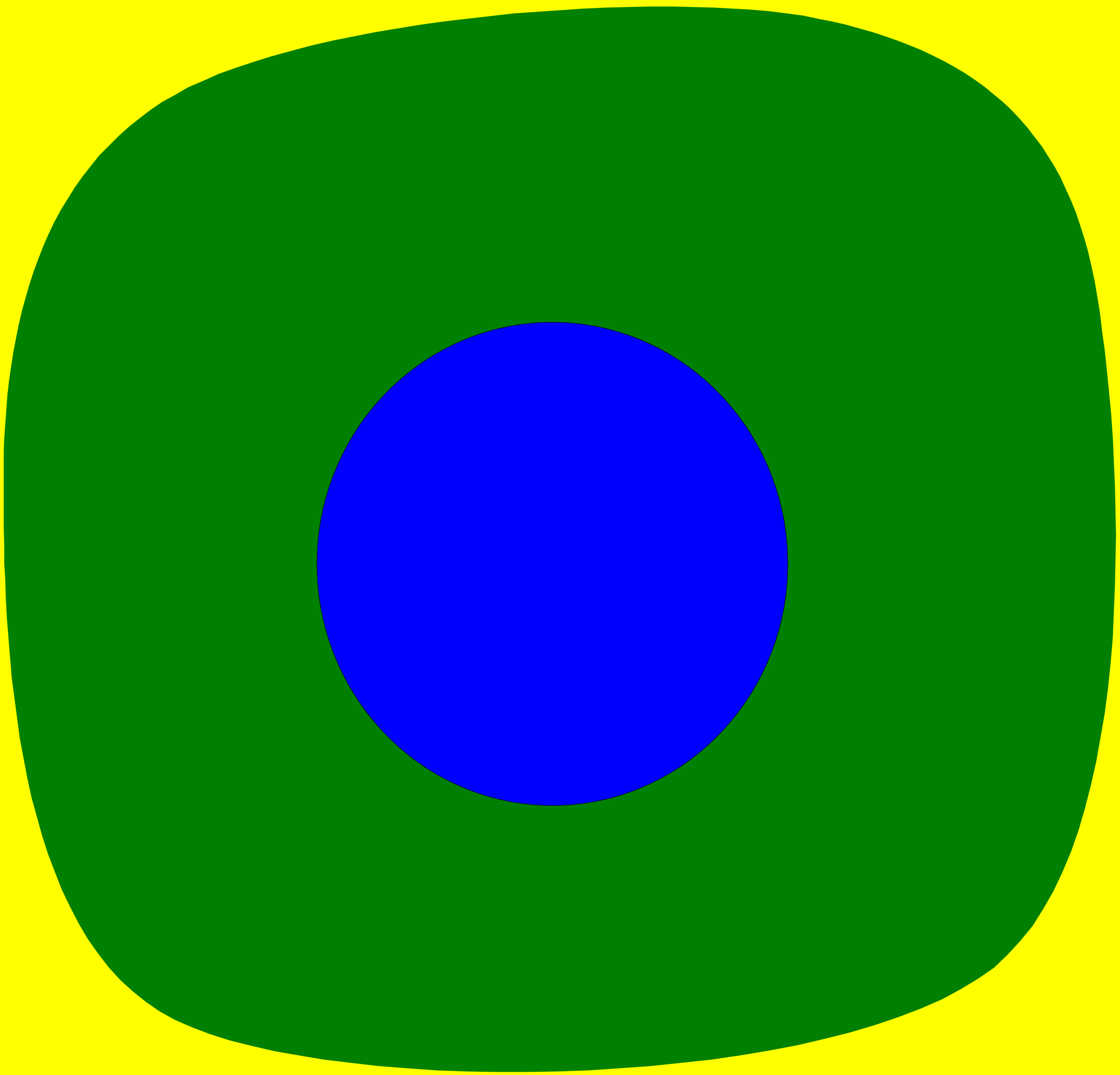

Crystal inside of an amorphous phase

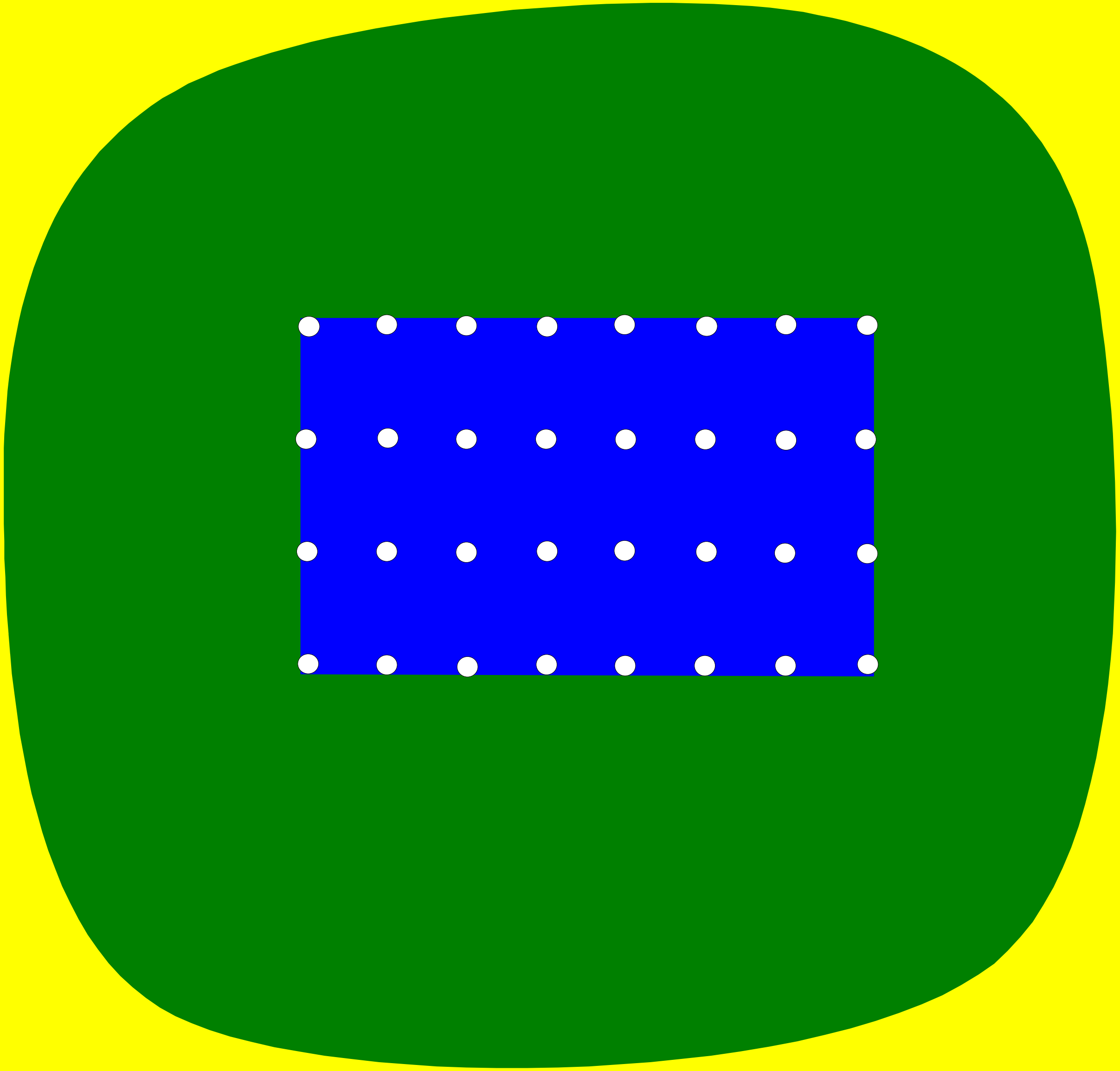

Two crystalline lattices

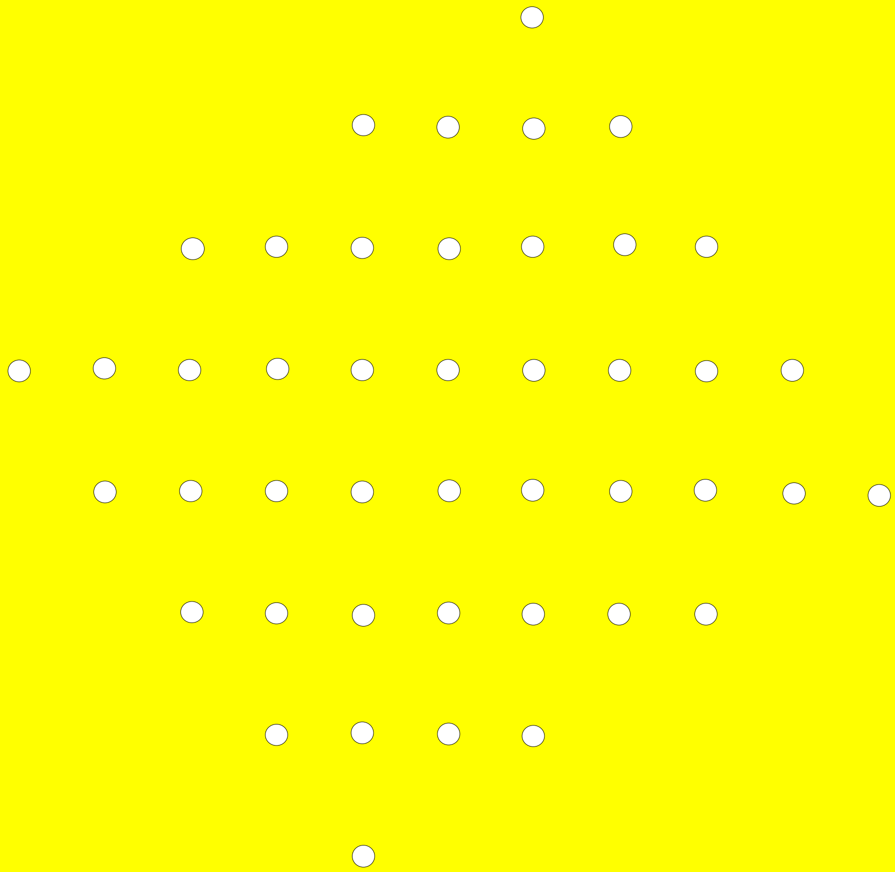

Two crystalline lattices

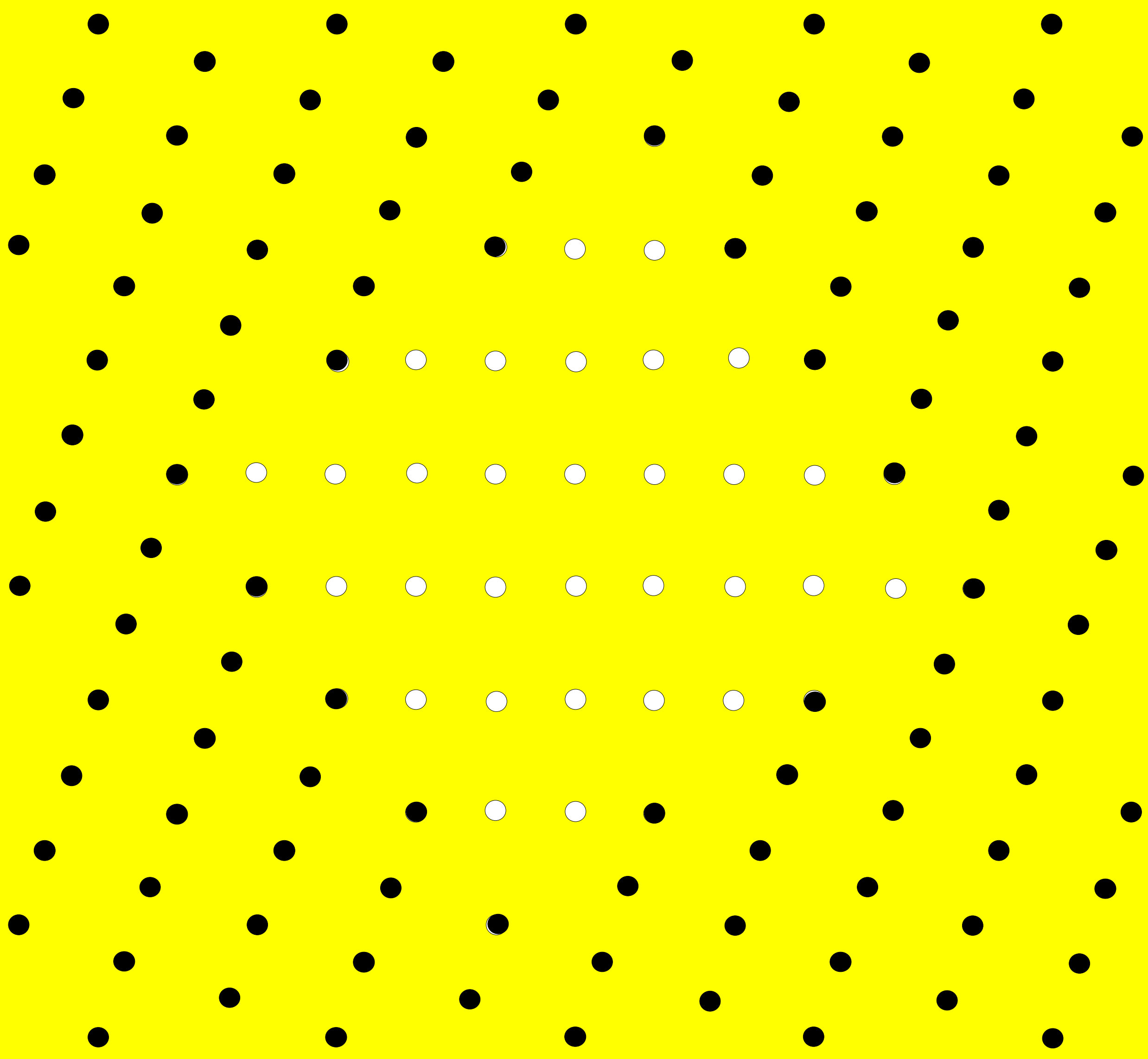

Two lattices: coincidence site lattice

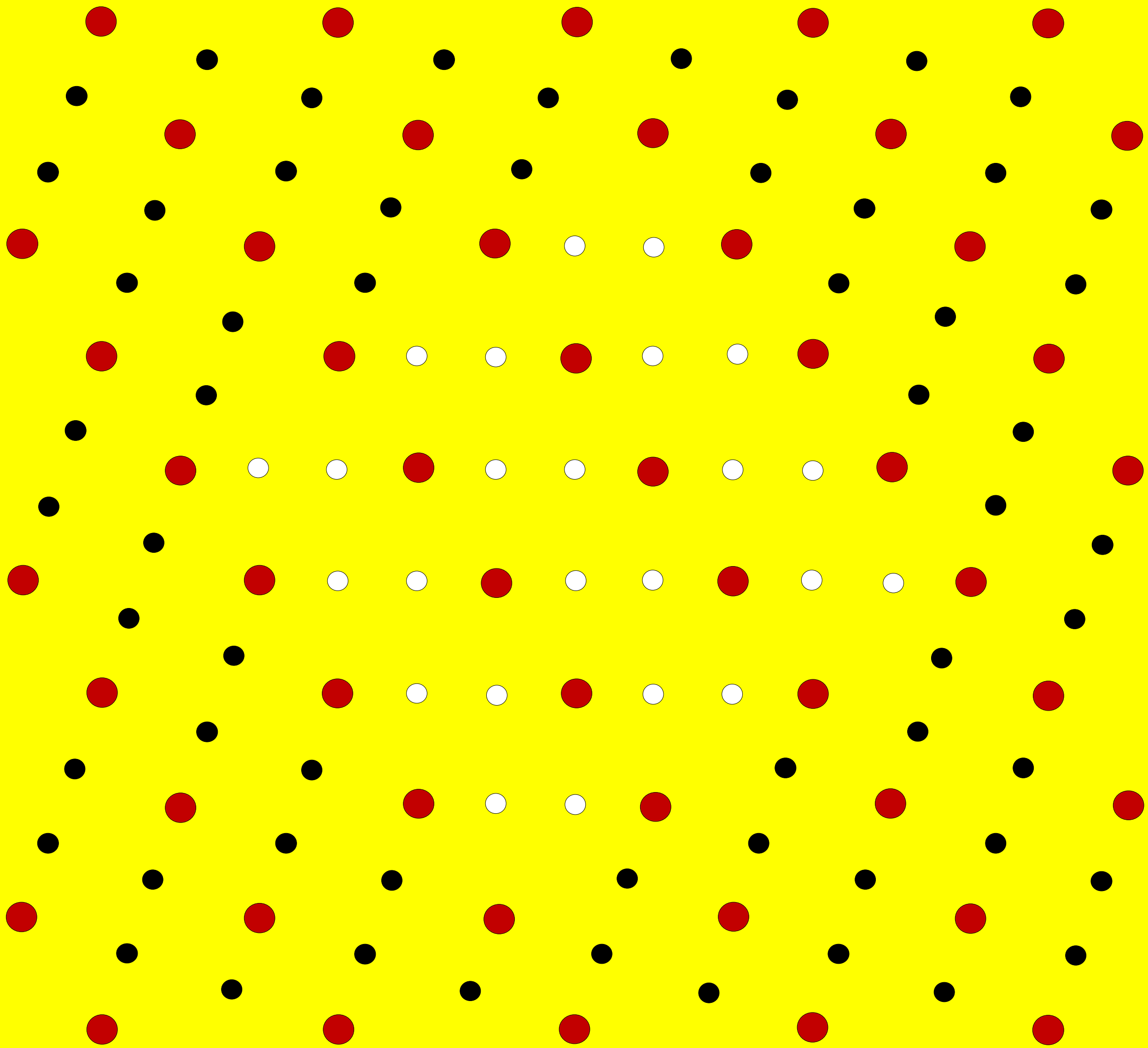

Facets in the coincidence site lattice

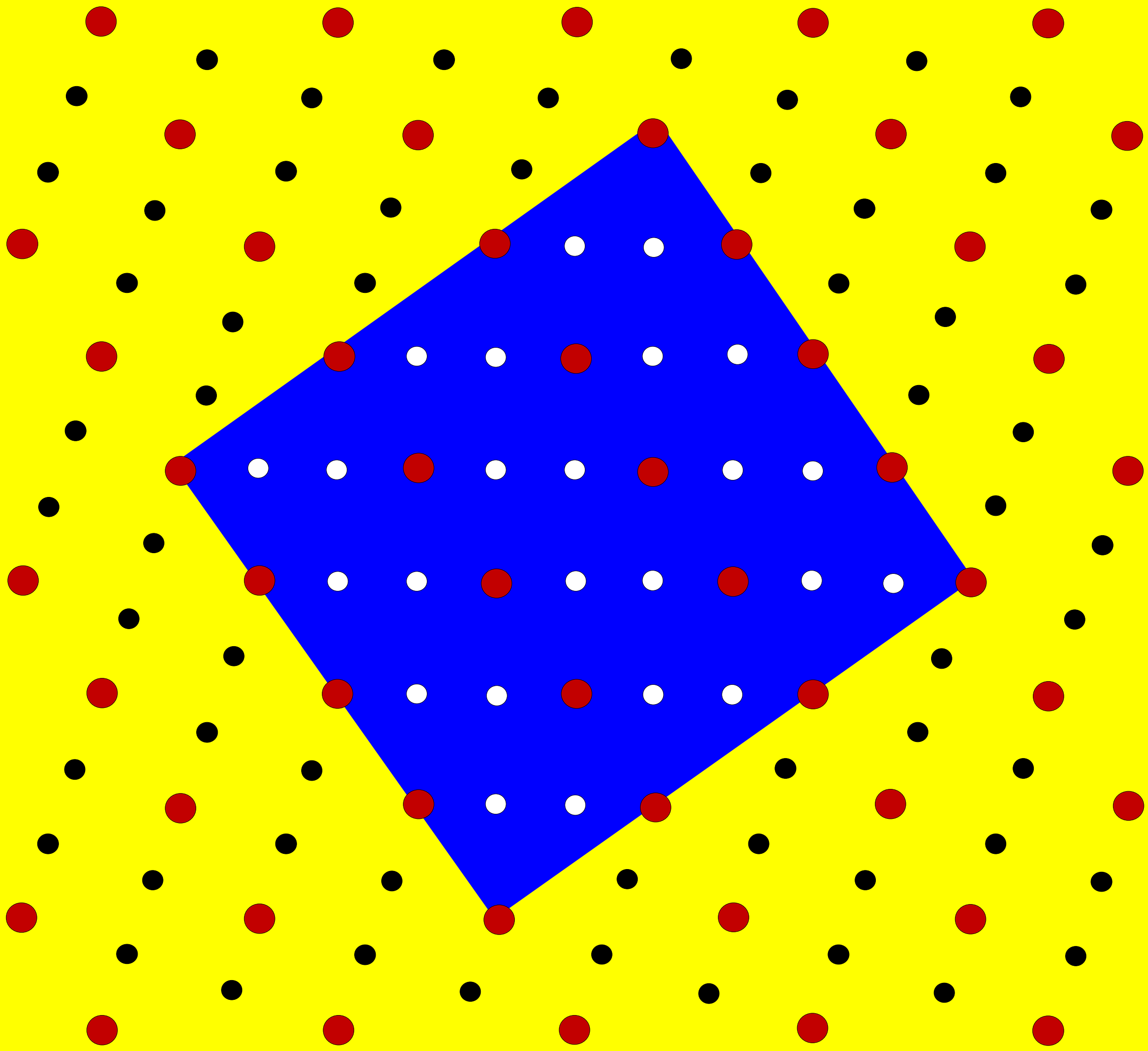

Facets in the coincidence site lattice

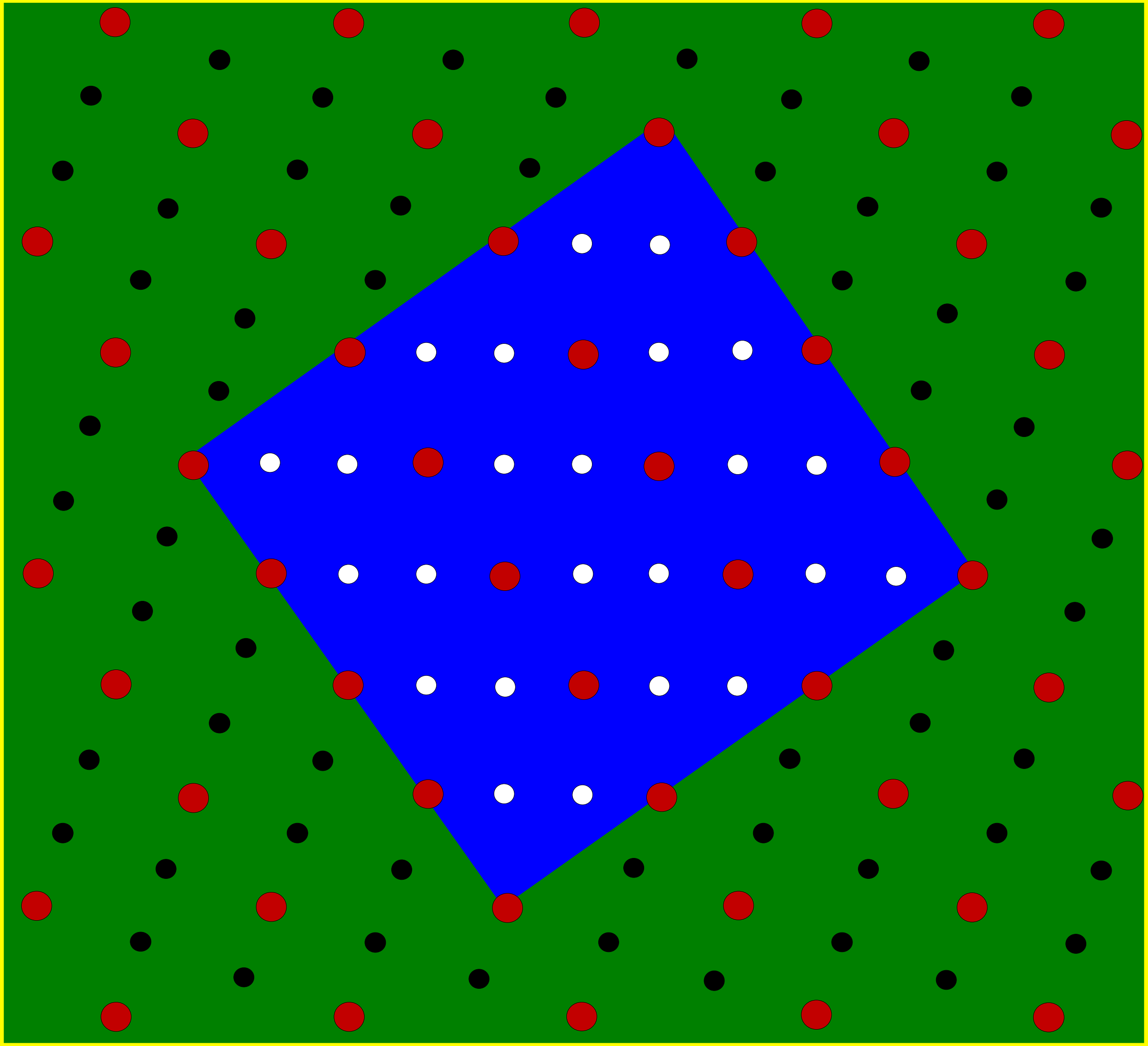

Coincidence sites lattice Σ3

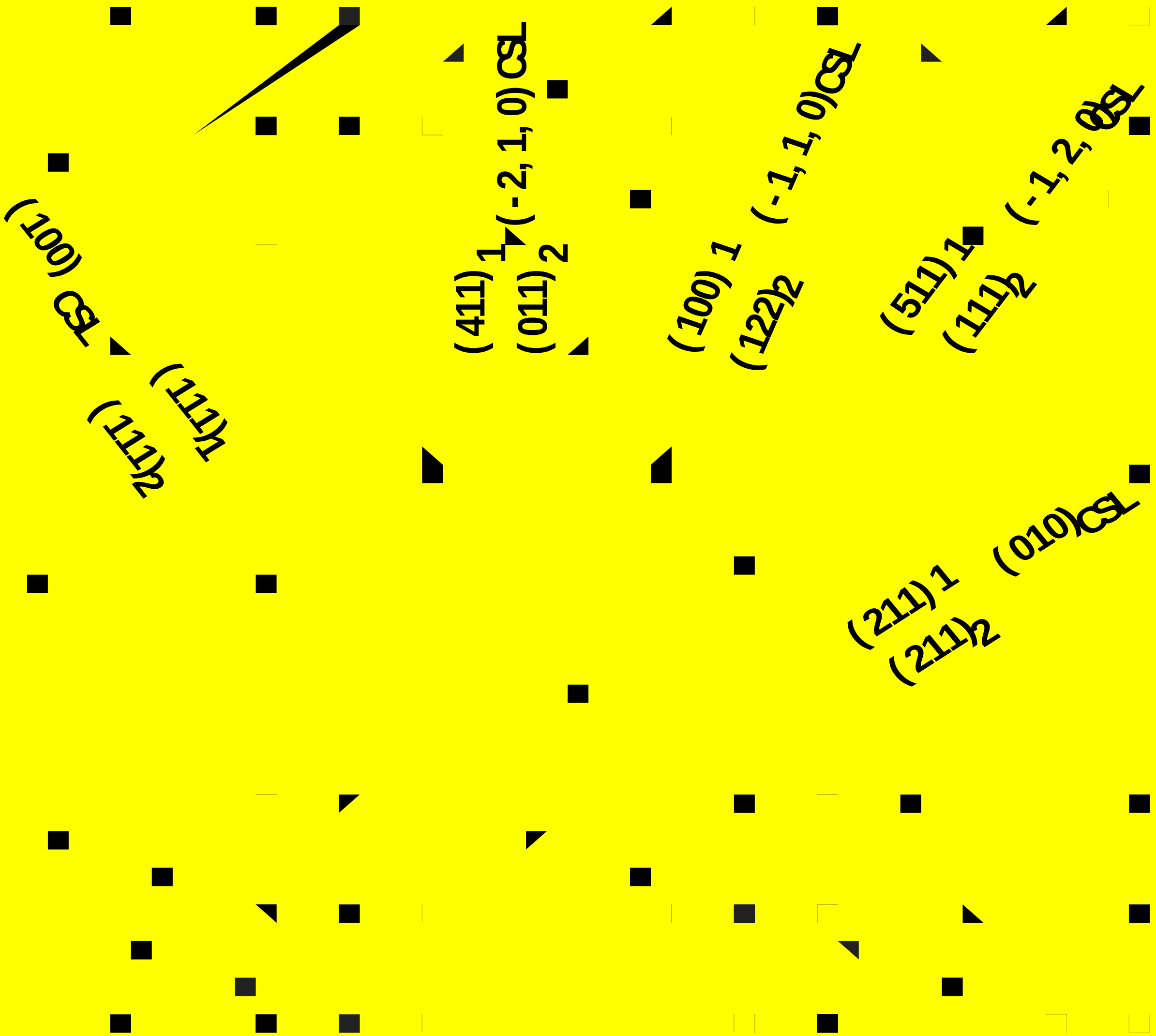

Coincidence sites lattice Σ3 (thick lines) and displacement shift lattice (thin lines)

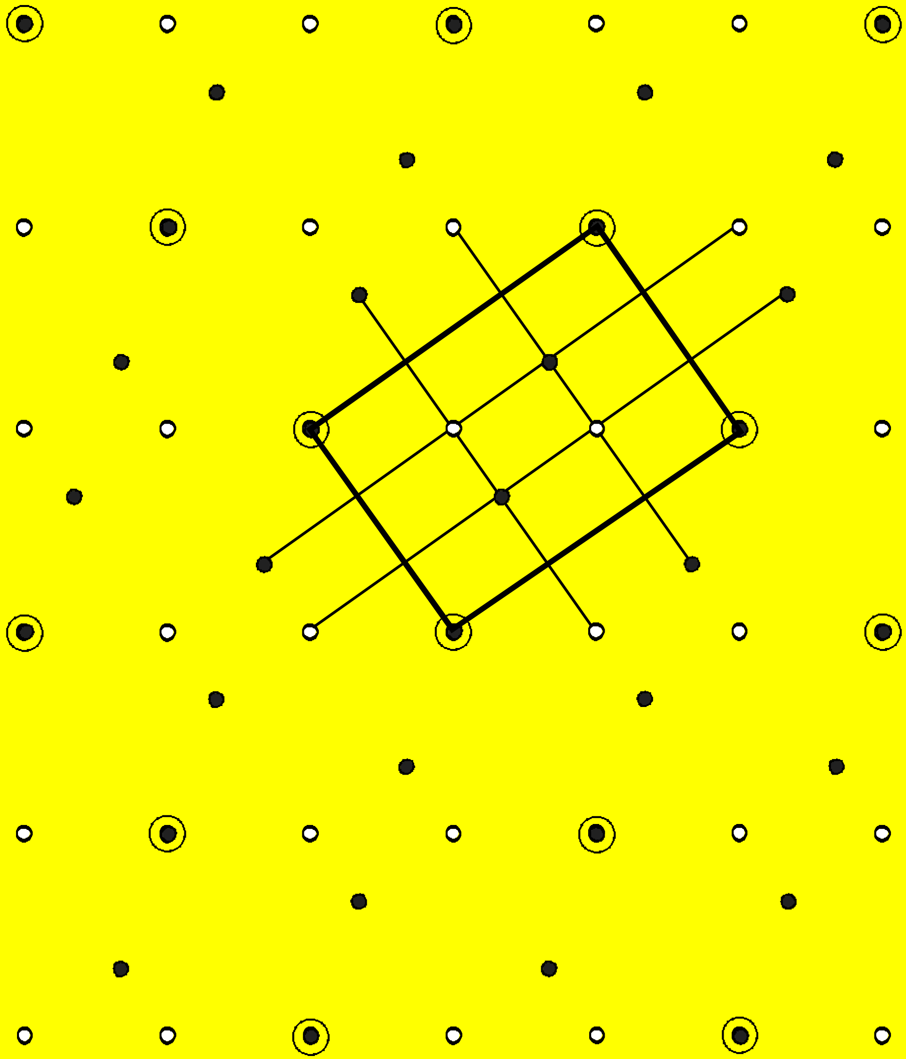

Scheme of Cu bicrystal with coaxial Σ3 GBs

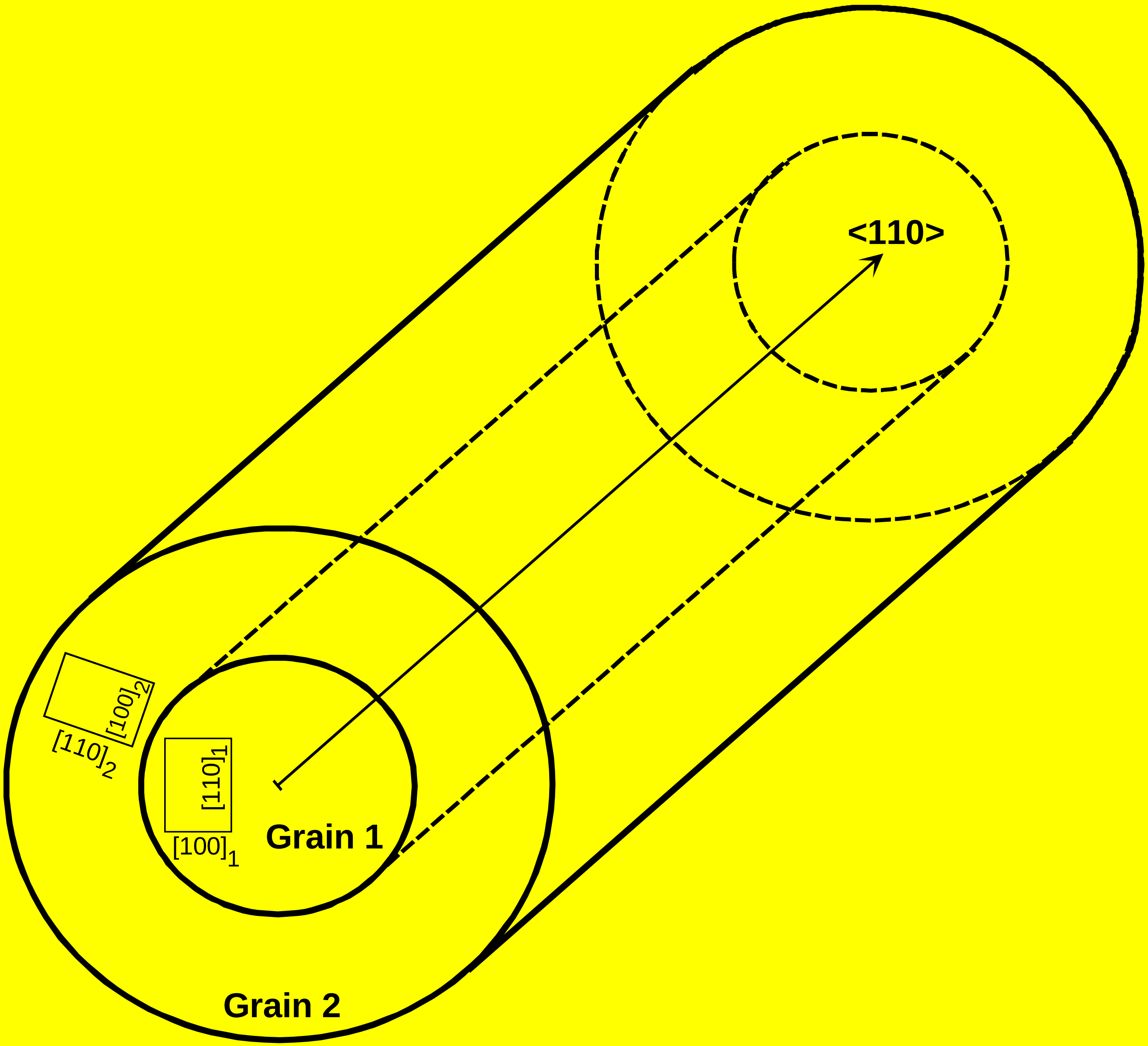

Cu bicrystal with cylindric Σ9/Σ3 GBs

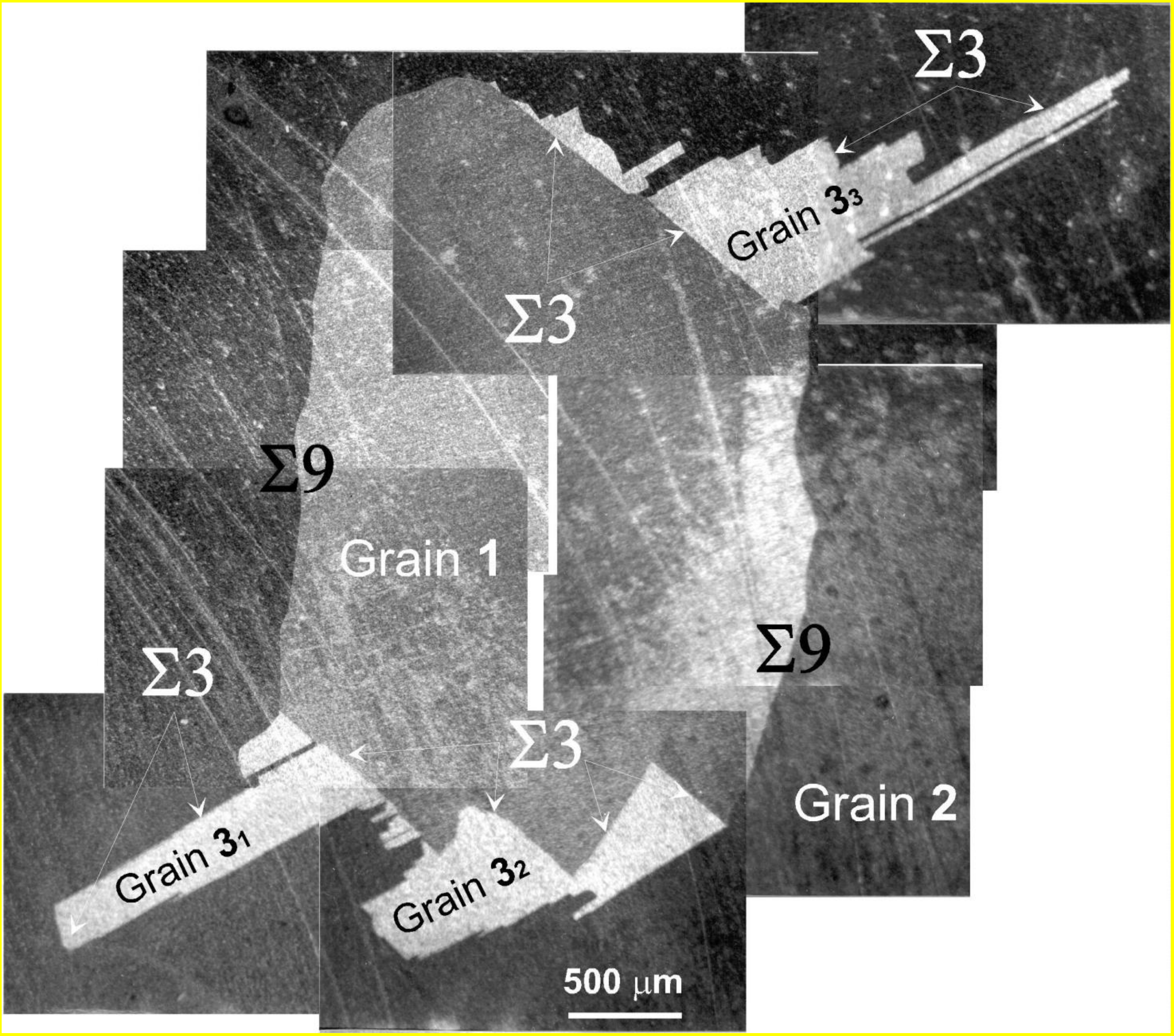

Section of Cu bicrystal with cylindric Σ9/Σ3 GBs, 1020°C, 48 h

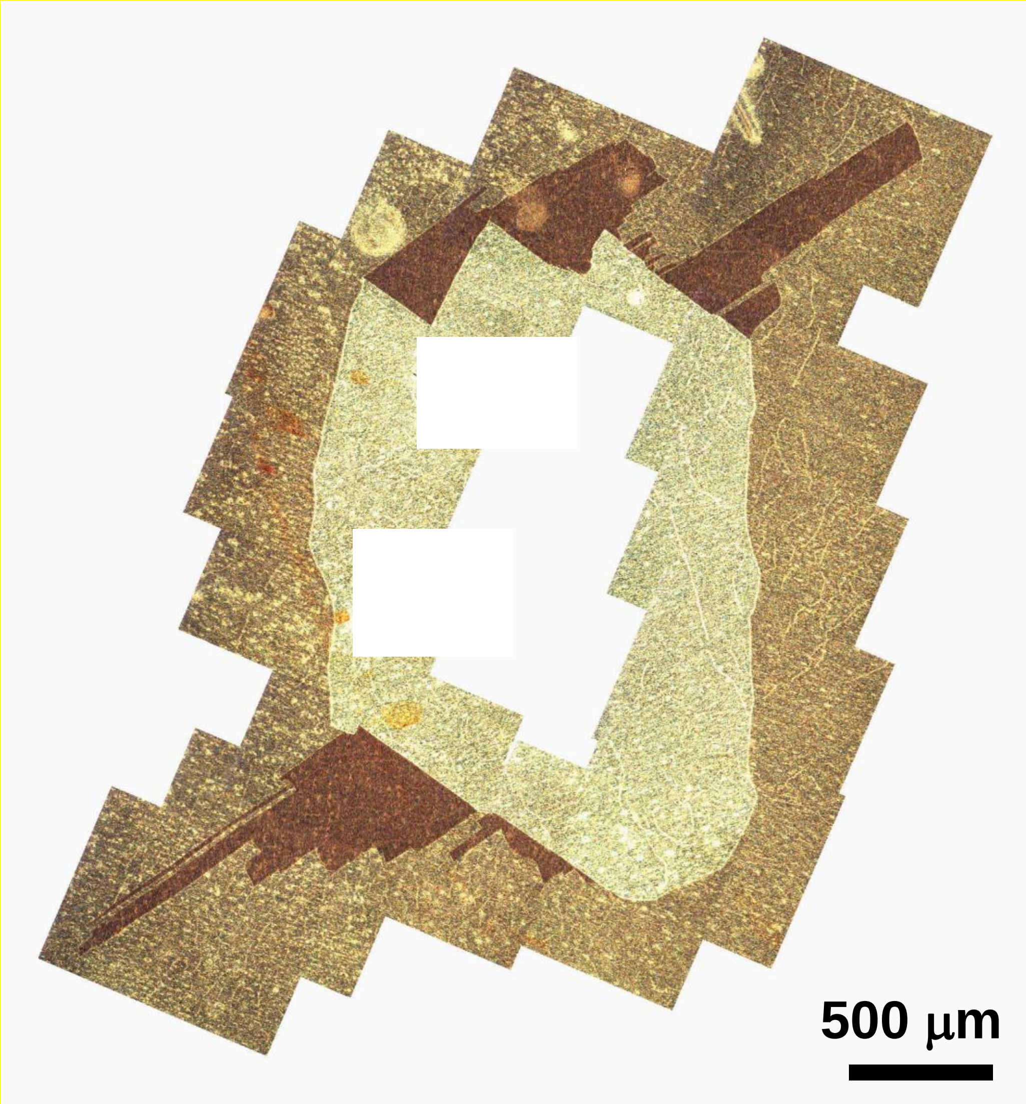

Σ3 tilt GB in Cu, 1020°C
$(100)_{CSL}$ and 9*R* non-CSL facets
(twin plates are not rectangular)

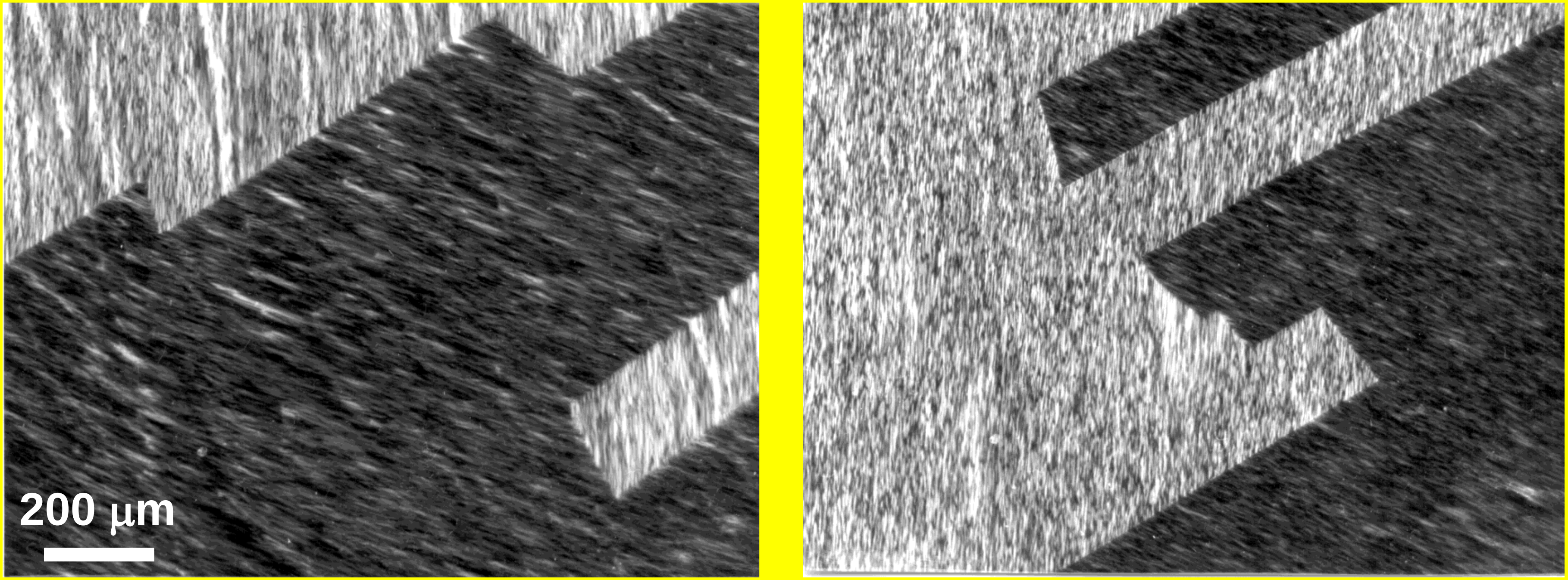

Σ3 tilt grain boundary in Cu, 1020°C
$(100)_{CSL}$ and 9*R* non-CSL facets

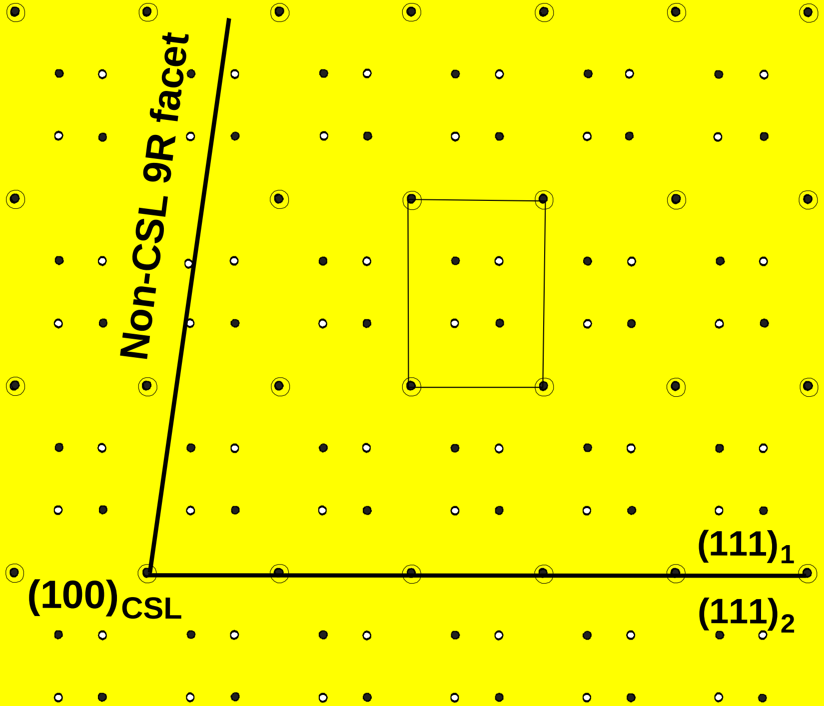

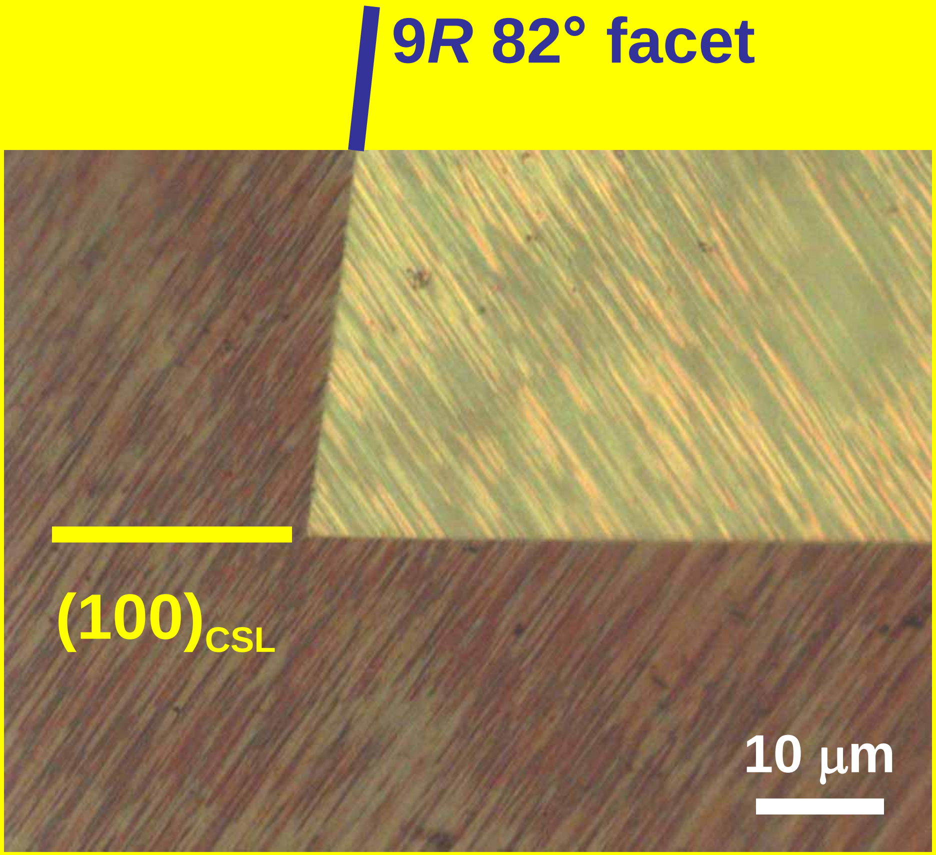

Non-CSL 9*R* facet of the Σ3 tilt GB (HRTEM)

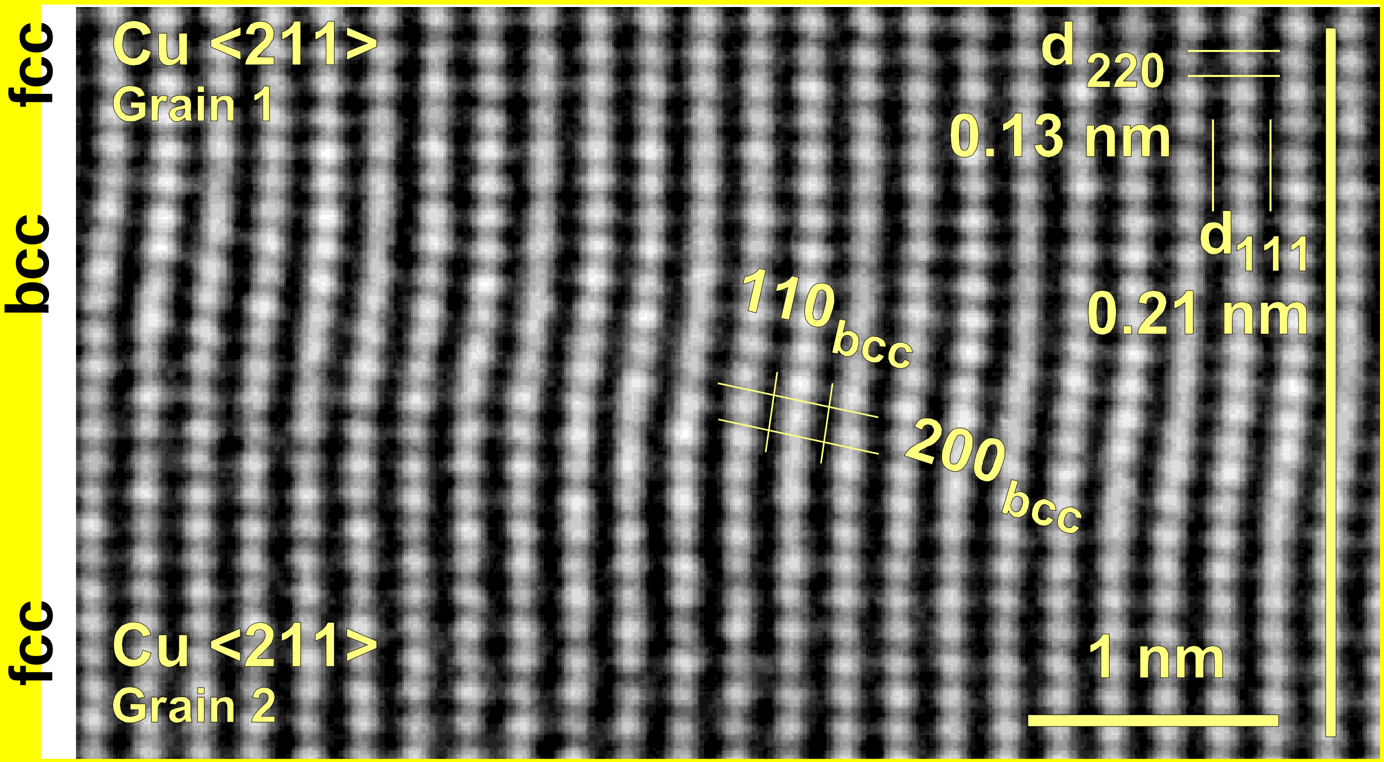

Step height 0.58*a*, equal to that of $(010)_{CSL}$

Phase diagram for the Σ3 GBs in Cu

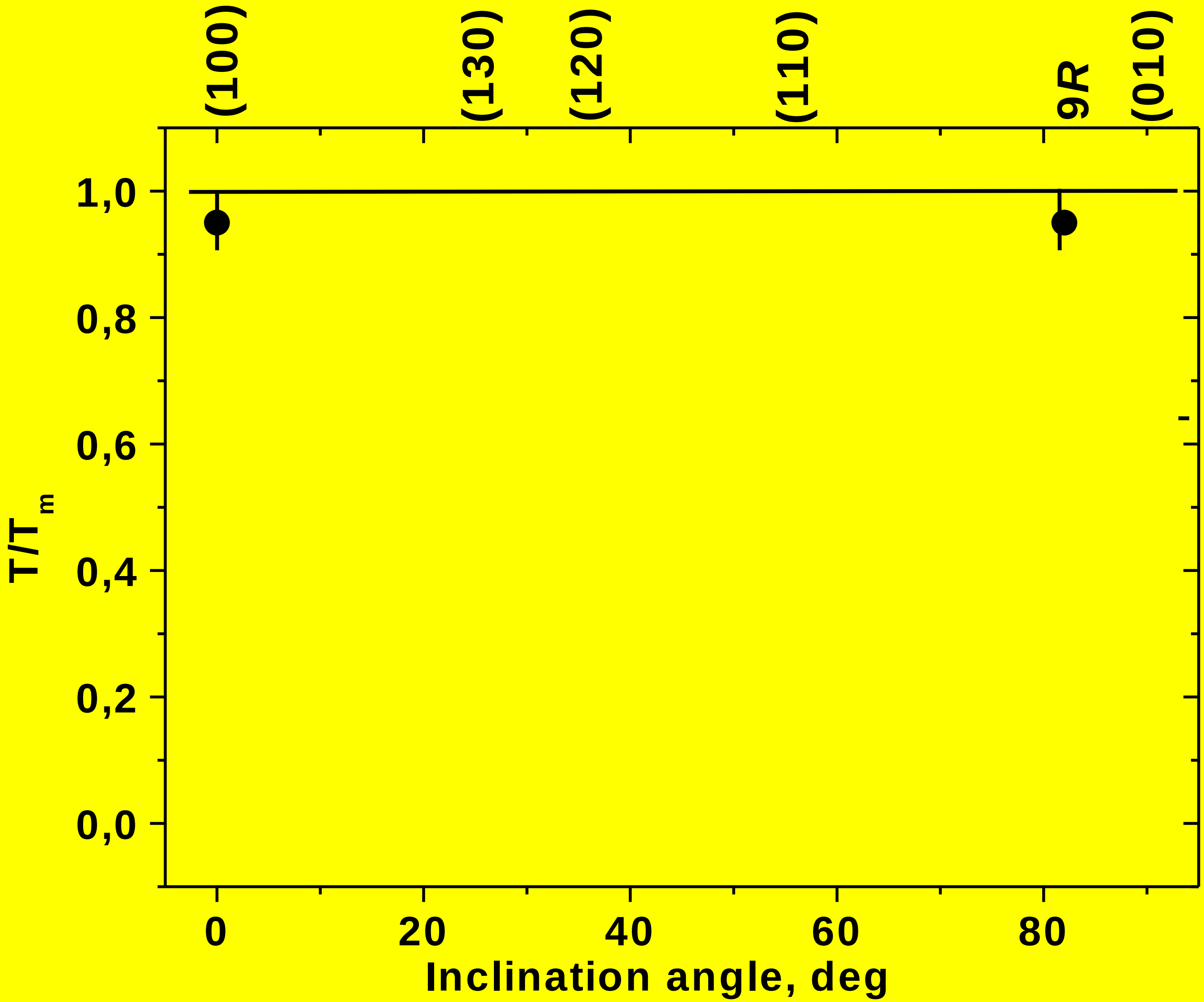

Rectangular facets in Au

$(100)_{CSL}$ and $(010)_{CSL}$ facets

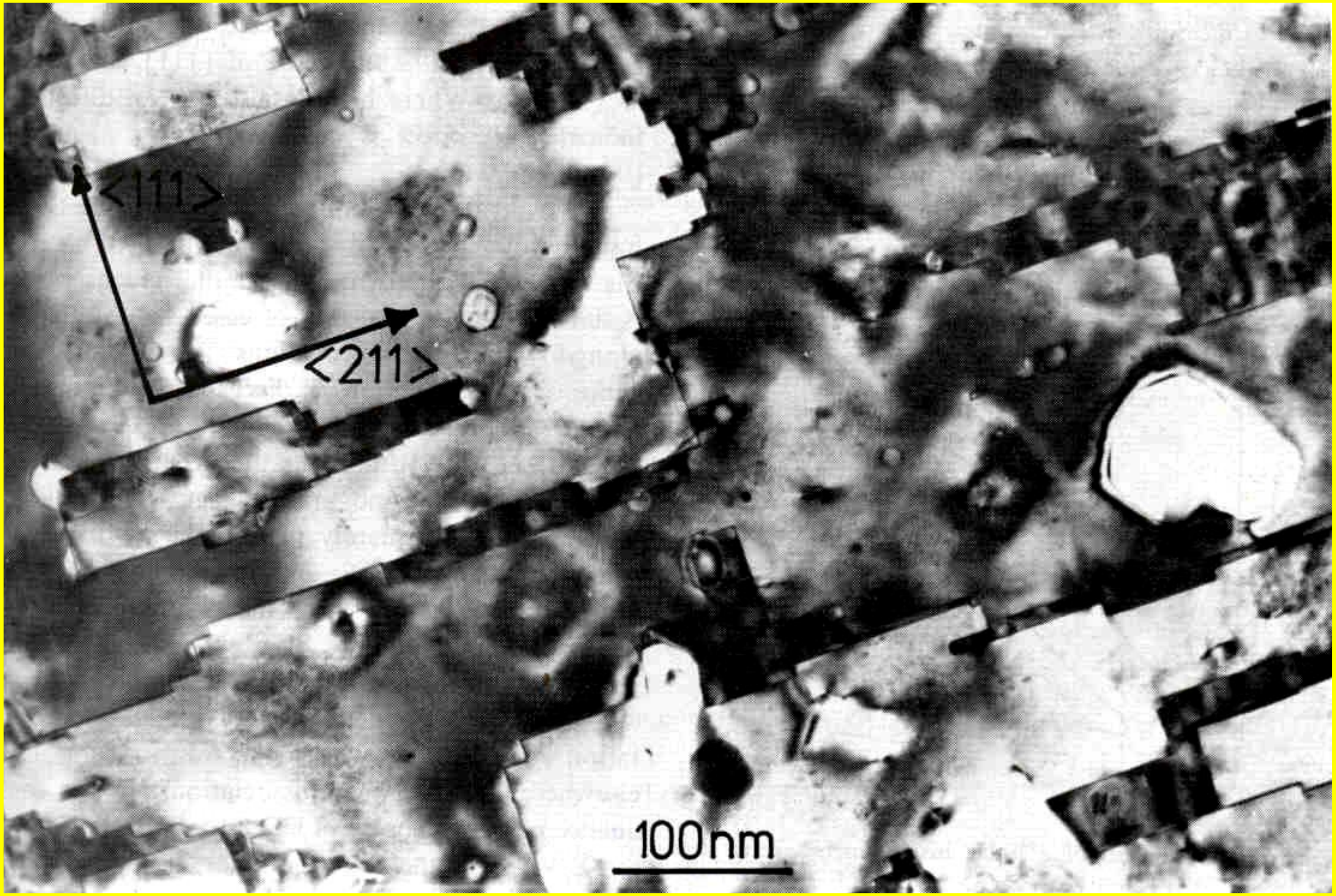

P.J. Goodhew, T.Y. Tan, R.W. Balluffi, *Acta Metall.* **26** (1978) 557–567

Σ3 tilt grain boundary in Cu, 800°C
$(100)_{CSL}$ and 9*R* non-CSL facets

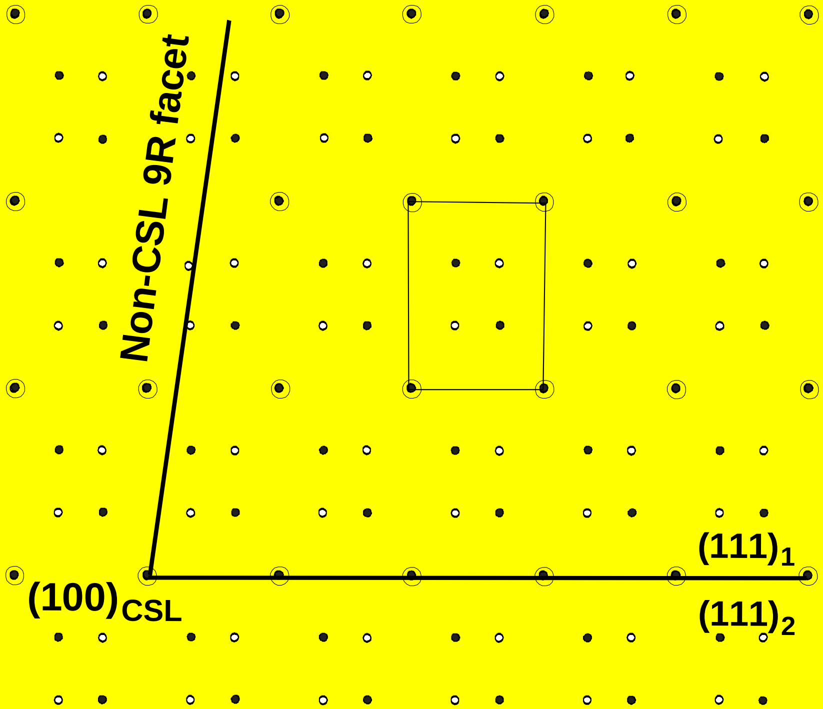

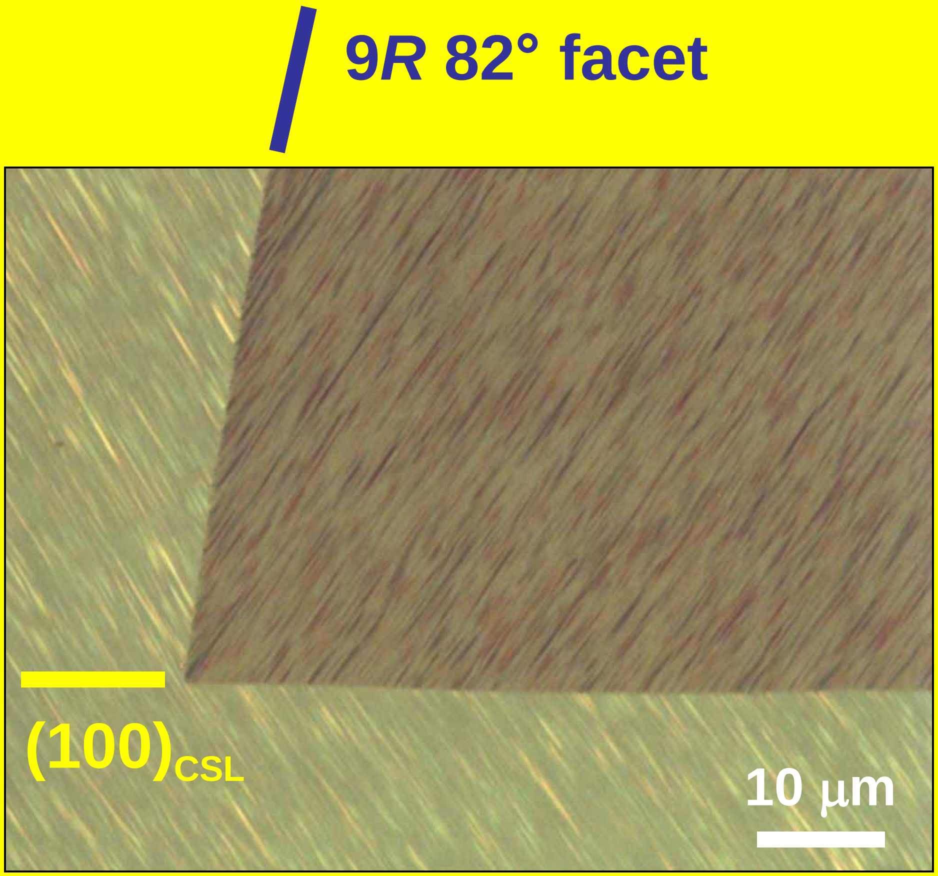

Phase diagram for the Σ3 GBs in Cu

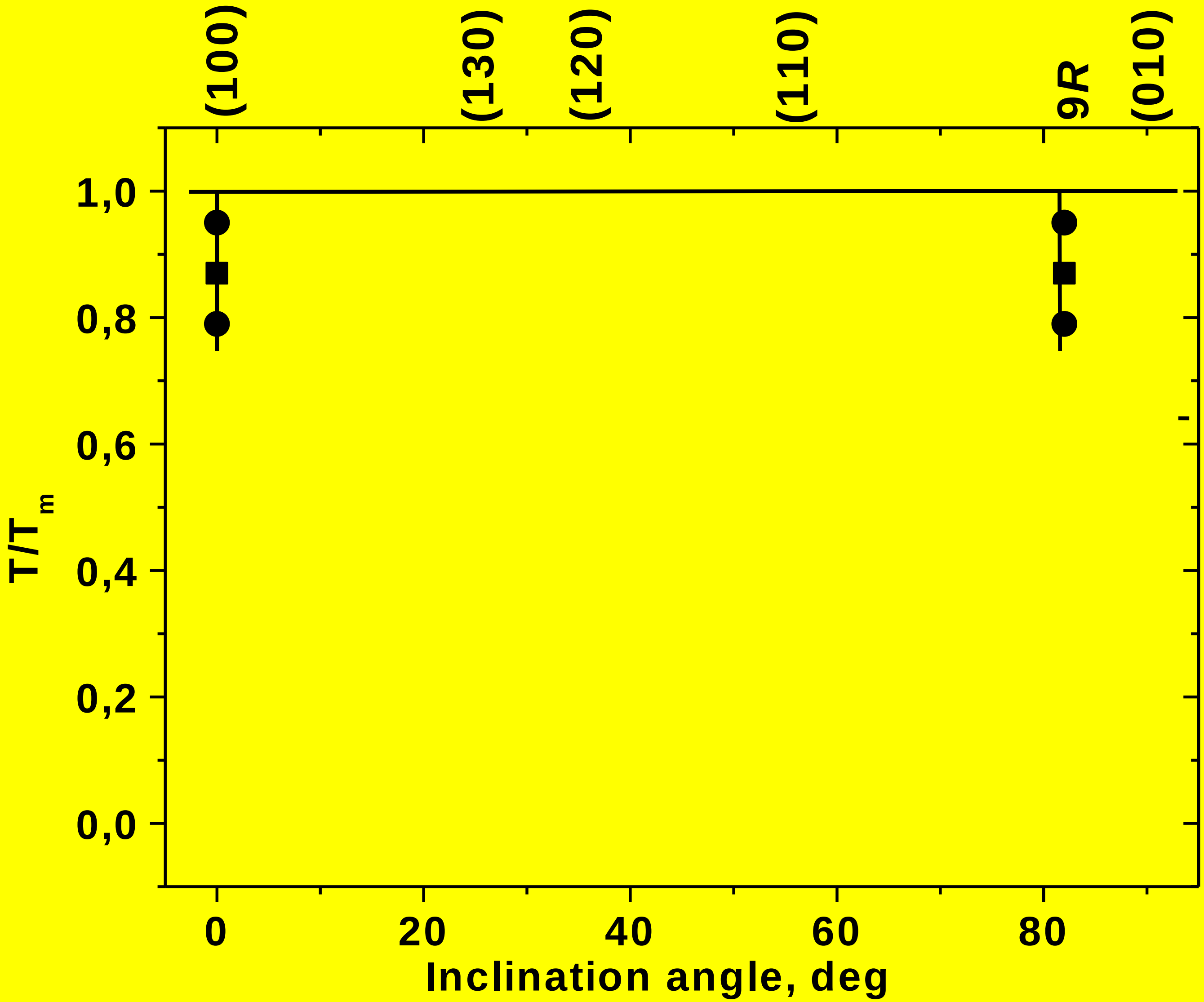

Σ3 tilt grain boundary in Cu, 650°C
$(100)_{CSL}$ and $(110)_{CSL}$ facets

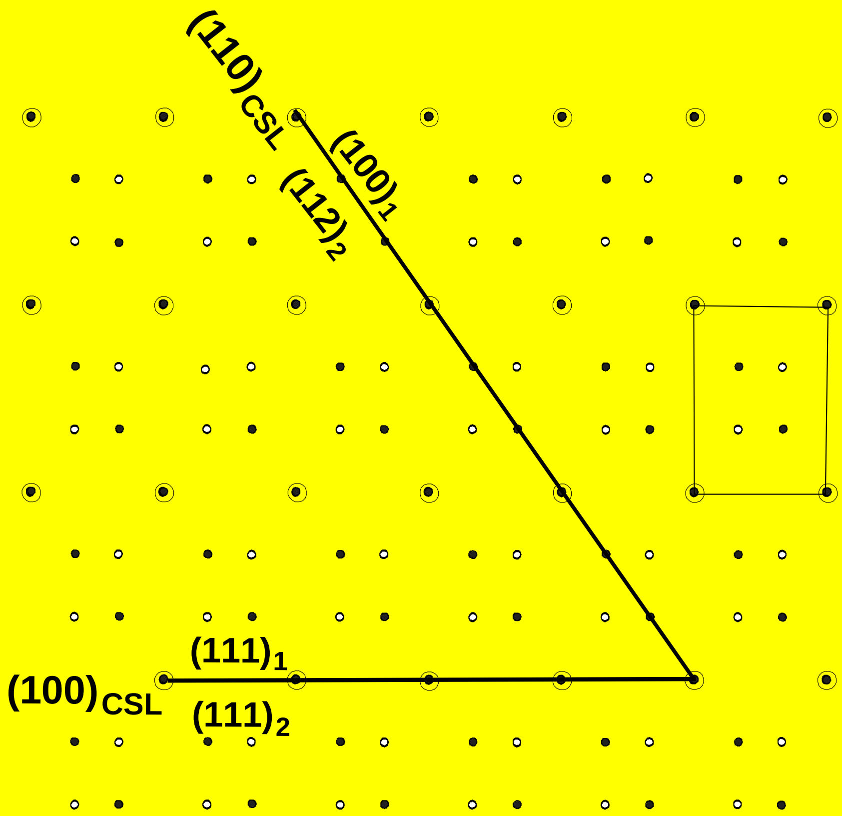

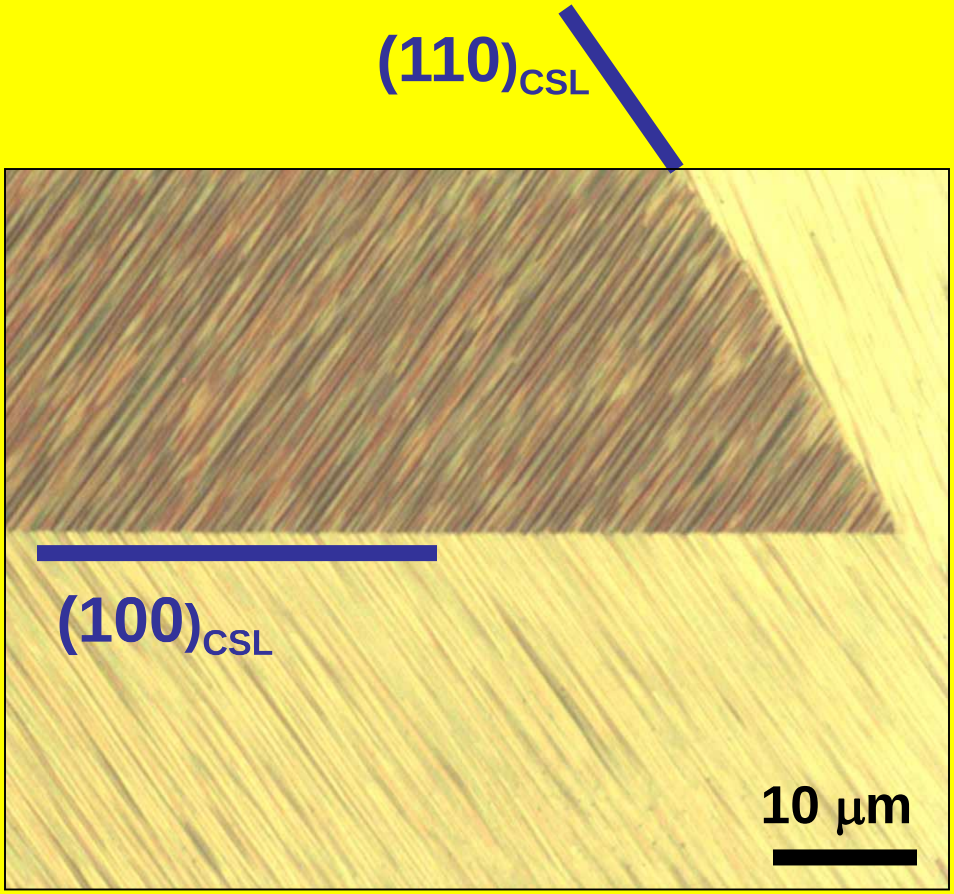

Σ3 tilt grain boundary in Cu, 650°C
$(100)_{CSL}$ and $(130)_{CSL}$ facets

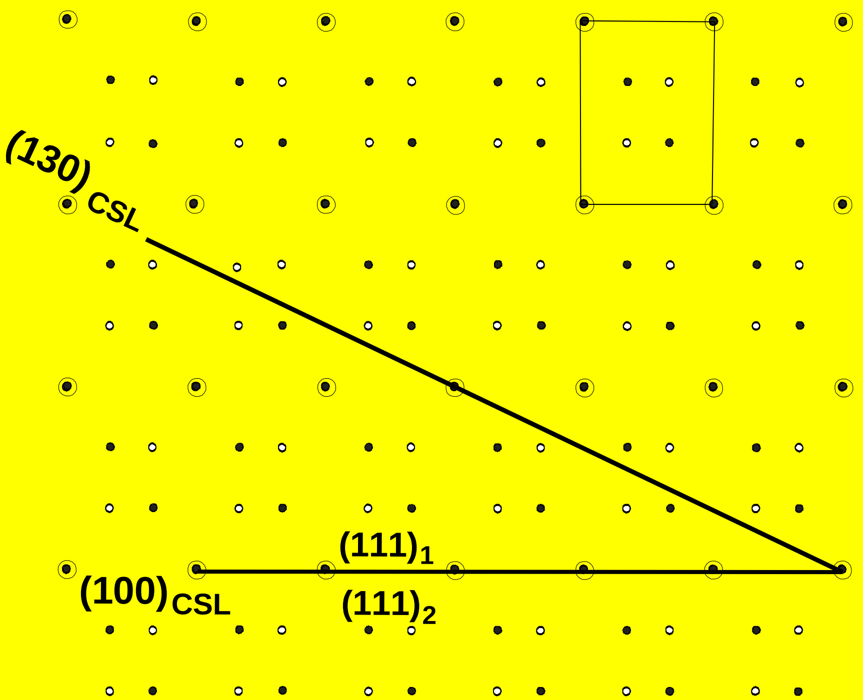

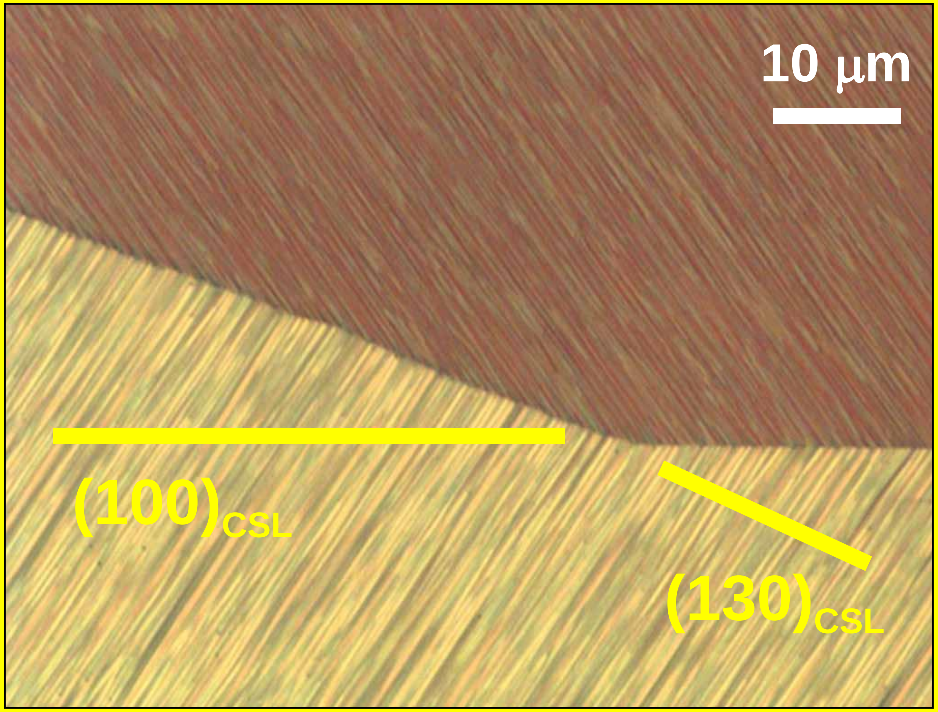

Phase diagram for the Σ3 GBs in Cu

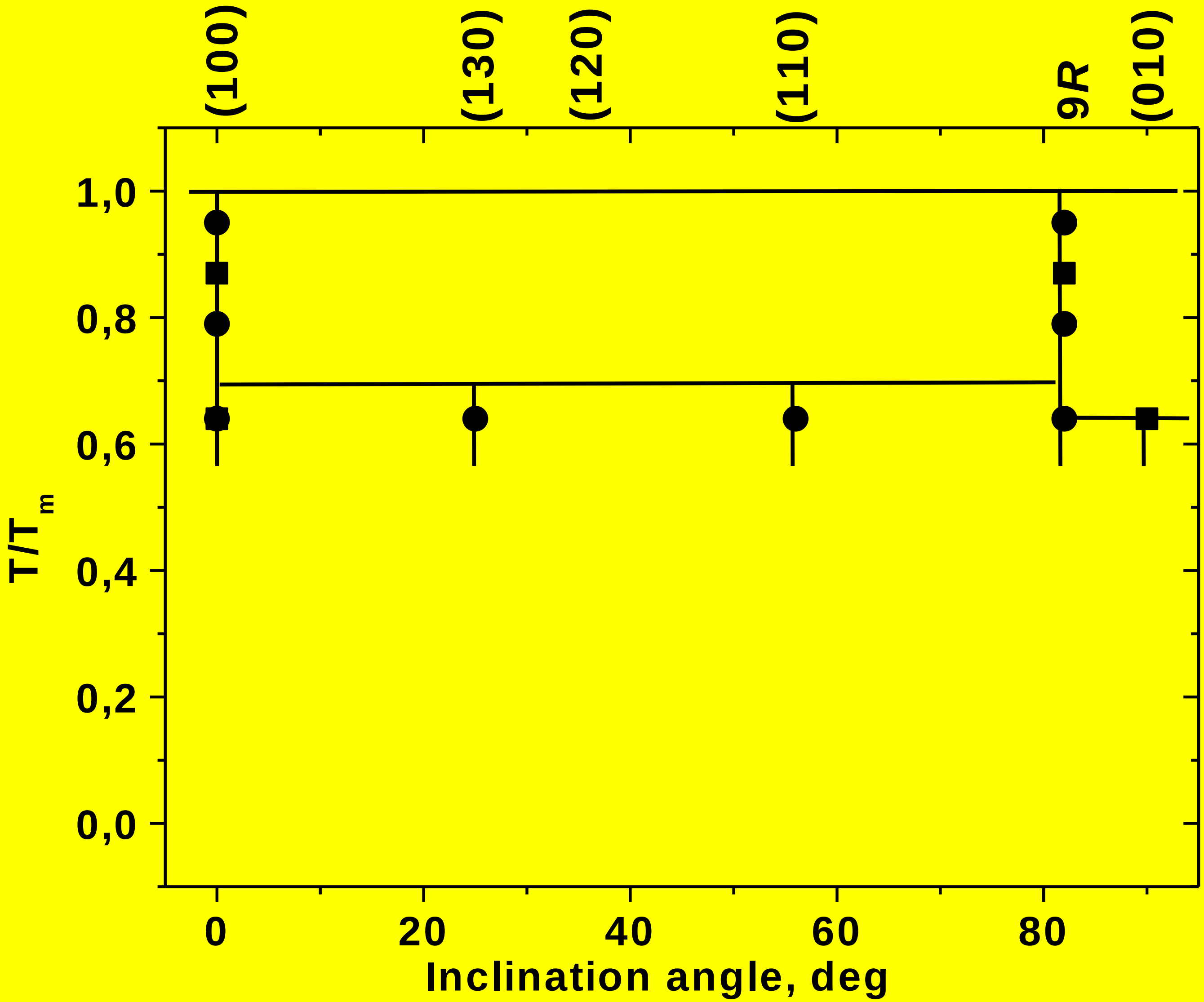

Σ3 tilt grain boundary in Cu, 400°C
$(100)_{CSL}$ and $(010)_{CSL}$ facets

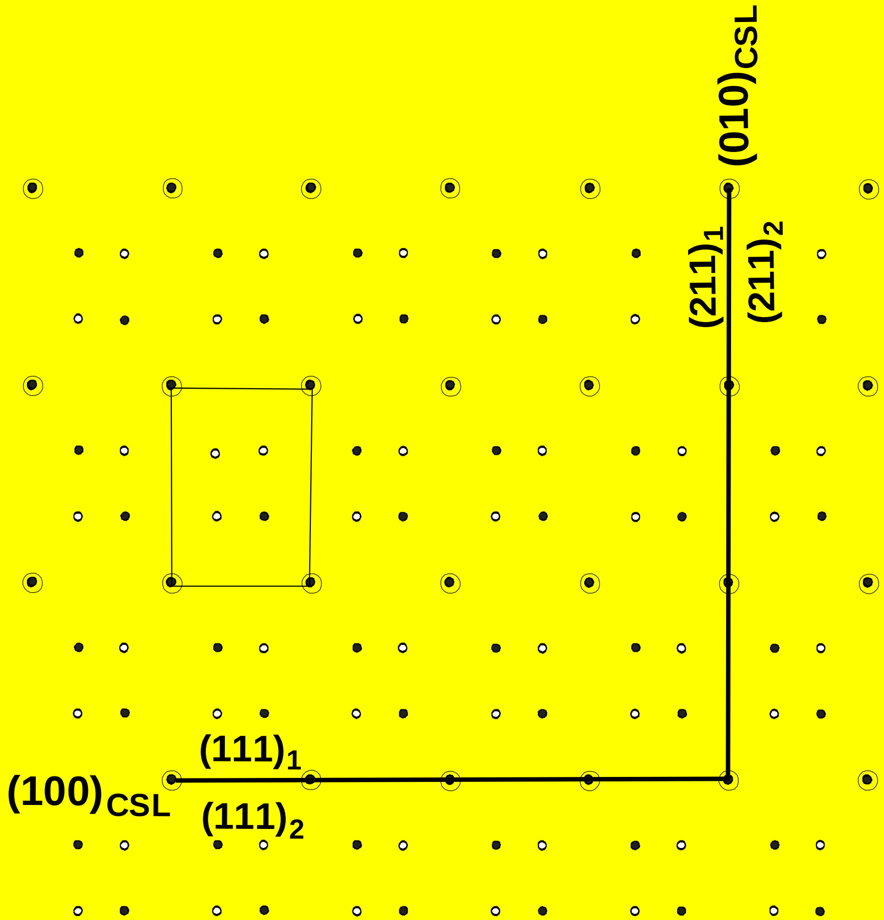

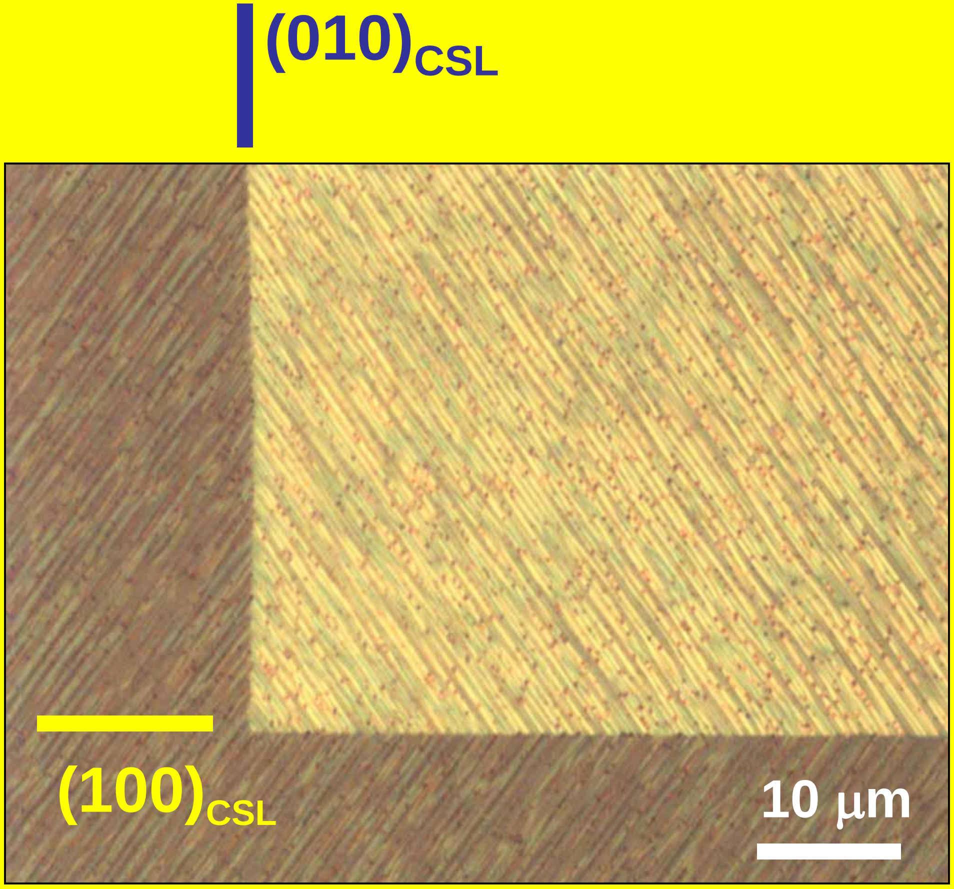

Σ3 tilt grain boundary in Cu, 400°C
$(100)_{CSL}$, $(130)_{CSL}$ and $(120)_{CSL}$ facets

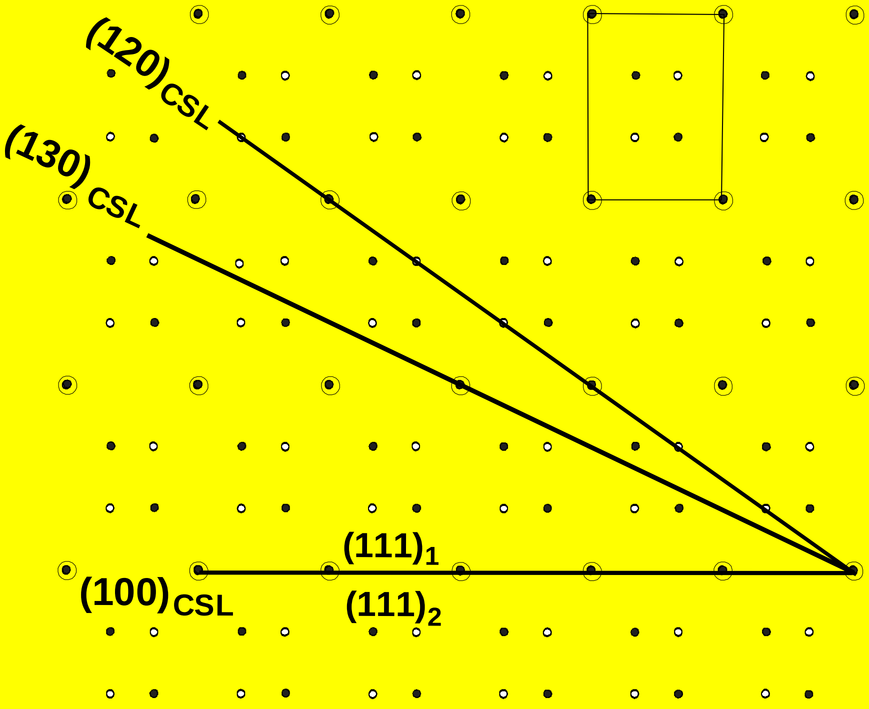

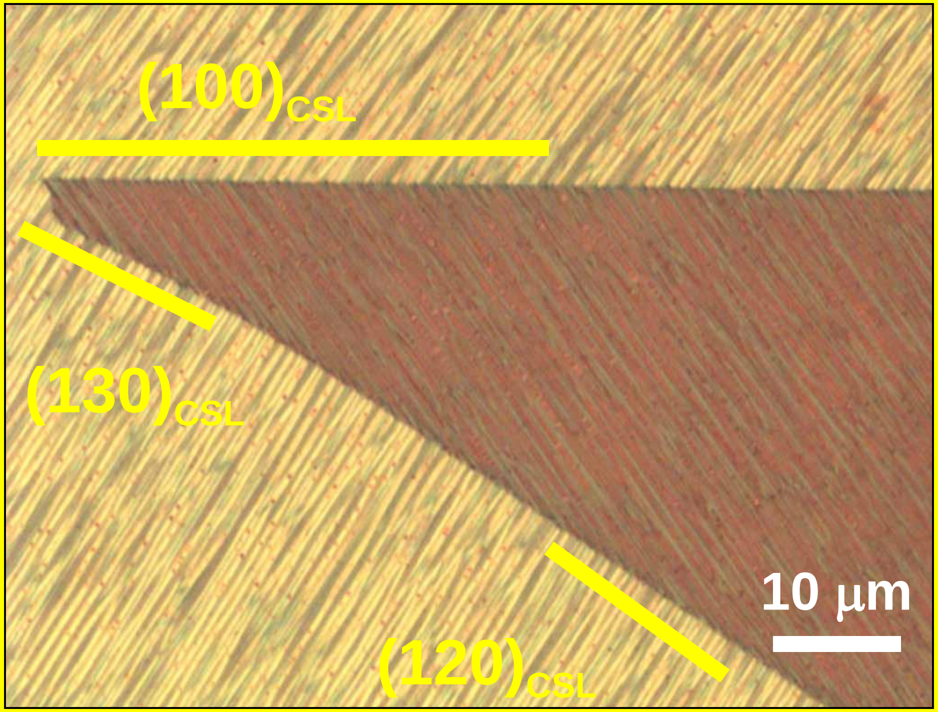

Phase diagram for the Σ3 GBs in Cu

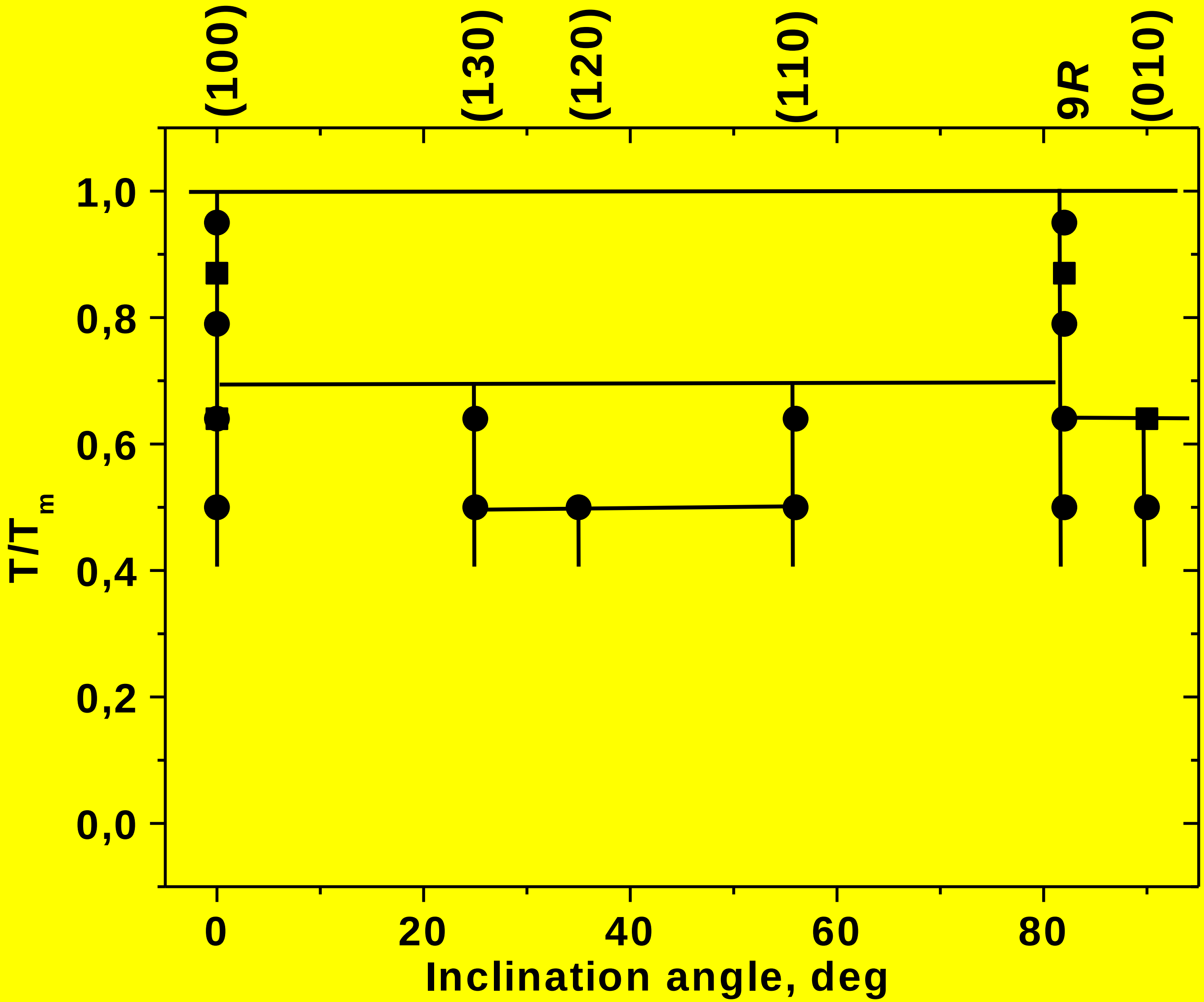

Phase diagram for the Σ3 GBs in Cu

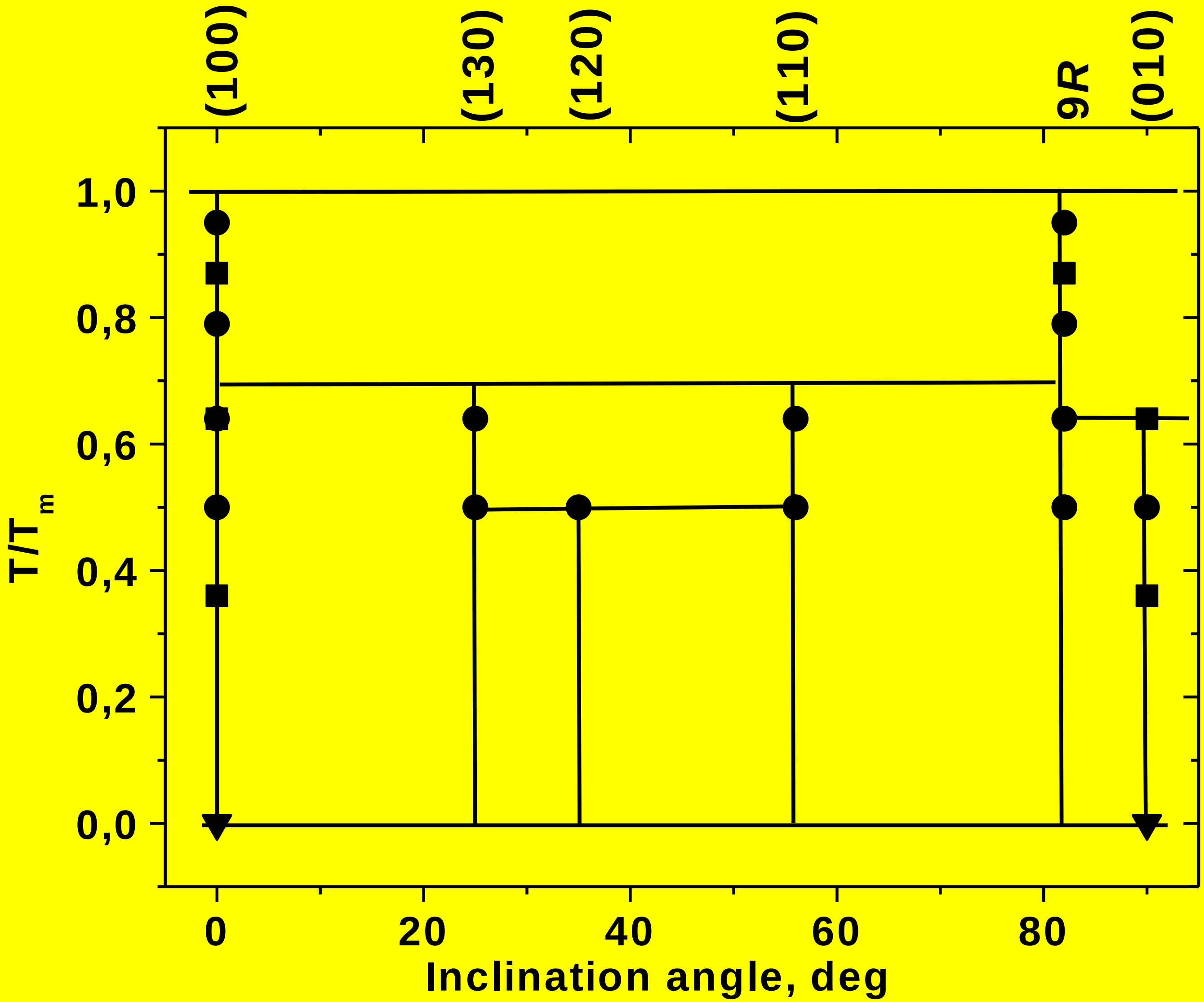

Σ3 tilt GB in Cu: increase of number of facets with decreasing temperature

800°C

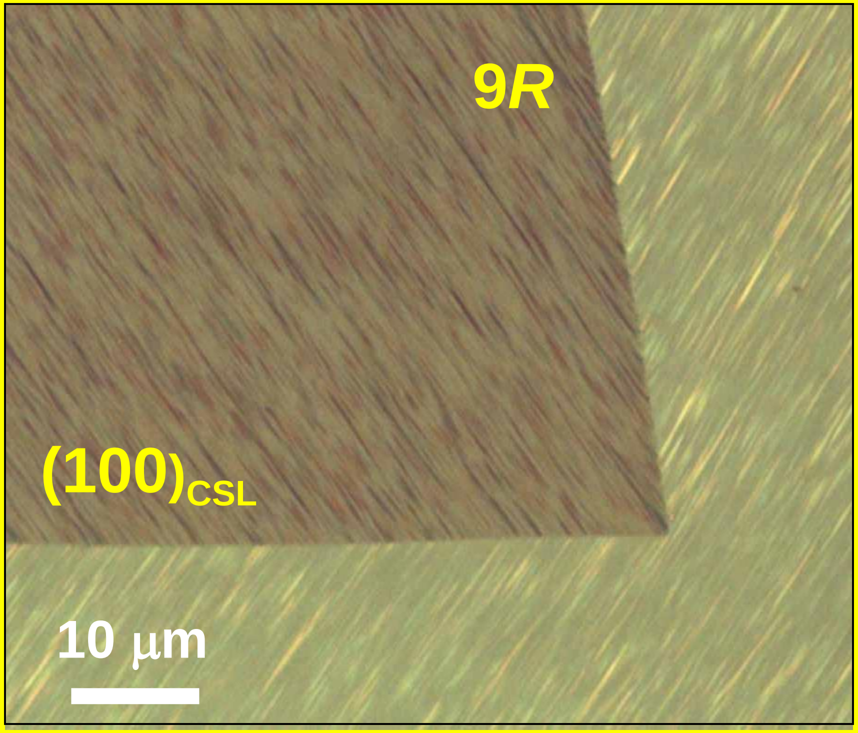

400°C

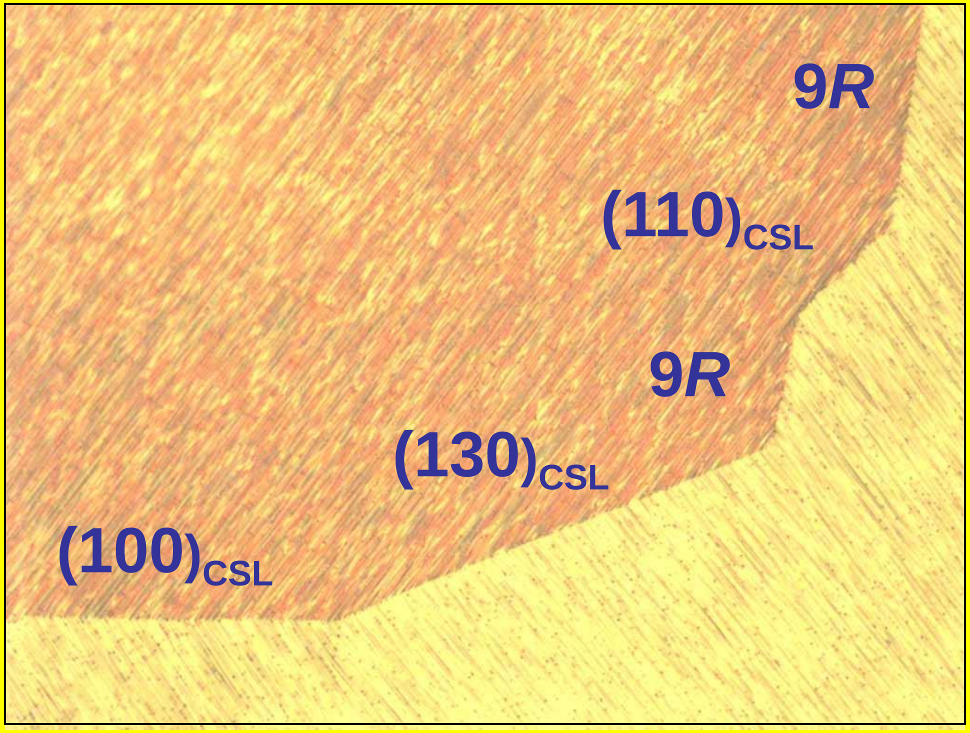

Σ3 tilt GB in Cu: increase of number of facets with decreasing temperature

650°C

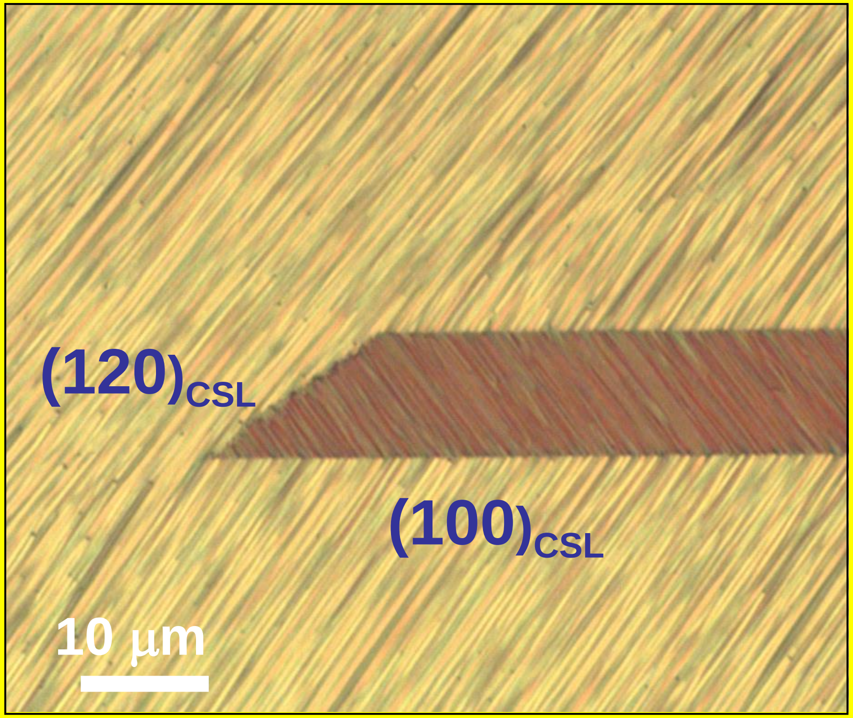

400°C

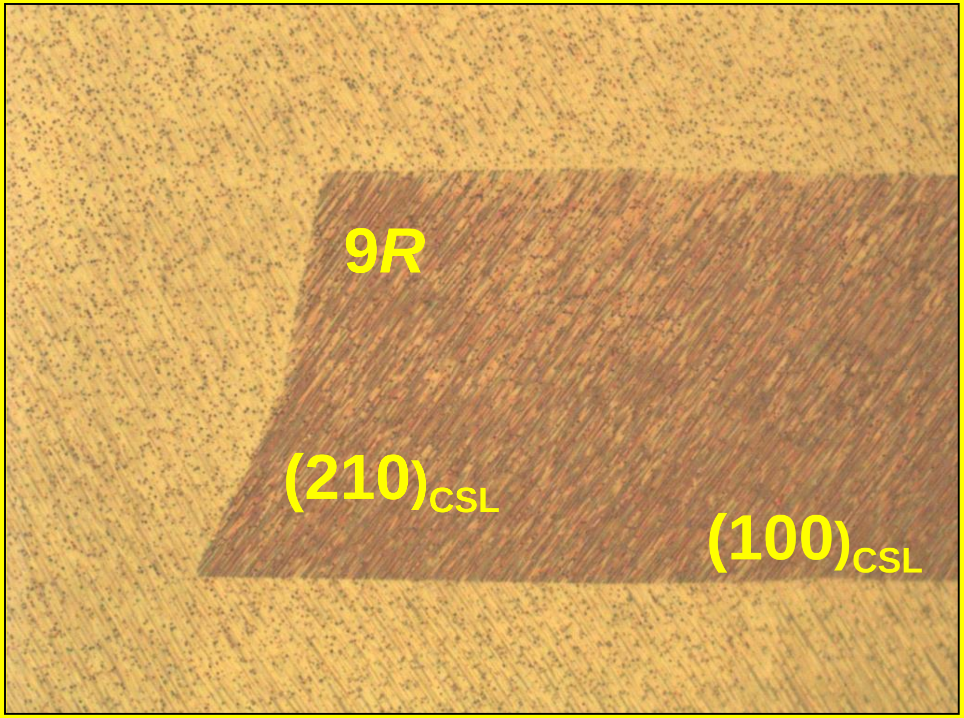

Σ3 and Σ9 grain boundaries in Cu. Experiment:

- By temperature decrease the number of (crystallographically different) facets increases up to six
- The GB facets are not separated by the rough GB portions. The facets form sharp edges.

Scheme of Mo bicrystal with coaxial Σ3 GBs

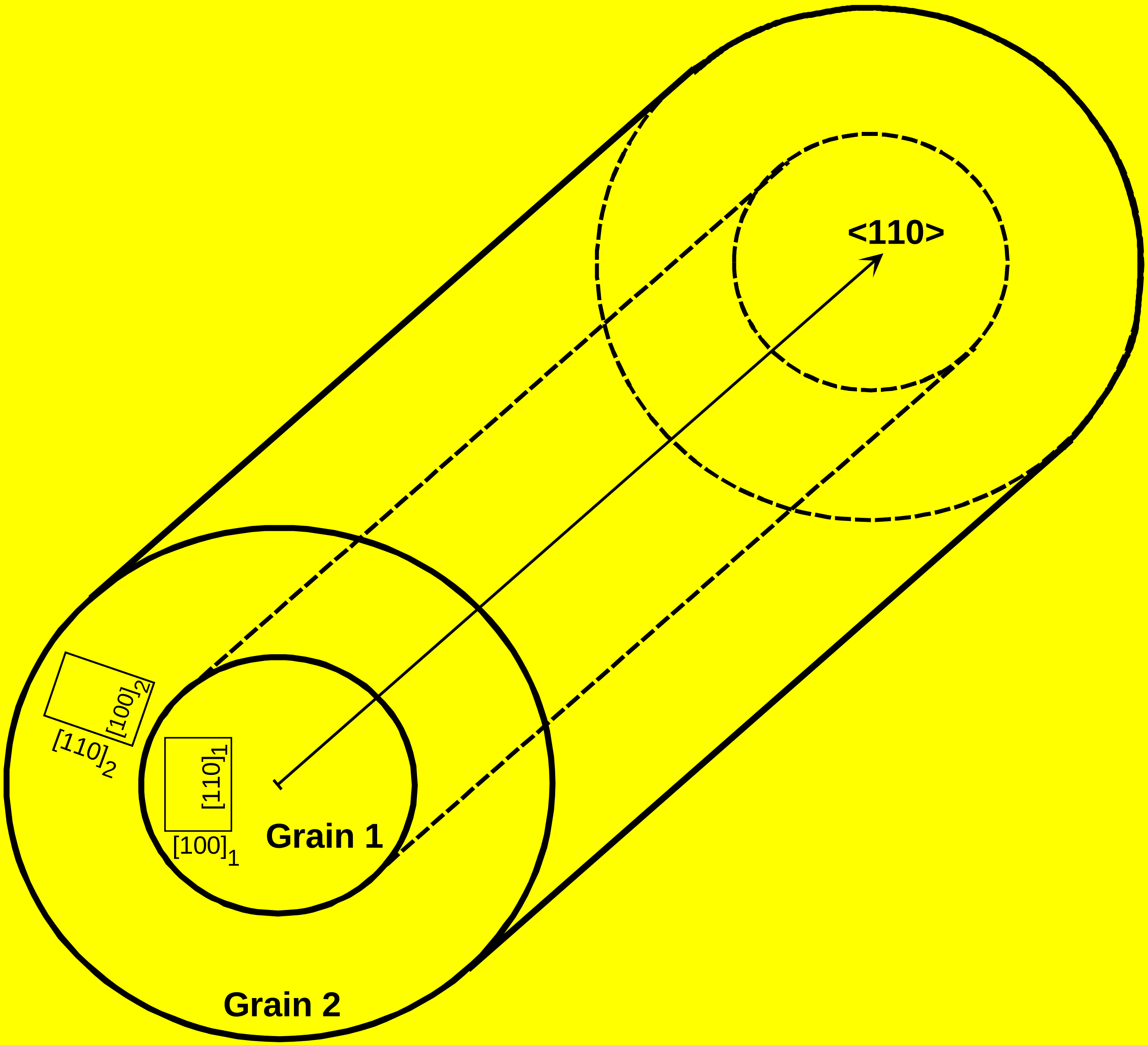

Shape of Σ3 tilt GB in Mo

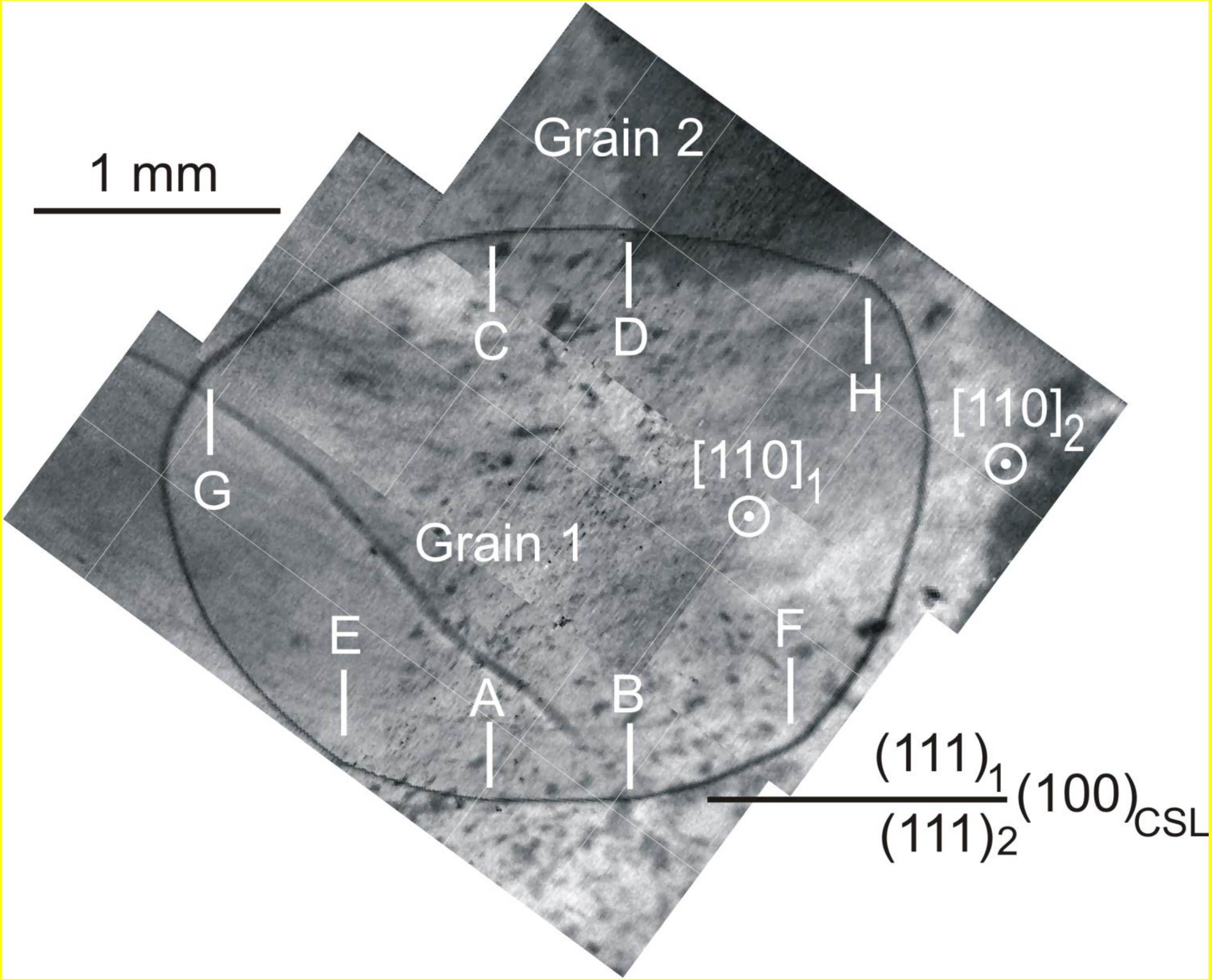

How a facet contacts curved (rough) surface or interface

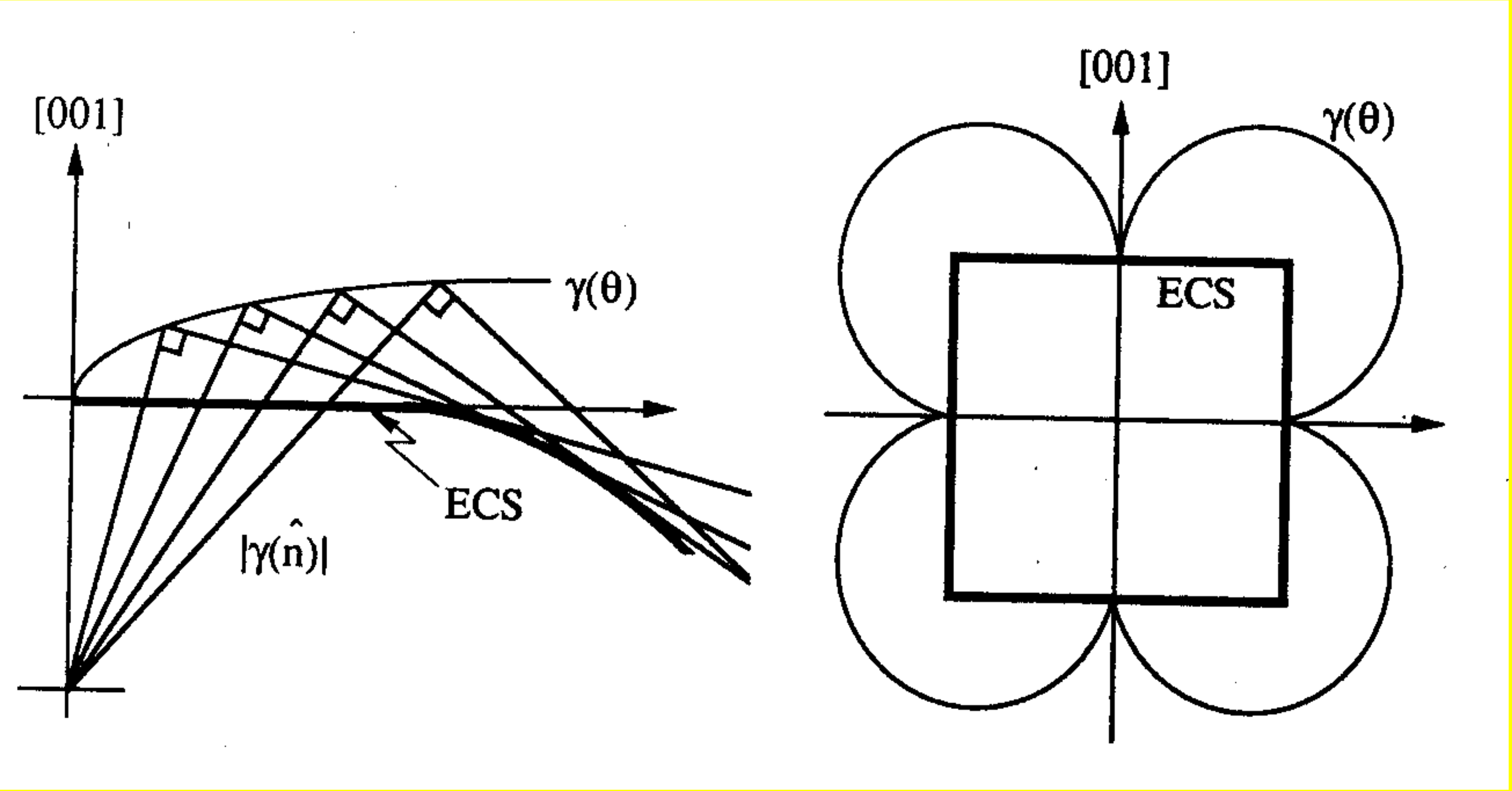

Roughening of Pb surfaces: P-T behaviour

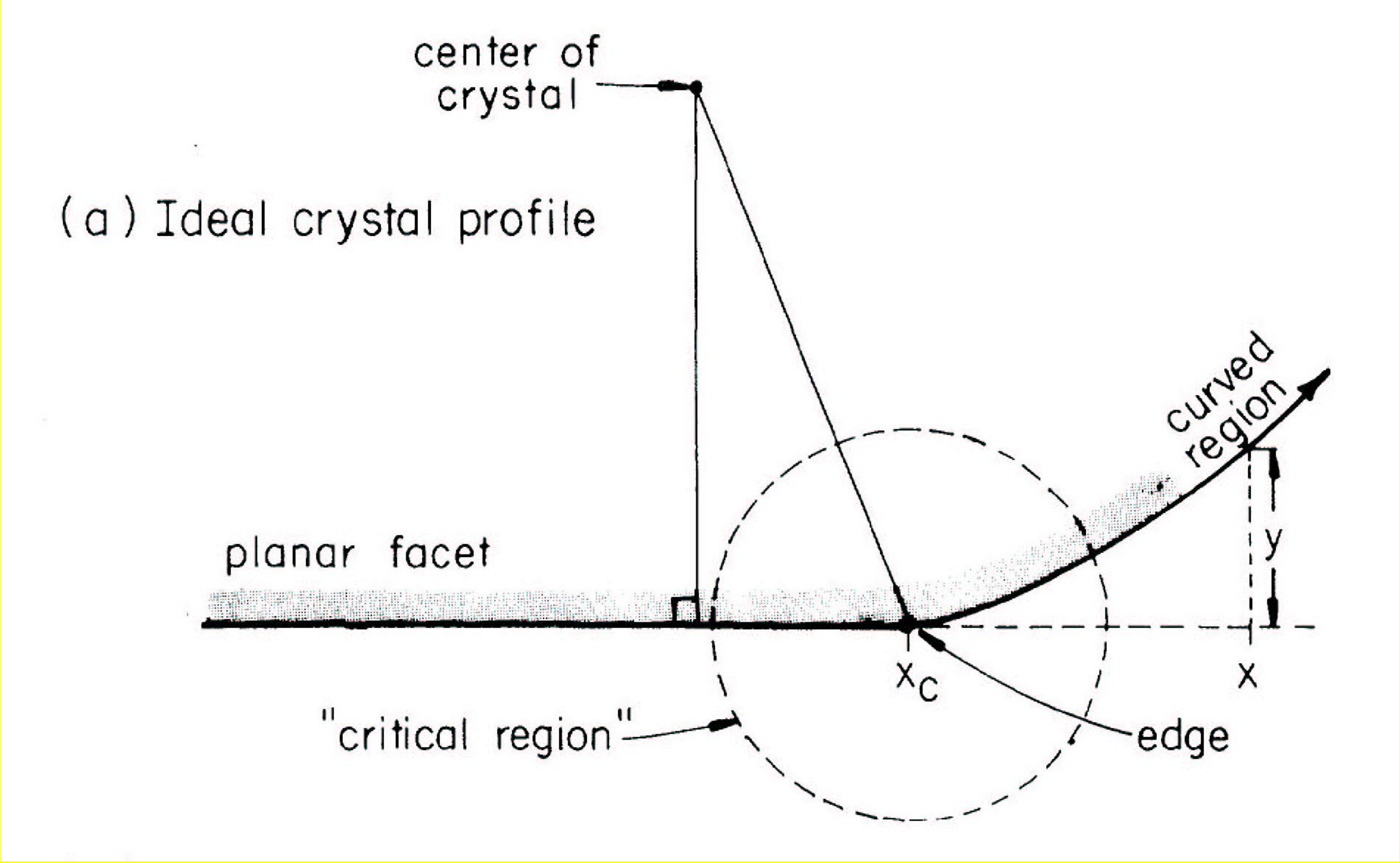

C. Rottman, R. Wortis, J.C. Heyraud, J.J. Mètois. *PRL* 52 (1984) 1009

Rounding near cristal facet

$$y = A(x - x_c)^\theta + \text{higher order terms}$$

Andreev theory (mean-field approximation):

$\theta = 2$

Pokrovsky-Talapov theory (including fluctuations):

$\theta = 3/2$

A.F. Andreev. *Zh.Eksp.Teor.Fiz.* 79 (1981) 2042

V.L. Pokrovsky, A.L. Talapov. *PRL* 42 (1979) 65 and *Zh.Eksp.Teor.Fiz.* 78 (1980) 269

Roughening of Pb surfaces: P-T behaviour

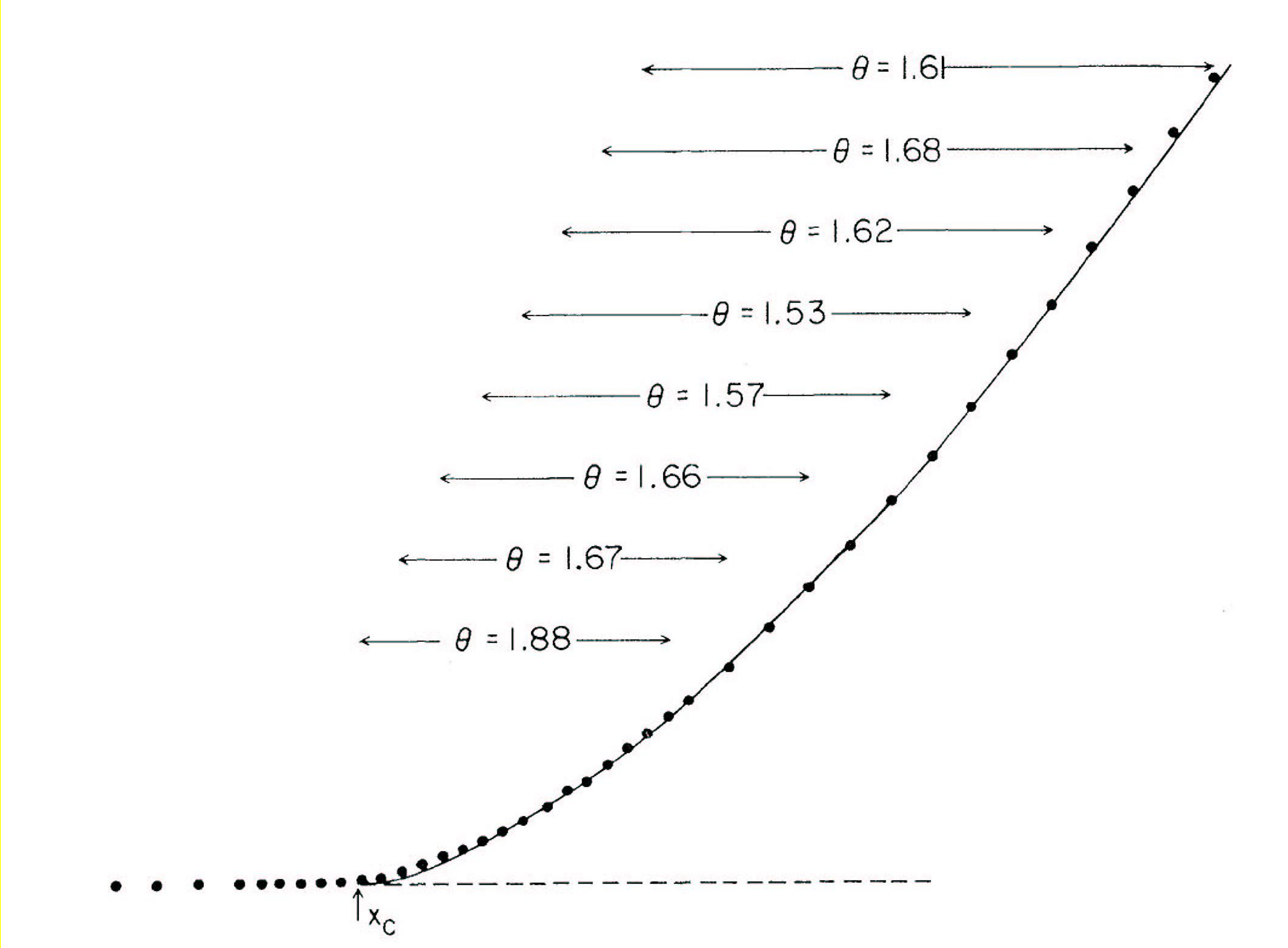

C. Rottman, R. Wortis, J.C. Heyraud, J.J. Mėtois. *PRL* 52 (1984) 1009

Shape of Σ3 GB in scaling coordinates

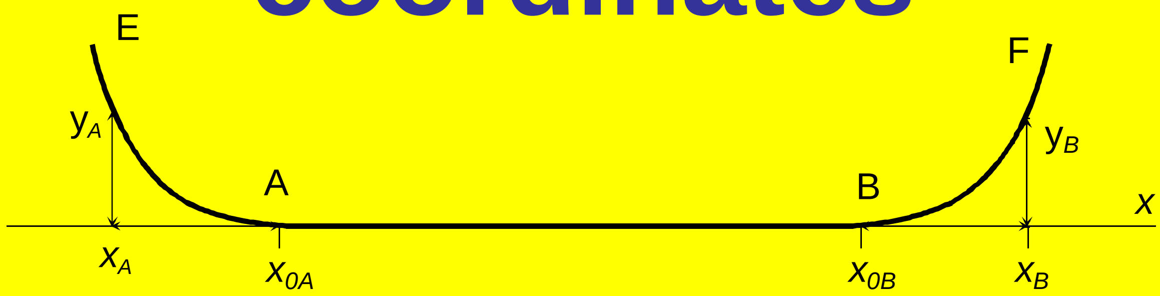

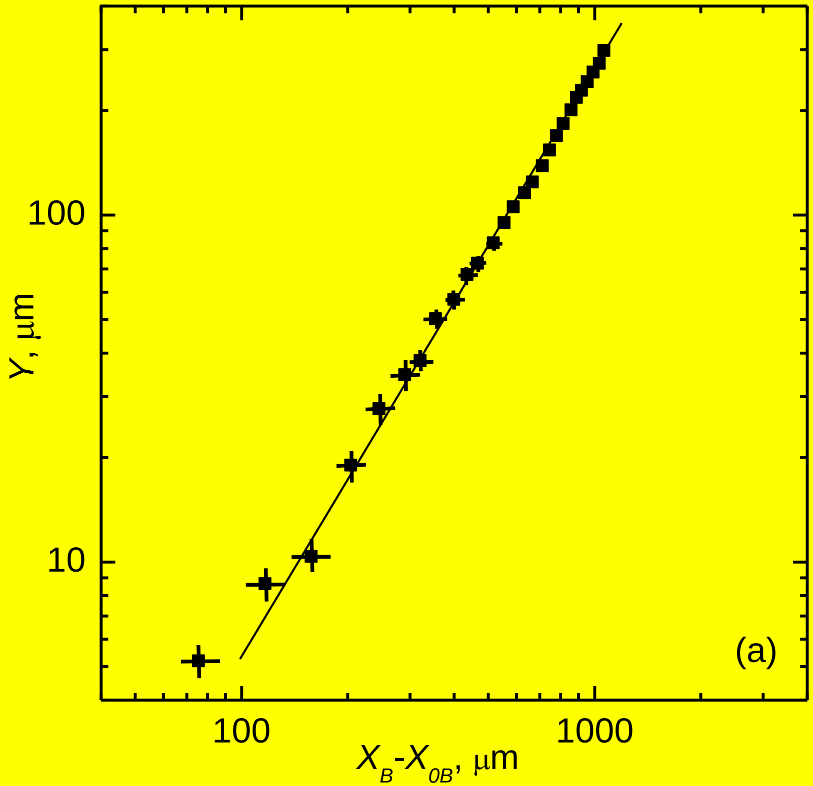

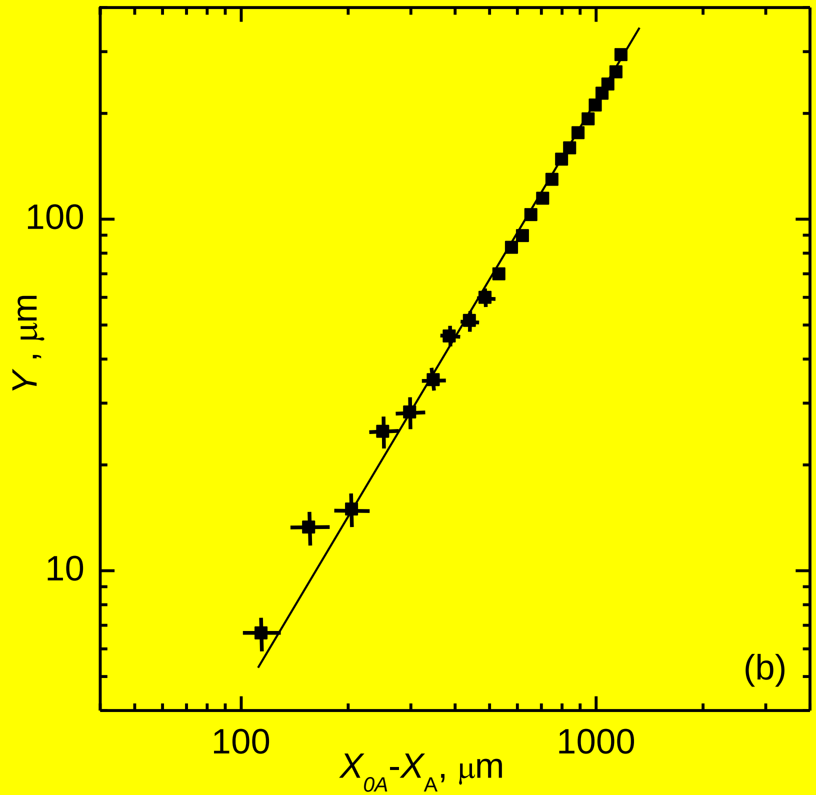

Shape of Σ3 tilt GB in Mo

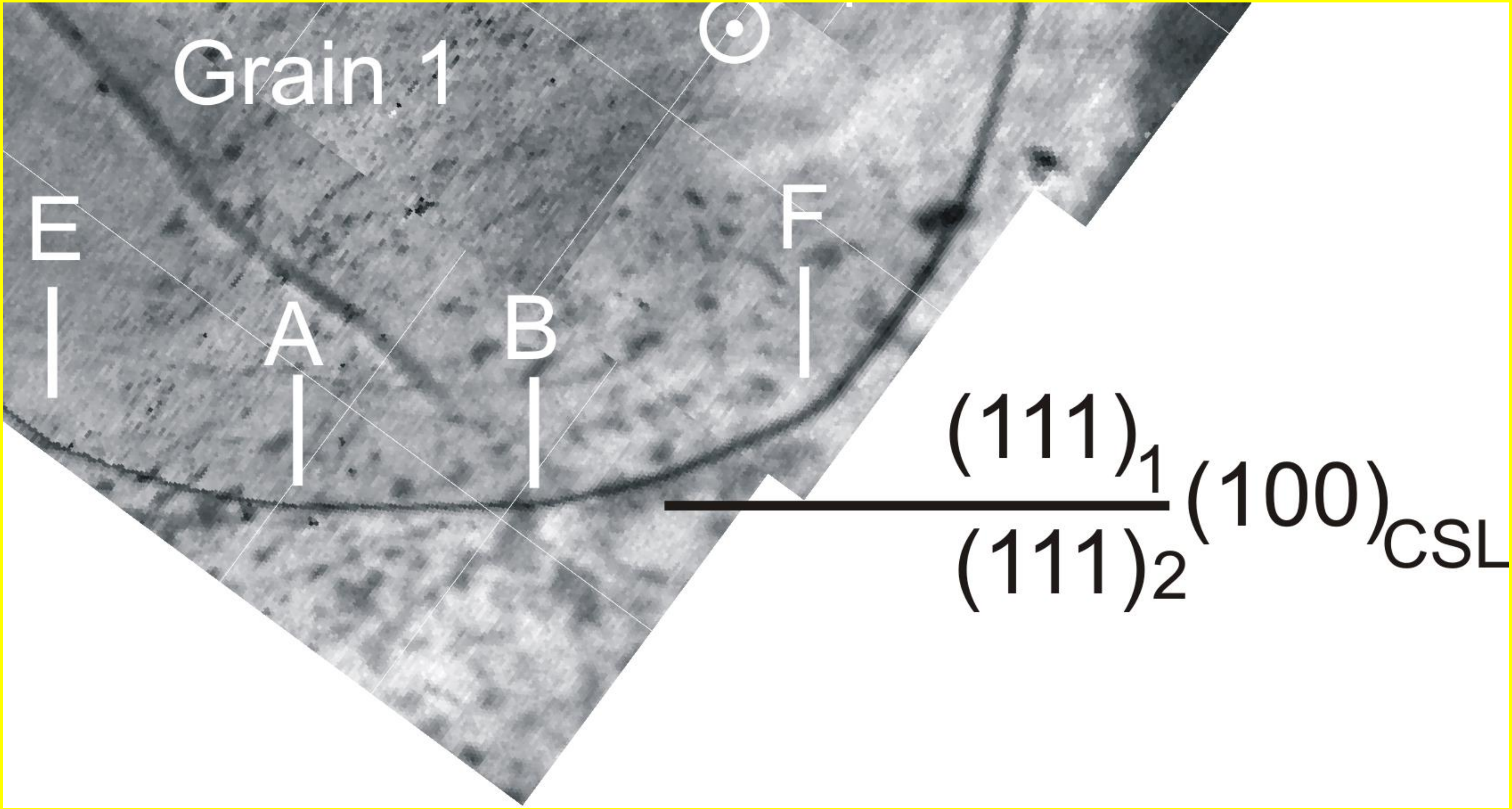

Roughening of 2nd order: Pokrovsky-Talapov behaviour

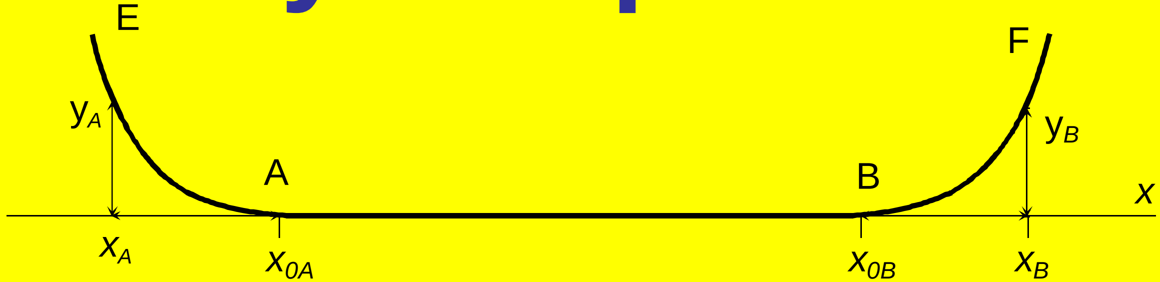

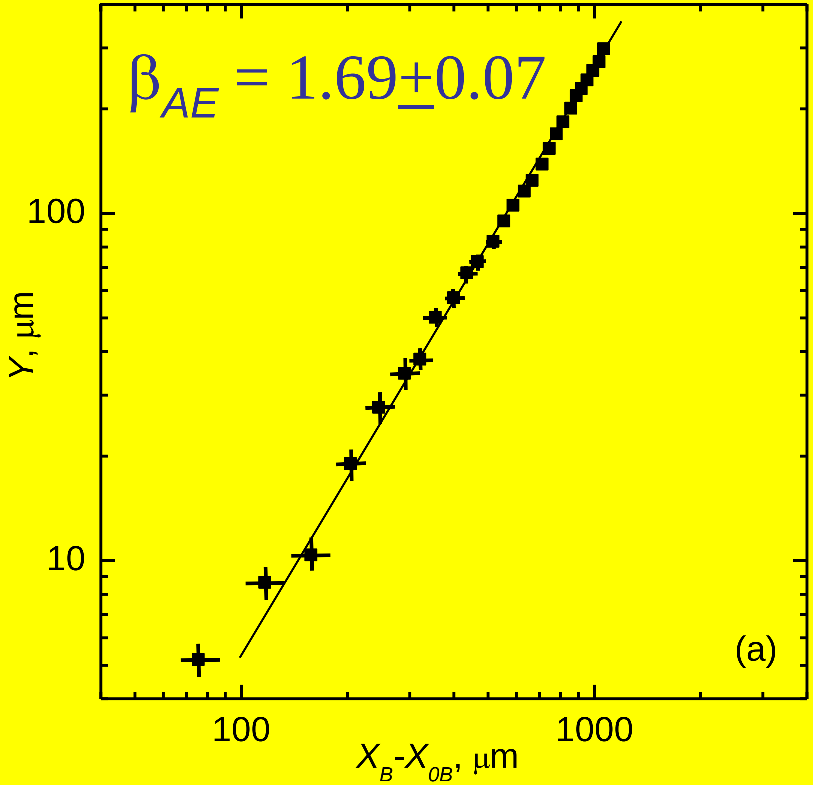

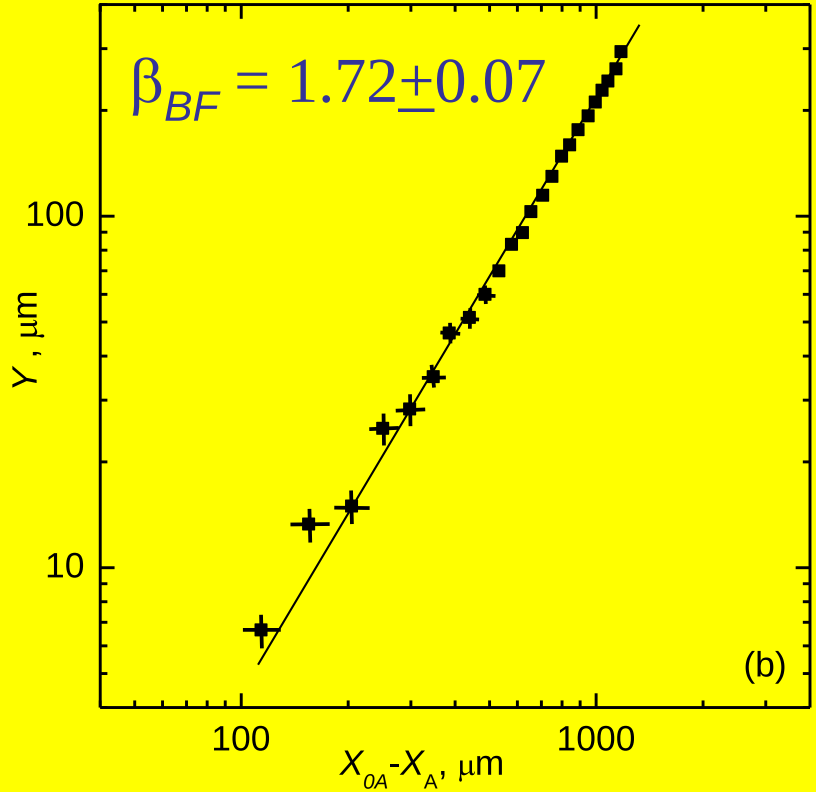

Фазовые превращения:

-- на внутренних границах раздела (смачивание)

Смачивание внешней поверхности

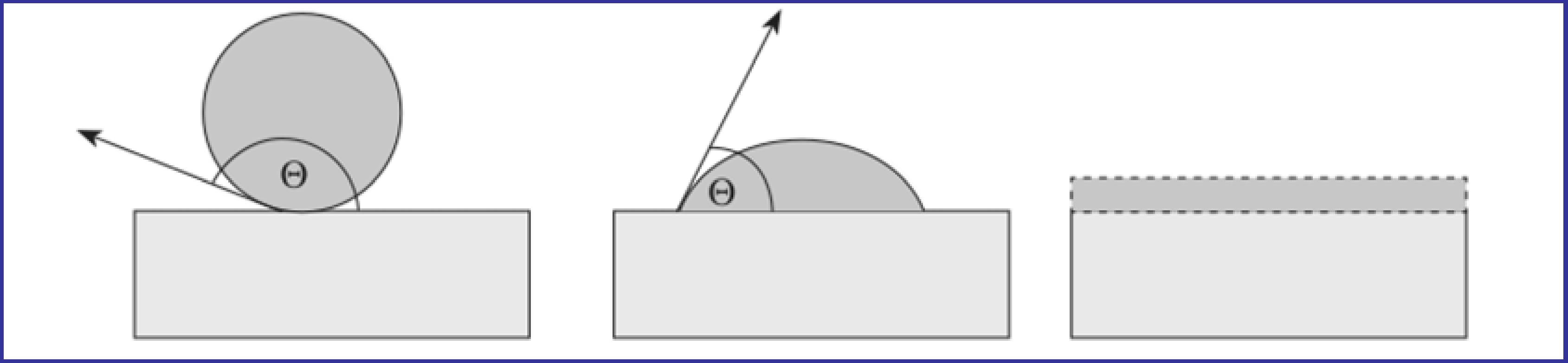

Фазовый переход смачивания на ГЗ

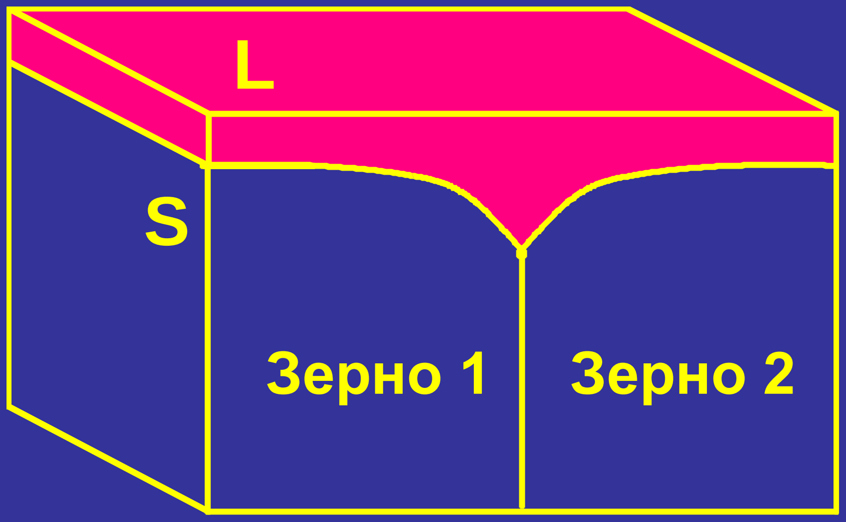

Фазовый переход смачивания на ГЗ

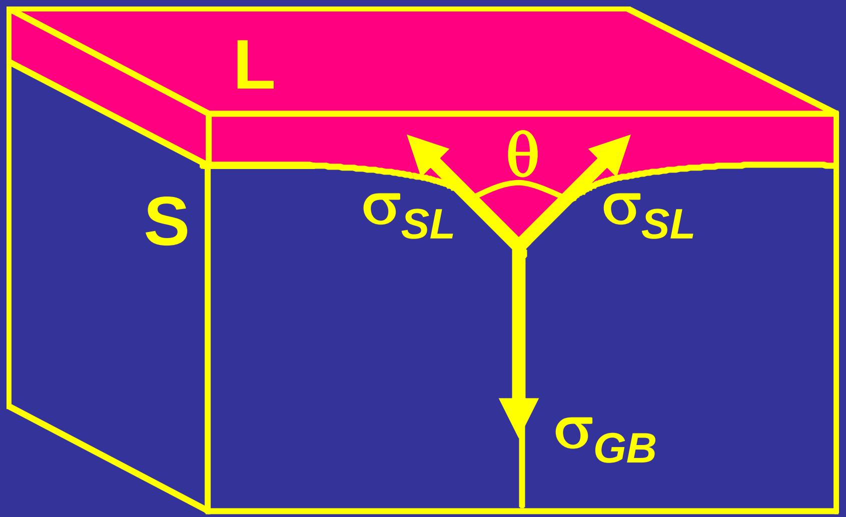

$\sigma_{GB} < 2\sigma_{SL}$, $\theta > 0$

Фазовый переход смачивания на ГЗ

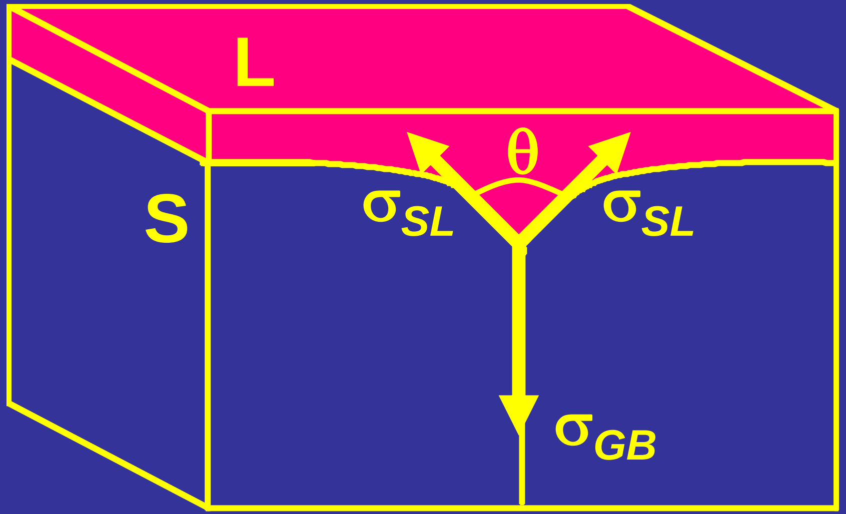

$\sigma_{GB} < 2\sigma_{SL}$, $\theta > 0$

Граница зерен в контакте с расплавом устойчива

Фазовый переход смачивания на ГЗ

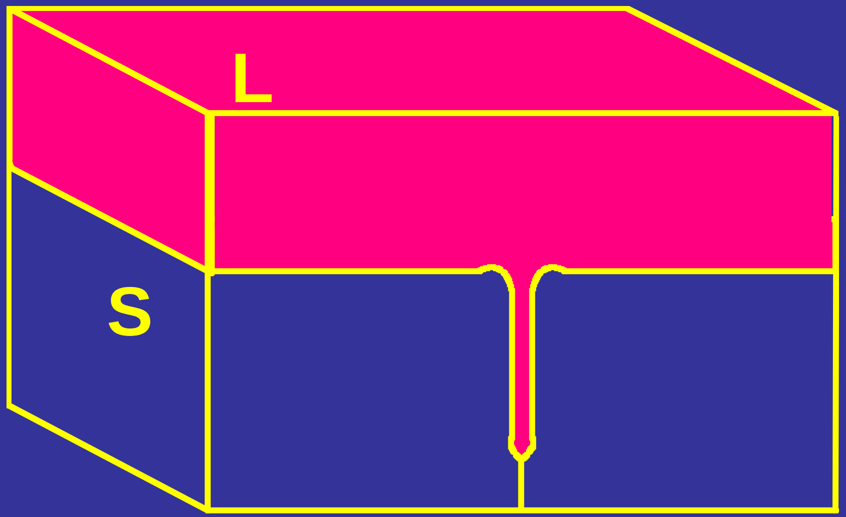

$\sigma_{GB} > 2\sigma_{SL}$, $\theta = 0$

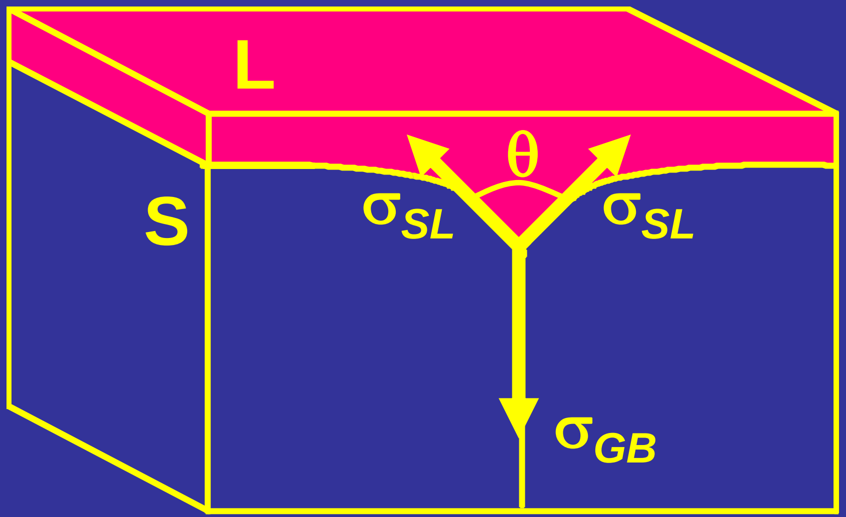

$\sigma_{GB} < 2\sigma_{SL}$, $\theta > 0$

Граница зерен в контакте с расплавом устойчива

Фазовый переход смачивания на ГЗ

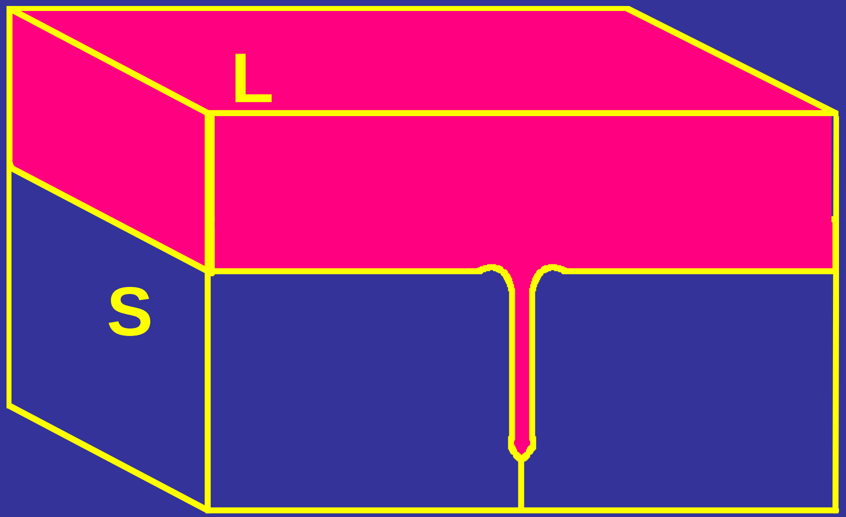

$\sigma_{GB} > 2\sigma_{SL}$, $\theta = 0$

Граница зерен в контакте с расплавом неустойчива и должна заменяться жидкой прослойкой

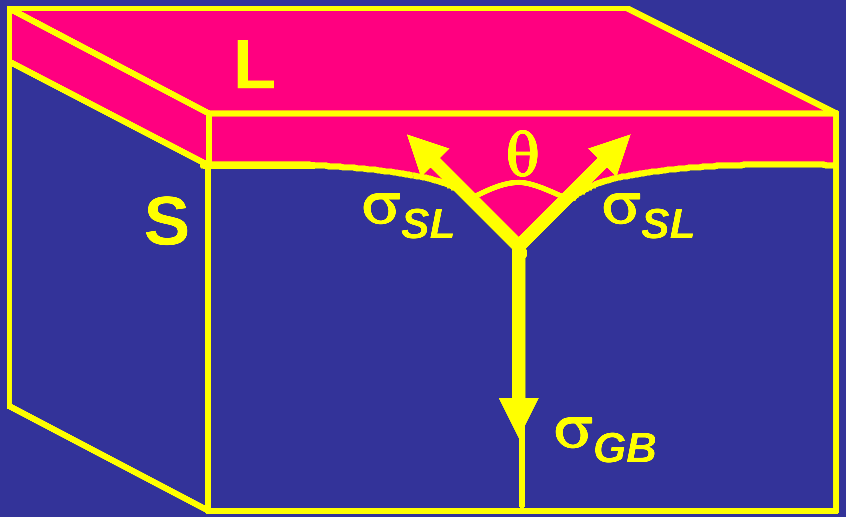

$\sigma_{GB} < 2\sigma_{SL}$, $\theta > 0$

Граница зерен в контакте с расплавом устойчива

Фазовый переход смачивания на ГЗ

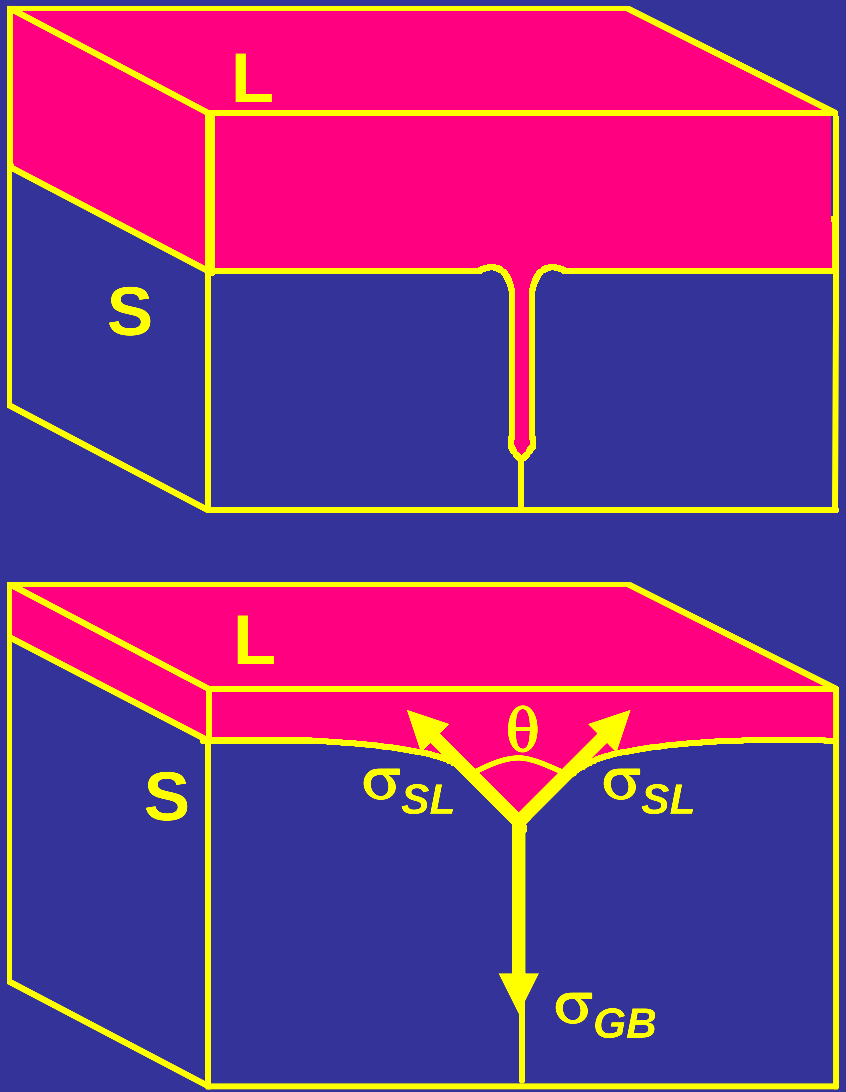

Есть системы,
в которых такое
превращение
происходит с
повышением
температуры

Фазовый переход смачивания на ГЗ

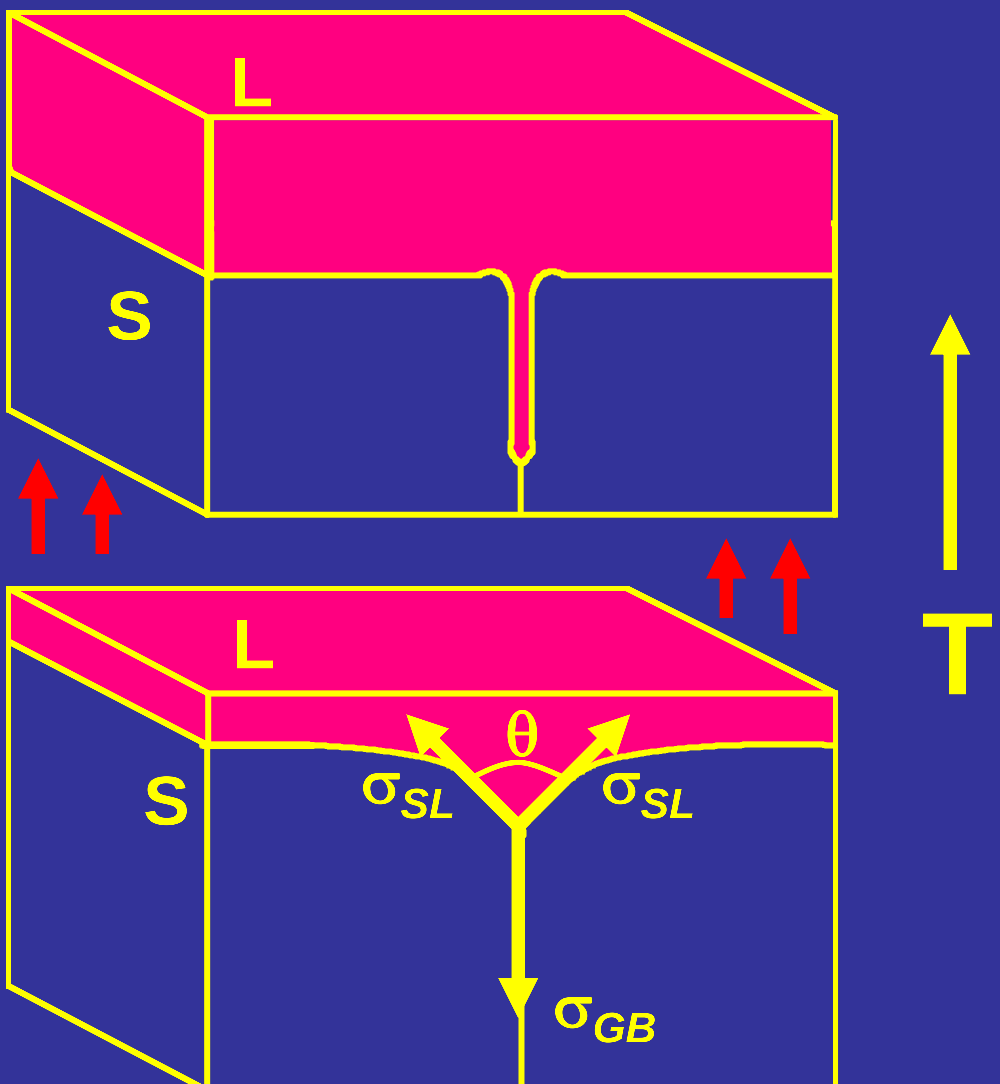

Есть системы, в которых такое превращение происходит с повышением температуры

Фазовый переход смачивания на ГЗ

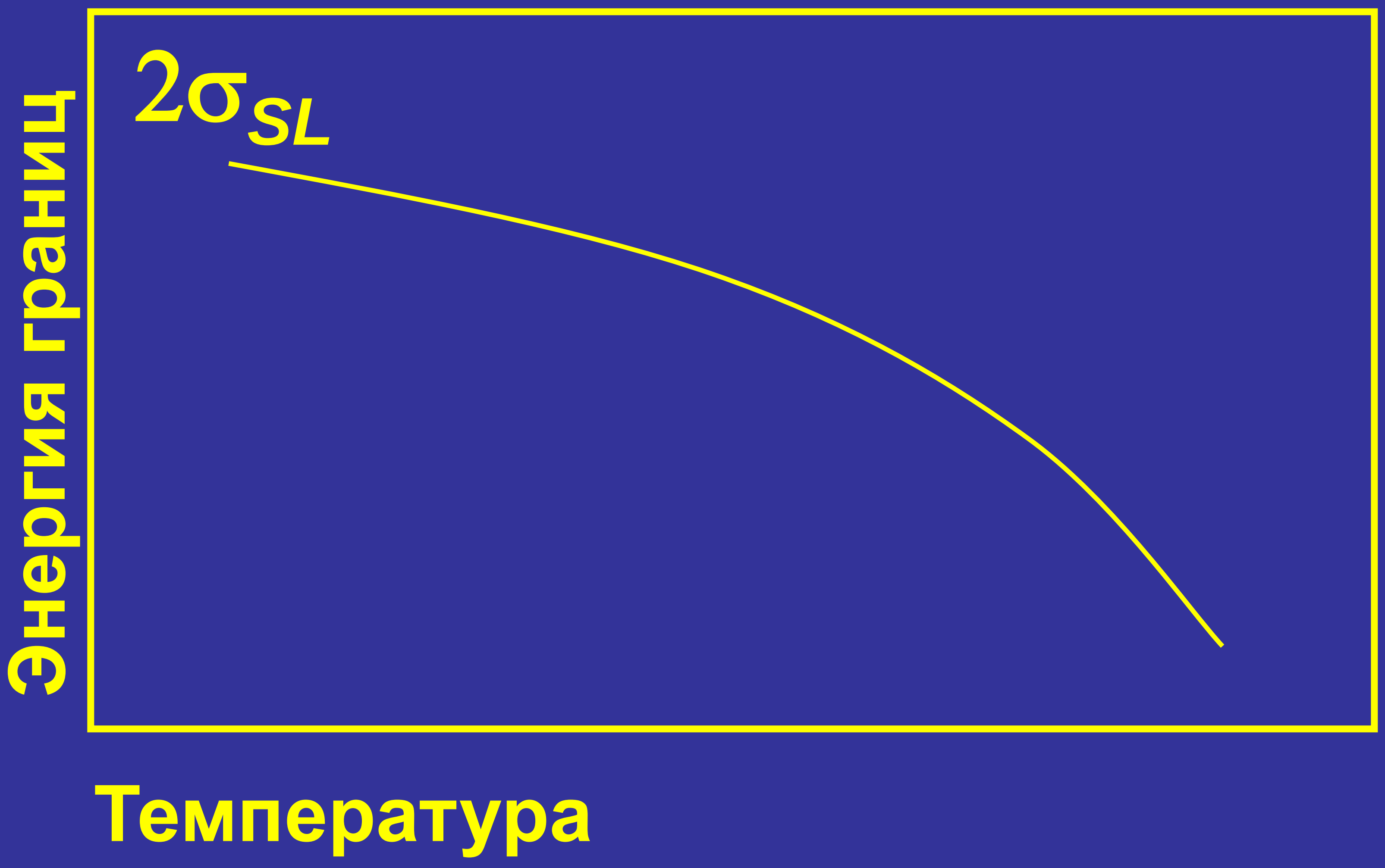

Фазовый переход смачивания на ГЗ

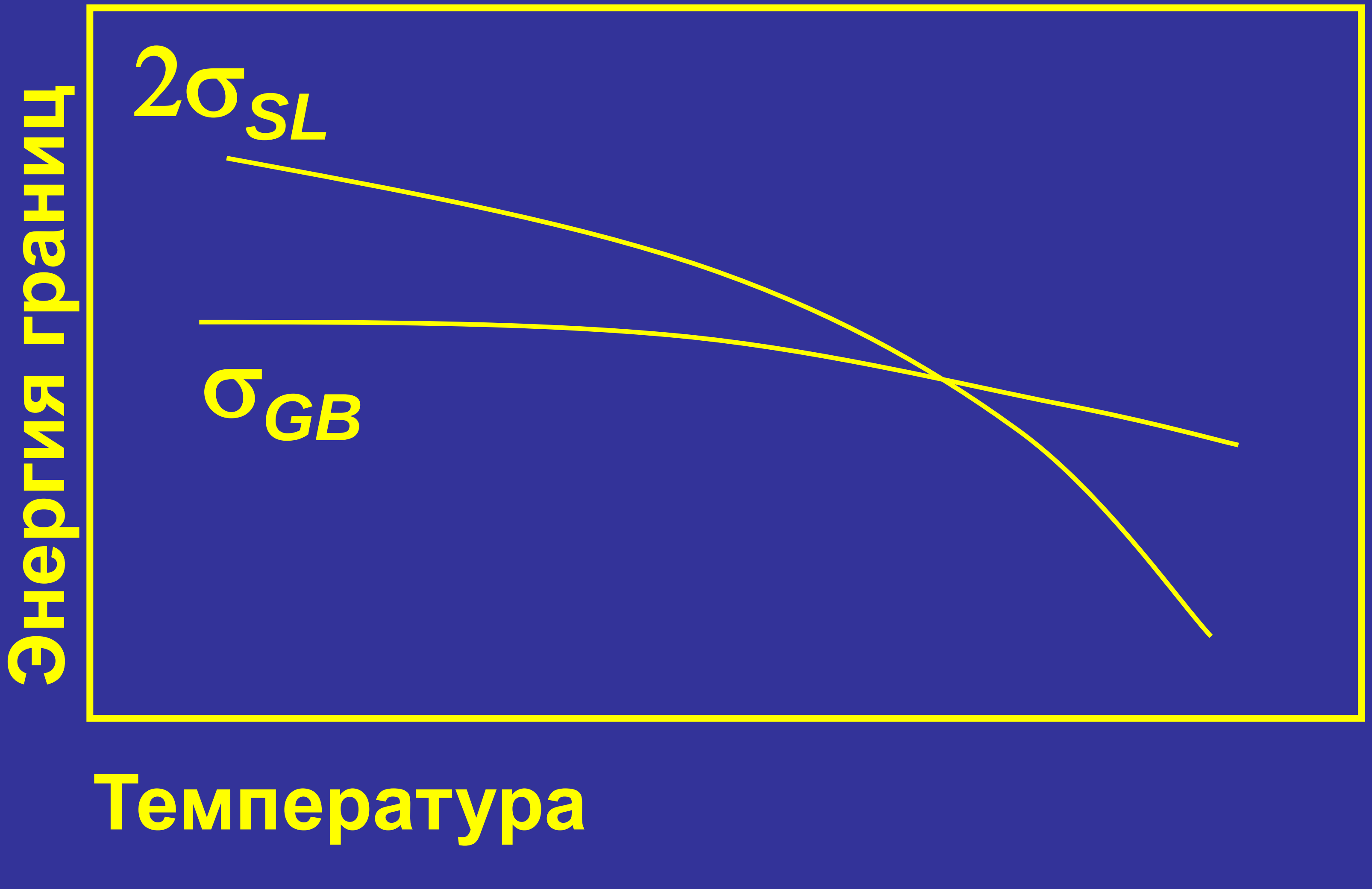

Фазовый переход смачивания на ГЗ

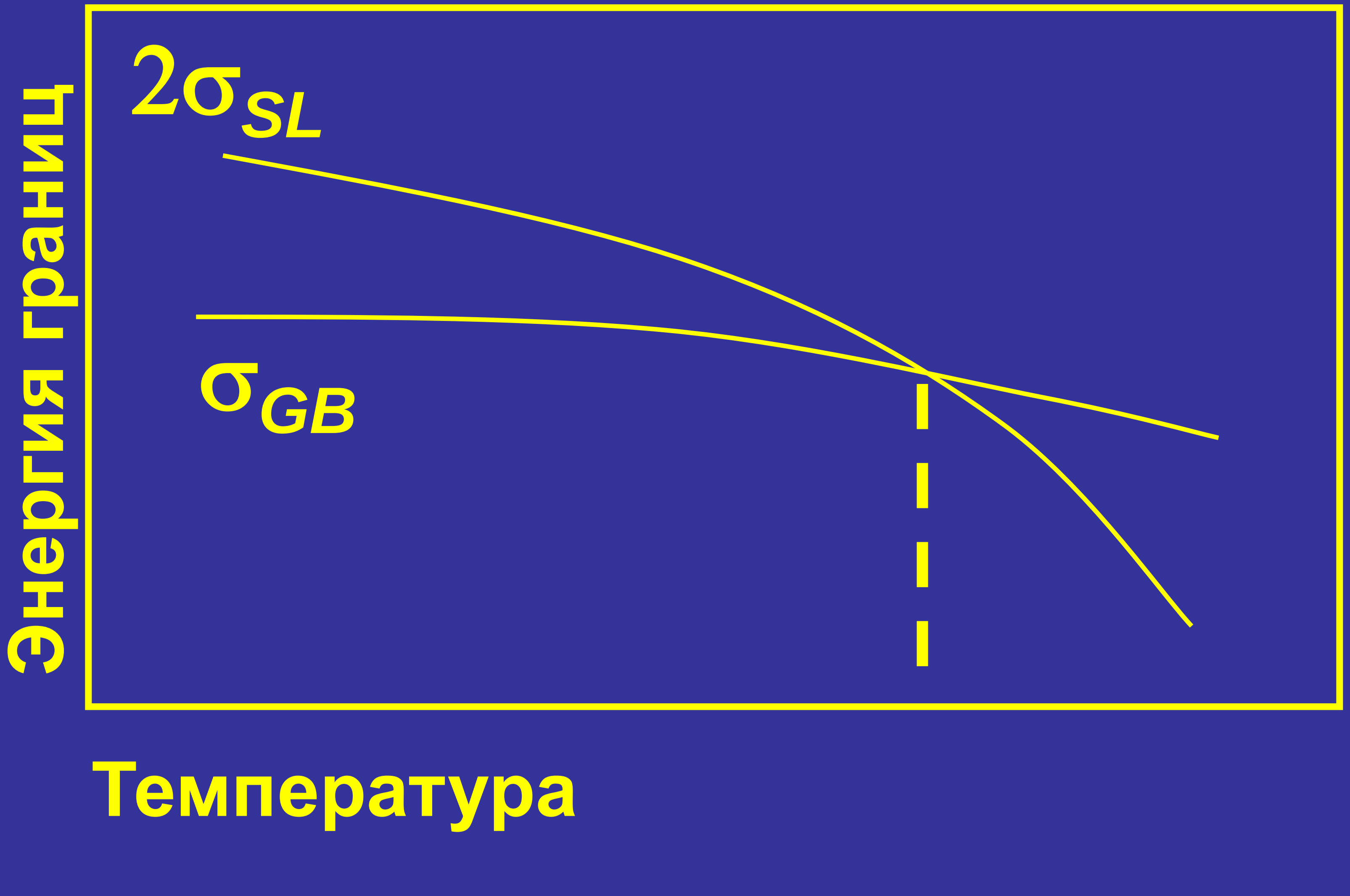

Фазовый переход смачивания на ГЗ

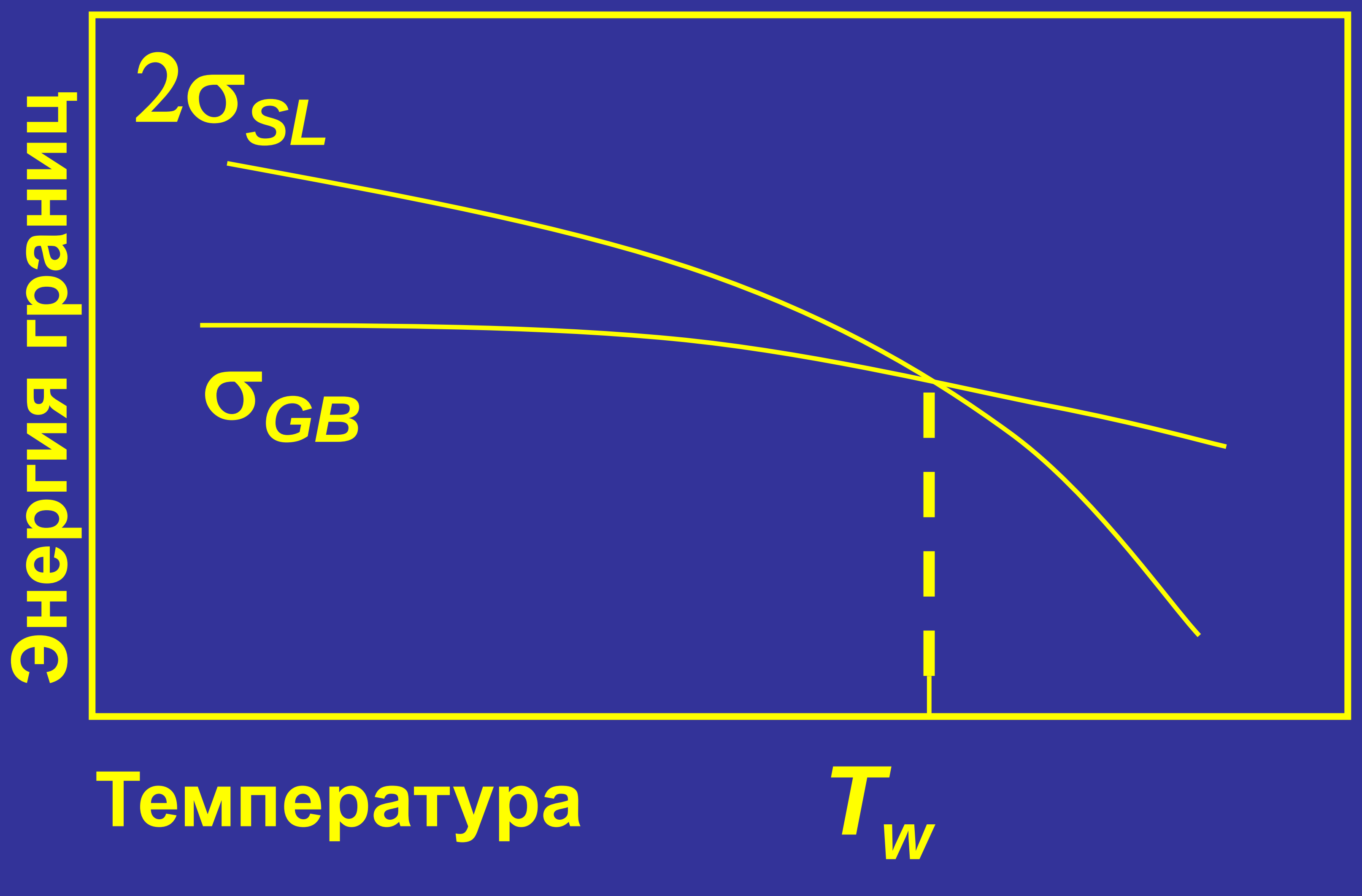

Фазовый переход смачивания на ГЗ

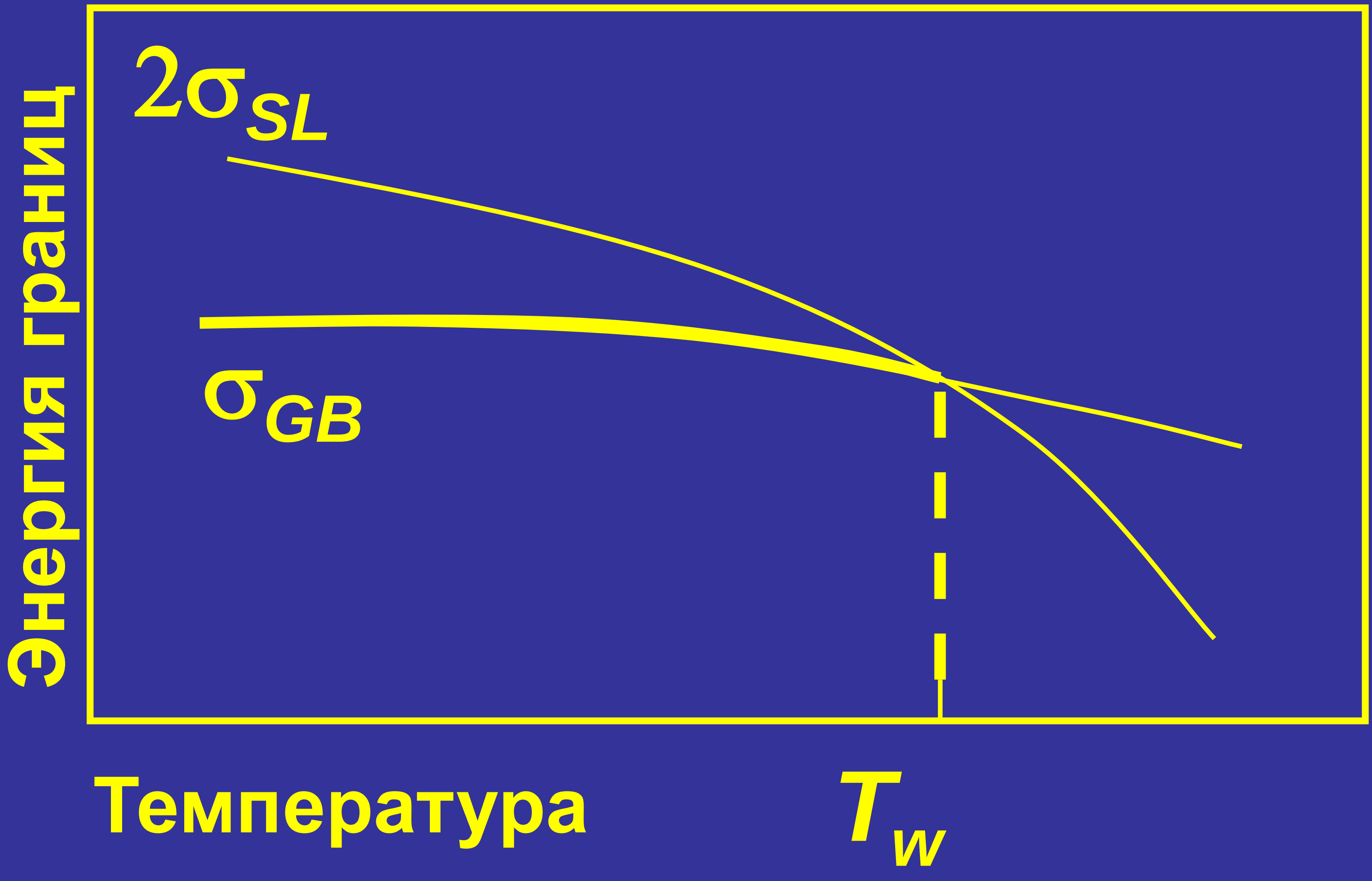

Фазовый переход смачивания на ГЗ

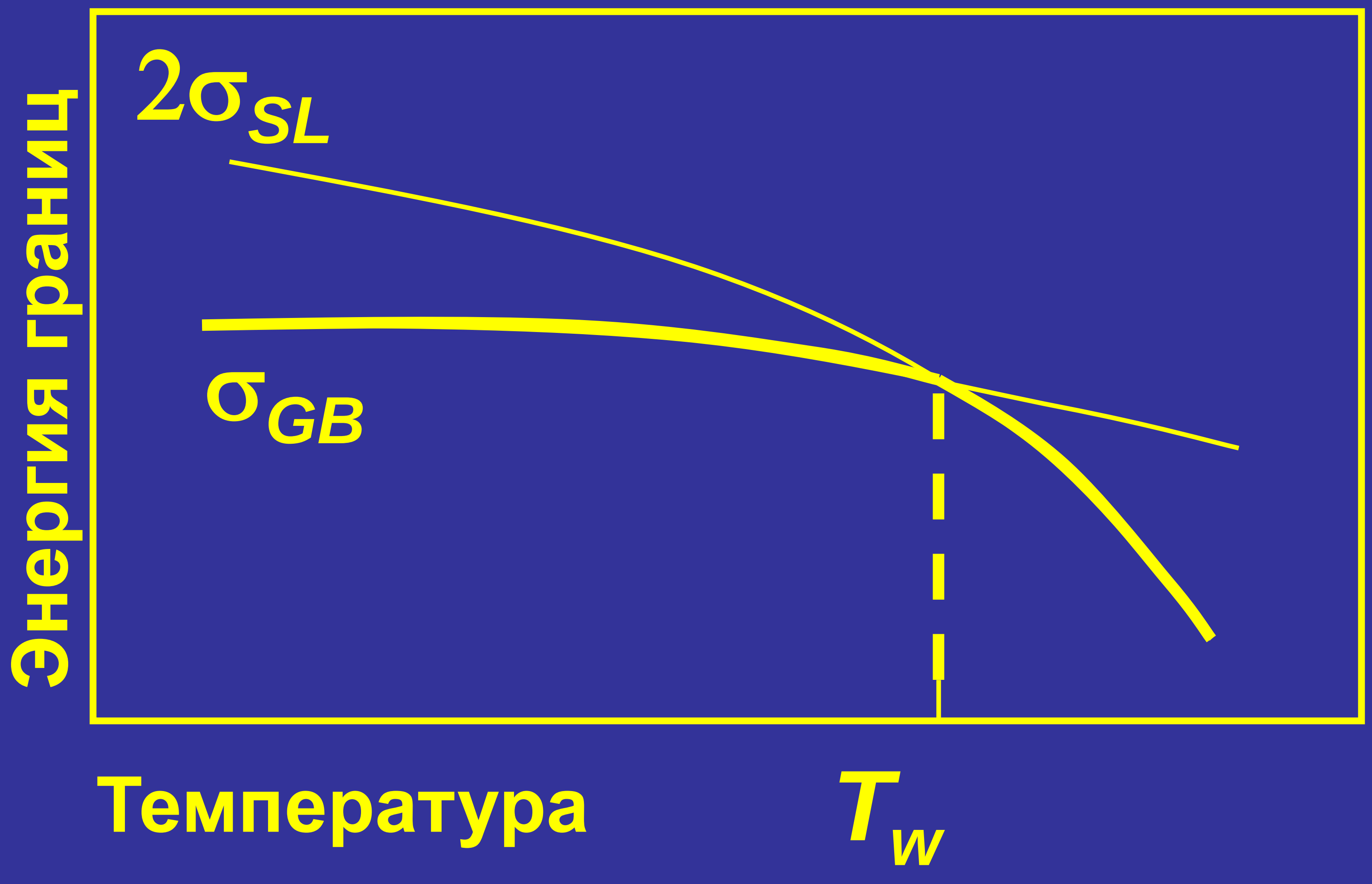

Фазовый переход смачивания на ГЗ

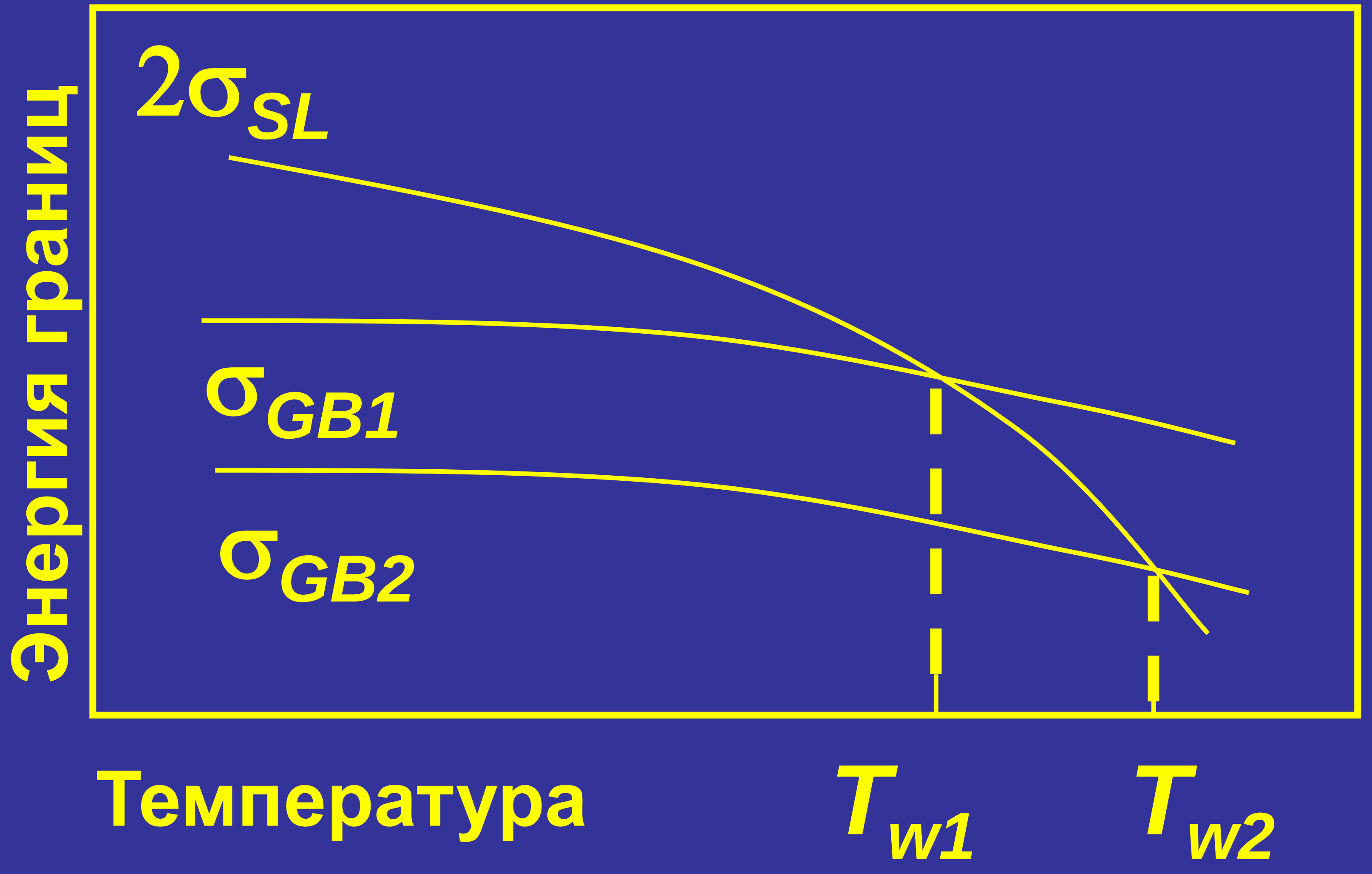

Фазовый переход смачивания на ГЗ

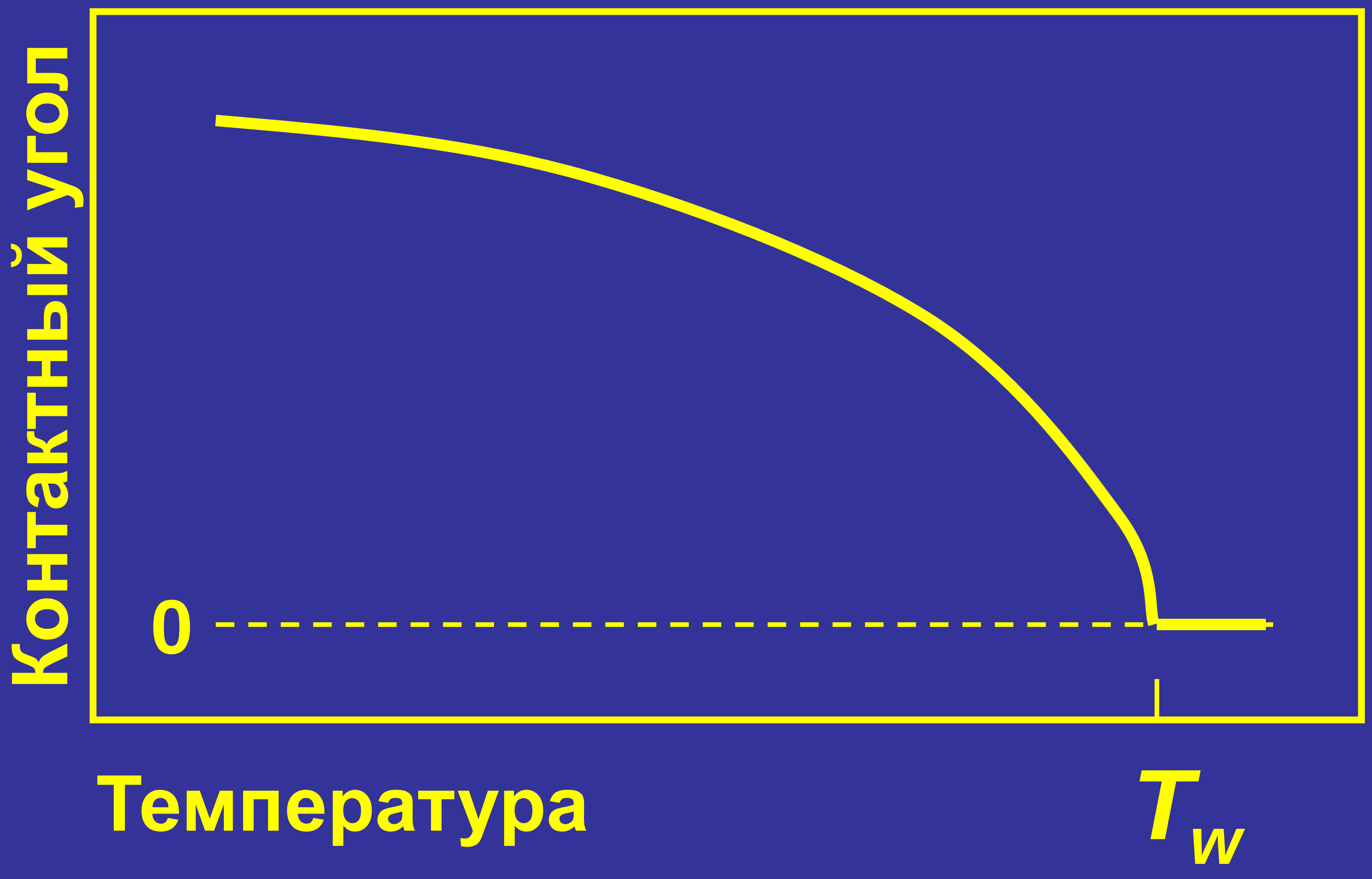

Фазовый переход смачивания на ГЗ

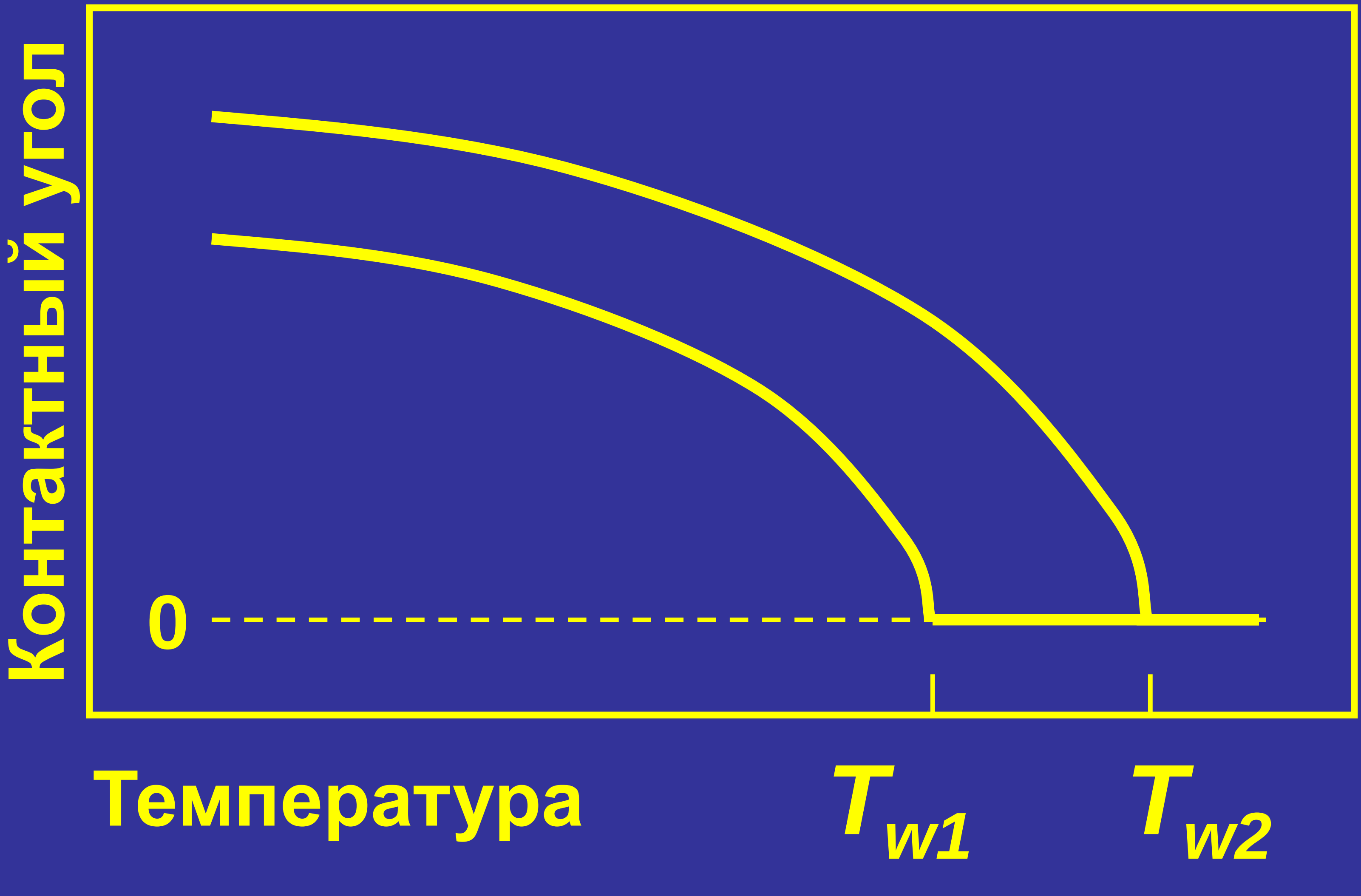

Система Al-Sn

граница наклона

$\langle 011\rangle\{001\}$ $\theta = 38{,}5°$

С повышением температуры контактный угол понижается, становится равным нулю при 617°С и остается равным нулю при дальнейшем повышении температуры

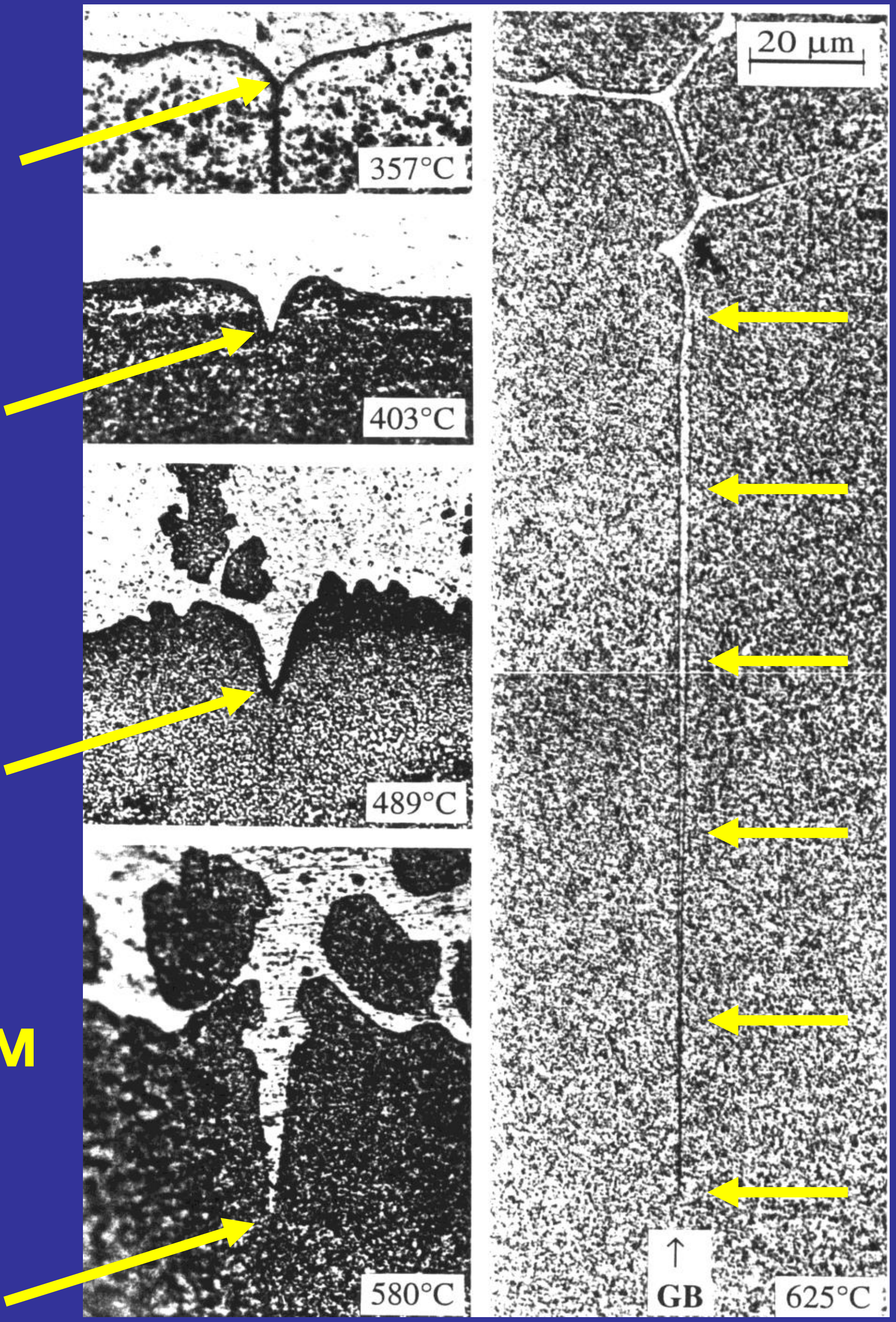

Фазовый переход смачивания на ГЗ

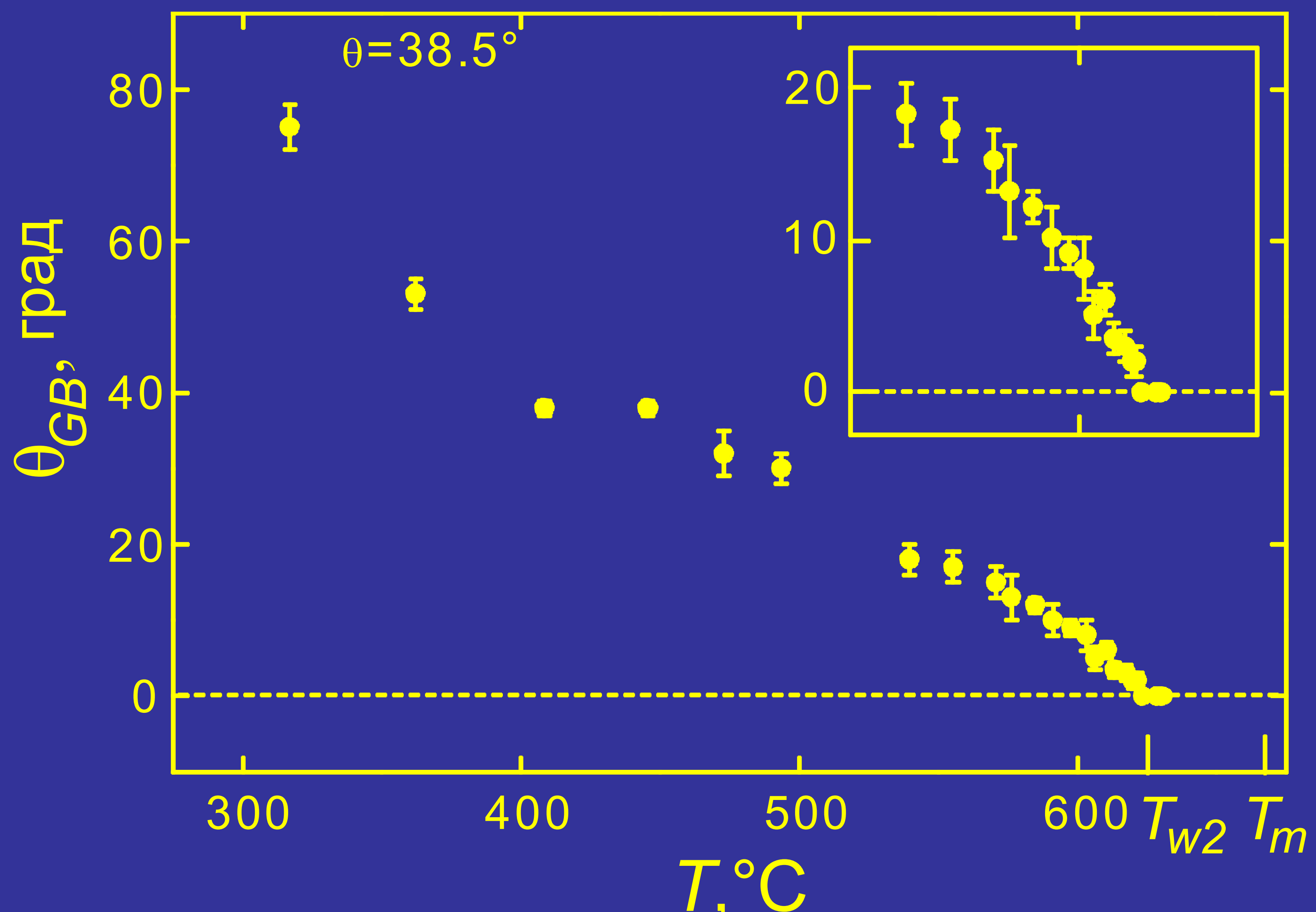

Вторая (смачивающая) фаза может быть твёрдой

Fe–1.3 вес.% C, 915°C, все γ-ГЗ “смочены” Fe_3C

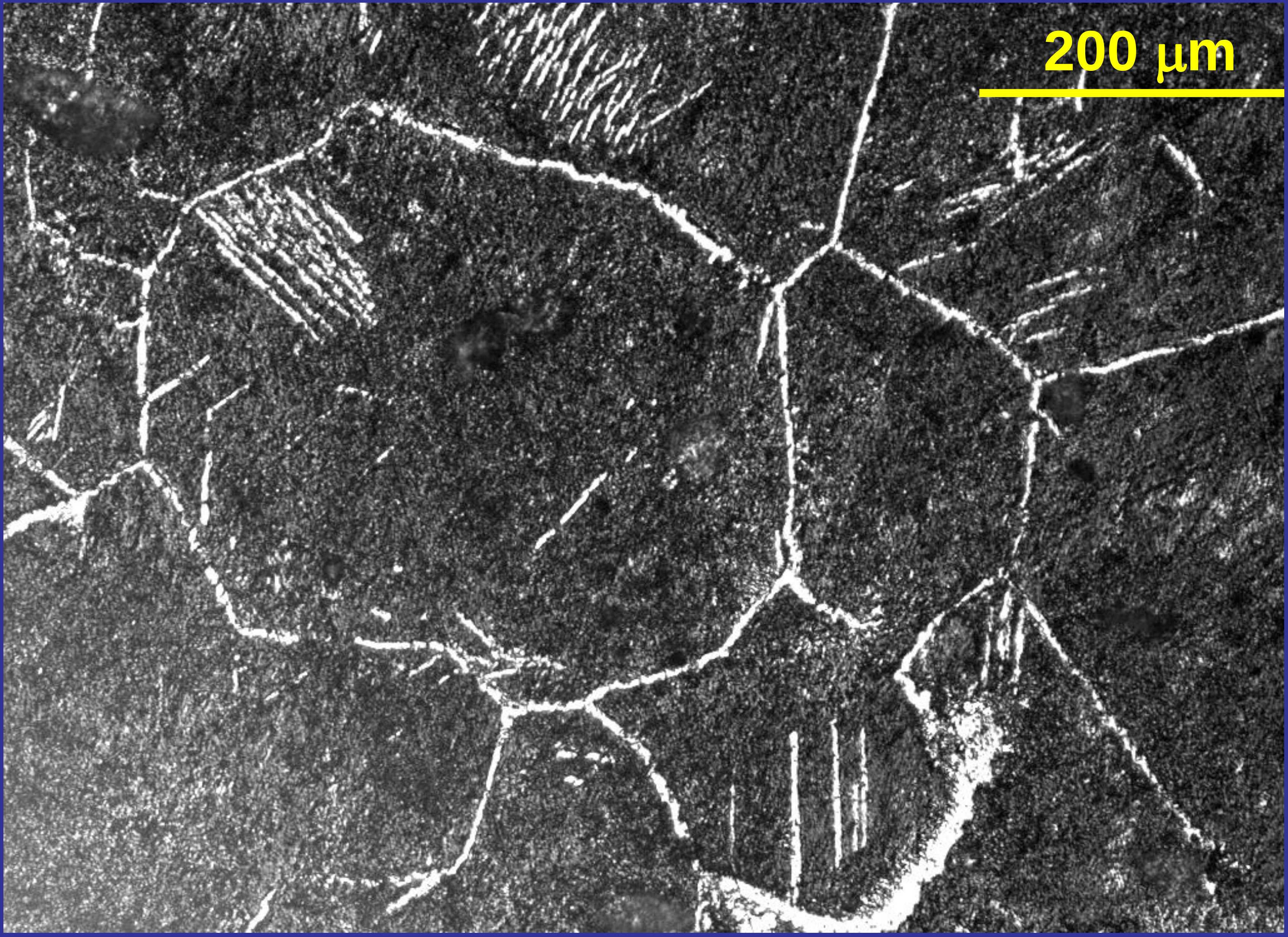

Выше 905°C все γ-ГЗ “смочены” фазой Fe_3C

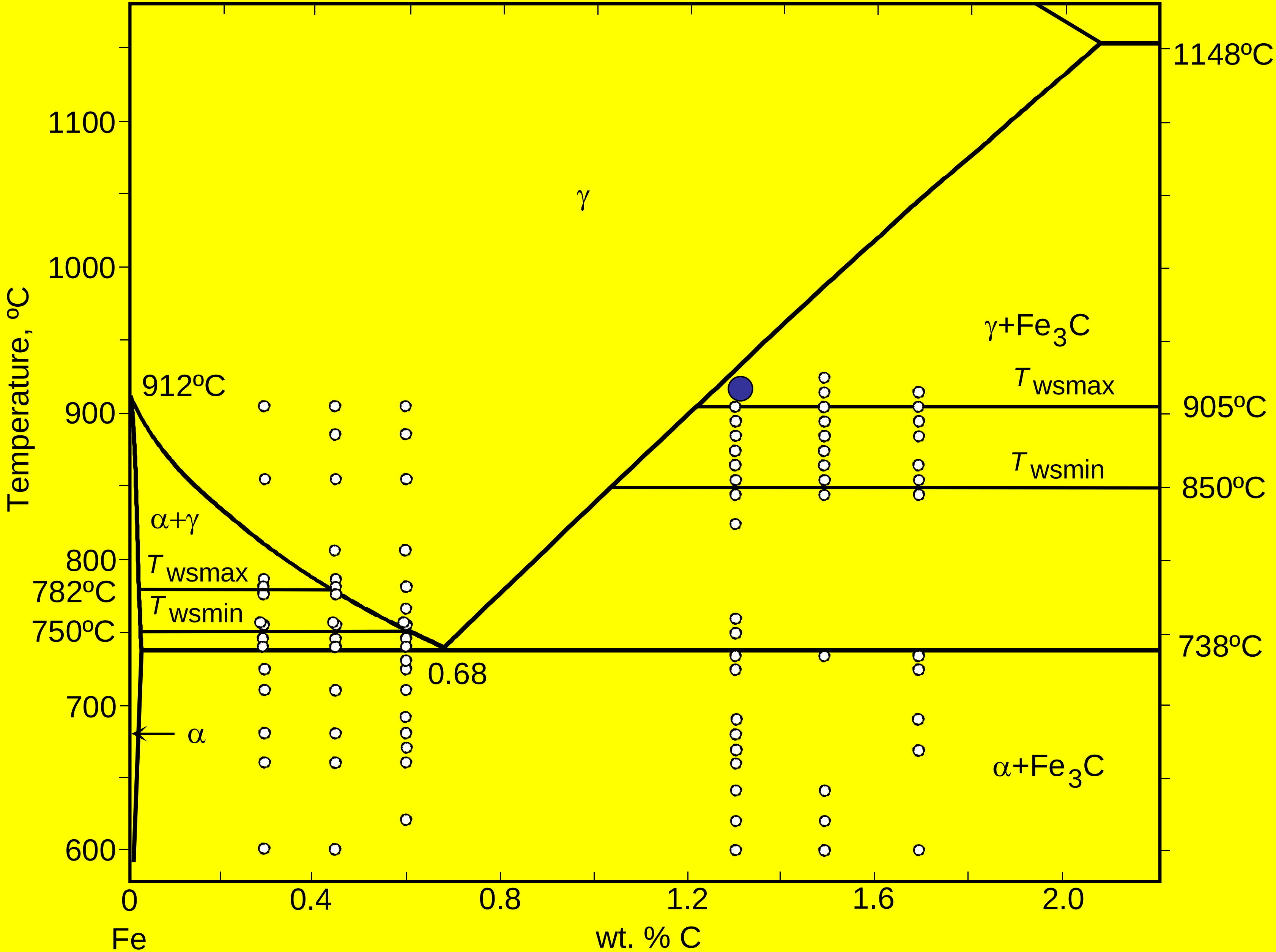

Между 850 и 905°C часть γ-ГЗ "смочена" Fe_3C

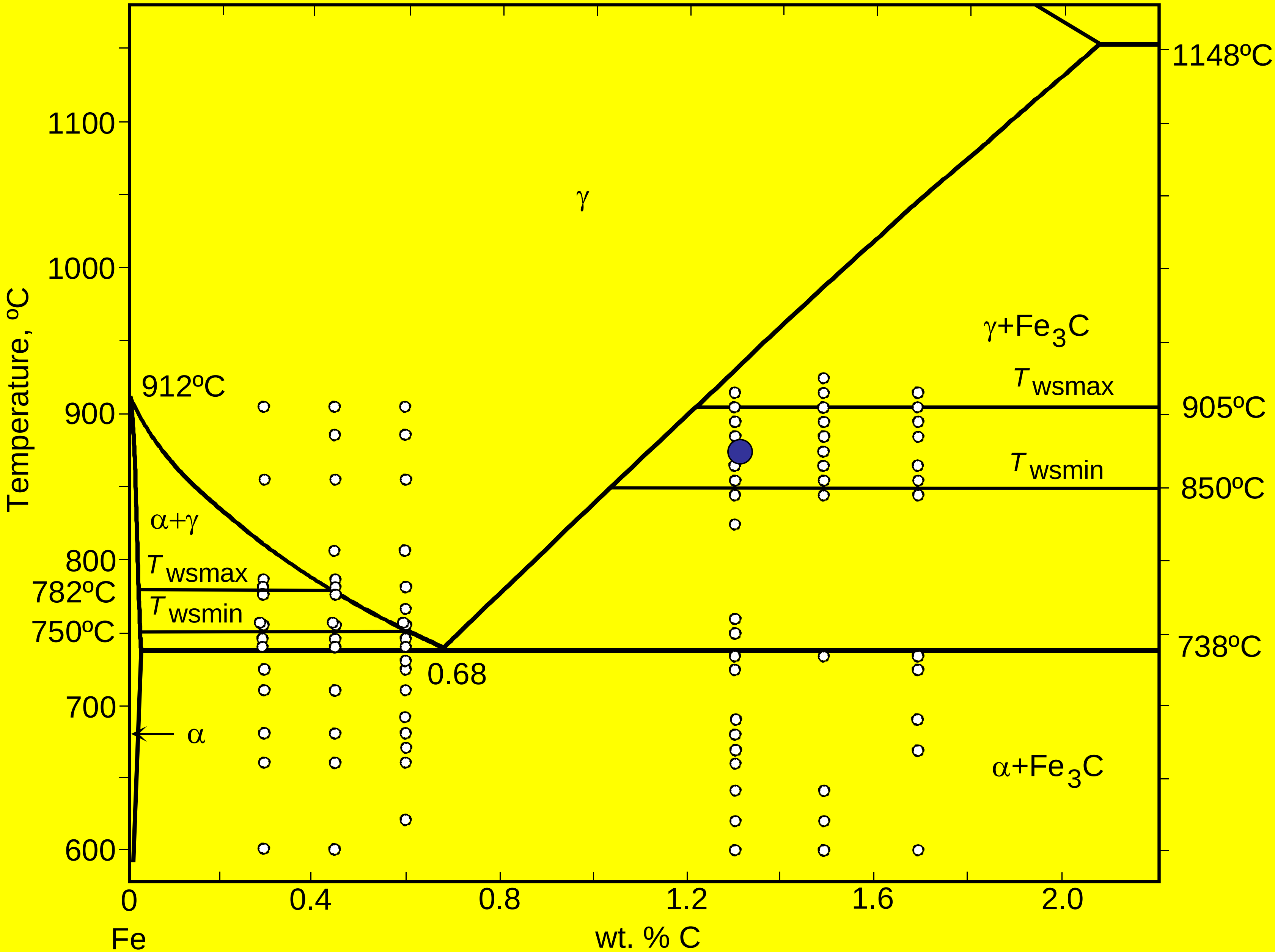

Fe–1.3 вес.% C, 885°C, часть γ-ГЗ “смочена” Fe_3C

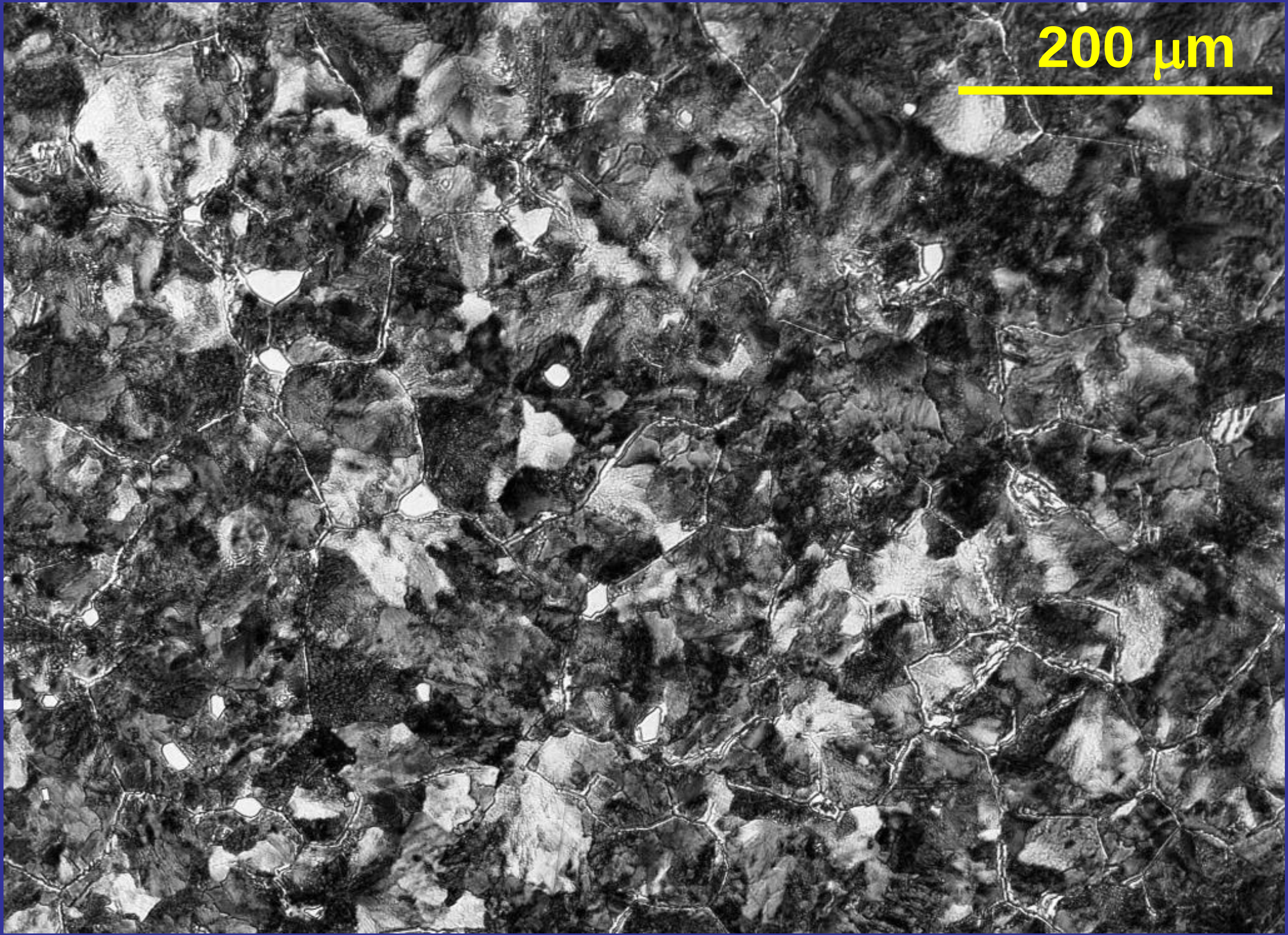

Ниже 850°C нет γ-ГЗ "смоченных" фазой Fe_3C

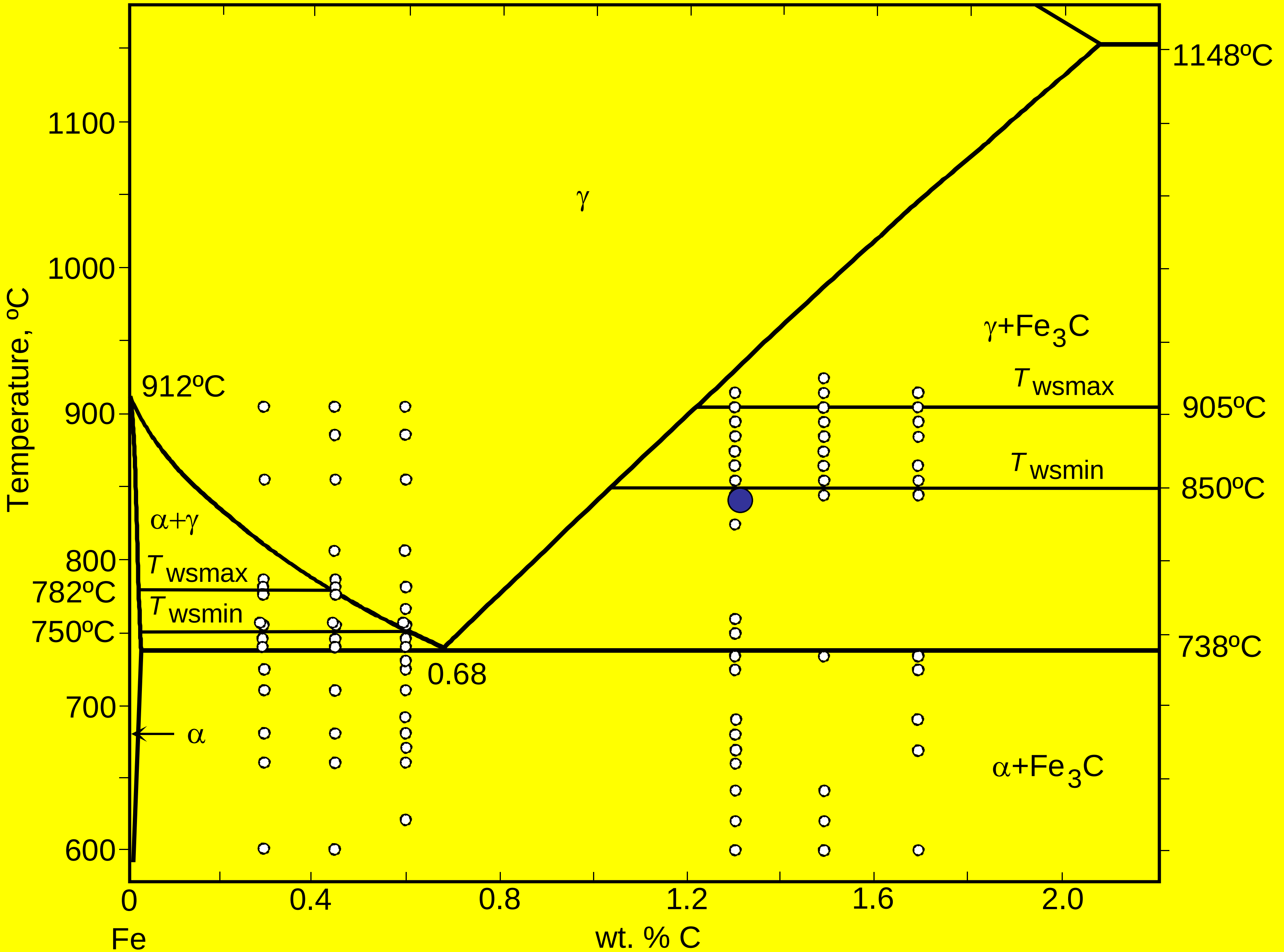

Fe–1.3 вес.% C, 885°C, часть γ-ГЗ “смочена” Fe_3C

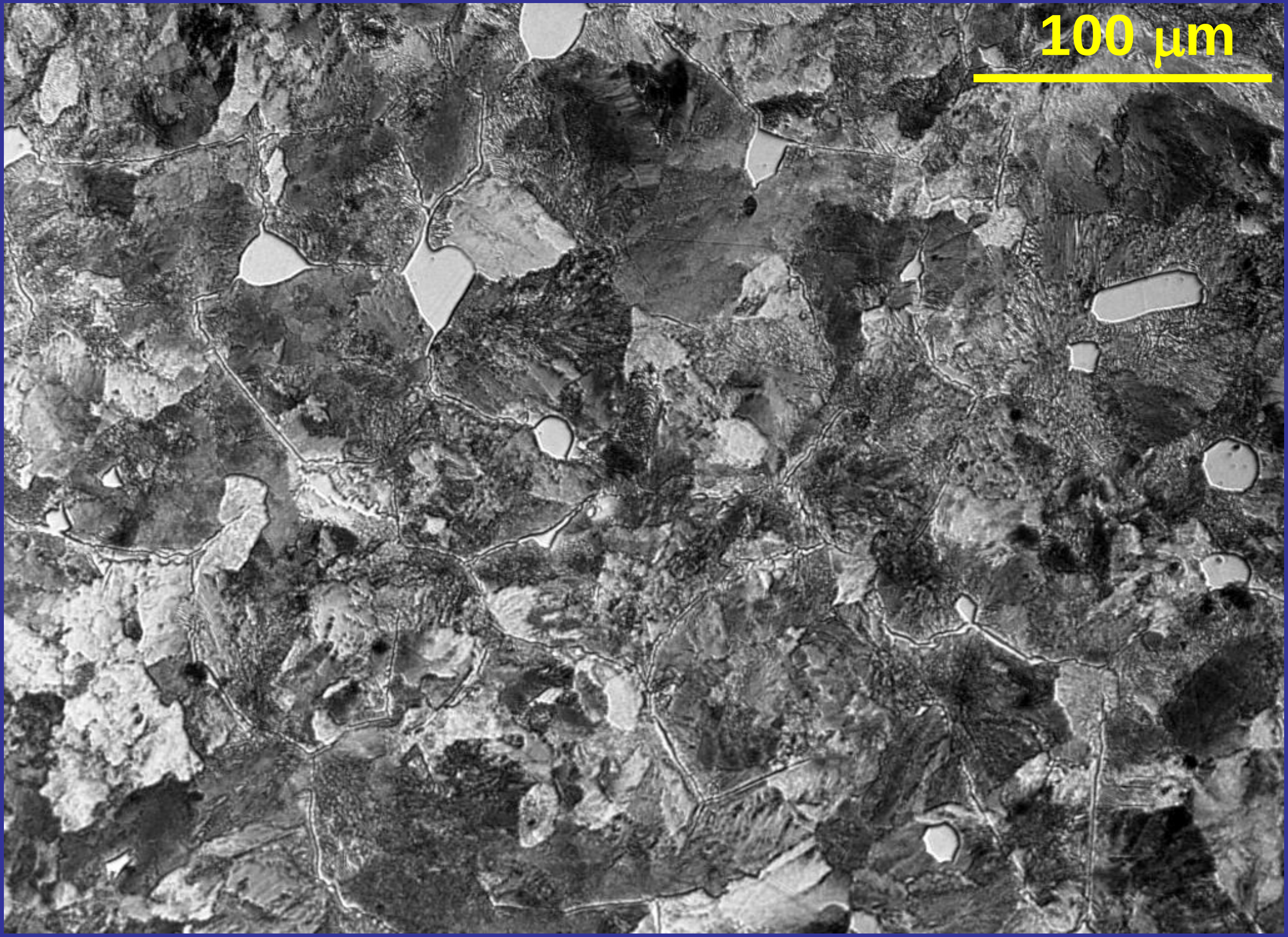

Булатная сабля, Стамбул 1656
(Подарок купца И. Булгакова царю Алексею Михайловичу, коллекция Оружейной палаты московского Кремля)

Булатная сабля, Стамбул 1656
(Подарок купца И. Булгакова царю Алексею Михайловичу, коллекция Оружейной палаты московского Кремля)

Предсмачивание, предплавление

GB segregation: fracture surfaces of Cu–50 at. ppm Bi polycrystals

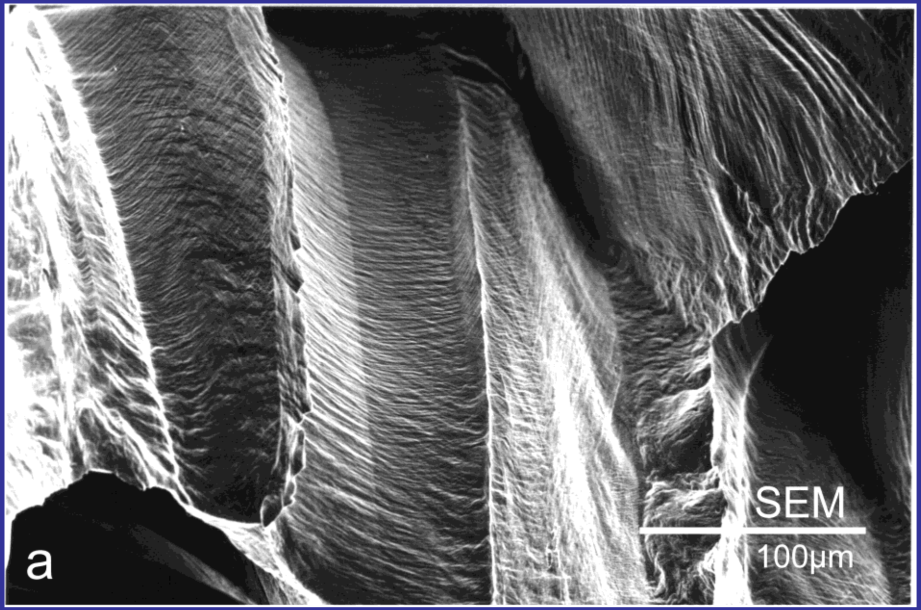

800°C

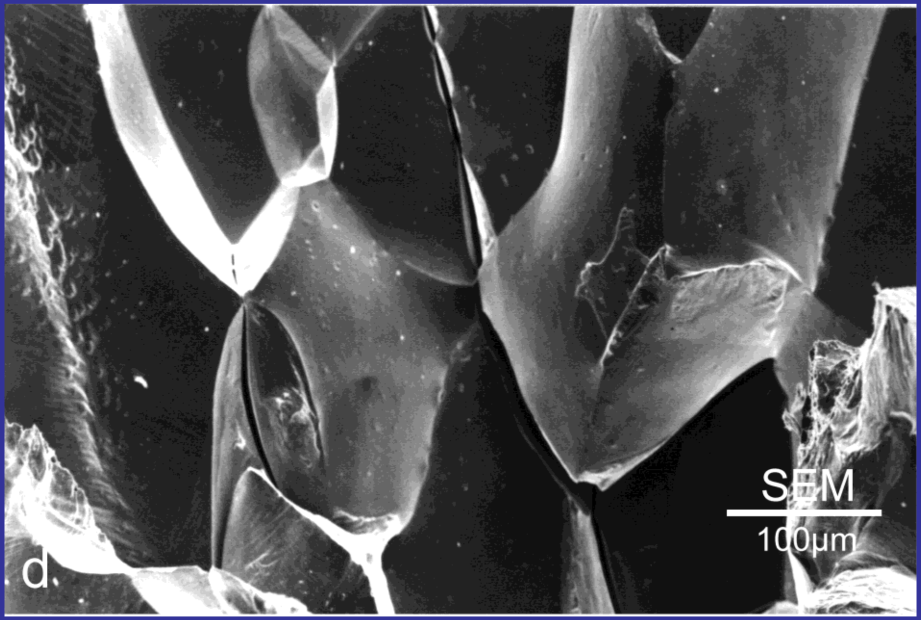

500°C

GB segregation: fracture surfaces of Cu–100 at. ppm Bi bicrystals

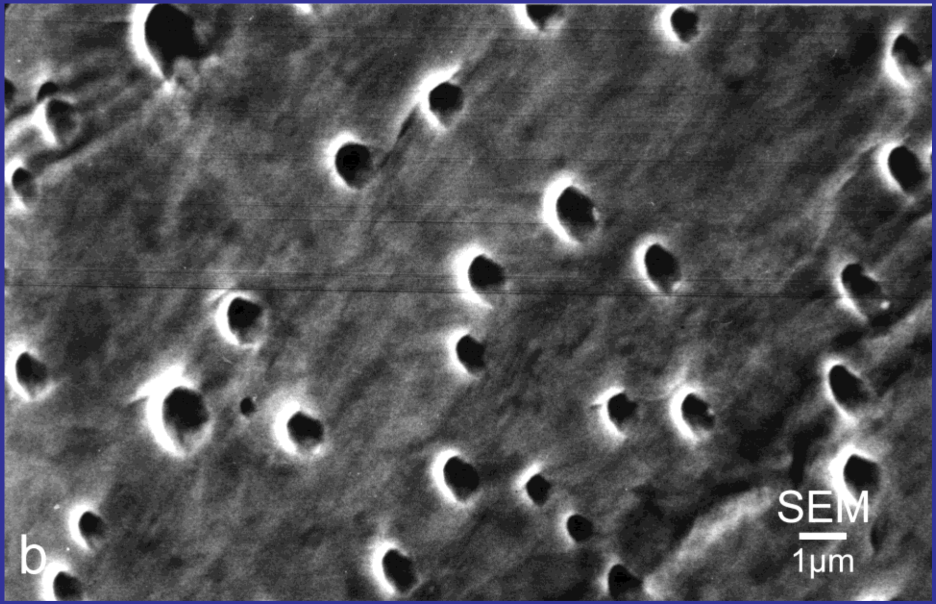

GB 33.2 °<100>
900°C

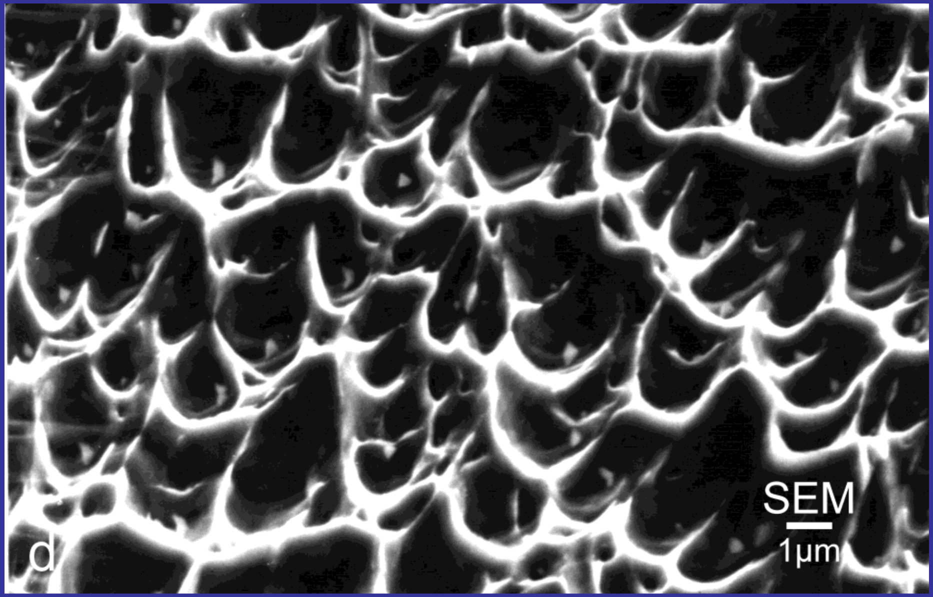

GB 36.5 °<100>
800°C

PSEUDOPARTIAL WETTING: BETWEEN COMPLETE AND PARTIAL

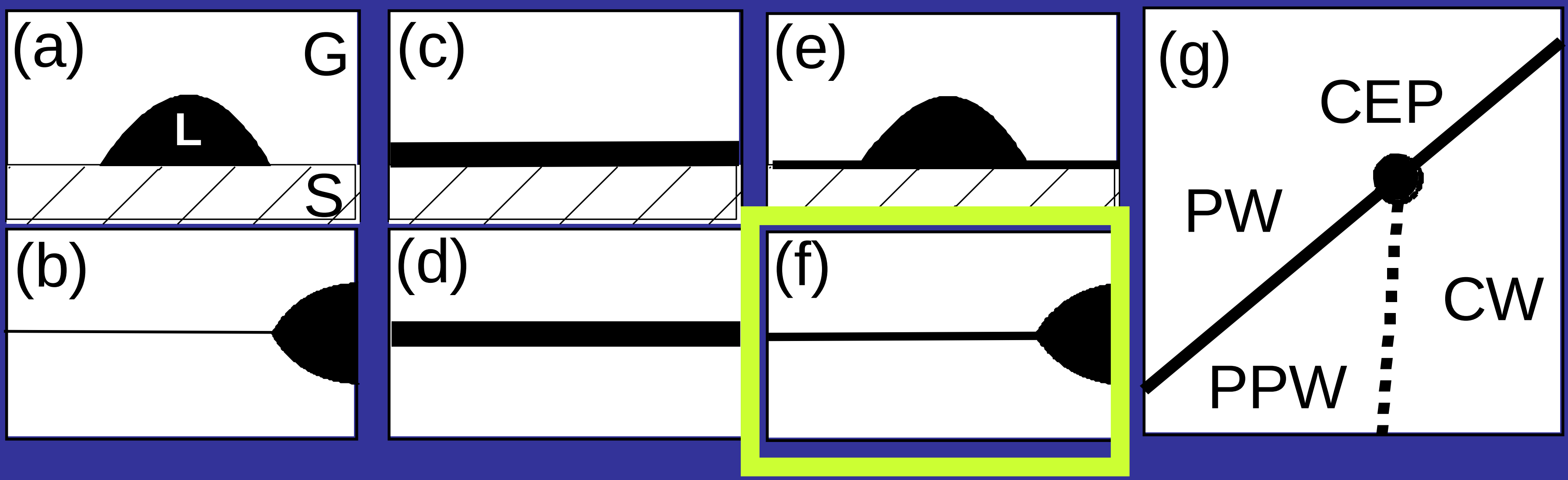

Pseudopartial wetting for grain boundaries=

Al-30wt.% Zn after HPT: no completely wetted GBs

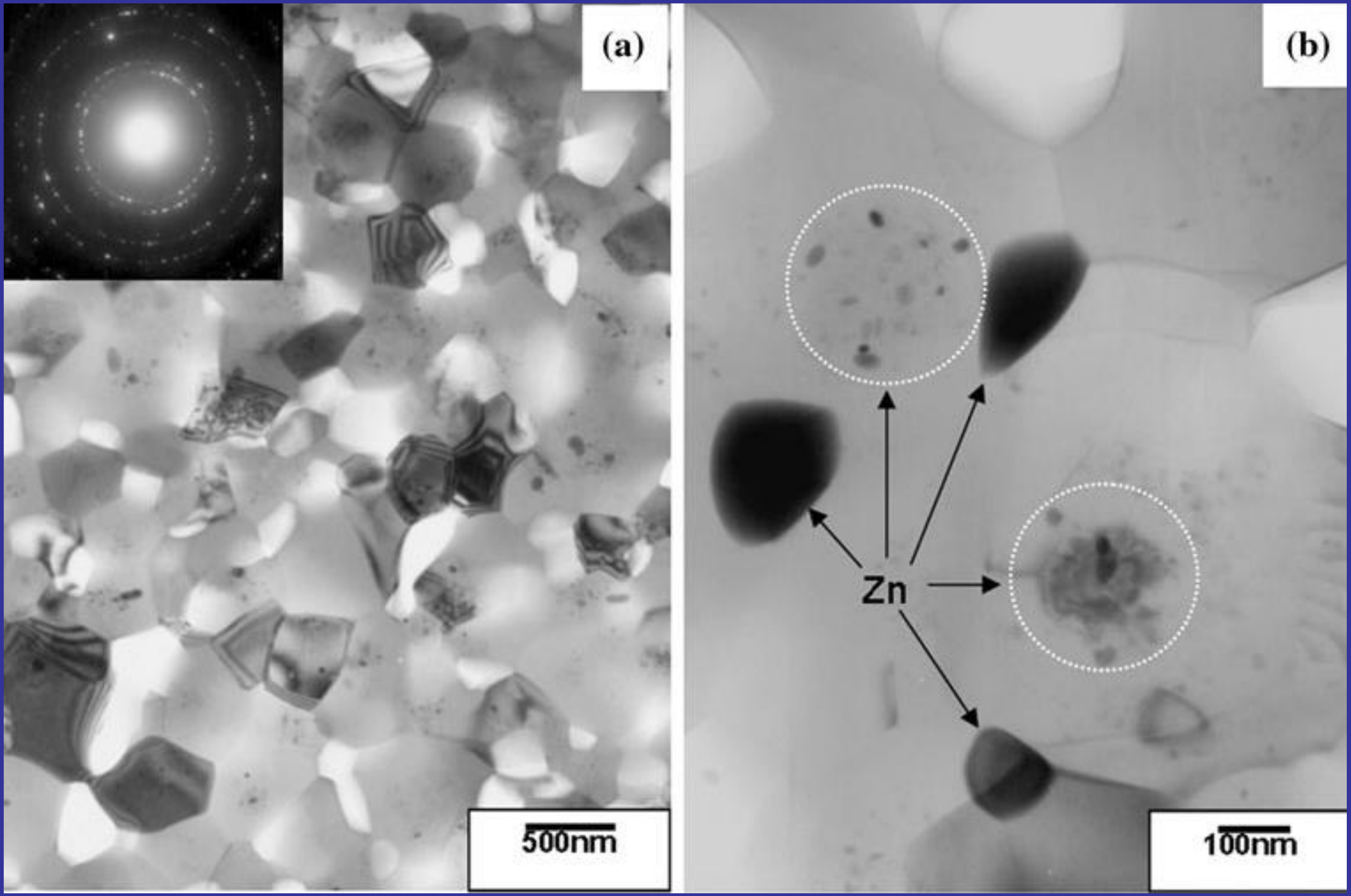

Al - 30 wt. % Zn, 5 GPa, 1 rpm, 5 rot

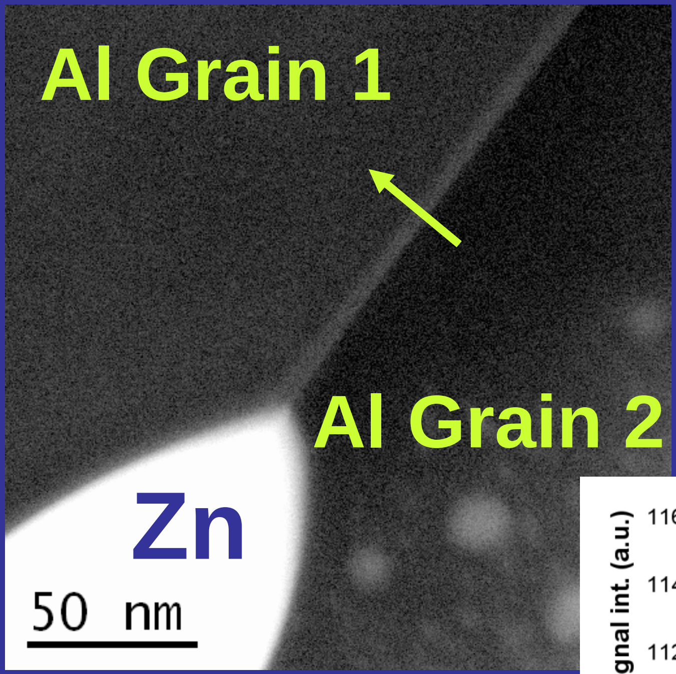

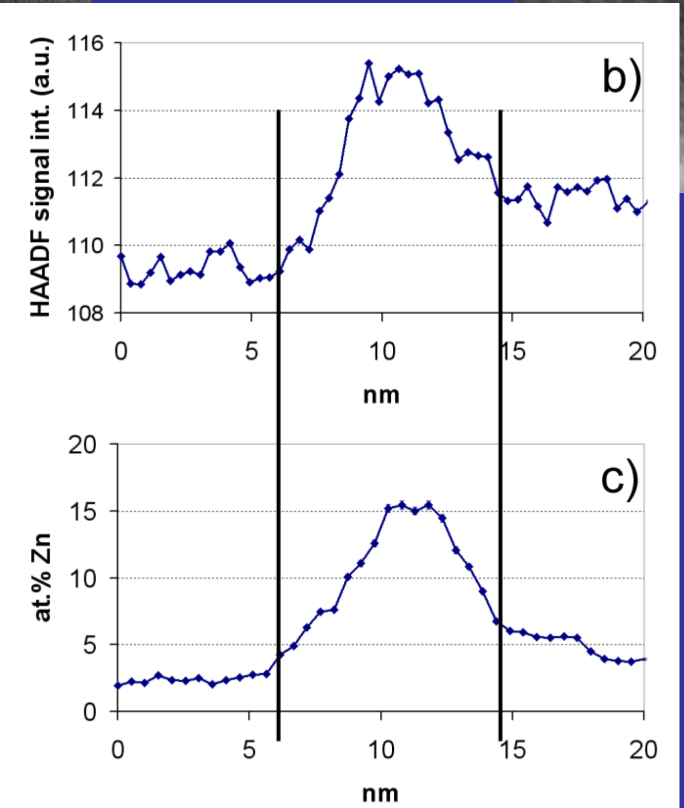

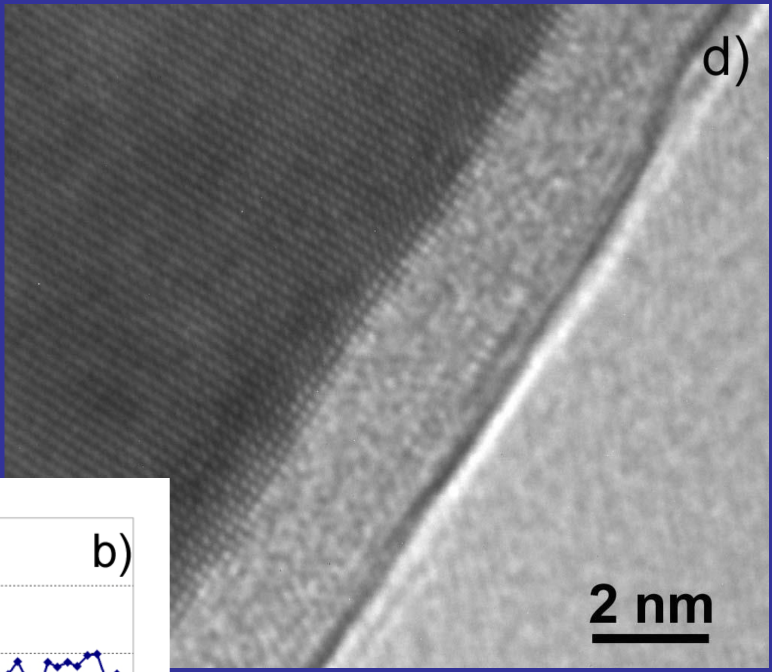

Pseudo-partially wetted GBs!!!

About 20% of all Al GBs

WC-Co CEMENTED CARBIDES

Thin GB layer of Co, θ = 88º

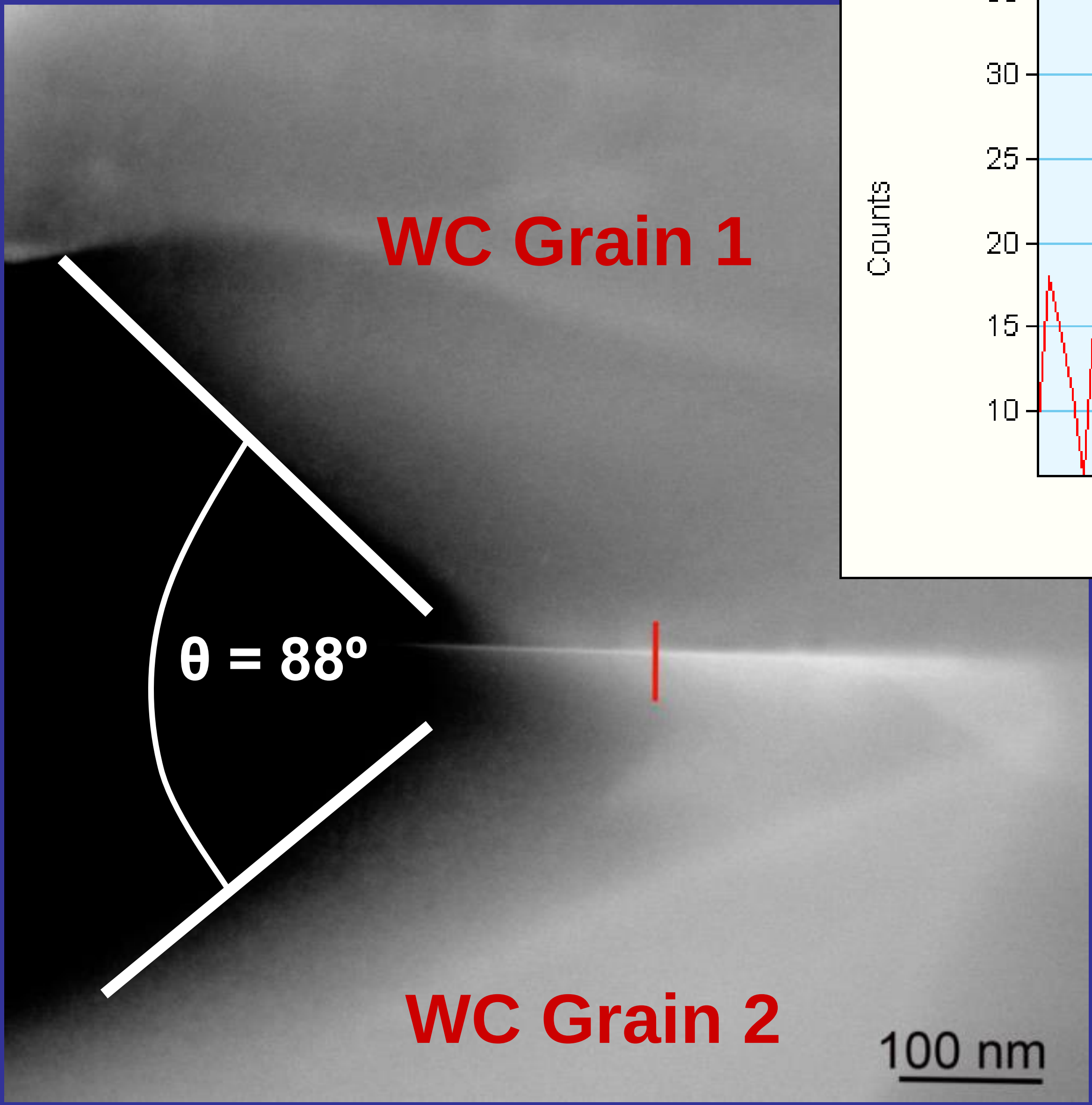

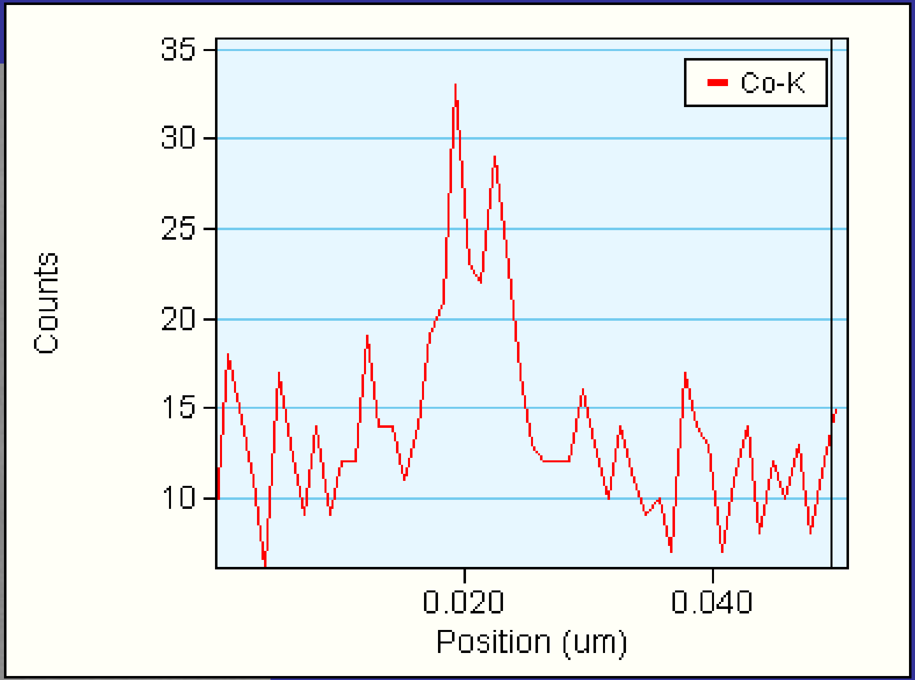

Pseudo-partially wetted GBs!!!

Прикладное значение

- Жидкоподобные равновесные ГЗ прослойки с высокой диффузионной проницаемостью:
  + активированное спекание
  – охрупчивание ГЗ или катастрофическая электромиграция
- Висмут в припоях для меди: область безопасных концентраций

Фазовые превращения:
-- в объеме
под воздействием кручения под высоким давлением

What is severe plastic deformation?

Material is strained,
but
--it cannot break and
--conserves its shape

Principle of High Pressure Torsion

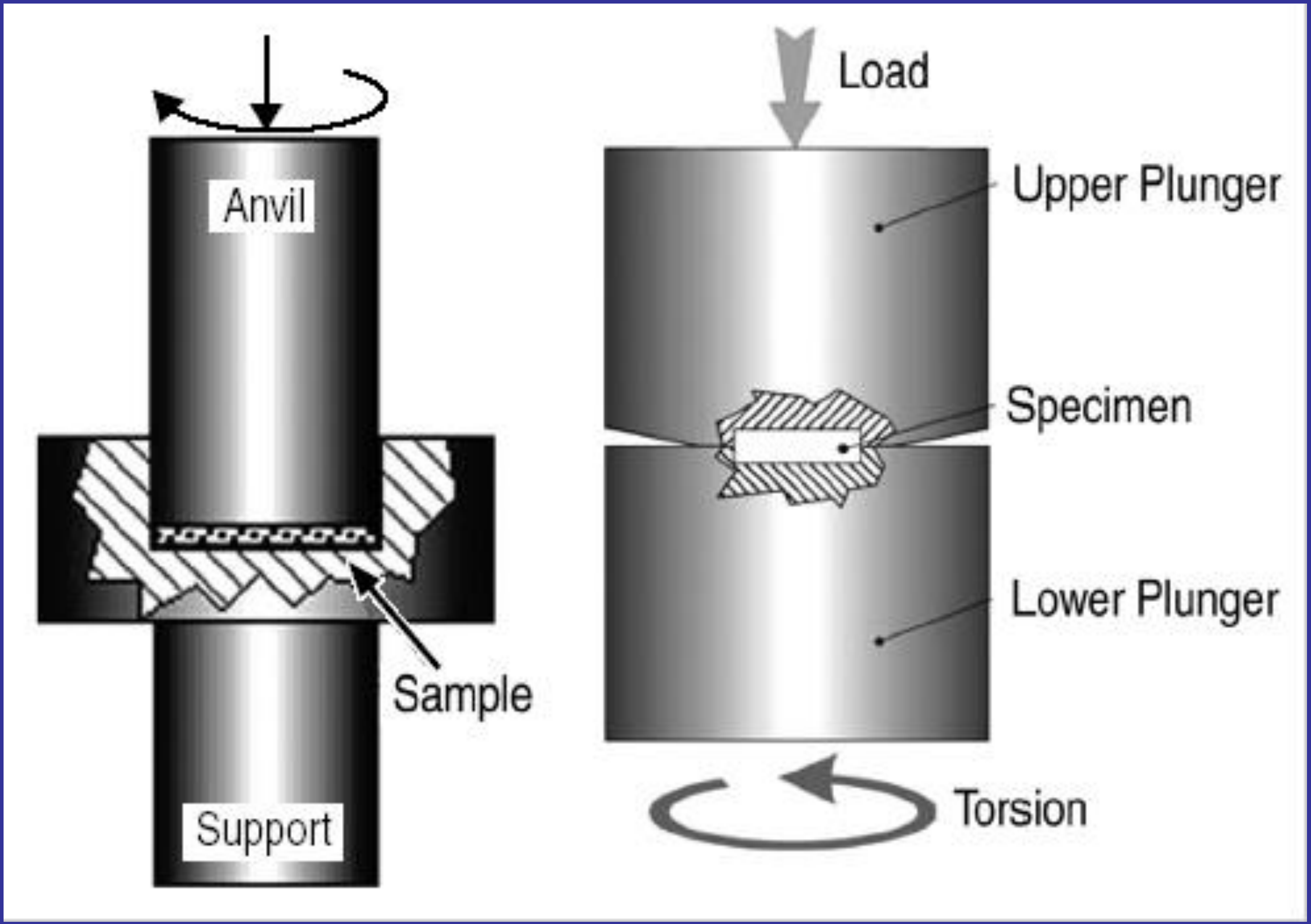

Tool with a sample located within a cavity in a support anvil

Tool with cavities in both anvils

Principle of Equal Channel Angular Pressing

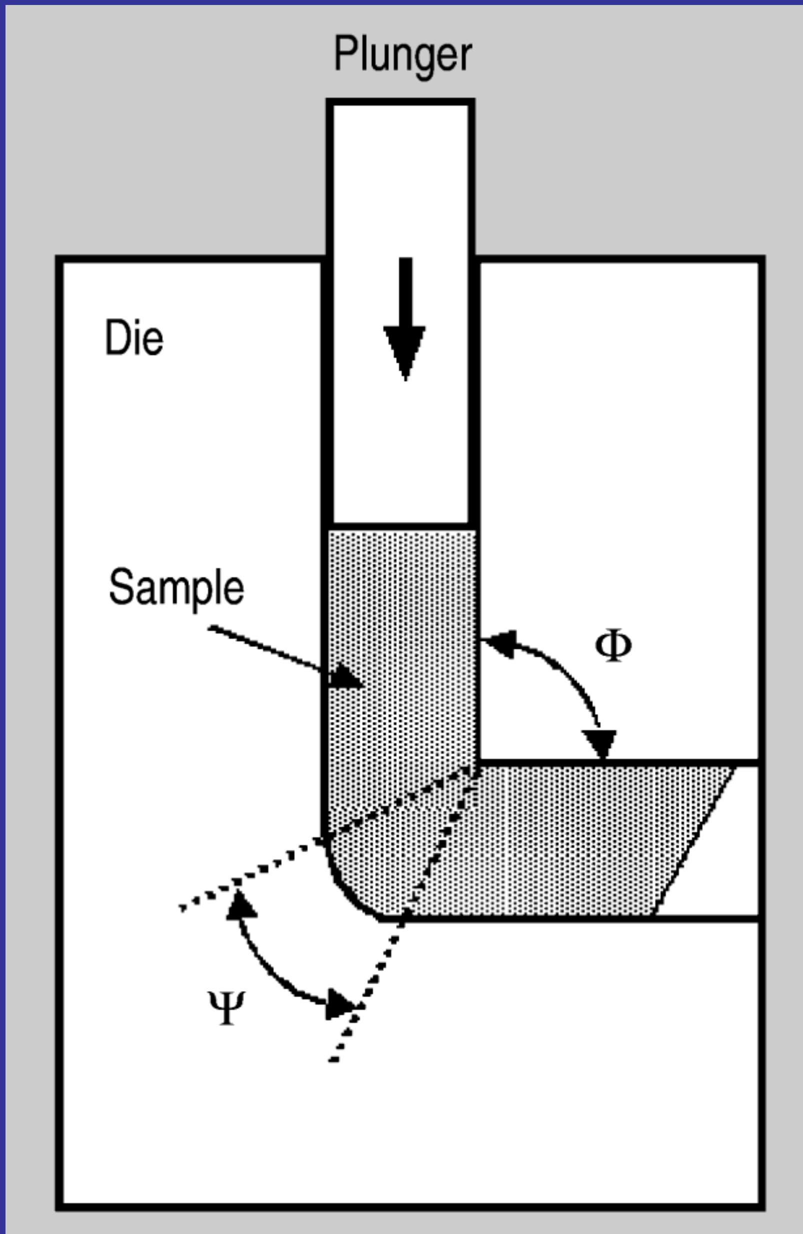

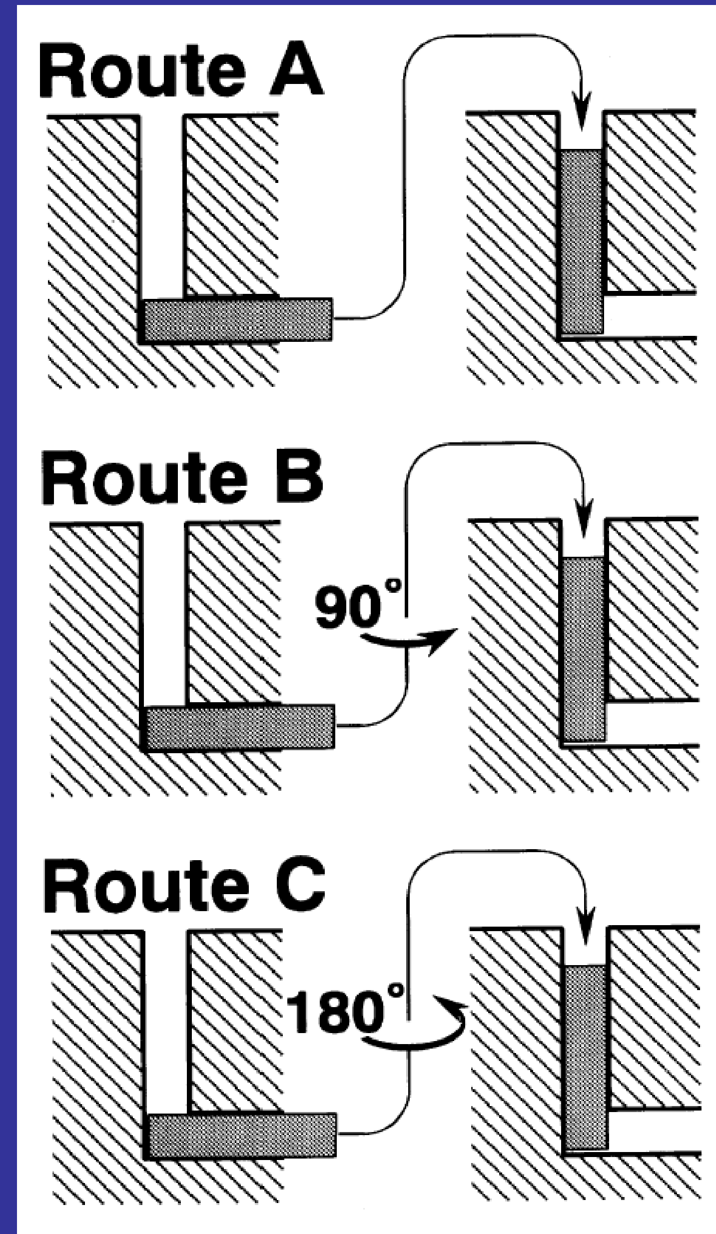

Principle of Accumulative Roll Bonding

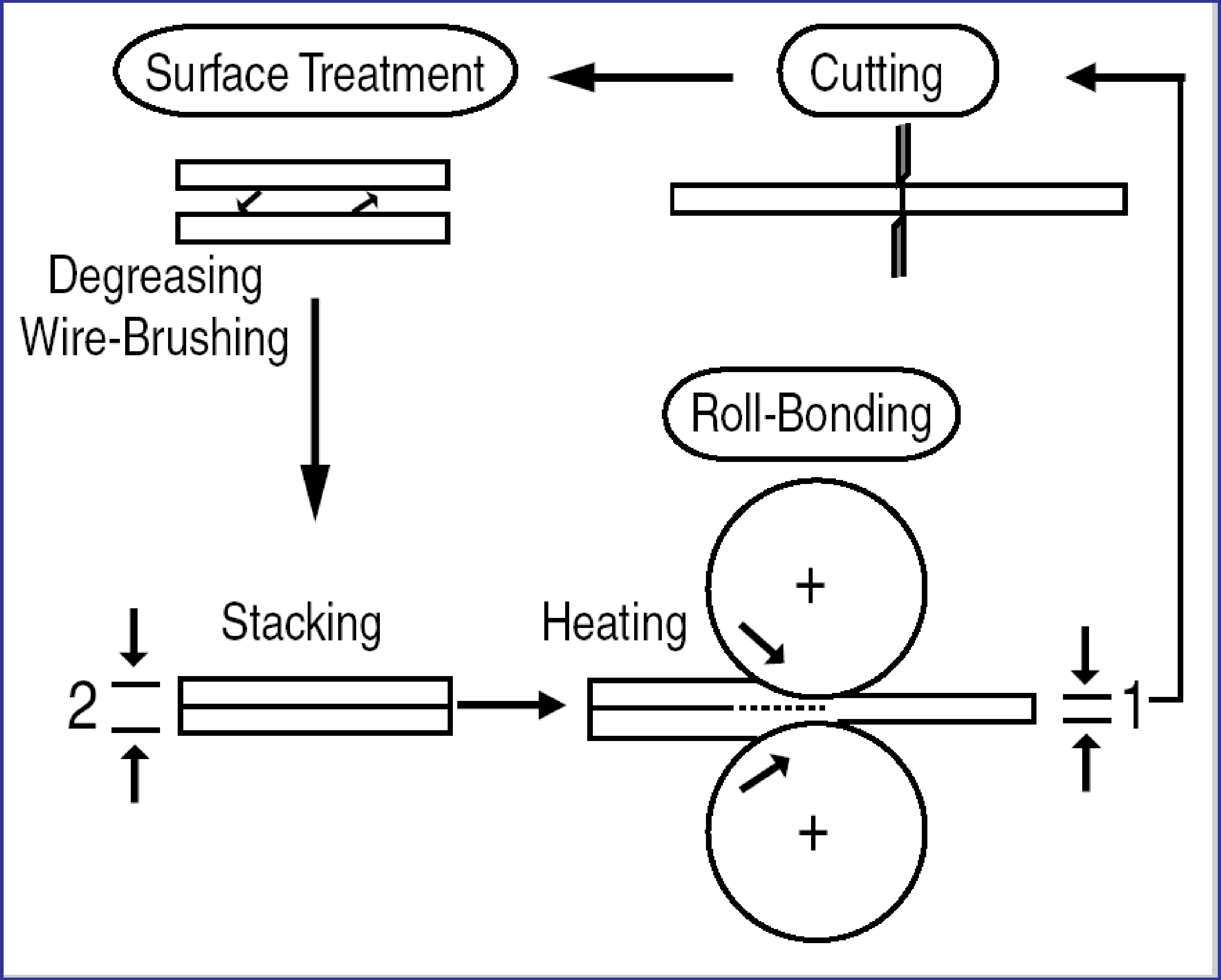

Principle of Cyclic Extrusion and Compression

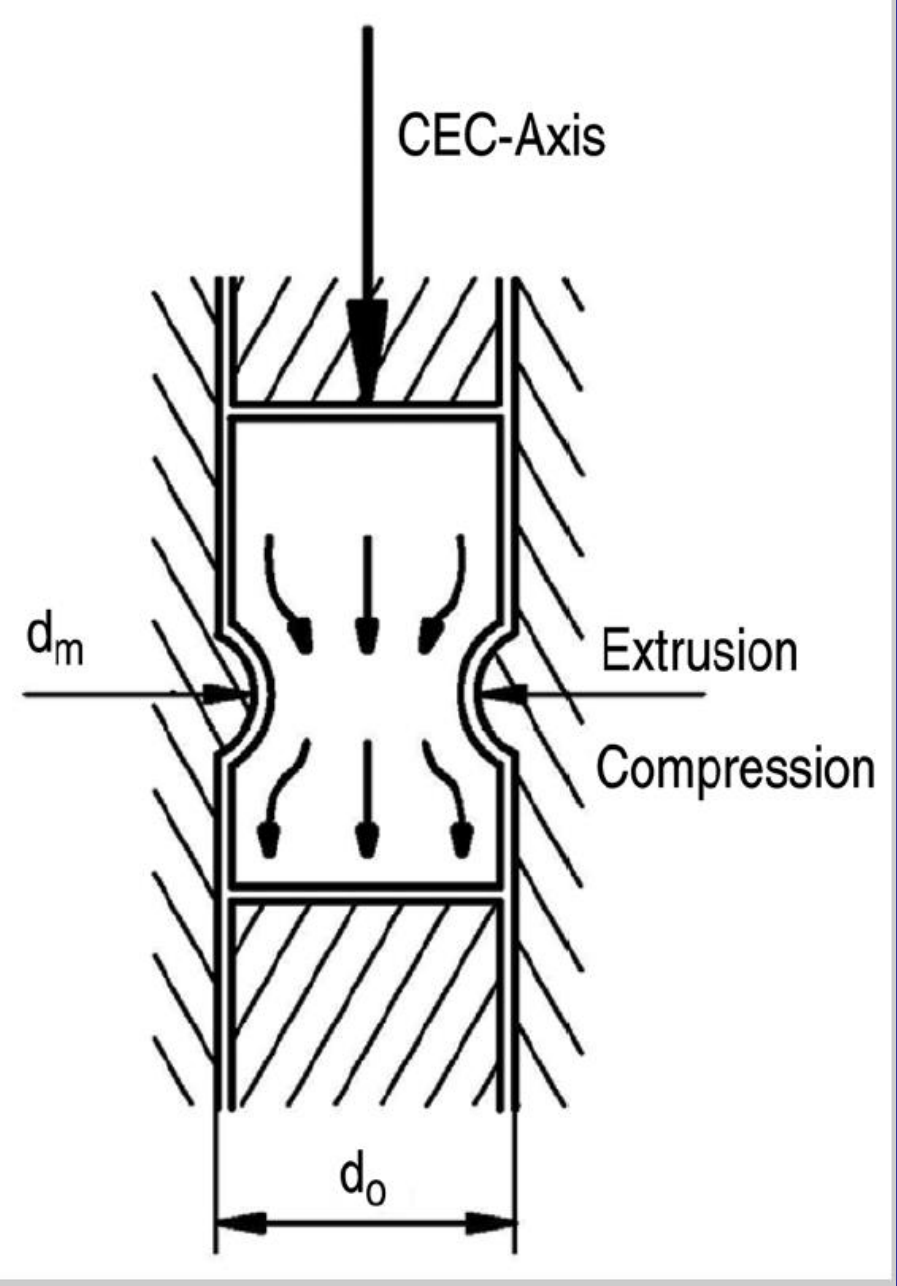

Principle of Twist Extrusion

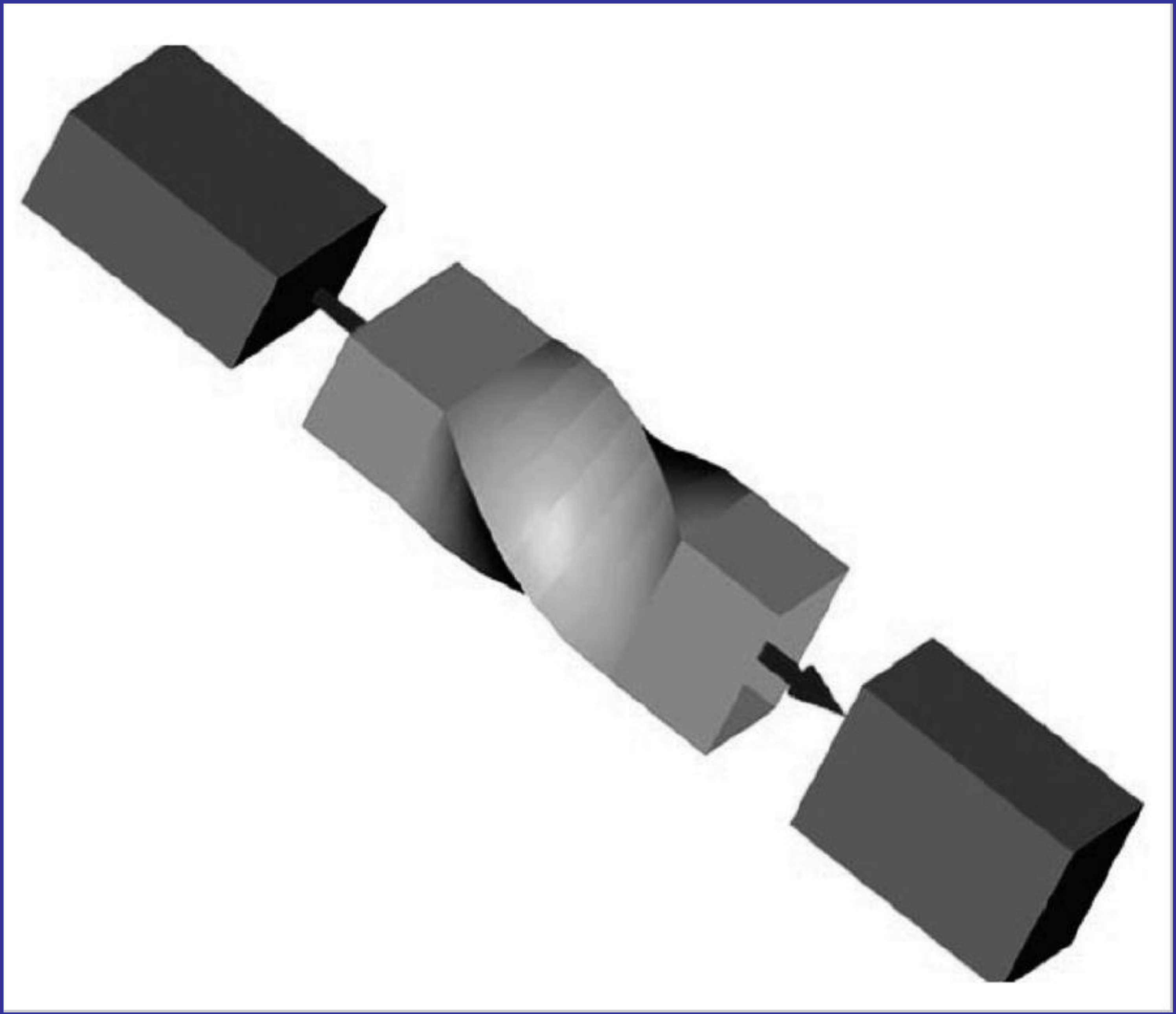

Severe plastic deformation accelerates diffusion and drives phase transitions:

- **Decomposition of supersaturated solid solutions**
  Al–Zn, Cu–Ni, Cu–Co, Cu–Ag
- **Formation of supersaturated solid solutions**
  Cu–Co, Cu–Ag
- **Crystalline phase ➔ one or two amorphous phases**
  NiTi, NdFeB, Ni–Nb–Y
- **Amorphous phase ➔ Crystalline phases**
  NiFeSiB, FeSiB, CuZrTi...
- **fcc-Fe ➔ bcc-Fe, fcc-Co ➔ hcp-Co, αTi↔βTi↔ωTi**
- **Grain boundary phases**

Can we predict, what happens with phases by SPD?

Steady-state and grain refinement

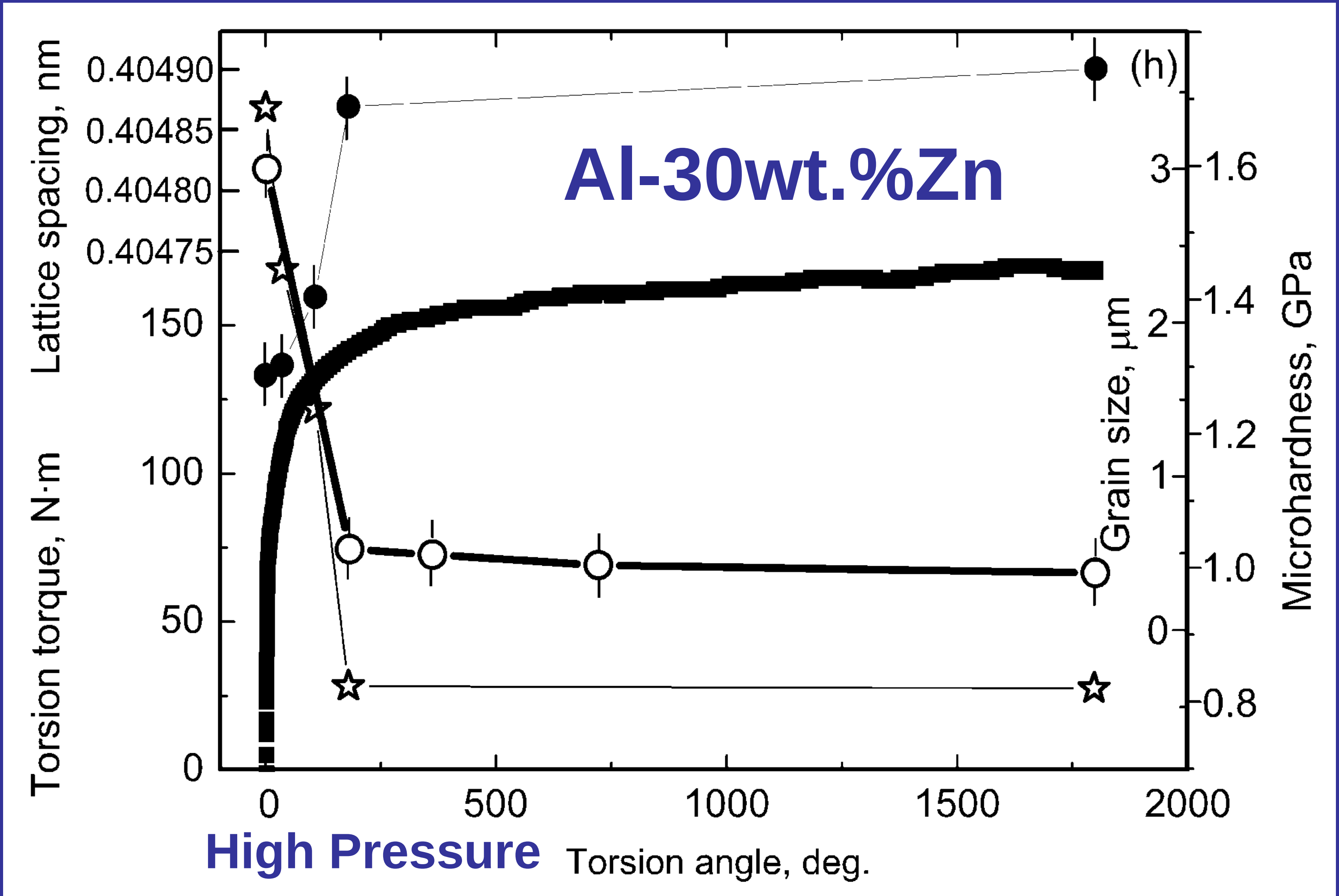

B.B. Straumal et al Scripta Mater **70** (2014) 59

Steady-state (saturation) during SPD

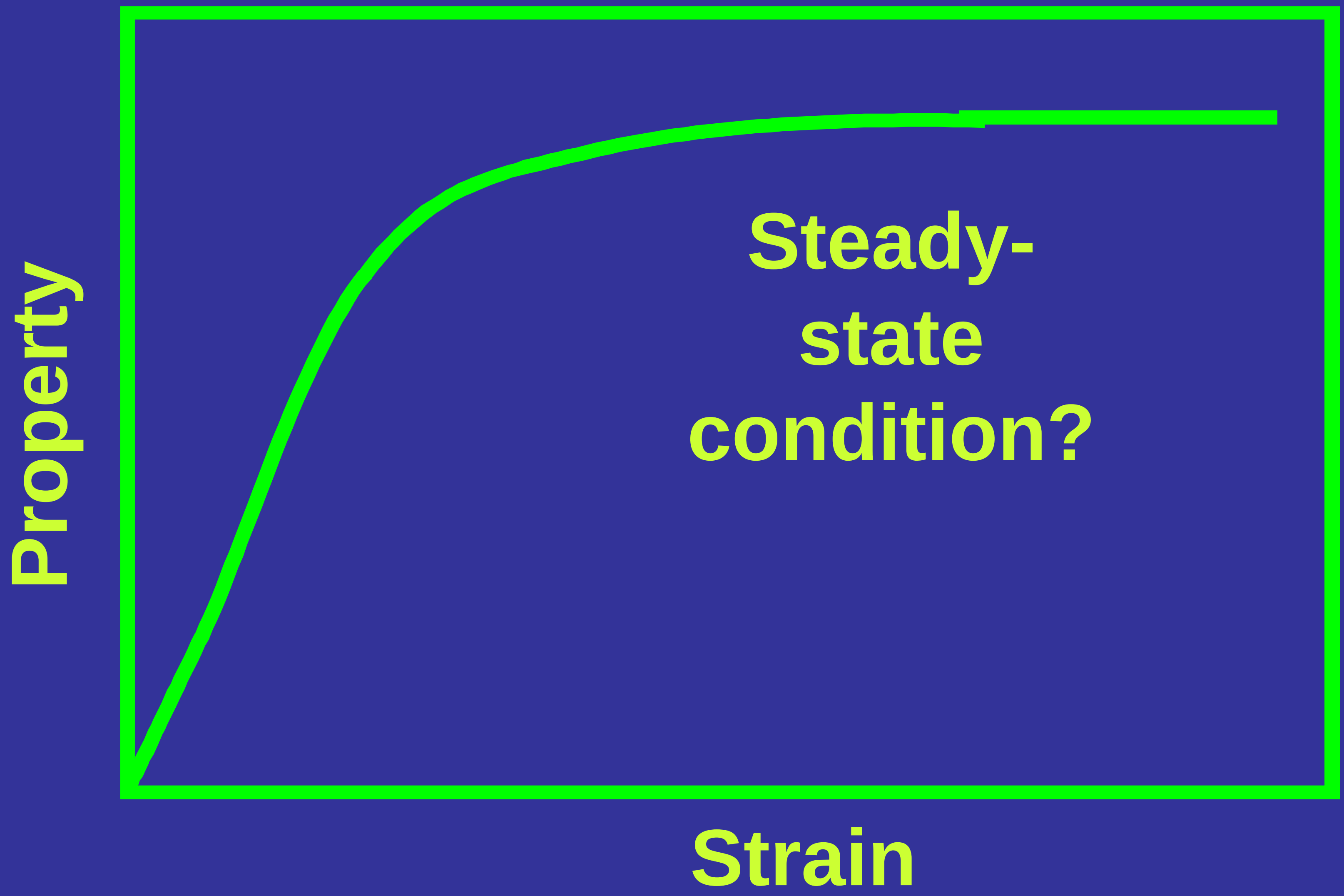

Steady-state (saturation) during SPD

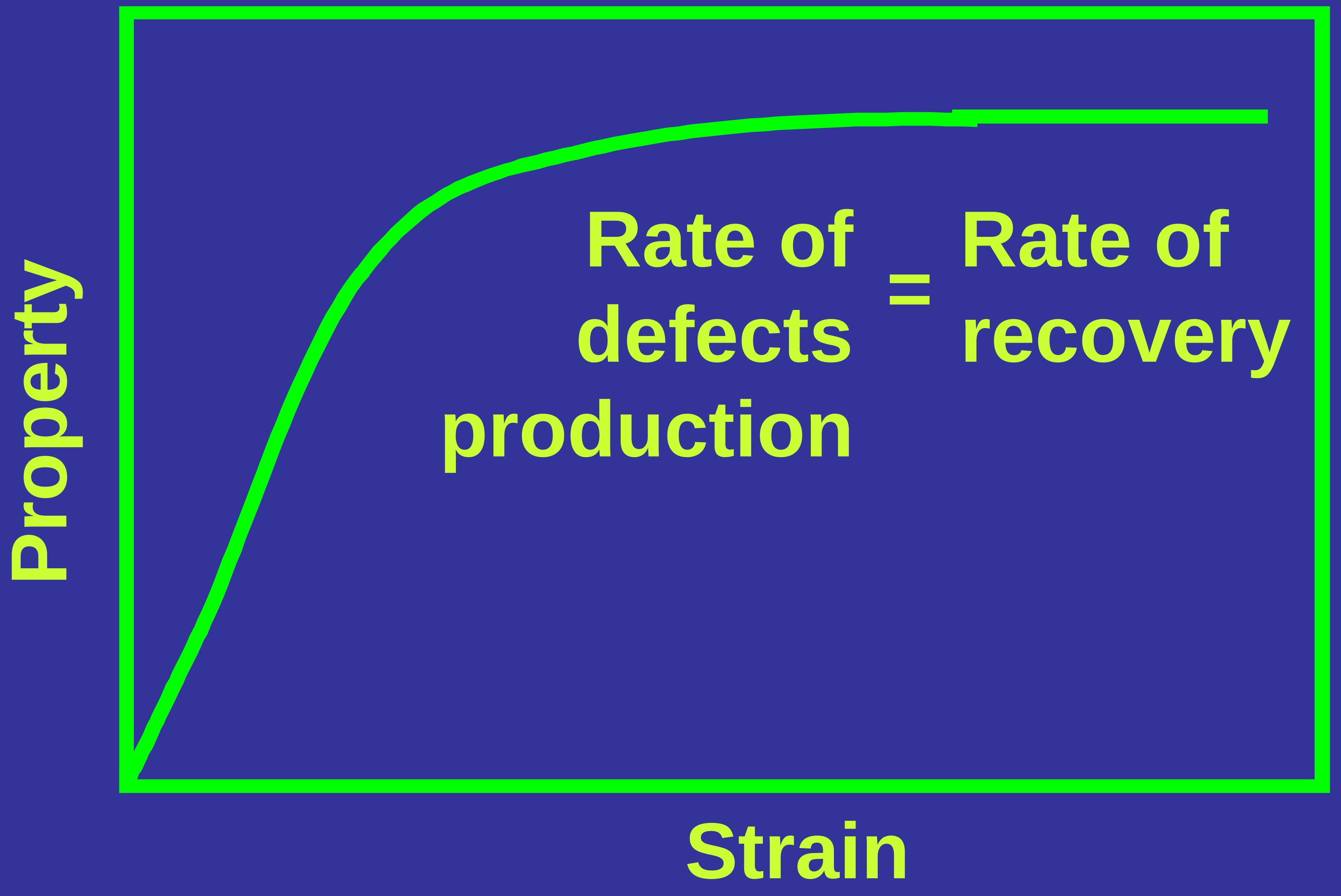

Grain size in steel, „up and down“

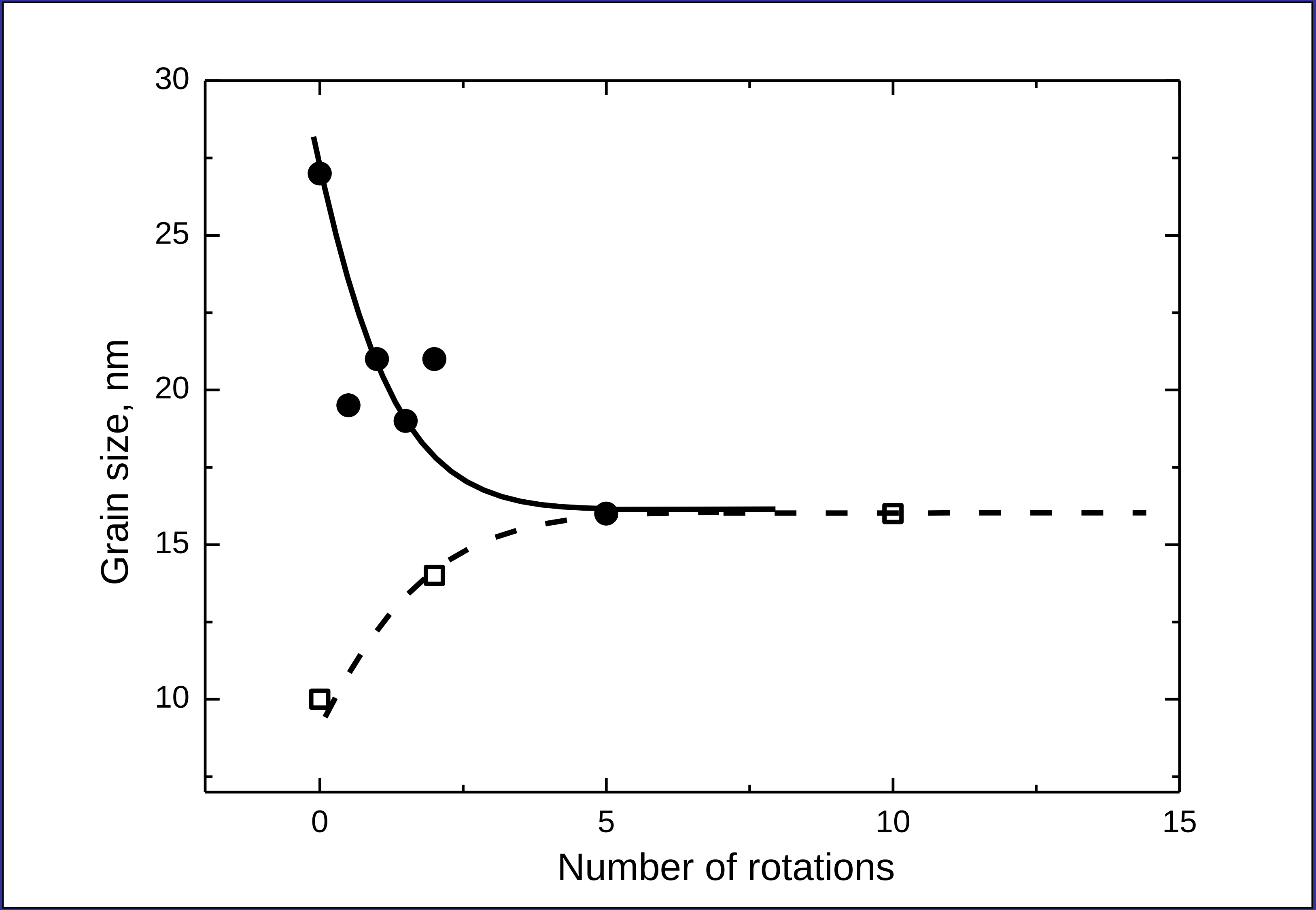

Y. Ivanisenko et. al Acta Mater. **51** (2003) 5555
S. Lee, Z. Horita: Mater. Trans. **53** (2012) 38

Grain size in Ni, „up and down"

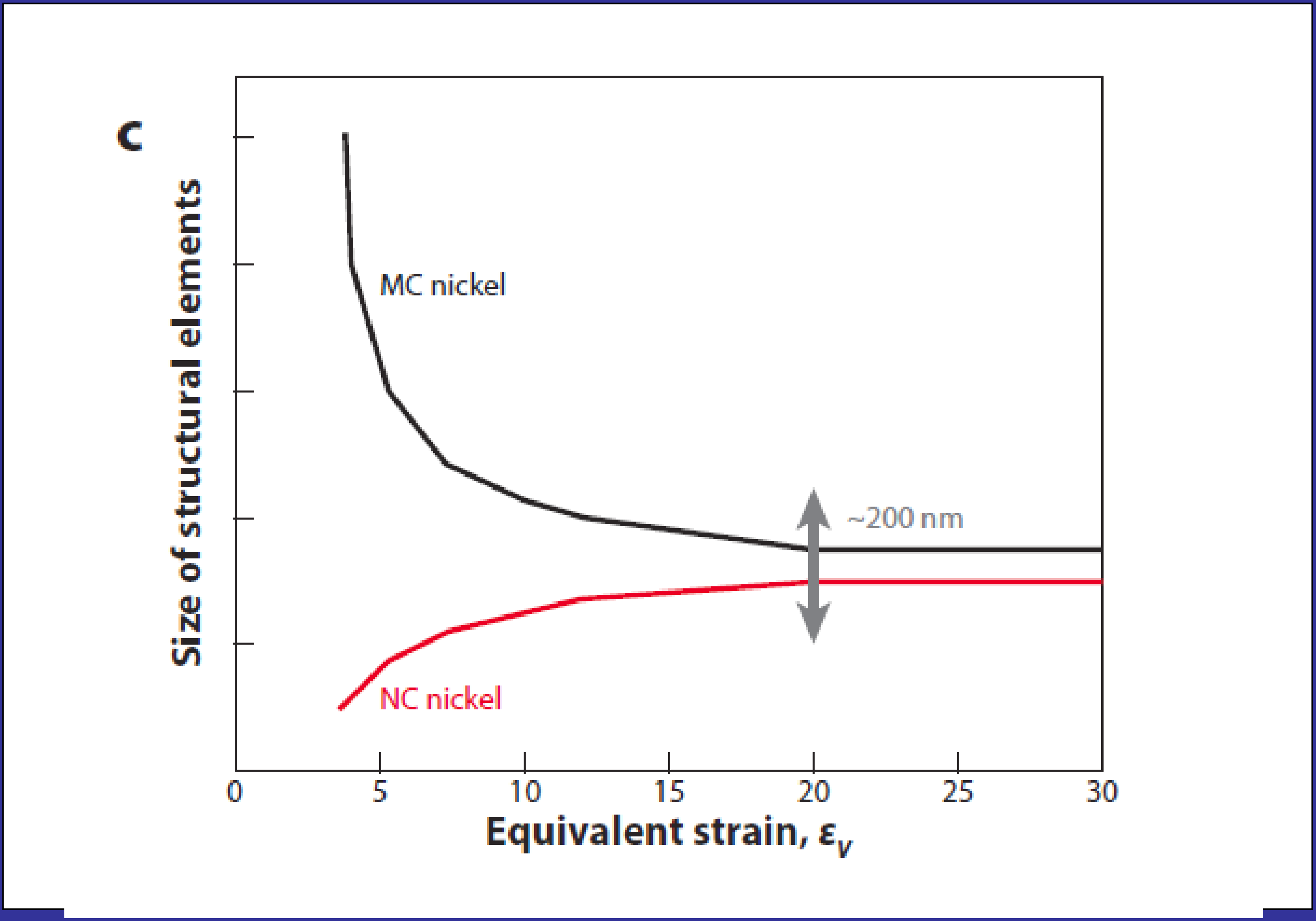

R. Pippan et. al Annu. Rev. Mater. Res. 40 (2010) 319

Diffusive phase transfromations

With change of the composition of phases and mass transfer

Displacive (martensitic) phase transformations

Without change of the composition of phases
Without mass transfer
Atoms conserve their neighbors
Orientation relationships

Let us consider pure diffusive Phase transformations

- Decomposition of supersaturated solid solutions
- Formation of supersaturated solid solutions

Principle of High Pressure Torsion

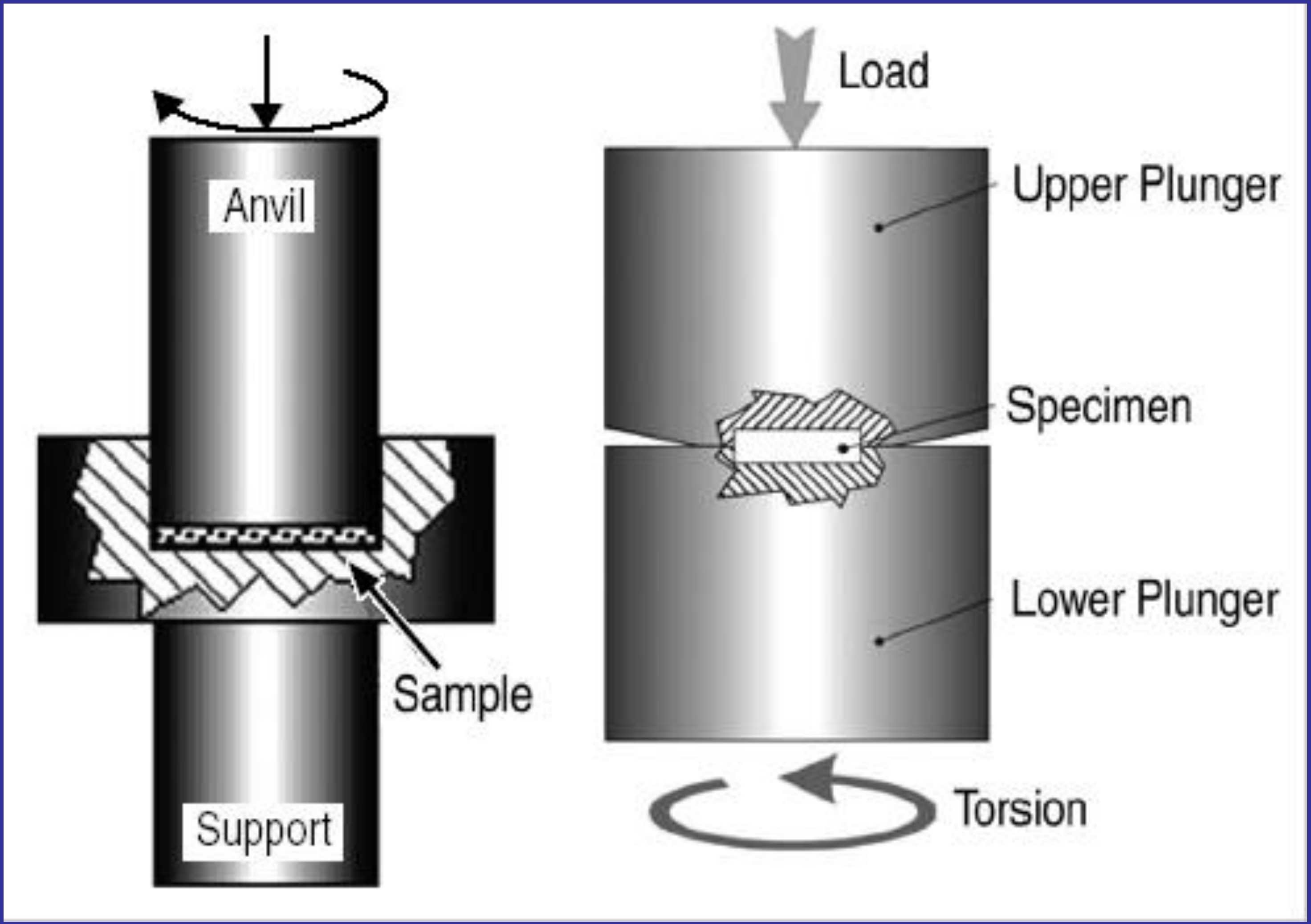

Tool with a sample located within a cavity in a support anvil

Tool with cavities in both anvils

Does the composition of phases after SPD depend on the composition of phases before SPD??

What happens, if we deform fully homogenized and fully precipitated alloy???

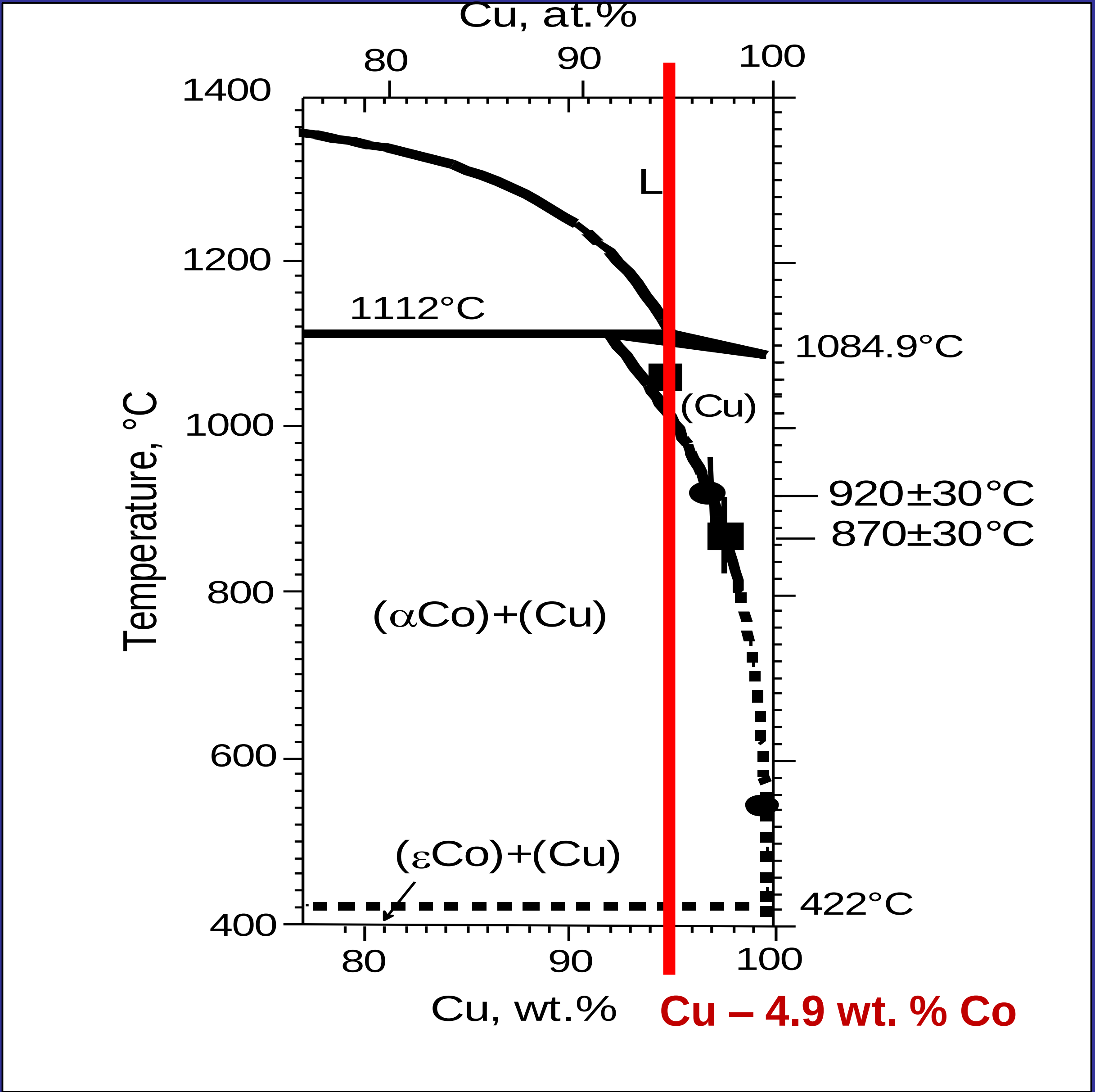

Mater. Lett. **118 (2014) 111**

What happens, if we deform fully homogenized and fully precipitated alloy???

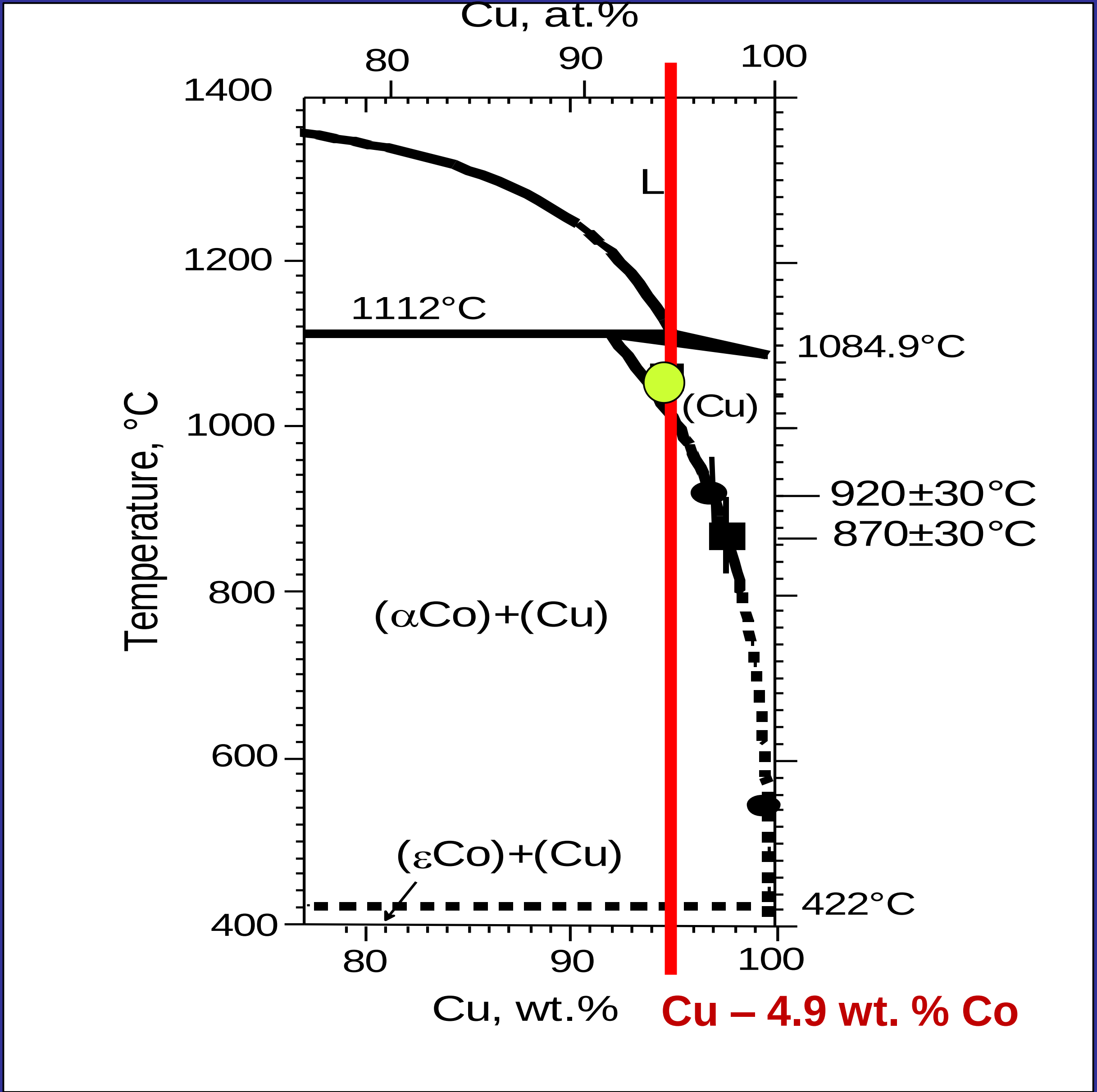

Mater. Lett. **118 (2014) 111**

What happens, if we deform fully homogenized and fully precipitated alloy???

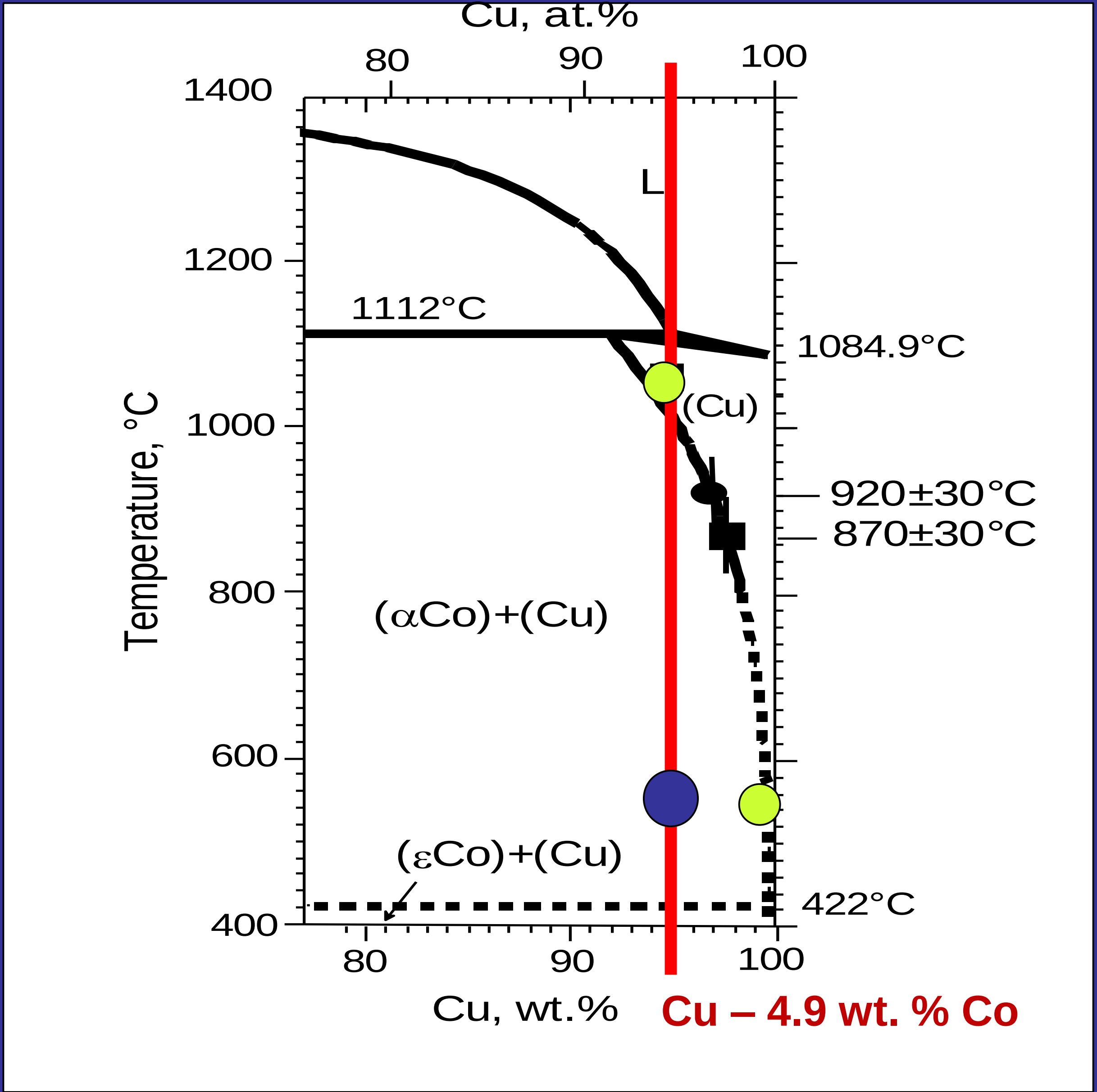

Mater. Lett. **118 (2014) 111**

Torsion torque reaches steady state after 1.5 rot.

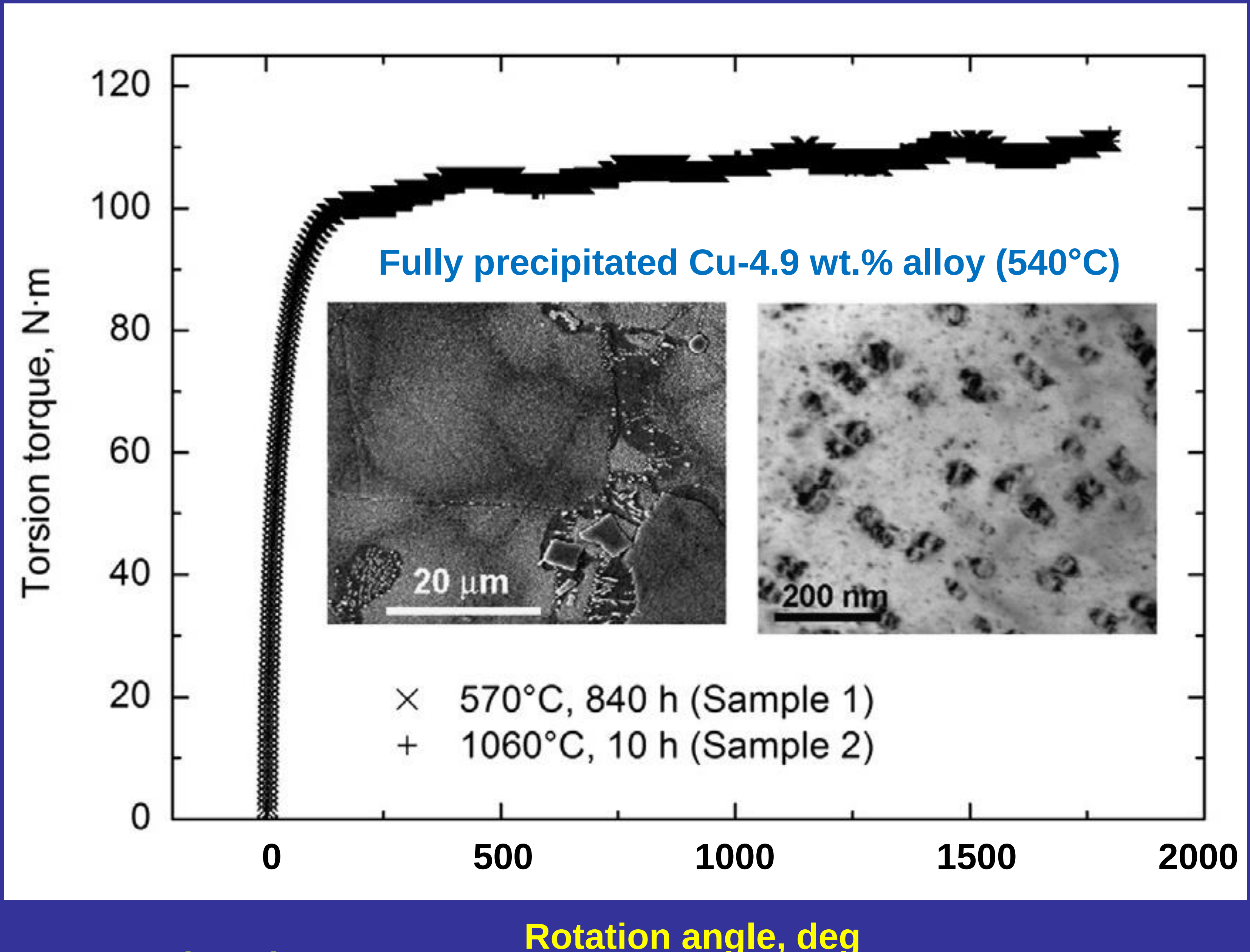

Mater. Lett. 118 (2014) 111

Lattice spacing and Co content in Cu-matrix

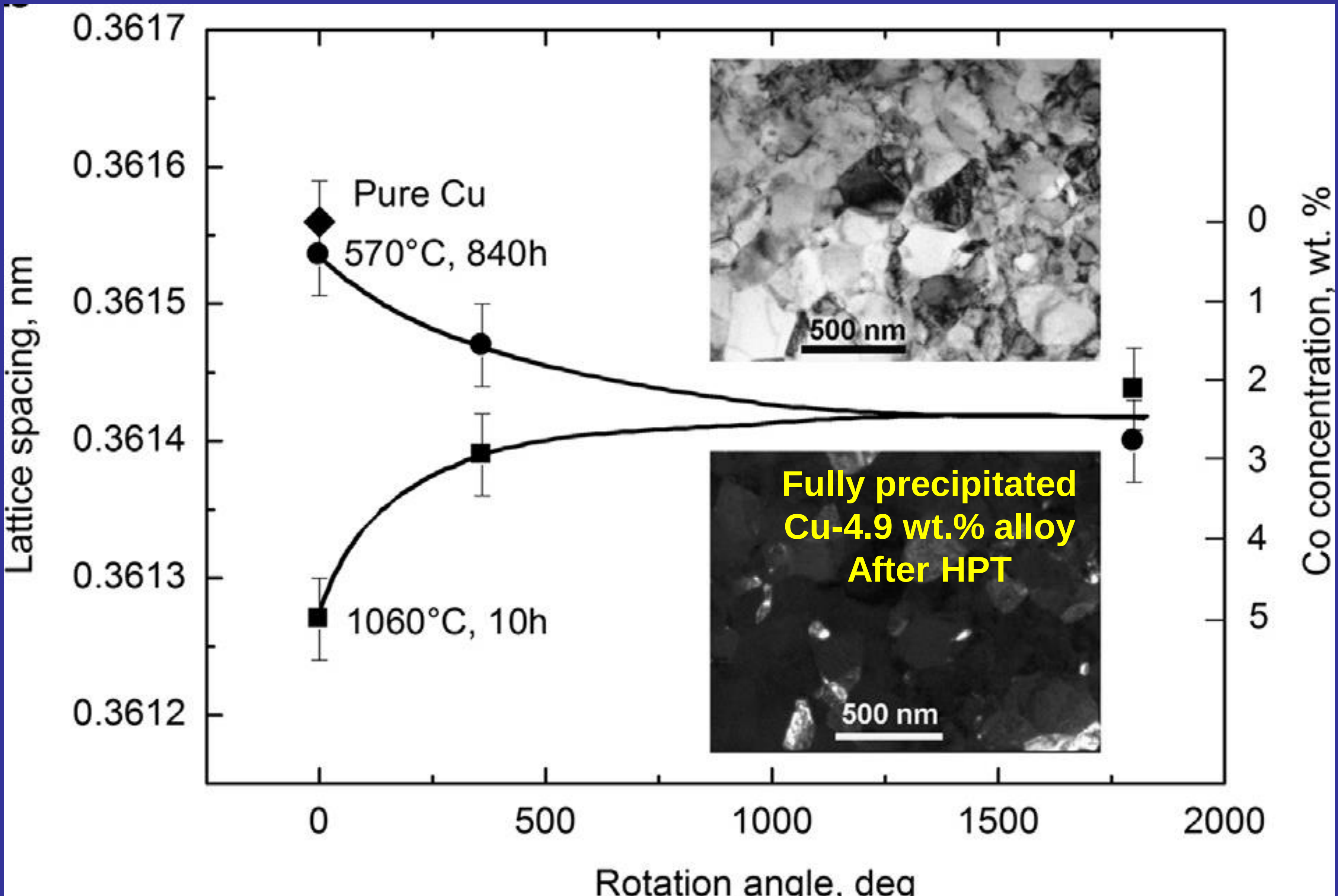

Mater. Lett. 118 (2014) 111

Lattice spacing and Co content in Cu-matrix

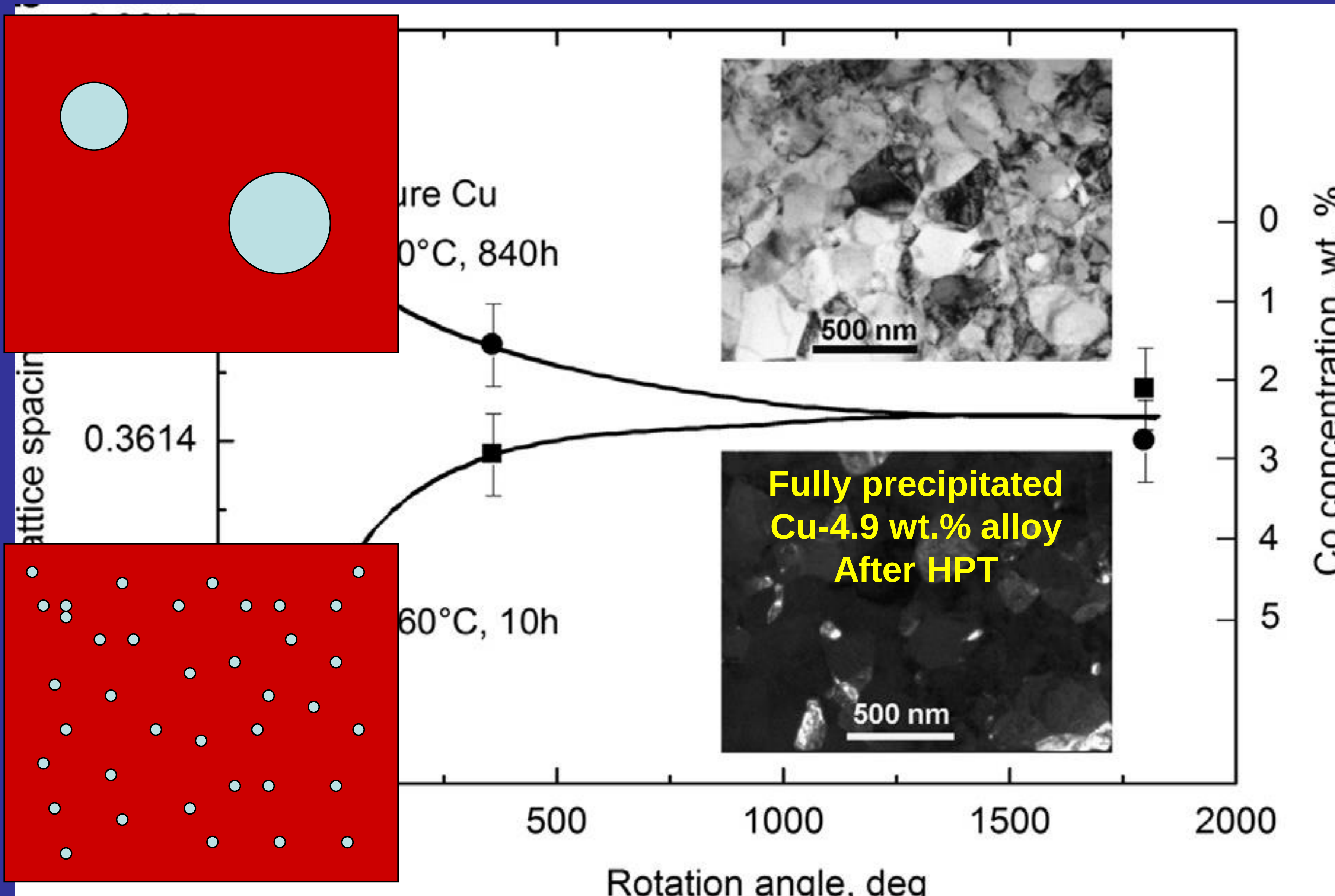

Mater. Lett. 118 (2014) 111

Lattice spacing and Co content in Cu-matrix

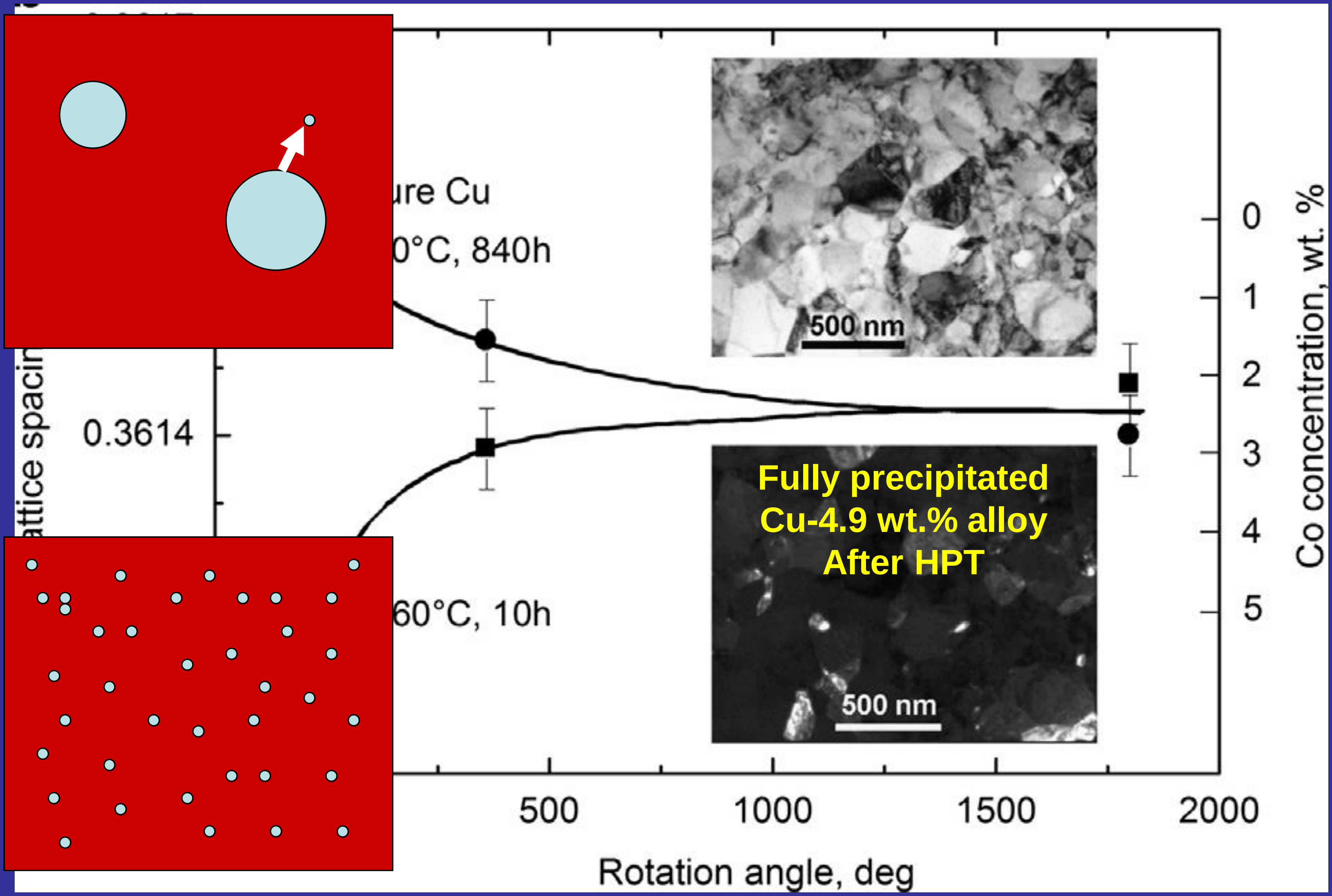

Mater. Lett. 118 (2014) 111

Lattice spacing and Co content in Cu-matrix

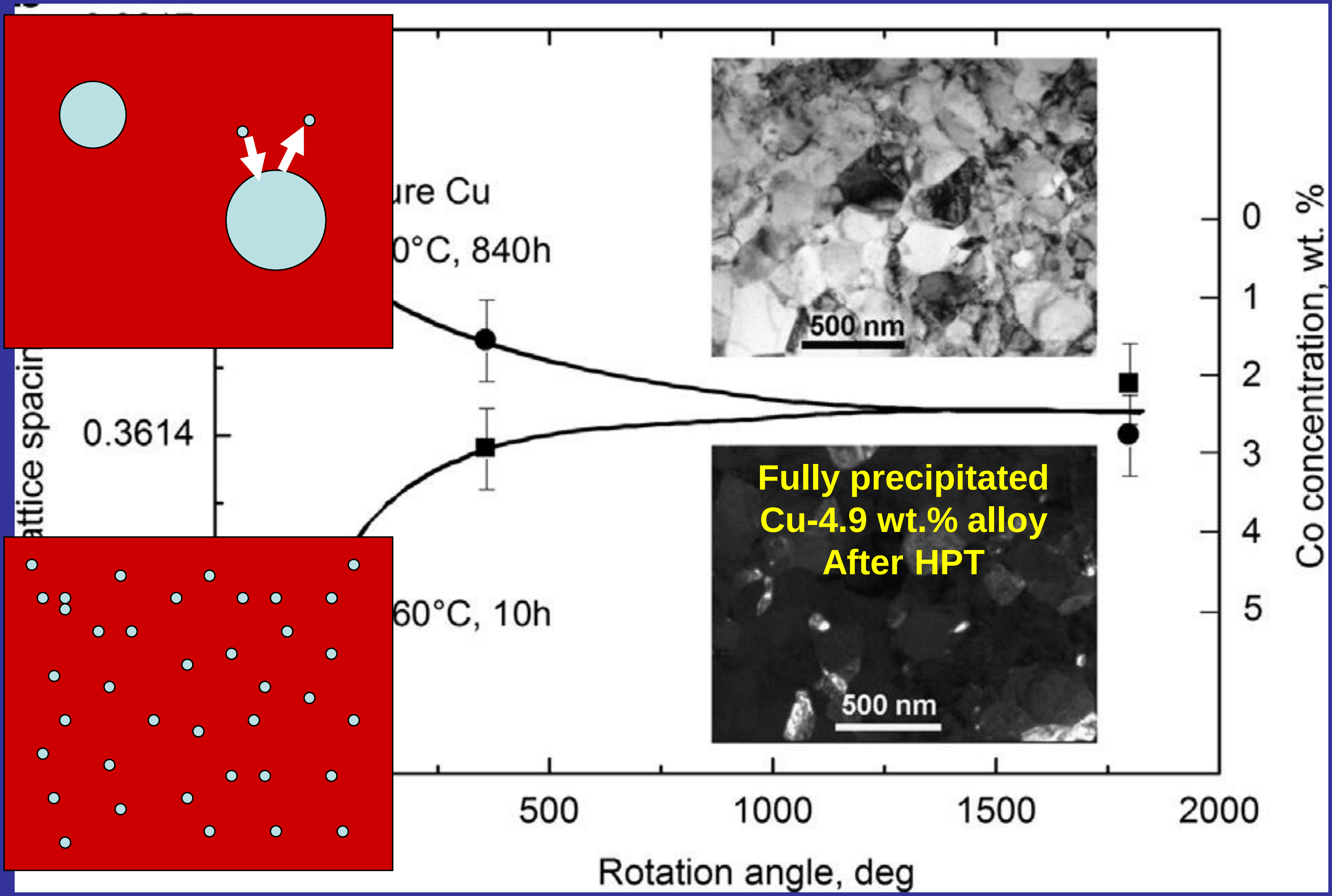

Mater. Lett. 118 (2014) 111

Lattice spacing and Co content in Cu-matrix

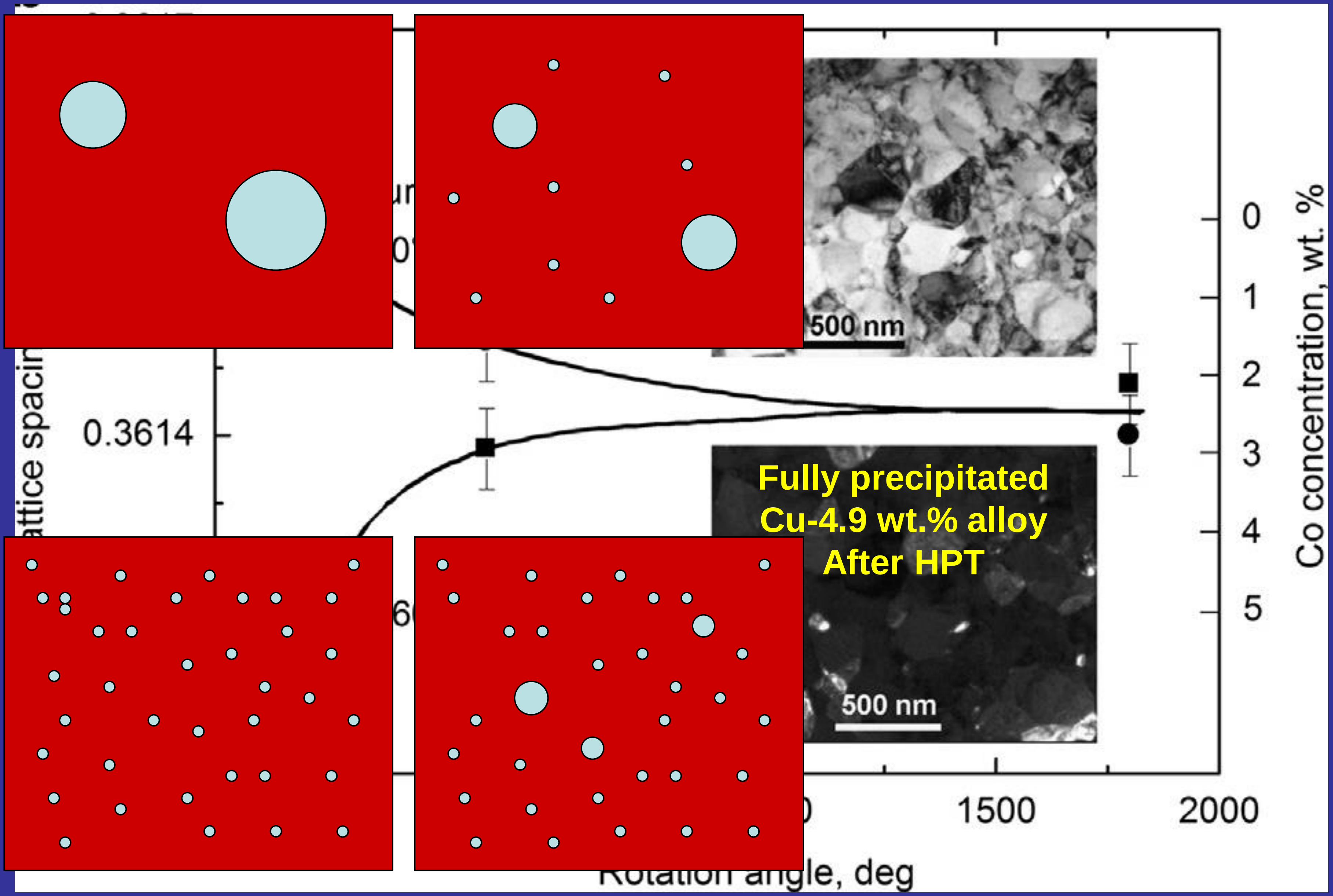

Mater. Lett. 118 (2014) 111

Lattice spacing and Co content in Cu-matrix

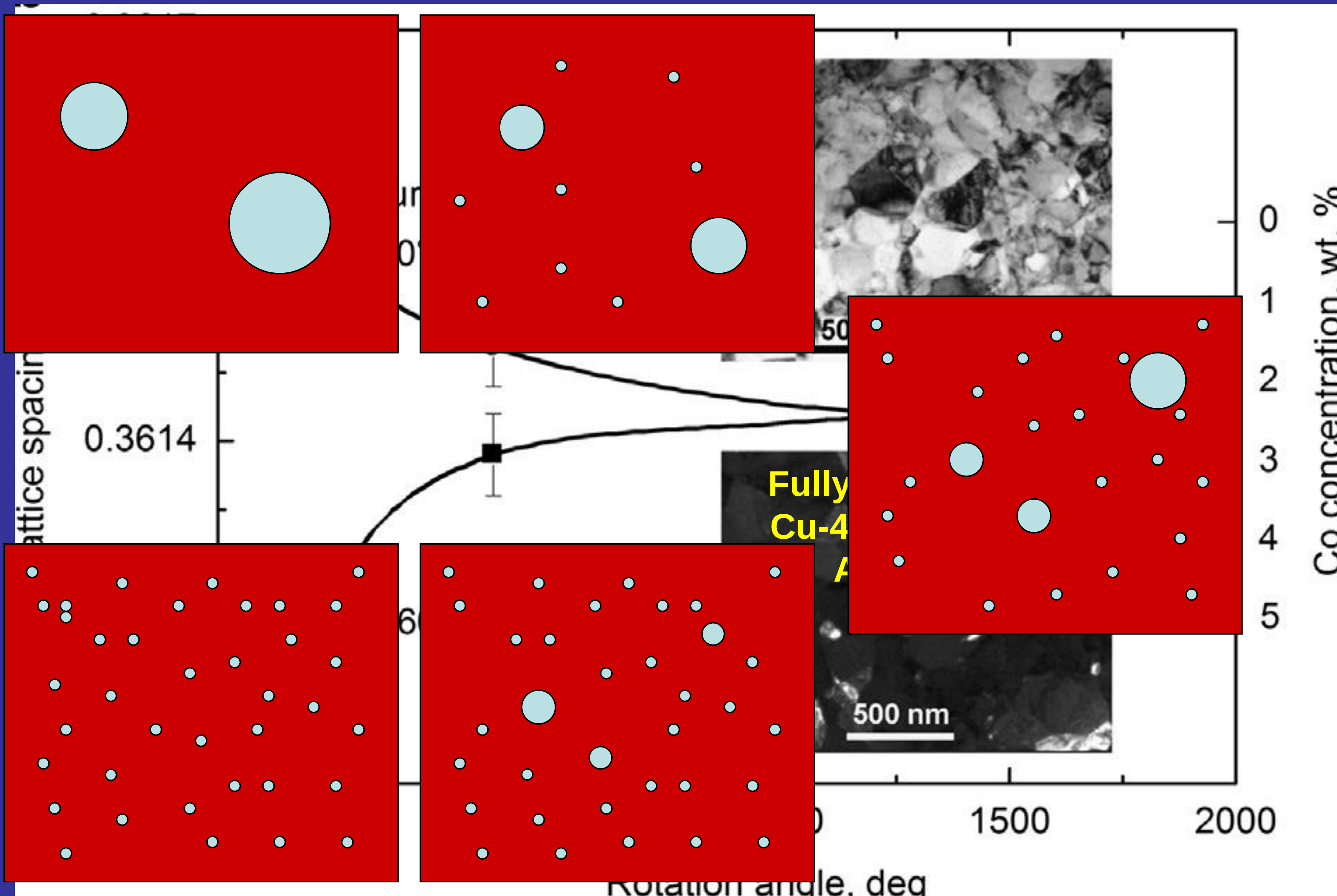

Mater. Lett. 118 (2014) 111

Supersaturated solid solution partially decomposes to 2.5 wt.% Co.

Co precipitates partially dissolve in the Cu-based solid solution up to 2.5 wt.% Co in (Cu)

Dissolution and precipitation proceed simultaneous and compete with each other

What happens, if we deform fully homogenized and fully precipitated alloy???

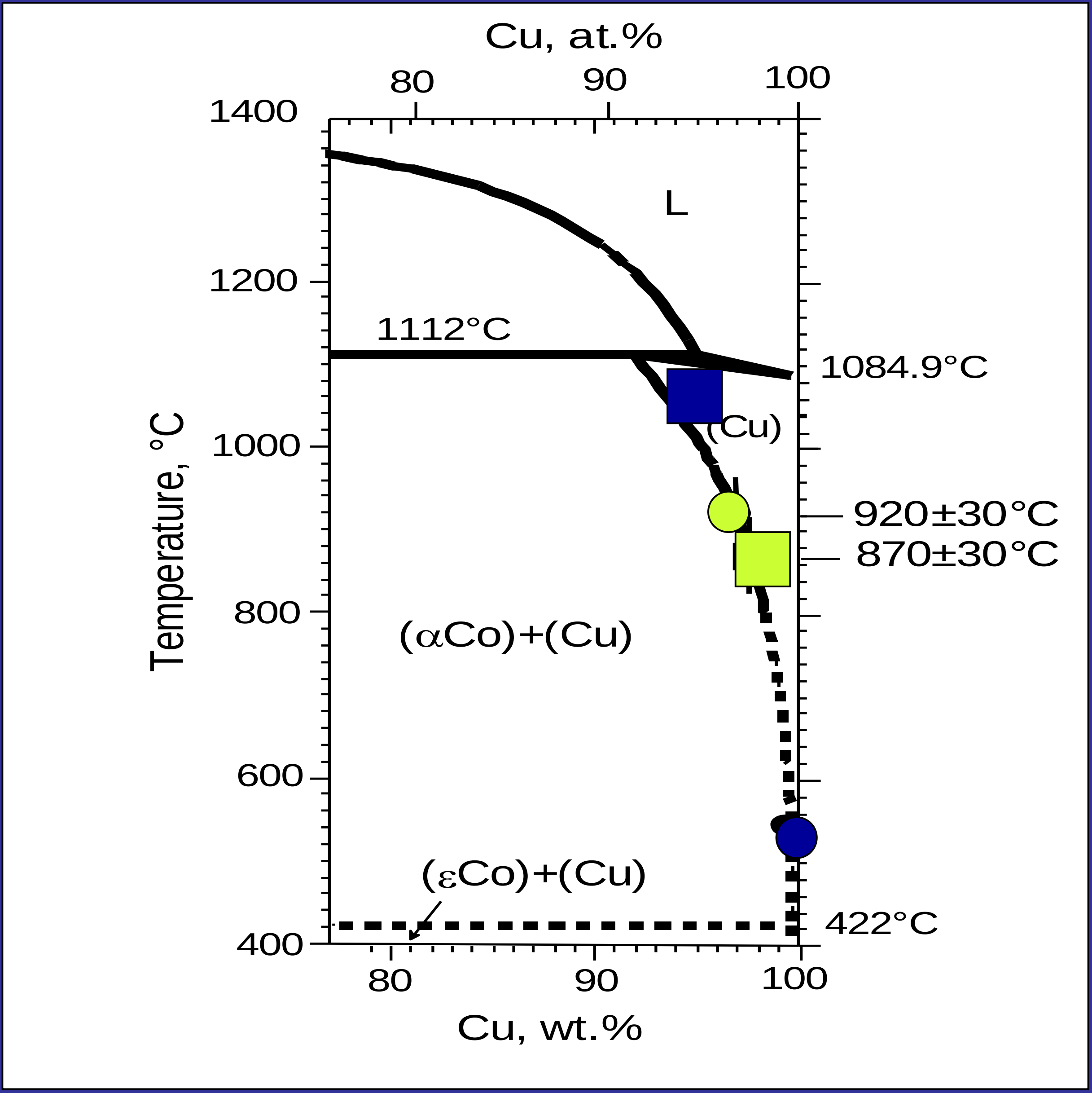

Mater. Lett. 118 (2014) 111

What happens, if we deform fully homogenized and fully precipitated alloy???

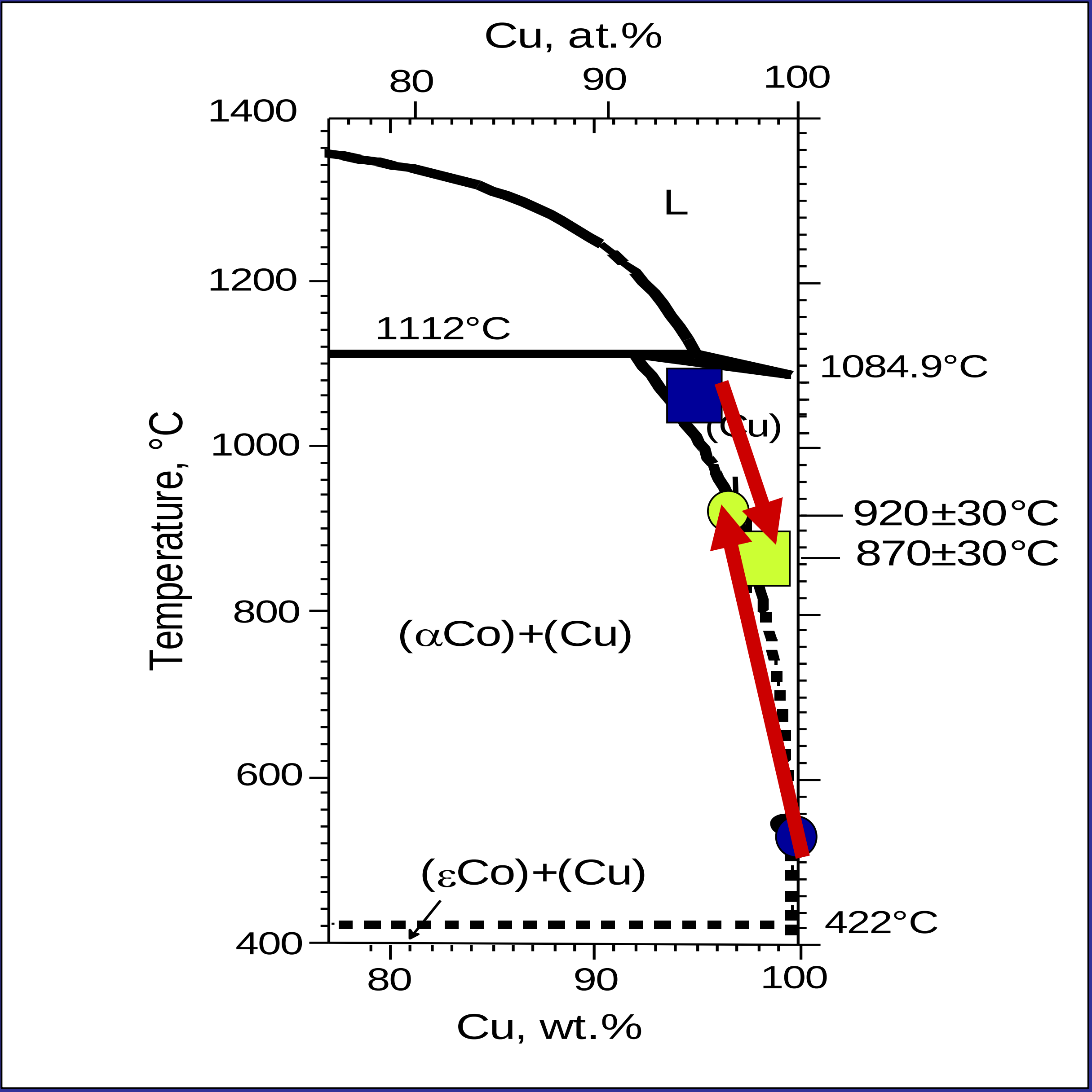

T_{eff}= 900°C

Mater. Lett. 118 (2014) 111

Does the composition of phases after SPD depend on the composition of phases before SPD??

No!!!

(equifinality)

The composition of phases
after SPD
is as if they were annealed
at 900°C

(so called equivalent
or effective temperature)

SPD-driven mass transfer is equivalent to the bulk diffusion with $D_{SPD} \sim 10^{-16}$ m²/s

Extrapolated bulk diffusion coefficient at 300K is $D_{SPD} \sim 10^{-35}$ m²/s

Bulk diffusion coefficient at T_{eff} is $D_{eff} \sim 10^{-14}$ m²/s

The SPD-driven mass transfer is equivalent to the annealing at 900°C

(equivalent or effective temperature)

Why T_{eff} is equal to 900°C?

What happens in other Cu-based alloys?

Concentration "corridor" in Cu-Ag alloys

Acta Mater.
195 (2020) 184

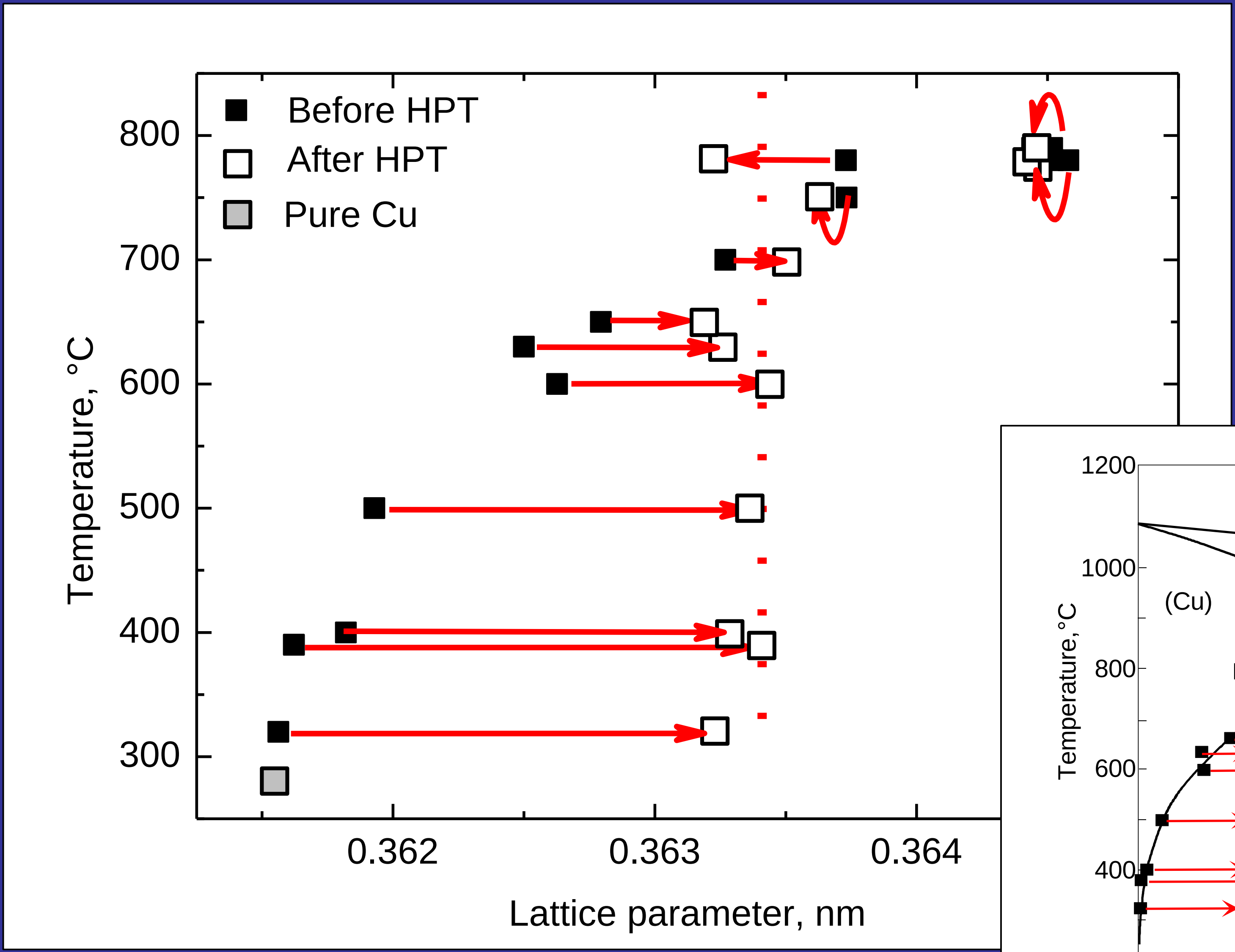

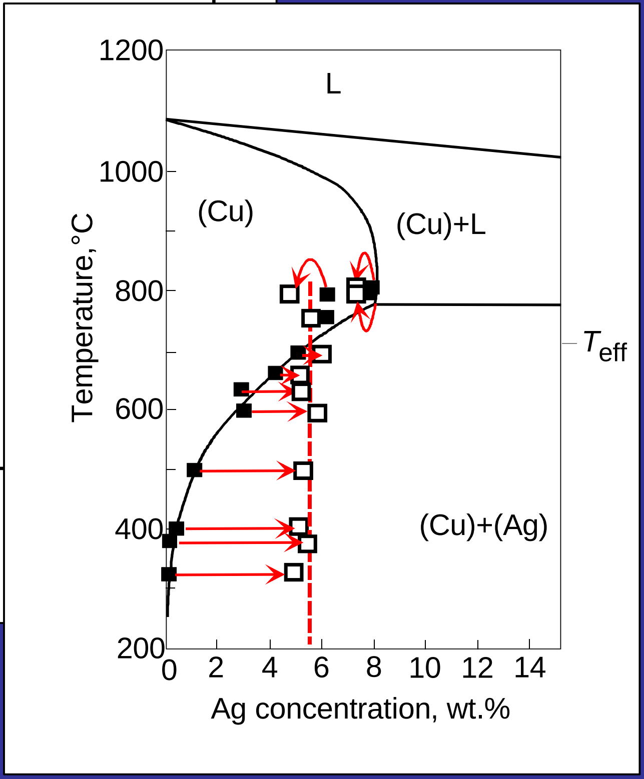

Concentration "corridor" in Cu-Sn alloys

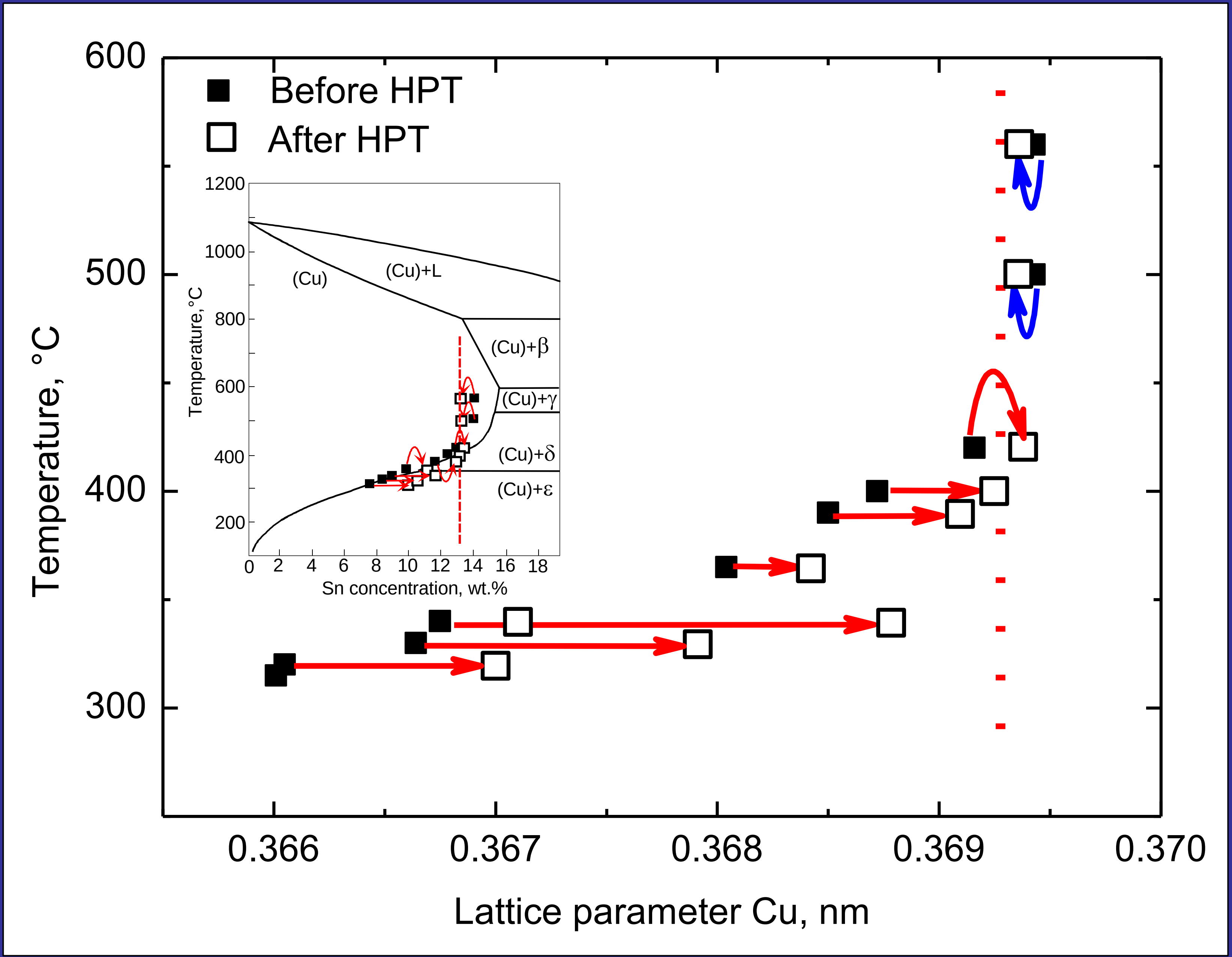

Acta Mater. **195** (2020) 184

Correlation between T_{eff} and activation enthalpy of bulk diffusion of the dopant

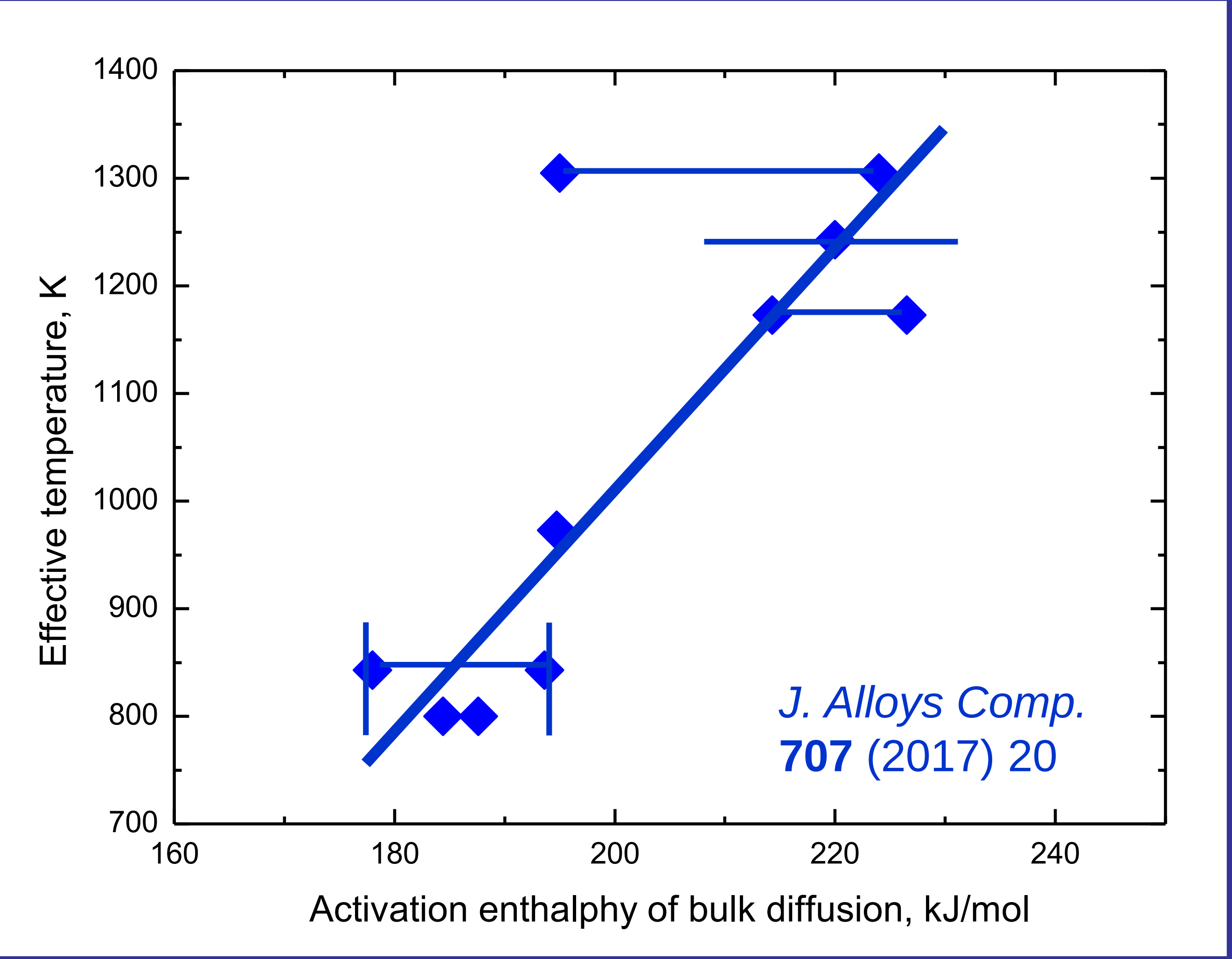

При перемещении в соседний узел атом преодолевает энергетический барьер

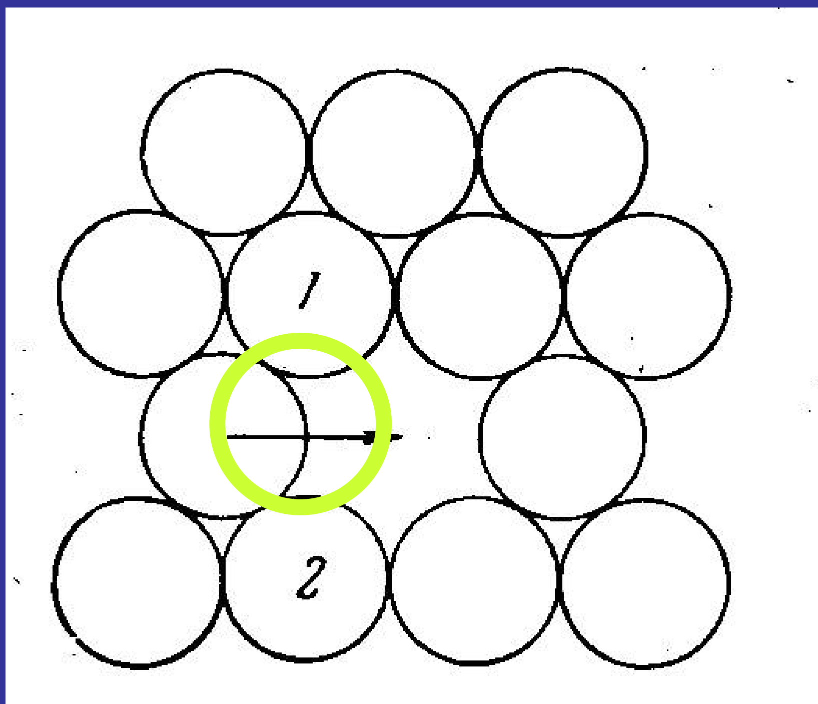

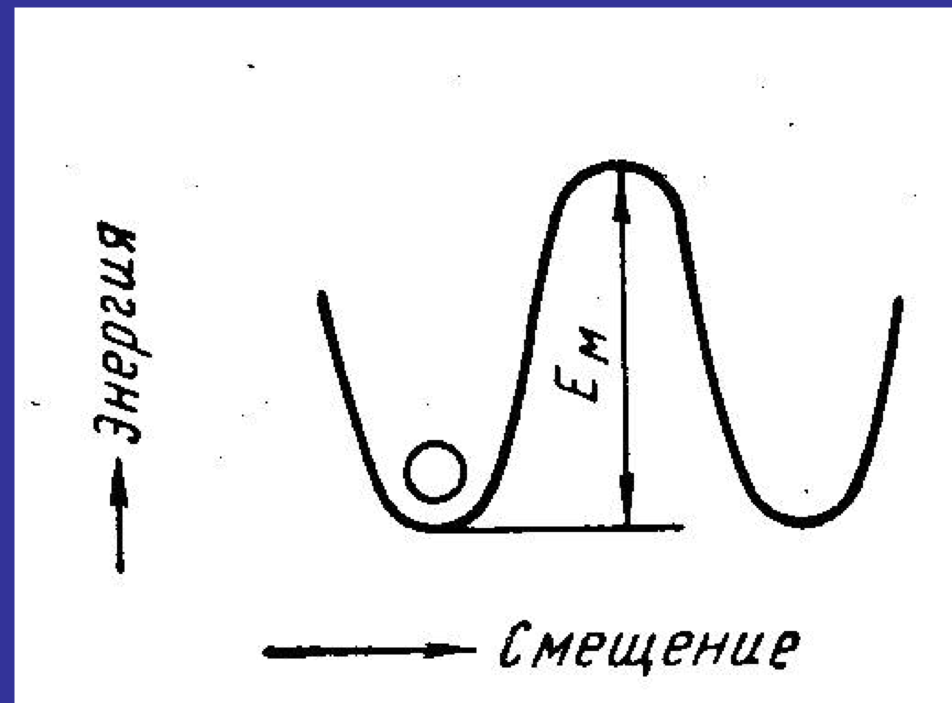

Correlation between T_{eff} and T_m of the dopant

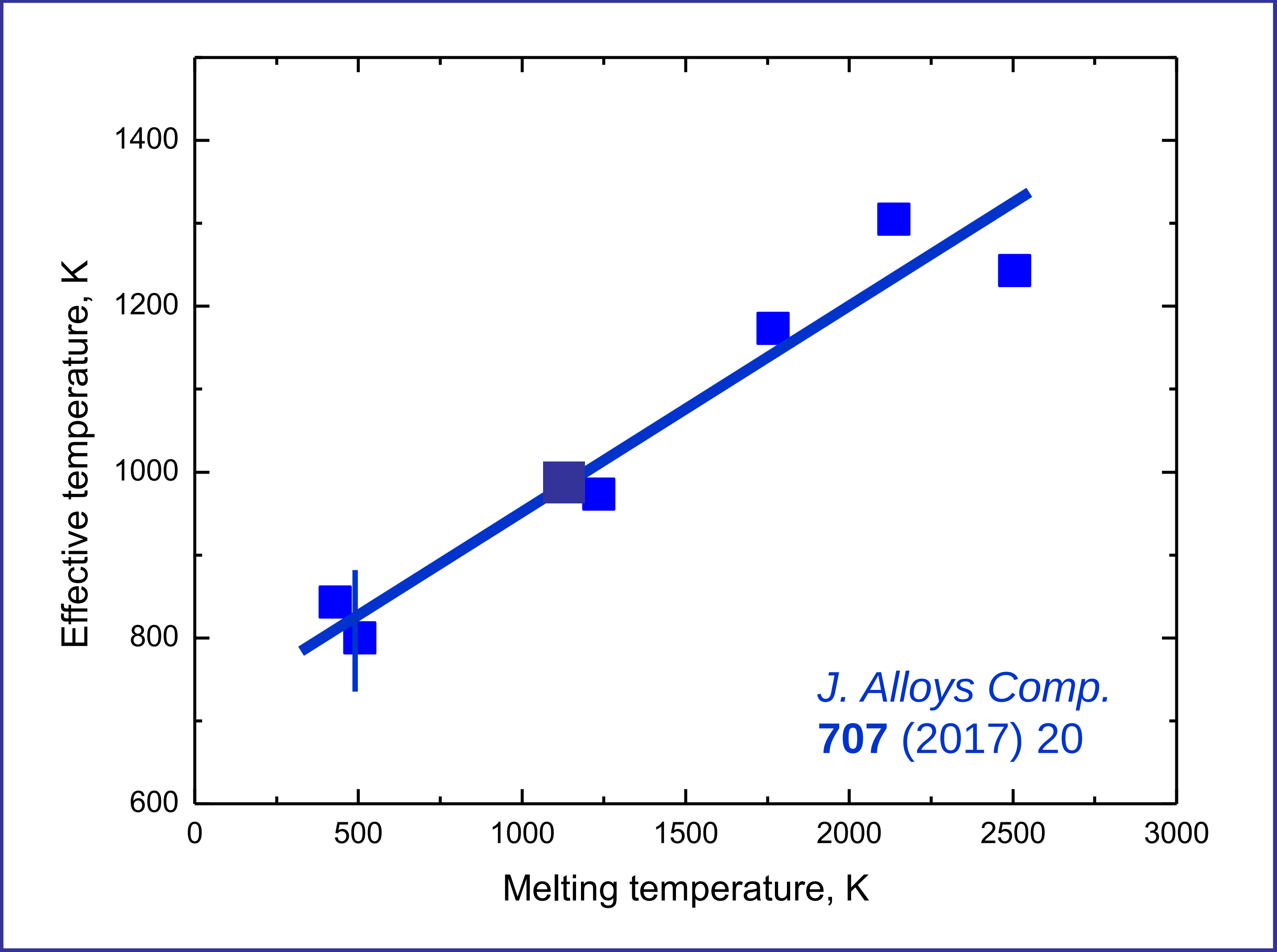

Correlation between activation enthalpy of bulk diffusion and T_m of the dopant

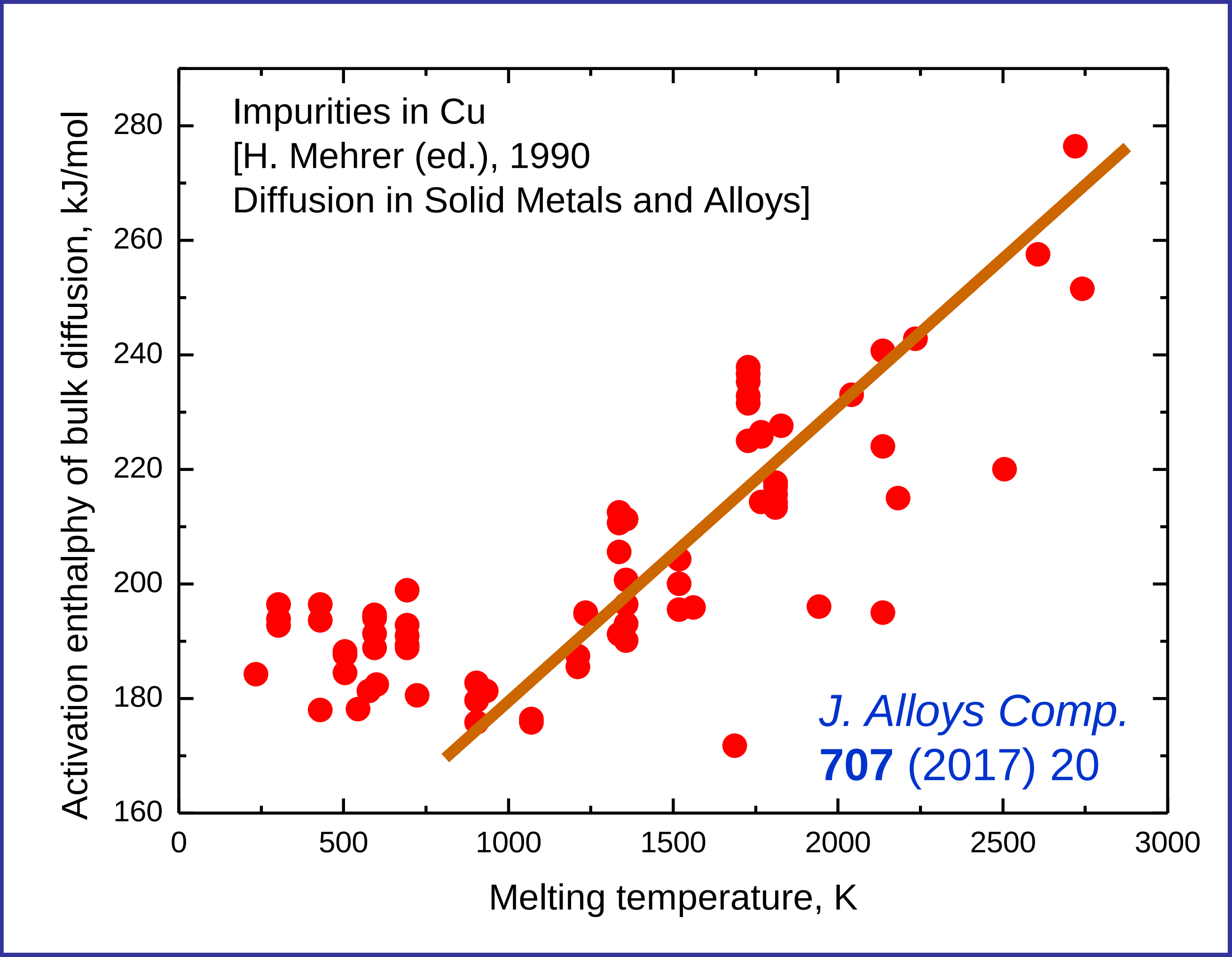

Facets in twin GBs in pure Cu after HPT are as if the sample was annealed at 900±50°C

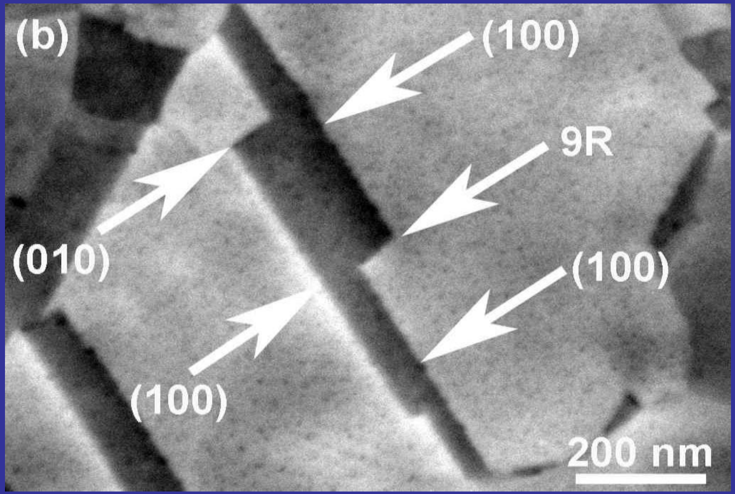

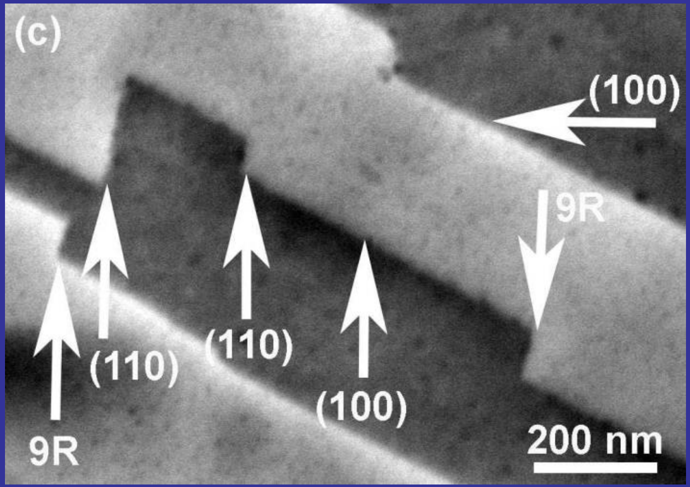

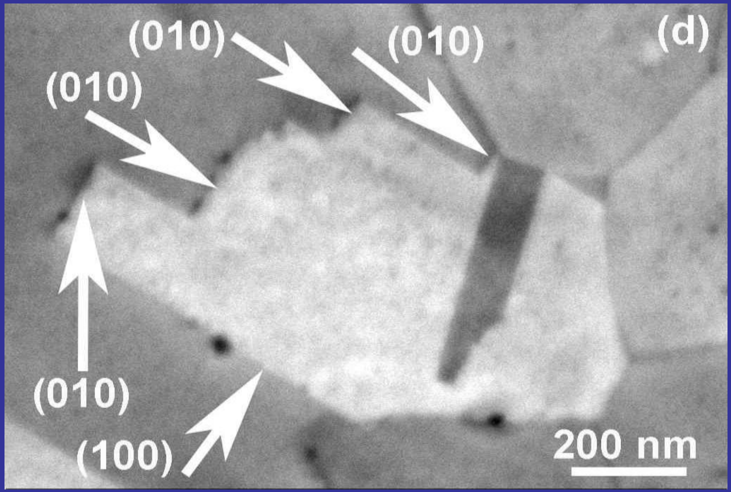

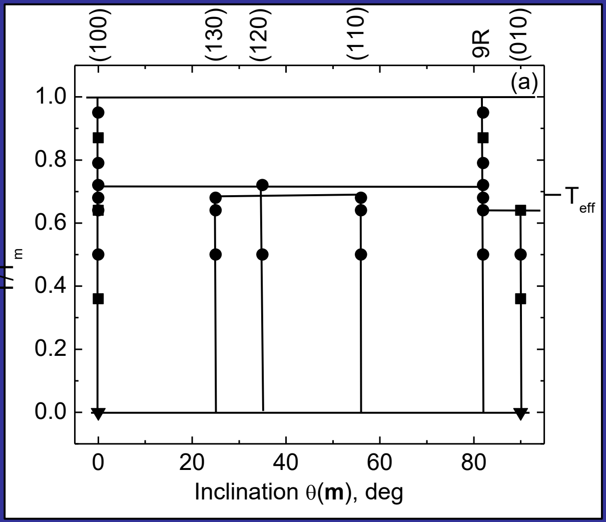

ADEM (2020) 1900589

If T_{HPT} increases, then T_{eff} decreases

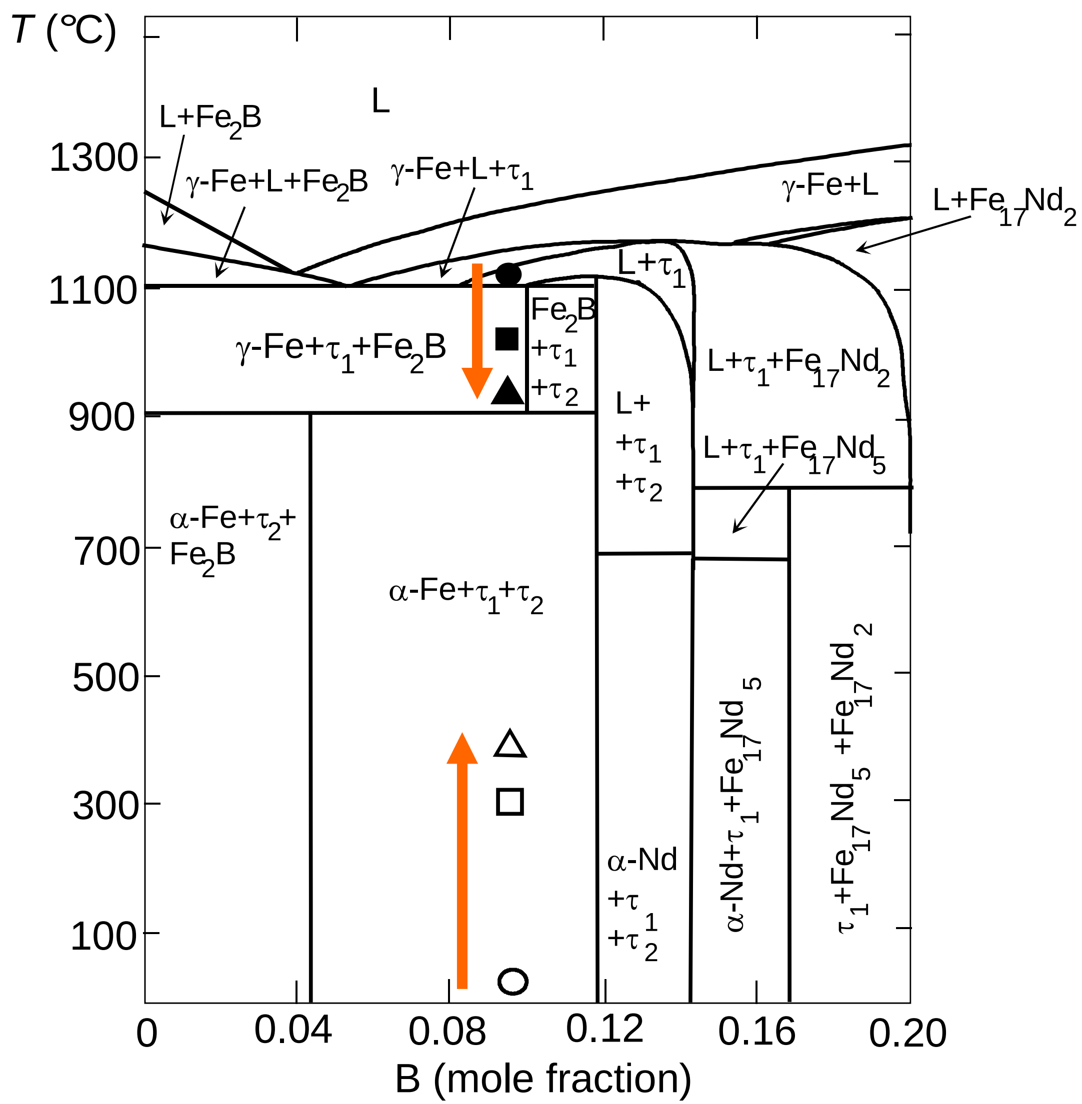

JETP Letters
112 (2020) 37
Письма в ЖЭТФ
112 (2020) 45

Diffusion- and diffusionless (martensitic) phase transformations

Ti-Fe alloys

αTi↔βTi↔ωTi

αTi↔βTi↔ωTi transformations

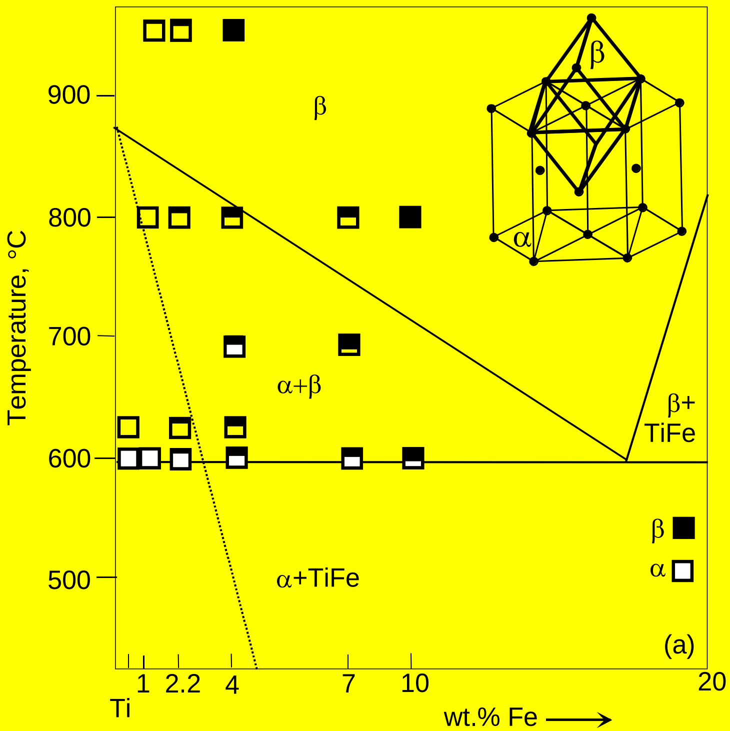

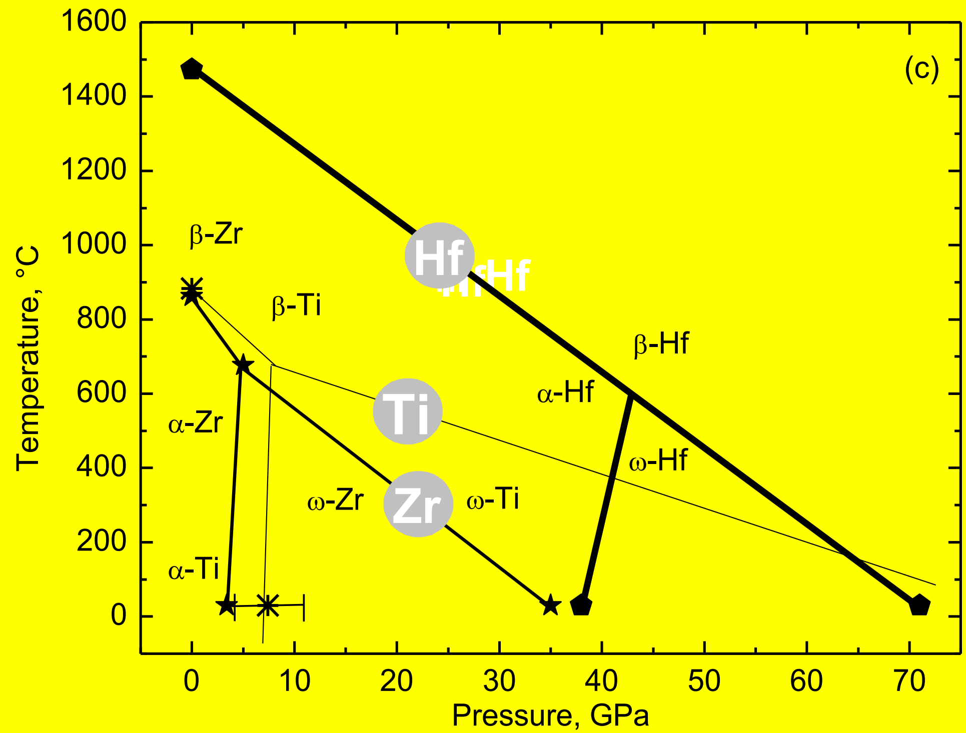

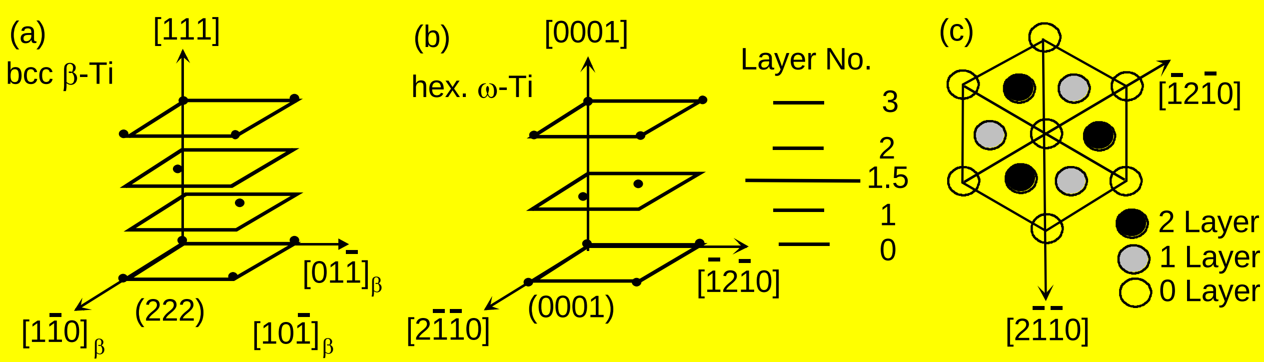

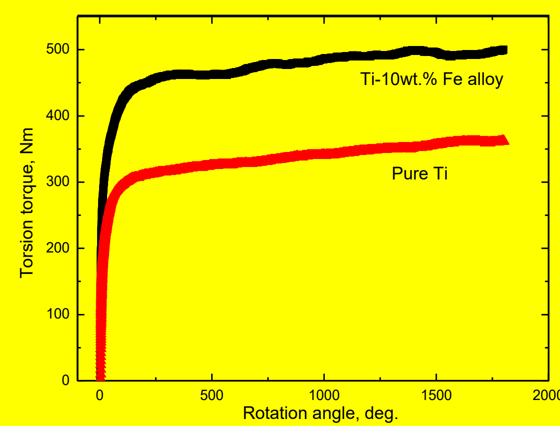

αTi↔βTi↔ωTi transformations

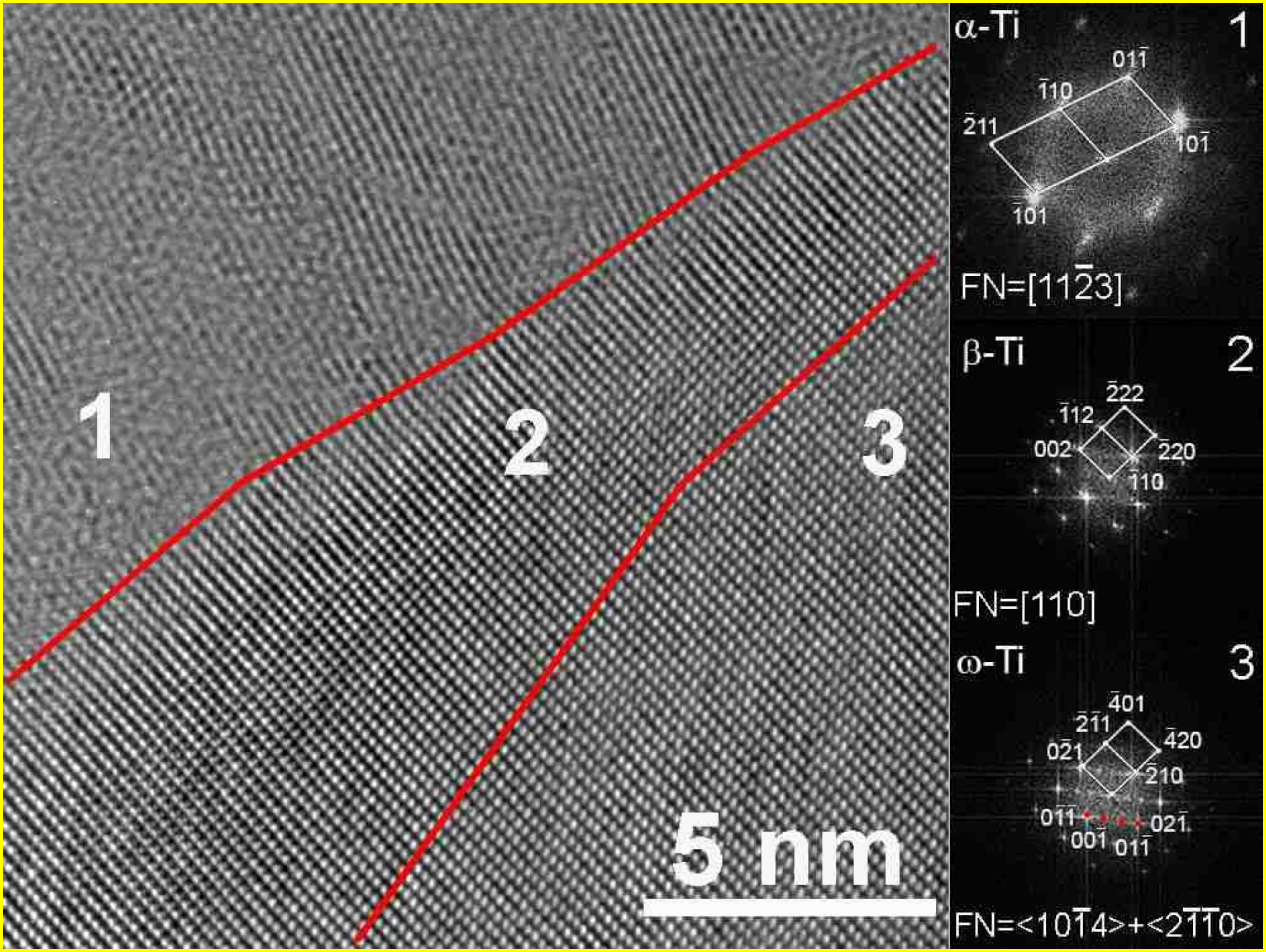

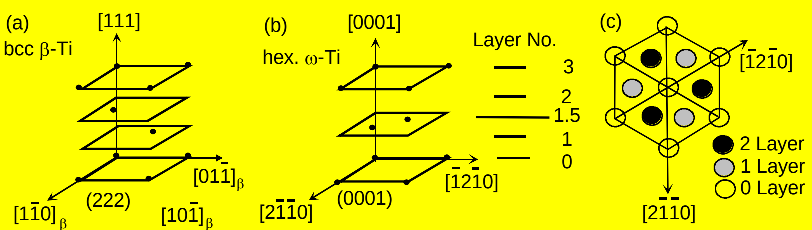

Acta Mater. **144** (2018) 337

αTi↔βTi↔ωTi transformations

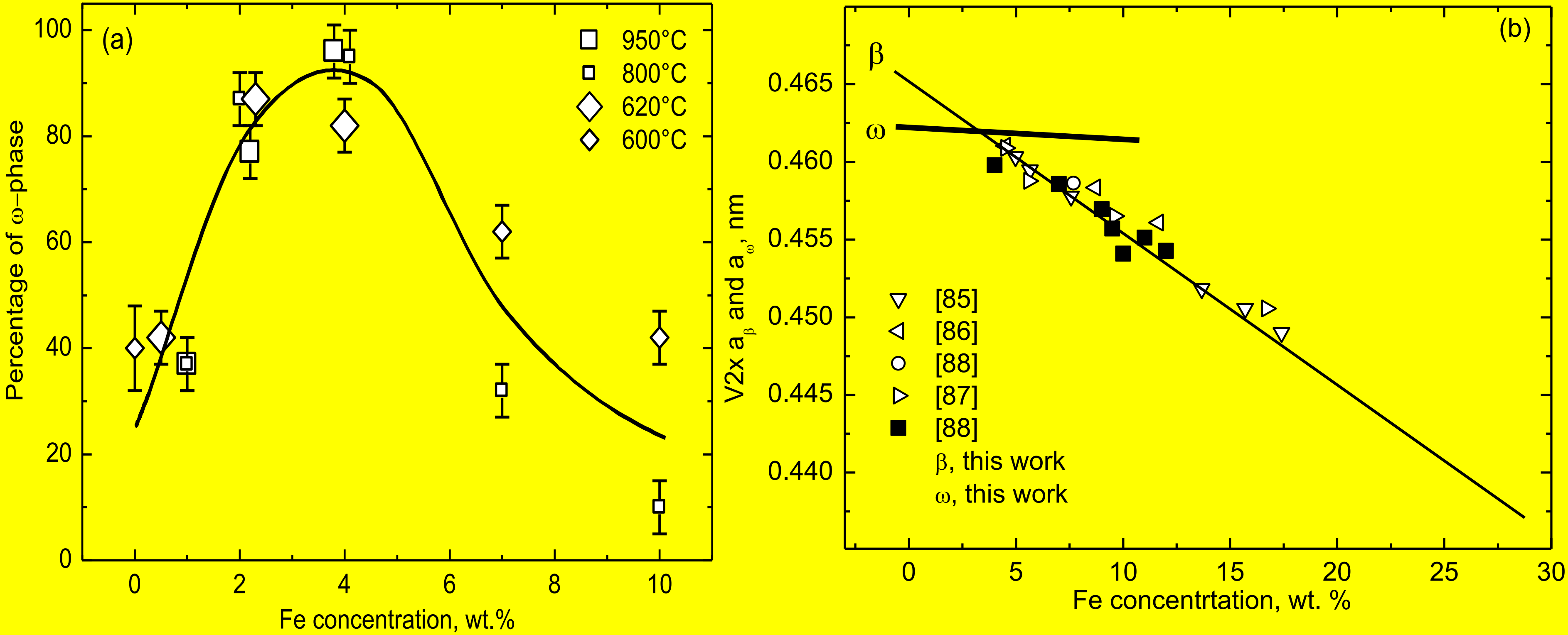

Best fit between βTi and ωTi phases is at 4 wt. % Fe

Acta Mater. **144** (2018) 337

Conclusions

1. Composition of phases after HPT does not depend on that before HPT.
It is, therefore, equifinal.
2. It is equal to that after equlibrium annealing at certain T_{eff}.
3. Reason: high steady-state concentration of lattice defects in dynamic equilibrium
4. T_{eff} ~ (T_m and Q_b) of the dopant
5. Diffusion- and diffusionless (martensitic) phase transformations

Фазовые превращения:

-- на внутренних границах раздела